Systematic investigation of the interplay between biomaterials and the immune system in vitro

Dissertation

der Mathematisch-Naturwissenschaftlichen Fakultät

der Eberhard Karls Universität Tübingen

zur Erlangung des Grades eines

Doktors der Naturwissenschaften

(Dr. rer. nat.)

vorgelegt von

M.Sc. Florian Billing

aus Tübingen

Tübingen

2021

Gedruckt mit Genehmigung der Mathematisch-Naturwissenschaftlichen Fakultät der Eberhard Karls Universität Tübingen.

Tag der mündlichen Qualifikation:	27.04.2022
Dekan:	Prof. Dr. Thilo Stehle
1. Berichterstatterin:	Prof. Dr. Katja Schenke-Layland
2. Berichterstatter:	Prof. Dr. Alexander Weber

Table of contents

Abstract ..... **III**
Zusammenfassung ..... **V**
Abbreviations ..... **VII**
List of Figures and Tables ..... **VIII**
List of Publications contributing to cumulative theses ..... **IX**
Contributions ..... **IX**
List of further publications ..... **X**
1 Introduction **3**
Preface 3
1.1 Biocompatibility of medical devices 4
1.1.1 The role of surface topography 6
1.1.2 The role of surface wettability 7
1.2 Protein adsorption to biomaterial substrates 9
1.2.1 Surface-dependent adsorption of plasma proteins 10
1.2.2 Protein-dependent effects on immunological responses 11
1.3 Immunological response to biomaterials 12
1.3.1 Adverse effects of an excessive immune response 15
1.3.2 Immune cell populations and the PBMC in vitro model 16
1.4 Modulation of biomaterials for targeted application 17
1.4.1 Surface treatments 18
1.4.2 Surface coatings 19
2 Objectives of the thesis **23**
3 Results I: Defining the role of different immune cell populations **27**
3.1 Surface characteristics of clinically-used titanium dental implants 28
3.2 Immune responses towards surface-treated titanium dental implants 29
3.3 The role of innate and adaptive immune cells 29
4 Results II: Systematic investigation of biomaterial surface roughness **35**
4.1 Creation and characterization of polyurethane samples 36
4.2 Cellular responses to polyurethane surface topography 37
5 Results III: Interrelation between wettability, protein adsorption & immune response **43**
5.1 Characterisation of surface properties and inflammatory response 44
5.2 Adsorbed proteins as potential causes of the observed immune response . 45
5.3 The MAPK signalling pathway as a candidate factor in driving monocyte immune response 46
6 General discussion and conclusion **51**
6.1 Role of innate and adaptive immune cells in response to biomaterial surfaces…… 51
6.2 Surface property-driven immune response 54
6.3 Modulation of biocompatibility via PEM surface coating 56

6.4 Protein adsorption as essential marker for biocompatibility 57
6.5 Conclusion 59
References 61
Acknowledgements 71
Declaration 72
Appendices 73
Appendix I 73
Appendix II 90
Appendix III 106

Abstract

Medical implants are widely used nowadays. Following tissue contact, proteins adhere to the device's surface and surrounding cells become activated, causing an initial inflammatory host response. If this host response develops into a chronic inflammatory state, significant adverse effects such as implant rejection and loss might occur. The physico-chemical qualities of the biomaterials employed have a substantial influence on the degree of the immune response. Therefore, modulating surface properties such as topography or wettability may be a viable strategy for altering the immune response. However, the complex interrelation between surface properties, highly sensitive adsorption of proteins, and multifaceted immune response remains largely unresolved. This thesis aims at investigating the interplay of all three of these critical factors determining a device's biocompatibility in order to enable effective modulation of the immune response to biomedical implants.

In the first part of this thesis, investigation of the contributing role of different immune cell types identified monocytes/macrophages as essential mediators of the initial inflammatory response, while involvement of T and NK cells was just minor during this phase. Analysis of titanium dental implant specimen revealed surface-dependent immune responses related to wettability and roughness. In contrast, systematic analysis of the influence of surface roughness of polymer materials in the second part of the thesis showed similar immunological activation irrespective of the applied surface roughness throughout the tested range. This was independent of the biological complexity of the cell culture system used (macrophage cell line, PBMCs, whole blood). The final section of the thesis examined wettability-mediated effects on immune cell activity using PEM coatings and discovered that pro- and anti-inflammatory cytokine responses are highly dependent on wettability, with lower pro-inflammatory effects reported on the more hydrophilic PEM surface. Experiments using serum-free cell culture medium demonstrated that the observed effects are clearly dependent on the presence of serum proteins at the biomaterial surface. Significant changes in the type and amount of adsorbed proteins were discovered using mass spectrometry analysis. The observed immunological differences could be correlated with the presence of specific apolipoproteins at the surfaces, implying that apolipoproteins might play a significant role in the modulation of biomaterial immune responses. These

findings may aid in the targeted design of immunomodulatory surfaces to promote healing and implant integration. In addition, they place a larger emphasis on adsorption of proteins such as apolipoproteins as crucial class of immune cell mediators.

Zusammenfassung

Die Nutzung medizinischer Implantate ist heutzutage weit verbreitet. Unmittelbar nach Gewebekontakt haften Proteine an der Oberfläche des Implantats an und es kommt zu einer Aktivierung der umgebenden Zellen, was zu einer initialen Entzündungsreaktion führt. Entwickelt sich diese Reaktion zu einem chronischen Entzündungszustand, können erhebliche negative Auswirkungen wie die Abstoßung und der Verlust des Implantats auftreten. Das Ausmaß der Immunreaktion wird dabei stark von den physikalisch-chemischen Eigenschaften der verwendeten Biomaterialien beeinflusst. Daher kann die Modulation von Oberflächeneigenschaften wie Topographie oder Benetzbarkeit eine praktikable Strategie zur Veränderung der Immunreaktion sein. Die komplexe Beziehung zwischen den Oberflächen-eigenschaften, der hochsensiblen Adsorption von Proteinen, und der vielschichtigen Immunantwort ist jedoch noch weitgehend ungelöst. Ziel dieser Arbeit ist es, das Zusammenspiel dieser drei kritischen Faktoren, welche die Biokompatibilität eines Implantats bestimmen, zu untersuchen, um eine wirksame Modulation der Immunantwort auf biomedizinische Implantate zu ermöglichen.

Im ersten Teil dieser Arbeit wurde die Rolle der verschiedenen Immunzellarten untersucht, wobei Monozyten/Makrophagen als wesentliche Vermittler der initialen Entzündungsreaktion identifiziert wurden, während die Beteiligung von T- und NK-Zellen in dieser Phase nur gering war. Die Untersuchung von Zahnimplantatproben aus Titan offenbarte oberflächenabhängige Immunreaktionen in Abhängigkeit von Benetzbarkeit und Rauheit. Im Gegensatz dazu zeigte die systematische Analyse des Einflusses der Oberflächenrauheit von Polymermaterialien im zweiten Teil der Arbeit eine ähnliche immunologische Aktivierung, unabhängig von der untersuchten Oberflächenrauheit im gesamten Testbereich. Diese war unabhängig von der biologischen Komplexität des verwendeten Zellkultursystems (Makrophagenzelllinie, PBMCs, Vollblut). Der letzte Teil der Arbeit untersuchte die durch die Benetzbarkeit vermittelten Auswirkungen auf die Aktivität von Immunzellen unter Verwendung von PEM Beschichtungen und stellte fest, dass pro- und anti-inflammatorische Zytokinreaktionen in hohem Maße von der Benetzbarkeit abhängig waren, wobei die pro-inflammatorischen Effekte bei Oberflächen mit größerer Hydrophilie geringer ausfielen. Experimente mit serumfreiem Zellkulturmedium zeigten, dass die

beobachteten Effekte eindeutig von der Anwesenheit von Serumproteinen auf der Biomaterialoberfläche abhängig sind. Mittels massenspektrometrischer Analyse wurden signifikante Veränderungen in der Art und Menge der adsorbierten Proteine festgestellt. Die beobachteten immunologischen Unterschiede konnten mit dem Vorhandensein spezifischer Apolipoproteine auf den Oberflächen korreliert werden, was darauf hindeutet, dass Apolipoproteine eine wichtige Rolle bei der Modulation der Immunantwort von Biomaterialien spielen könnten. Diese Ergebnisse könnten die gezielte Konzipierung immunmodulatorischer Oberflächen unterstützen, um die Heilung und Implantatintegration zu fördern. Darüber hinaus legen sie einen größeren Schwerpunkt auf die Adsorption von Proteinen wie Apolipoproteinen als entscheidende Klasse von Immunzellmediatoren.

Abbreviations

AFM	atomic force microscopy
CD	cluster of differentiation
ECM	extracellular matrix
FBGC	foreign-body giant cell
h	hour
IL	Interleukin
LC-MS/MS	liquid chromatography-mass spectrometry
NK cells	natural killer cells
PAH	polyallylamine hydrochloride
PBMC	peripheral blood mononuclear cells
PEM	polyelectrolyte multilayer coating
PSS	polystyrene sulfonate
SEM	scanning electron microscopy
SLA	sandblasted and acid etched (titanium surf.)
SLActive	sandblasted and acid etched titanium surface including hydrophilic treatment
T_c cells	cytotoxic T cells
T_h cells	helper T cells
THP-1	human monocytic cell line THP-1
XPS	X-ray photoelectron spectroscopy

List of Figures and Tables

Figures

Figure 1:	Biocompatibility of medical devices	4
Figure 2:	Biomaterial properties with potential influence on the host response	5
Figure 3:	Characterisation of surface wettability	8
Figure 4:	Effect of wettability on protein adsorption and cell adhesion	10
Figure 5:	Overview of the immunological response to biomaterials over time	13
Figure 6:	Schematic view of possible strategies for targeted modulation of biomaterials	17
Figure 7:	Schematic overview of the generation and application of PEMs	20
Figure 8:	Investigation of the immune response to titanium biomaterials and the role of individual immune cell populations	28
Figure 9:	Systematic investigation of biomaterial surface roughness	36
Figure 10:	Schematic overview of the interrelation between surface wettability, protein adsorption and immune response	47
Figure 11:	Example of similar topographical profiles with distinct roughness parameter Ra	55

Tables

Table 1:	Overview of important cytokines / chemokines and their function in the immune response to biomaterials	14

List of Publications contributing to cumulative theses

1. **Billing F.,** Jakobi M., Martin D. et al. The immune response to the SLActive titanium dental implant surface in vitro is predominantly driven by innate immune cells. *Journal of Immunology and Regenerative Medicine, Volume 13, 100047* (2021). *https://doi.org/10.1016/j.regen.2021.100047*
2. Segan S., Jakobi M., Khokhani P., Klimosch S., **Billing F.** et al. Systematic Investigation of Polyurethane Biomaterial Surface Roughness on Human Immune Responses in vitro. *BioMed Research International*, *Volume 2020, Article ID 3481549* (2020). *https://doi.org/10.1155/2020/3481549*
3. **Billing F.,** Walter B., Fink S. et al. Altered pro-inflammatory responses to polyelectrolyte multilayer coatings are associated with differences in protein adsorption and wettability. *ACS Applied Material Interfaces, Volume 13, Issue 46, pages 55534–55549* (2021). *https://doi.org/10.1021/acsami.1c16175*

Contributions

No.	Accepted for publi-cation	Number of authors	Position of the candi-date in the list of authors	Scientific ideas by candidate (%)	Data generation by candi-date (%)	Interpreta-tion and analysis by candidate (%)	Paper writing by candidate (%)
1	**Yes**	**9**	**1**	**50**	**65**	**65**	**60**
2	**Yes**	**21**	**5**	**10**	**10**	**20**	**10**
3	**Yes**	**16**	**1**	**55**	**45**	**55**	**65**

List of further publications

- Feuerer N., Marzi J., Brauchle E.M., Berrio D.A.C., **Billing F.** et al. Lipidome profiling with Raman Spectroscopy identifies macrophage response to biomaterials. *Proceedings of the National Academy of Sciences, Volume 118, Issue 52* (2021). *https://doi.org/10.1073/pnas.2113694118*
- Feuerer N., Berrio D.A.C., **Billing F.** et al. Raman microspectroscopy identifies biochemical activation fingerprints in THP-1- and PBMC-derived macrophages. *Biomedicines*, *Volume 10, Issue 5, 989* (2022). *https://doi.org/10.3390/biomedicines10050989*

Chapter 1

Introduction

1 Introduction

Preface

For several decades, the use of biomaterials in the treatment of medical pathology or malfunction has been well established as standard procedure. Even though there is a relatively high success rate for the majority of implants, implant failure, or the development of patient side effects, remains a critical issue in the field.[1–3] Upon implantation into the body, all materials inevitable initiate a host response. The extent and type of immune response experienced plays a major role in determining a medical device's biocompatibility. This host response includes adsorption of plasma proteins to the implant surface as the first interaction between the body and the foreign material. Following this, inflammatory cell migration occurs, which can induce acute inflammation and may result in a foreign body reaction.[4] In this regard, the nature of the response by the immune cells recruited to the implant site plays a deciding role in whether the material will successfully perform its intended function after the primary inflammatory response is resolved, or whether adverse immune responses will occur. Adverse immune responses often result from chronic excessive inflammation and can lead to fibrotic encapsulation, tissue destruction, or even isolation and rejection of the medical device.[5,6] In this context, the surface characteristics of the biomaterial are crucial in influencing the early immune response following implantation.[4,7] Physico-chemical properties on the surface of the implant, including surface roughness and wettability, can influence the immune response towards a biomaterial, resulting in either a pro-healing and tissue regenerative response or in the development of chronic inflammation being associated with negative effects on wound healing, tissue homeostasis, bone implementation and implant stability.[4,7,8] Therefore, one strategy for modulating the host response to materials is the modification of material surfaces.[7,9,10] Rather than developing entirely new materials, surface modification may provide an effective technique of imparting materials with favourable physical properties resulting in a substantially improved degree of biocompatibility. To enable finely tuned immune strategies, a more in depth understanding of the processes taking place at the interface between biomaterial and the immune system is required.

1.1 Biocompatibility of medical devices

Biomaterials are distinguished from other classes of materials by their capacity to be exposed to human body tissue without causing an unacceptable degree of harm to those tissues. This characteristic of both the biomaterial and the biological host system is termed biocompatibility and is defined by the Williams Dictionary of Biomaterials as "the ability of a material to perform with an appropriate host response in a specific application".[11] Immediately following biomaterial contact, a generic host response is initiated, which can be caused by the adsorption and desorption of host proteins at the biomaterial surface, the adhesion of platelets and components of the complement system, the exposure of mechanical forces, or the partial degradation of the biomaterial. Most essential factor in the development of the host response towards a biomaterial implant is the human immune system. In the progression of the host response, the activity of the immune system determines if the host response will be resolved and the medical device tolerated and successfully integrated into the body, or if the host response develops into a chronic state, causing clinically relevant side effects for the patient. These adverse effects may include the formation of inflammation-promoting foreign body giant cells, the deposition of excessive granulation tissue leading to fibrotic encapsulation, the destruction of peri-implant tissue, or the triggering of allergic reactions, all potentially leading to the rejection of a medical device.[12,13] Figure 1 depicts a schematic representation of the processes that define implant biocompatibility.

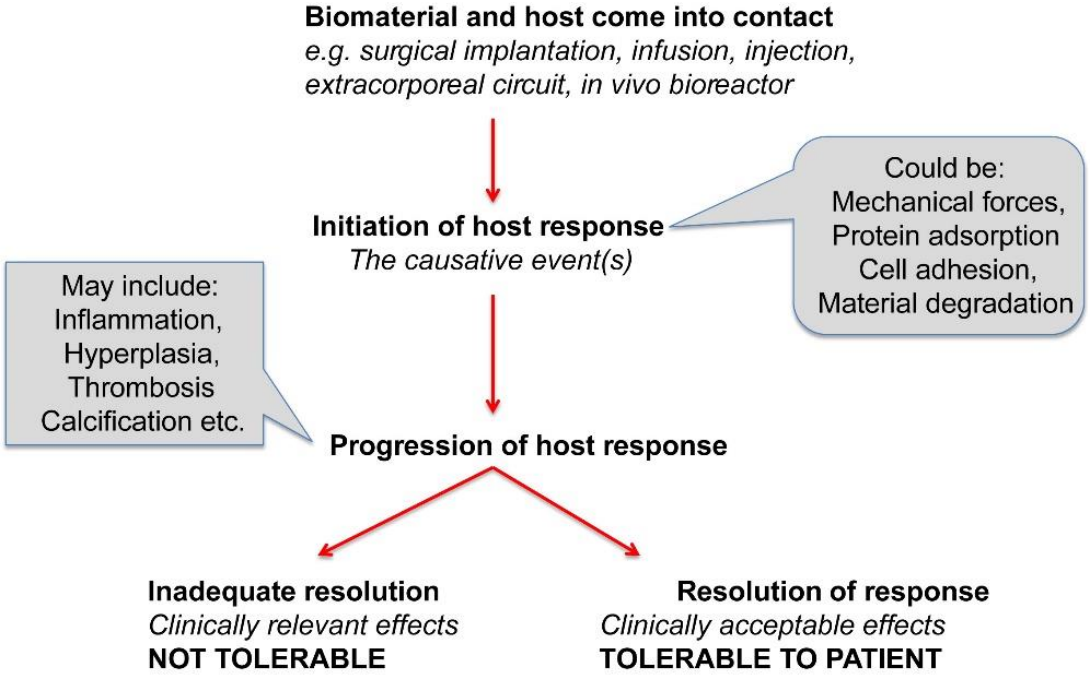

Figure 1: Biocompatibility of medical devices. The contact between biomaterial and host initiates a tissue response. Causative events can be mechanical forces, the adsorption of specific proteins, the adhesion of a broad spectrum of cell types, or the degradation of the material. As the host response progresses, there may be clinically acceptable outcomes associated with medical device tolerance or excessive activation associated with clinically unacceptable symptoms for the patient. Adapted from Williams (2014).[13]

The type of immune response elicited by a certain biomaterial – and thus its biocompatibility – strongly depends on several characteristics of the biomaterial surface like topography, surface energy, charge and wettability (Figure 2).[4,8,14–16] Since these characteristics can often be modulated without impairing the intended function of the medical device, they provide potential cues to direct implant biocompatibility. For the manufacturing of implants, a thorough understanding of the interplay between surface characteristics and immune response is required. However, adjusting more than one of the surface features at the same time can result in combinatorial effects that make predictions about the expected immunological response challenging. As a result, our understanding of surface-related processes is still limited. To gain a better understanding, the influence of each individual surface parameter must be investigated separately. The biological effects of the parameters surface topography and wettability known so far are described in detail in the following sections.

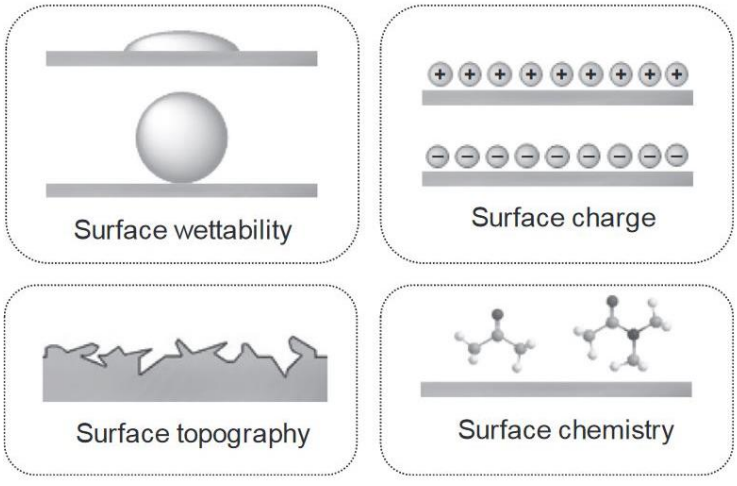

Figure 2: Biomaterial properties with potential influence on the host response. Surface-specific characteristics like wettability, charge, topography and chemistry are known modulators of the immune response towards medical devices. Adopted from Nouri and Wen.[14]

1.1.1 The role of surface topography

Surface topography refers to the three-dimensional structure of a material's surface. Topographical characteristics can be organized, such as pillars, grooves and pores, or they can be randomly dispersed, such as peaks, valleys and cavities. Surface roughness, which pertains to the texture of the uppermost layer of a material and is quantified by measuring protrusions and depressions at the surface, is a common parameter used to describe substrate topography. Common techniques investigating surface roughness include stylus profilometer, atomic force microscopy (AFM), and optical methods like confocal scanning microscropy.[17] The R_a value, which reflects a surface's average roughness in 2D dimension, is the most common roughness parameter in the biomaterial field and will be used in this work as well. However, roughness can also be quantified using a variety of other metrics.

Surface topography of a medical device has far-reaching effects on adhesion, motility, proliferation, differentiation and gene expression of various cellular populations of the host, which all play an essential role in the successful integration, tissue healing and biocompatibility of an implant material.[18,19] As such, implant topography has been shown to influence differentiation and proliferation of osteoblasts. Osteoblasts are crucial regulators of osseointegration, determining the stability of bone implants such as dental implants or hip replacements. It was found that the roughness of biomaterial surfaces impairs osteoblast attachment, proliferation and differentiation, as well as cytokine and growth factor production, thus affecting bone healing and integration of the implant.[20] For bone implants, an increase of surface roughness is generally associated with improved osseointegration and bone regeneration.[21] This was also observed in patients, where titanium specimens of a certain degree of roughness clearly improved bone response and osseointegration of dental implants compared to smooth specimens.[22,23] A further cell population influencing biocompatibility are the fibroblasts. In the context of biomaterials, these cells modulate the deposition of extracellular matrix surrounding the implant side, an effect that, if done excessively, can lead to severe tissue fibrosis.[24] Several studies demonstrated the activity of fibroblasts to be affected by the surface topography of the biomaterial used. Fibroblasts were significantly elongated, adhered more strongly, expressed elevated levels of fibronectin, increased extracellular matrix synthesis and upregulated proliferation when

cultured on grooved or micropatterned surfaces, generally showing increasing activation with decreasing height or size of the topographical features.[25–27] This effect can also be observed in vivo in breast implant recipients where fibroblast activity determines ECM formation and encapsulation of the implant, thus contributing to capsular contracture and fibrosis.[28] Studies investigating the effect of surface topography on capsular contracture in response to breast implants revealed diminished fibroblast activation, suppressed foreign body response and reduced capsule formation on textured silicone surfaces compared to smooth implants.[29,30] These findings highlight the critical role of surface topography in cell–surface interactions. A modification of biomaterial surface topography could be utilized to control the cellular host response to a medical device, and hence implant biocompatibility (see Chapter 4 for the modulation of biomaterials). However, the cellular response to topographical changes is dependent of the cell-type.

The myeloid population of monocytes and macrophages, both representing major players in the host immune response towards biomaterials (see Chapter 1.3), has also been shown to interact with biomaterial topography. It was observed that, in general, macrophages prefer to adhere to rough surfaces rather than flat topographies, independent of the biomaterial substrate.[31] In addition, migration, proliferation, gene expression and secretion of inflammation-inducing or inflammation-dampening cytokines and chemokines are clearly affected by micron-scale topography.[32] However, the effect of individual topographical parameters on the emerging immune response is still not fully understood. While some studies observe an initially increased release of pro-inflammatory cytokines in response to enlarged surface roughness, the effects on individual cytokines and the time point of expression can differ significantly.[33,34] In addition, many in vitro biocompatibility studies focus on cell adhesion but do not address immunological effects. Moreover, studies regarding immunological responses to surface topography are often conducted using cell lines only,[33,35,36] while results with primary immune cells are limited.

1.1.2 The role of surface wettability

Another essential regulator of the host response to medical devices is surface wettability. Wettability is the behaviour of liquids in contact with the surface of solid materials, and is determined by surface tension / energy and a force balance between

adhesive forces between liquid and solid as well as cohesive forces within the liquid.[37] The most common approach to gain insight into the wetting behaviour of a solid material is the contact angle measurement using the sessile drop technique, which quantifies the angle between the tangent of a drop (typically water) at the solid/liquid/gas boundary and the horizontal baseline of the solid surface (Figure 3).[38] Surfaces with water contact angles lower than 90° are designated as hydrophilic, while surfaces with contact angles above 90° are considered hydrophobic. Other surface characteristics like surface roughness and chemical heterogeneity can influence the wettability of a material.

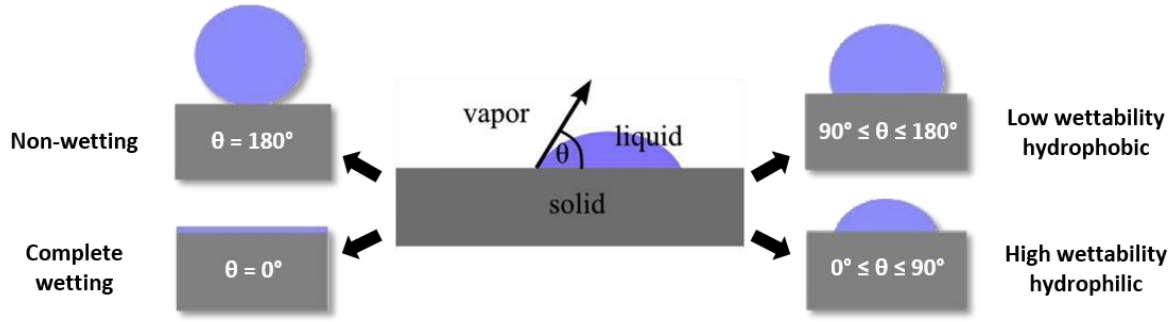

Figure 3: Characterisation of surface wettability. Wettability of a biomaterial is quantified by measurement of the contact angle θ between liquid phase (water droplet), gas phase (usually air), and the solid material. Surfaces with a contact angle above 90° possess low wettability and are considered hydrophobic, while surfaces with a contact angle below 90° possess a high level of wettability and are considered hydrophilic. Adopted and modified from Rupp et al.[38]

Similar to roughness, surface wettability influences the adhesion of osteoblasts,[39] endothelial cells,[40] and fibroblasts.[41] Moreover, especially monocytes and macrophages as essential components of the immune response to biomaterial substrates were discovered to be responsive to variations in surface wettability. This includes changes in adhesion, migration, and polarization of these cells, thus directly affecting biocompatibility.[42,43] In general, hydrophilic surfaces are related with enhanced cell adhesion and anti-inflammatory properties.[44–46] Comprehensive proteomics investigations demonstrated that when macrophages were cultivated on surface-modified polymers with hydrophobic, hydrophilic, and/or neutral chemistries, their protein expression profiles and cytokine/chemokine responses changed.[43] Surface wettability modification, induced by specific treatments or coatings, can thus

be a useful strategy for guiding the immunological activation and the general host response toward a favourable outcome (see Chapter 1.4.2).

However, in the interpretation of their results, many studies on surface wettability relate their findings to alterations of wetting behaviour only, ignoring the fact that the surfaces investigated in the respective studies often differed in terms of topography, chemistry, and other physicochemical variables as well, all of which can influence the immunological outcome in addition. This can lead to contrary findings. While one study on the wettability of silicone lenses found hydrophilic lenses to have beneficial immunological effects and enhance their biocompatibility compared to hydrophobic ones,[47] another study claimed that hydrophilic lenses led to a larger percentage of patients with inflammatory side effects than hydrophobic lenses, thus proposing a higher biocompatibility for the more hydrophobic implants.[48] These apparently contrasting results highlight a common problem in biomaterial-immune interaction research and increase the need for specific investigations to pinpoint immunological effects to surface wettability only.

1.2 Protein adsorption to biomaterial substrates

The host response to specific surface properties is not caused by direct contact between the surrounding cells and the biomaterial, but is mediated by an intermediate factor: the layer of adsorbed proteins on the material's surface. Immediately after implantation, a biomaterial substrate inevitable gets in contact with plasma proteins, interstitial fluids, and proteins of the extracellular matrix. These proteins form a protective coating, surrounding the implant, preventing direct contact between the material and the cells and providing the surface with a new biological identity.[49] Hence, the only surface dependent stimulus available to adherent host cells is the naturally occurring adsorbed protein layer, whose affinity, composition and conformation is dependent upon physico-chemical surface characteristics and the properties of the specific proteins.[50] Understanding the fundamental principles of protein adsorption may allow a more guided protein deposition to influence subsequent biological processes such as cell contact and immune response in vivo.

1.2.1 Surface-dependent adsorption of plasma proteins

Material properties have a considerable impact on the protein layer's composition. Several reviews precisely describe the principles underlying biomaterial-protein interactions.[51–53] In particular, surface energy, polarity, wettability, charge and roughness have been characterized as key determinants of protein absorption. Substrates with more topographical features will expose more surface area for possible interaction with proteins while differences in wettability influence the affinity of individual proteins to a biomaterial. As a consequence, adsorption of plasma proteins such as albumin, fibronectin/fibrinogen, immunoglobulins and others is altered on hydrophobic surfaces compared to hydrophilic substrates.[54] In general, hydrophobic materials are thought to be more protein-adsorbent than hydrophilic materials because of the strong hydrophobic interactions that occur at their surfaces, which results in a gain of entropy in the system.[55,56] In addition to affinity, wettability can also alter the structural confirmation of the adsorbed proteins. Hydrophilic surfaces, for example, are thought to promote protein attachment in its natural state, whereas proteins on hydrophobic surfaces frequently undergo conformational reorientation.[54] As the protein conformation determines which receptor binding sites are available for immune cells like monocytes and macrophages, the conformational state can influence the activation of the surrounding tissue cells (Figure 4).

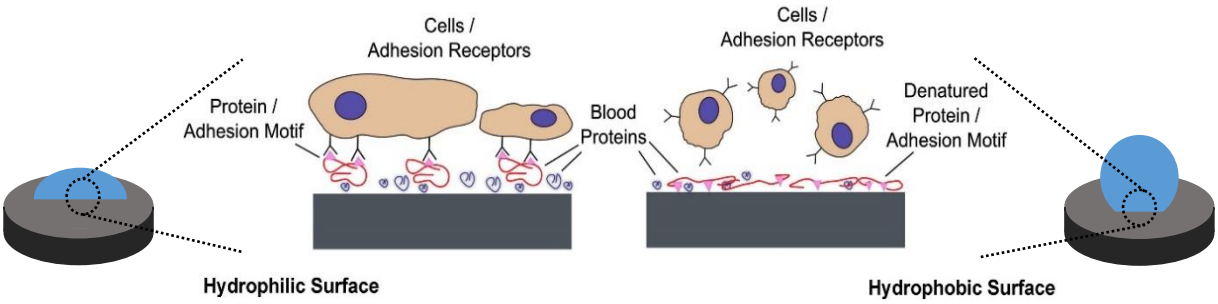

Figure 4: Effect of wettability on protein adsorption and cell adhesion. In contact with blood and biological fluids, hydrophilic surfaces tend to provoke protein adsorption in a conformational state that exposes adhesion motifs and improves cell attachment. Hydrophobic surfaces on the other side can partially denature proteins, making cell-binding sites less accessible and result in decreased cell adhesion. Adopted and modified from Gittens et al.[57]

When studying protein adsorption to a biomaterial surface, it is important to note that the layer of adsorbed proteins is not a static state but a kinetic phenomenon involving a succession of adsorptions and displacement steps until a "steady state" is reached: This is known as the Vroman effect. The effect describes that proteins with a high concentration but a low affinity for a surface are gradually displaced, whereas proteins with a low concentration but a high affinity for a surface might accumulate over time.[58,59] While numerous studies demonstrated surface-dependent effects on individual protein adsorption, only a few had looked at the composition of the protein layer on a biomaterial exposed to the whole spectrum of human serum proteins. However, as proteins can affect each other's adsorption patterns, and due to the Vroman effect, data from studies examining the adsorption kinetics of individual proteins are rarely applicable to the actual situation in vivo. Therefore, it is crucial to investigate adsorption from heterogeneous protein mixtures such as human serum in order to anticipate in vivo adsorption, and thus the biological response to the implant.

1.2.2 Protein-dependent effects on immunological responses

The presence of specific serum proteins on the surface of a biomaterial substrate has a significant impact on the immunological response of the host. As such, adsorbed proteins mediate coagulation, the deposition of proteins of the complement system, and the adhesion of platelets, all affecting the biocompatibility of a device.[54] For the initial immune response, the adhesion rate of immune cells is a critical factor. Cellular adhesion and activation are determined by the presence of adsorbed protein ligands on a surface in conjunction with expressed cellular receptors. These events set the foundation for the further course of the inflammatory response. The presence of specific adhesive proteins affects the adhesion, differentiation and survival of macrophages and the formation of foreign-body giant cells (FBGC); effects which can contribute to the degradation of a material surface.[60–62] Furthermore, protein layer-dependent immune cell adhesion is a decisive factor in the cytokine response and impacts the generation of pro-inflammatory signalling molecules, thus modulating inflammatory and wound healing responses.[63] Due to altered protein binding, hydrophilic surfaces for example were observed to significantly inhibit leukocyte adhesion and macrophage fusion, which resulted in decreased cytokine secretion and attenuated inflammatory reactions.[61,64] These results highlight the importance of protein adsorption in the progression of the host response towards a biomaterial.

However, knowledge about the specific immunological effect of individual proteins adhered to a biomedical substrate is limited to a very small number of human serum proteins. For the bulk of serum compounds, however, effects on immune cells following adsorption onto material surfaces is unknown.

1.3 Immunological response to biomaterials

Classically known for its defence against bacterial and viral infections, the immune system is also activated by foreign bodies such as implanted biomaterials. The processes underlying the immune response to biomaterials are schematically depicted in Figure 5. Upon implantation into the body, the injury through the surgical procedure initiates an inflammatory response. Within nanoseconds after the first contact, blood proteins and coagulation factors adhere to the surface (described in Chapter 1.2) and a provisional matrix is formed. Subsequently, inflammatory cells – predominantly neutrophils and monocytes – migrate towards the implant side, guided by chemoattractants, injured cells, mast cell degranulation, the presence of complement proteins, and autocrine attraction. At the implant site, these cells are responsible for the acute inflammatory response.[4,7] Depending on the foreign material characteristics and the layer of adsorbed proteins, neutrophils and monocytes adhesion and their subsequent cell activation are mediated via integrin receptors.[5] Activated monocytes mature into macrophages and, in synergistic effects with neutrophils, direct the chemotaxis of additional monocytes and macrophages by secreting effective chemoattractants and inflammatory cytokines like IL-6, IL-8, MCP-1 or MIP-1β (see Table 1 for a list of essential pro- and anti-inflammatory cytokines).[43,65] These cytokines and chemokines characterise the initial inflammatory response and are therefore frequently used as read out parameters in experimental and clinical research. Circulating monocytes are attracted by these chemoattractants, become activated and differentiate into pro-inflammatory macrophages (M1-like). Both myeloid cell types have the ability to initiate subsequent inflammatory responses such as the activation of the adaptive immune system by recruiting B and T cells from the blood by producing additional immunomodulating cytokines. The interaction between activated macrophages and lymphoid cells is an important regulator in immune response progression that should not be overlooked.[66]

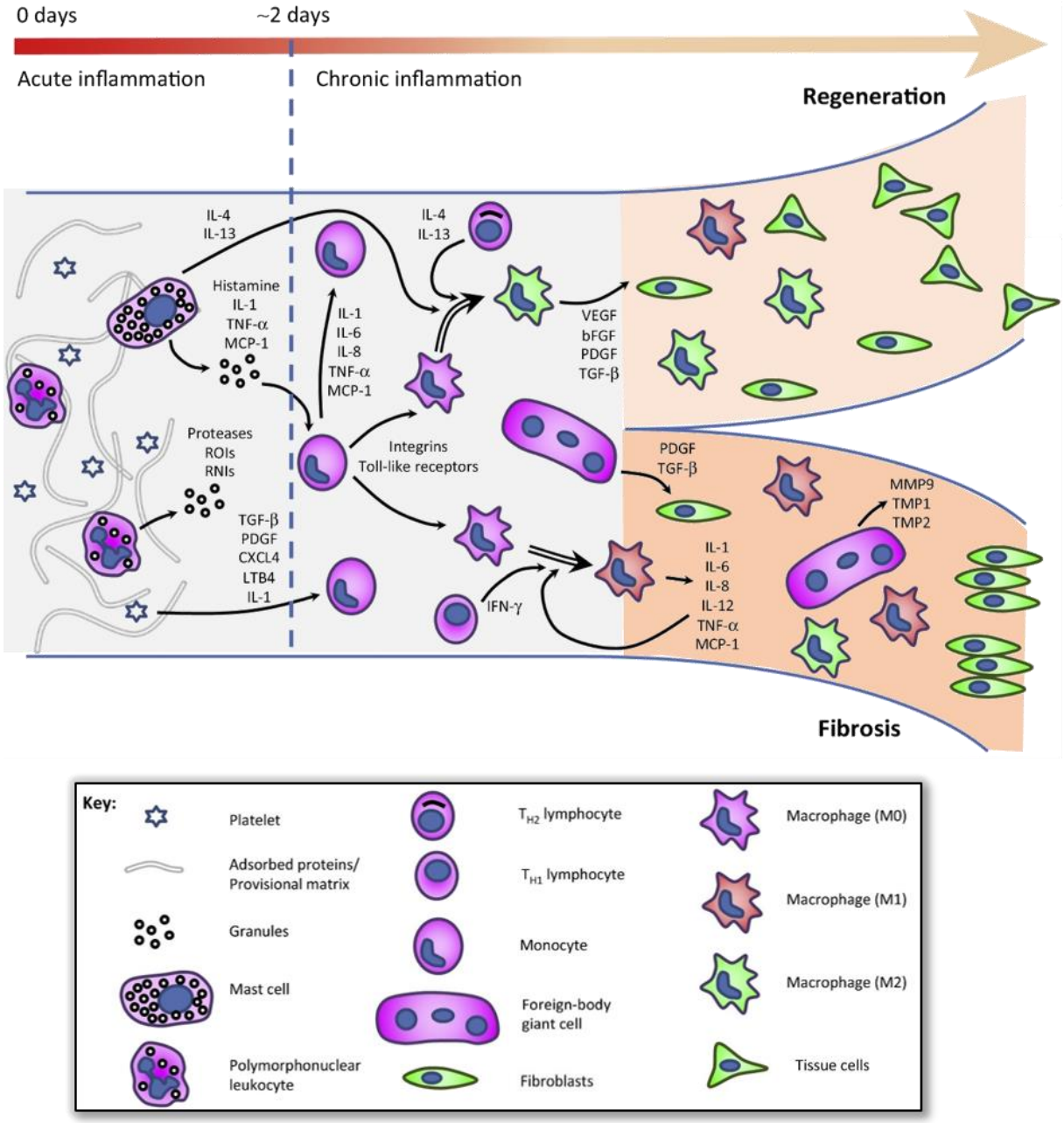

Figure 5: Overview of the immunological response to biomaterials over time. Implantation of a biomaterial triggers an acute inflammatory response, which is mediated by adsorbed proteins, platelet adhesion, mast cells, and polymorphonuclear leukocytes like neutrophils. Mononuclear cells are recruited by chemokines and growth factors. Activated inflammation-inducing M1-like macrophages, FBGCs, and T_{H1} lymphocytes can all contribute to a persistent state of inflammation, promoting tissue fibrosis and implant rejection. Based on beneficial material properties and other factors, the initial inflammation can also be followed by the secretion of immune-dampening stimuli and macrophage polarisation to a pro-healing phenotype (M2-like), inducing successful tissue regeneration. Adopted from Vishwakarma et al.[9]

These initial immunological responses can be observed in a similar way for most biomaterials. However, they do not represent the end of the immunological activity and can continue in a variety of ways. Following the initial inflammatory phase, the accumulation of large numbers of activated macrophages on the surface can lead to macrophage fusion, which results in the formation of FBGCs, a hallmark of chronic inflammation. FBGCs can release mediators of degradation such as reactive oxygen intermediates and degradative enzymes.[4] Together with further inflammatory signals from macrophages of a pro-inflammatory phenotype, this can develop into a phase of chronic inflammation and can finally promote the formation of fibrotic tissue.[5] However, the initial inflammatory phase does not necessarily have to progress to a chronic state. Beneficial material properties, the stimulatory activities of specific T cells, and other factors can all contribute to a reduction in the inflammatory response in its early phase. The release of anti-inflammatory cytokines like IL-4 and VEGF can result in the formation of pro-healing macrophages (M2), which can dampen the immune response and can lead to effective tissue regeneration.[4,5] The decision whether the initial inflammation resolves or persists as a chronic inflammation is determined by a variety of material-related parameters (see Chapters 1.1 and 1.2) and the cellular response. At the cellular level, the population of monocytes/macrophages plays a key role in this process due to their multifaceted reactions. Depending on their polarisation and activation state, they can either promote inflammatory effects like pro-inflammatory cytokine secretion and activation of additional immune cells, or induce inflammation-dampening effects like secretion of anti-inflammatory cytokines, improved bone regeneration or enhanced wound healing, thereby significantly influencing biocompatibility.[67,68] While the general concepts of the immune response are relatively well established, the precise effects of individual material characteristics and the specific interplay of the diverse sets of immune cell populations after contact with biomaterials are often still unknown.

Cytokine	Full name	Function	References
IL-1β	Interleukin 1β	Important mediator of the inflammatory response. Involved in a variety of cellular activities, including cell proliferation, differentiation, and apoptosis. Triggers secretion of IL-6 and IL-8. Produced by activated macrophages.	69,70
IL-6	Interleukin 6	Central role in activating and maintaining the inflammatory response. Promotes lymphocyte and monocyte differentiation. Anti-inflammatory effects by reducing neutrophil recruitment.	71–73
IL-8	Interleukin 8	Key mediator of the inflammatory response. Involved in acute inflammation. Induces neutrophil recruitment. Can be produced by every cell with a Toll-like receptor.	74–76

MCP-1	Monocyte chemo-attractant protein 1	Promotes inflammatory effects. Key chemokine regulating migration and infiltration of monocytes, T cells and NK cells. Potent factor in the polarisation of T cells. Secreted by monocytes, macrophages and dendritic cells.	77
MIP-1β	Macrophage inflam-matory protein 1β	Chemoattractant for NK cells, monocytes and lymphocytes. Enhances local inflammatory response. Produced by monocytes/macrophages but also other immune cells.	78
TNF-α	Tumour necrosis factor α	Inflammatory cytokine. Mediation of cell survival and pro-inflammatory response. Produced by macrophages/monocytes and T cells during acute inflammation.	79,80
IL-4	Interleukin 4	Anti-inflammatory cytokine. Diminishes inflammatory responses. Regulates cell proliferation, apoptosis, and gene expression of lymphocytes and macrophages. Mainly produced by activated T cells.	81,82
IL-10	Interleukin 10	Anti-inflammatory cytokine. Prevents release of IL-8 and TNF-α. Inhibits activation and differentiation of T cells, B cells, NK cells, and granulocytes. Promotes differentiation of regulatory T cells. Produced by almost all types of leukocytes.	83,84
VEGF	Vascular endothelial growth factor	Promotes wound healing. Key regulator of angiogenesis.	85

Table 1: Overview of important cytokines / chemokines and their function in the immune response to biomaterials. IL-4 and IL-10: anti-inflammatory cytokines. VEGF: wound healing marker. All remaining cytokines mediate pro-inflammatory effects.

1.3.1 Adverse effects of an excessive immune response

Neutrophil activity, monocyte/macrophage polarization, and lymphocyte differentiation into specific phenotypes can all directly affect the biocompatibility of a medical device. Excessive inflammatory activation (also known as foreign body reaction/response) can impair healing, promote tissue loss, induce fibrotic encapsulation, or even cause the medical device to be rejected. This excessive activation can occur regardless of the kind of biomaterial or the site of implantation. Patients with dental implants, for example, are frequently affected by peri-implantitis, a pathologic condition characterized by persistent excessive inflammation of the peri-implant tissue, which leads to progressive loss of supporting bone and, if left untreated, can cause implant loosening.[86] Excessive inflammation can also be a severe side effect of other medical devices that are implanted in the bone. As a result of a persistent inflammatory condition, increasing osteolysis can cause implant loosening 10 to 20 years following total hip arthroplasty, resulting in a complete loss of implant functionality.[87] This condition, known as aseptic loosening, is responsible for more than 70% of hip revisions, which entails an additional health burden for the patient.[88] Aseptic loosening, which is frequently induced by the presence of wear particles, is initiated by the cellular

response of monocytes and macrophages and involves the release of substantial amounts of osteoclastogenic and inflammatory cytokines. This activation results in increased osteoclast recruitment and activity around bone-implant interfaces, leading to osteolysis and implant instability.[89]

Excessive immunological activity might also lead to complications in other regions of the body, such as soft tissue. The most prevalent failures in female breast replacement are fibrotic encapsulation and capsular contracture formed around silicone implants. Histological studies have shown that increased capsular thickness is mainly found in patients with a severe inflammatory reaction at the implant side.[90] Patients with this finding also have a higher frequency of clinical symptoms. In general, the host's inflammatory response to the material is the primary driver of implant biocompatibility and the development of patient side effects for all types of medical implants. The magnitude of the inflammatory reaction has a significant impact on implant integration and performance. Further research regarding the modulation of material biocompatibility is required to reduce the risk of an excessive pro-inflammatory response.

1.3.2 Immune cell populations and the PBMC in vitro model

The immune response to biomaterial implants, as discussed in Chapter 1.3, is a well-coordinated process involving many distinct types of immune cell players. Thus, comprehensive in vitro studies on the biomaterial-host interaction require the use of complex models that encompass a wide spectrum of immune cell types. Peripheral blood mononuclear cells (PBMCs) are a type of immune cell suspension that includes myeloid cells (monocytes and macrophages), lymphocytes (T cells and B cells), dendritic cells, and natural killer (NK) cells. The PBMC cell suspension, which can be extracted directly from human blood using density gradient centrifugation, serves as a useful model to explore complex immunological interactions. Besides of its complexity, another advantage of the PBMC model is that it contains primary cells, as opposed to widely used cell line models. As shown in several studies, the choice of cellular model can impair the immunological outcomes. Comparisons between primary PBMC-derived monocytes and THP-1 cell line monocytes revealed differences in gene expression and cytokine secretion.[91,92] Thus, it is thought that the use of primary cells such as those in the PBMC model more closely resembles the in vivo situation.

1.4 Modulation of biomaterials for targeted application

The more we know about the interactions between material properties, immune response and tissue sensitivity, the more efforts are made to therapeutically improve the biocompatibility of medical devices. Turning away from designing ‘biologically inert’ biomaterials, the major goal today is the engineering of ‘immune interactive’ surfaces that harness the therapeutic effects of modifying the inflammatory response towards healing and regeneration.[93,94] Various strategies are currently developed to modulate the immune response in a passive way, for example by specific surface treatments or the application of coatings of organic or inorganic origin (Figure 6). These modulations of biomaterial surface properties often aim at limiting macrophage activation and fusion to FBGCs. Attempts are also undertaken to actively mitigate cell behaviour by the release of bioactive agents and pharmaceuticals at the implant side, either by application as a coating or by delayed release in degradable devices.[9] All strategies require a precise understanding of the effect of specific surface parameters for effective targeted modulation.

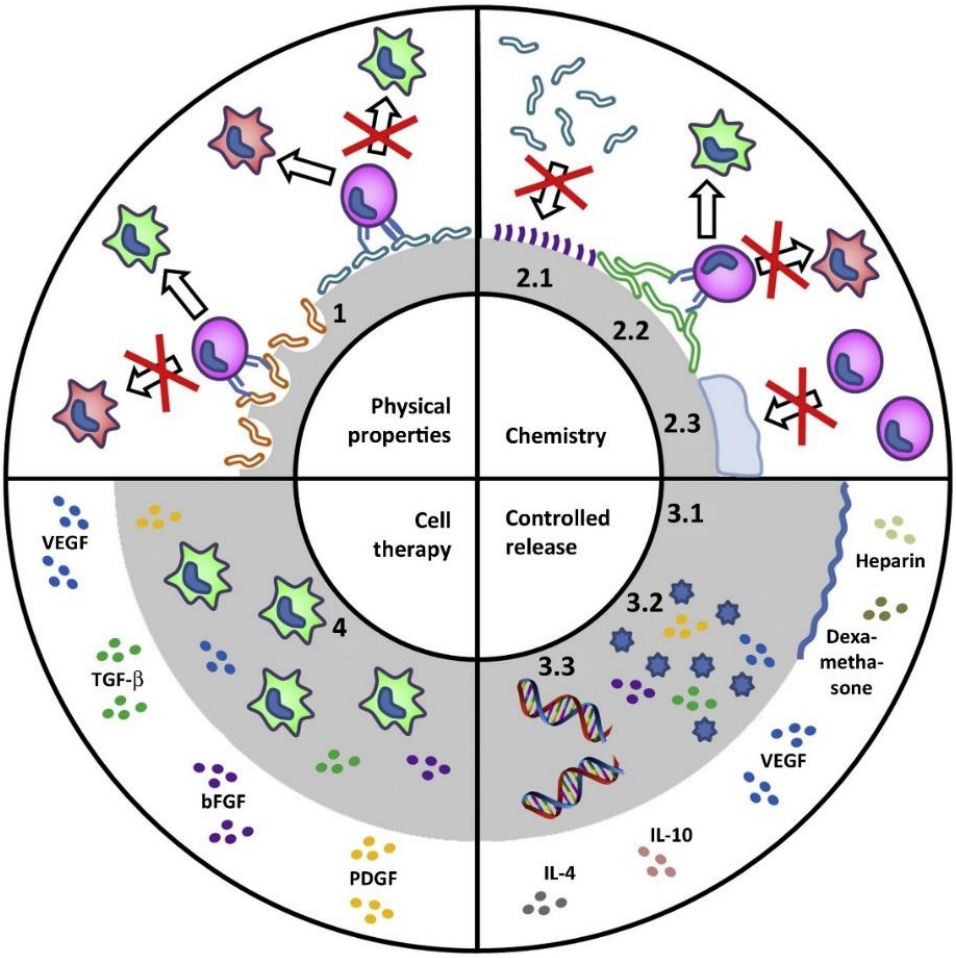

Figure 6: Schematic view of possible strategies for targeted modulation of biomaterials. Activity of immune cell populations in response to biomaterials can be mitigated in different ways. (1) Changes in physical properties such as topography and wettability modulate protein adhesion and thus polarisation of macrophages. The use of non-biofouling coatings to prevent protein adhesion (2.1), the deposition of biomimetic extracellular matrix components to disturb M1 activation of macrophages (2.2) and the application of hydrogels to prevent biomaterial-immune cell interaction (2.3) are approaches to alter the surface chemistry. Surfaces can also actively modulate immunological processes by the controlled release of anti-inflammatory agents through specific coatings (3.1) and embedded particles (3.2) or gene delivery systems (3.3). The use of embedded immune cells – although not widely applied yet – is another option for targeted modulation (4). Adapted from Vishwakarma et al.[9]

1.4.1 Surface treatments

As shown in chapters 1.1.1 and 1.1.2, surface properties have a significant impact on the nascent immune response. Depending on the nature of the material used, surface properties can be intentionally modified by a variety of techniques. This enables a more in-depth analysis of the link between the material surface and the immune system in experimental setups, and is a current strategy to alter the immune response of implants to improve clinical application. Mechanical surface treatments such as acid etching or sandblasting for example can be used to modify physicochemical features. These approaches increase the roughness of metallic surfaces, which has been linked to altered cellular adhesion of osteoblasts, endothelial cells and fibroblasts compared to smooth or polished surfaces.[95–97] Imprinting of structures on polymers using lithographic methods is another treatment to induce topographical alteration, which was shown to impair macrophage adhesion and morphology.[34] Besides of topography-modulating treatments, chemical modifications can be used to alter immune cell activity by changing surface energy and wettability of devices. Depending on type and surface, plasma treatment was observed to promote M1-like or M2-like macrophage differentiation.[98,99] Similarly, chemical modification using photograft copolymerisation can be used to alter the immune response of monocytes and macrophages.[100] These relatively simple techniques are representatives of the large spectrum of biomaterial treatments, and their immunological effects are further characterized in Chapter 3.

1.4.2 Surface coatings

The use of specific surface coatings is another method for altering surface characteristics and modulating the immune response to biomaterials. A passive approach is the use of non-fouling biological coatings like low-inflammatory proteins, polymeric films or hydrogels that can be used to prevent protein adsorption and corresponding downstream inflammatory responses. As such, semipermeable hydrogel surface coatings were able to diminish fibrinogen adsorption and human macrophage adhesion in vitro while also attenuating acute phase leukocyte adhesion and pro-inflammatory cytokine response in vivo.[101] Other passive coating strategies use the structure of the extracellular matrix (ECM) as a model, since coatings that mimic or directly use ECM components can generate a microenvironment that promotes natural wound healing and repair mechanisms. The presence of hyaluronan at the biomaterial surface, for example, can significantly reduce chronic M1 activation of macrophages and even stimulate M2-related cytokine release.[102]

A promising candidate for the targeted modulation of biocompatibility are coatings composing of polyelectrolyte multilayers (PEMs). Two types of alternatively charged polyelectrolytes can be sequentially deposited on biomaterial surfaces, where they self-assemble and form thin polymer film coatings due to the electrostatic interactions between the cationic and anionic charged polyelectrolytes.[103] To assemble PEMs, virtually any combination of cationic and anionic polyelectrolytes from synthetic and naturally occurring polymers can be employed. Due to their versatile nature, PEM coatings provide a powerful tool to modulate cell adhesion and host response. Being deposable on nearly any type of implant independent of biomaterial characteristics, PEMs have been found to change protein adsorption to biomaterial substrates[104] and modulate the surface adhesion, cellular differentiation and viability of monocytes,[105] fibroblasts,[106] endothelial cells[107] and osteoblast-like cells.[108] As a result, PEM coatings possess the ability of regulating the inflammatory response, paving the way for tissue engineering applications. A significant benefit of PEMs is the easy and precise adjustment of their physico-chemical surface properties by the choice of polyelectrolyte substrate and the pH of the assembly solution.[109] This can be used to impart specific surface properties to biomaterials in order to guide the immune response in a desired direction (Figure 7). Due to their ability of targeted modification, PEM coatings could

also prove to be a suitable tool to identify key effectors of biocompatibility. Their ability to specifically alter surface properties was used in this work to explore the influence of wettability on the adsorption of serum proteins and the elicited immune response, integrating three important parameters affecting implant biocompatibility.

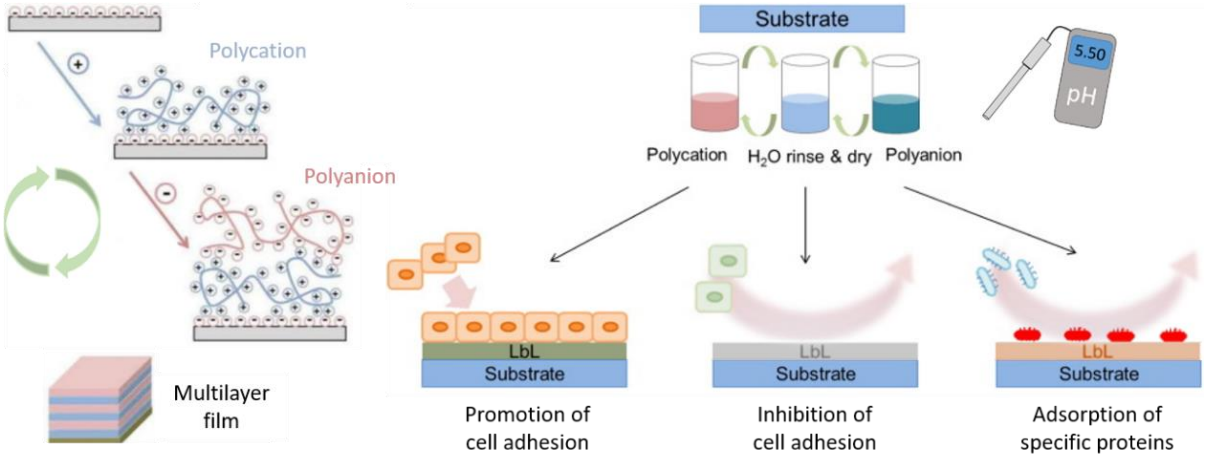

Figure 7: Schematic overview of the generation and application of PEMs. PEM coatings are generated by the alternating deposition of cationic and anionic polyelectrolytes (see left side). By choice of polyelectrolyte substrates and adjustment of the pH of the assembly solution, coatings of different surface properties can be created. As such, different PEMs can promote or inhibit the adhesion of specific cell types and influence the adsorption of specific proteins. Graphic adapted and modified from Criado-Gonzalez et al. and Guo et al.[110,111]

Chapter 2

Objectives of the thesis

2 Objectives of the thesis

The aim of this thesis was the development of a fundamental understanding of immune responses to biomaterial surfaces in the context of different classes of medical implant devices. The influence of surface characteristics, the role of adsorbed proteins, and the specific response of individual immune cell populations were all given significant attention. To accomplish this, the effects of biomaterials on both innate and adaptive immune responses, as well as material surface properties and the composition of the adsorbed layer of proteins were thoroughly investigated. This information was aimed to provide information to allow the rational modulation of immune response through the design of biomaterial, and hence provide a mechanism to modulate material biocompatibility in a targeted and precise manner.

The aim of the first study was to assess the immune response to clinically-used materials and identify key cell populations involved in the inflammatory response. To achieve this, five differently treated titanium surfaces, which differed in surface wettability, chemistry, and roughness, were investigated. The immune response was assessed by quantifying the secretion of pro- and anti-inflammatory cytokines using multiplexed bead-based sandwich immunoassays and by examining the expression of specific surface markers of cellular activation and differentiation using flow cytometry. The role of individual immune cell populations was identified by culturing cells separately and in defined ratios on the titanium surfaces. The information collected was placed in the context of the materials' clinical performance to develop an understanding of the connection between observed immune responses in vitro and performance in vivo and the contributing role of specific immune cell populations.

The second study aimed to systematically investigate the effect of surface topography on the cellular response. To elucidate if surface roughness alone could be a decisive factor determining biocompatibility, eight specimens of medical grade polyurethane with varying degree of roughness were compared regarding their effect on macrophage polarisation, inflammatory cytokine secretion, and surface marker expression. For the analysis, the immune response in three biological test systems of varying complexity was evaluated to test the sensitivity of different in vitro models towards topographical variations.

The third study sought to elucidate the relationship between varying levels of wettability and the ensuing protein adsorption at the material surface, as well as between the presence of certain proteins on a biomaterial surface and the resulting immune response. For this approach, three polyelectrolyte multilayer coatings with varying degrees of wettability were created and their surface properties as well as their immunological activity were quantified. Mass spectrometry was used to study the composition of the adsorbed protein layer, and the presence of particular types of proteins was linked to different immunological responses. Furthermore, changes in the expression of intracellular signalling pathways were evaluated and compared to the reported immune response using DigiWest analysis.

The knowledge gained from this work was aimed to contribute to improve the design of immunomodulatory materials in biomedicine and facilitate the development of material concepts for biomedical applications.

Chapter 3

Results I:

Defining the role of different immune cell populations

The contents of this chapter are based on:

Billing F., et al. The immune response to the SLActive titanium dental implant surface in vitro is predominantly driven by innate immune cells. *Journal of Immunology and Regenerative Medicine, Volume 13, 2021*

3 Results I: Defining the role of different immune cell populations

The type of response by the immune cells found at the cellular-material interface is a decisive factor for implant biocompatibility.[4] Besides neutrophils, the first cells that encounter biomaterial surfaces in the body are monocytes. Following biomaterial implantation, these innate immune cells have the ability to encourage the migration and differentiation of other types of immune cells by releasing chemoattractants and inflammatory cytokines in response to biomaterial properties, thus initiating a pro-inflammatory response and promoting the differentiation into pro-inflammatory macrophages (M1-like).[112] On the other hand, monocytes also play an important role in the resolution of inflammation and wound healing by maturating into anti-inflammatory macrophages (M2-like).[113] Which effects predominate in the long term is largely affected by the biomaterial surface properties, which determine the polarisation of the monocytes.[114,115] Besides of innate cells, adaptive immune cells like lymphocytes are also reported to influence the immune response to biomaterials. As such, it was demonstrated that lymphocyte populations can regulate monocyte adherence to biomaterial substrates and that innate and adaptive immune cells are able to influence each other bidirectionally.[116,117] Thus, lymphocytes could be crucial cellular determinants of biocompatible outcomes, with their response also being influenced by biomaterial surface characteristics.[66,118]

However, the understanding of the possible interactions between different immune cell populations is still limited in the context of biomaterials. To evaluate the role of innate and adaptive cell populations in the initial phase of biomaterial-induced immune responses, the biologically complex patient-derived PBMC model was employed. The aim of this study was the identification of key cellular populations responsible for driving the immune response within the heterogeneous collection of cells found in the PBMC model, namely monocytes, natural killer cells, helper T cells and cytotoxic T cells. Clinically used titanium dental implant materials with different surface modifications served as substrates. First, the surface characteristics roughness, wettability and chemistry of a set of five unique titanium specimens were assessed using confocal scanning microscopy, water contact angle measurement, and X-ray photoelectron spectroscopy (XPS). Luminex-based cytokine immunoassays and flow cytometry were employed to quantify the induced immunological response. To evaluate the extent to

which lymphocyte populations are involved in the immunological response, monocytes were isolated from whole PBMC and cultured in isolation or combined with lymphocytes at set ratios of varied monocyte levels on the titanium biomaterial. Cell specific cytokine production as well as surface marker expression were compared in monocyte and lymphocyte populations (Figure 8).

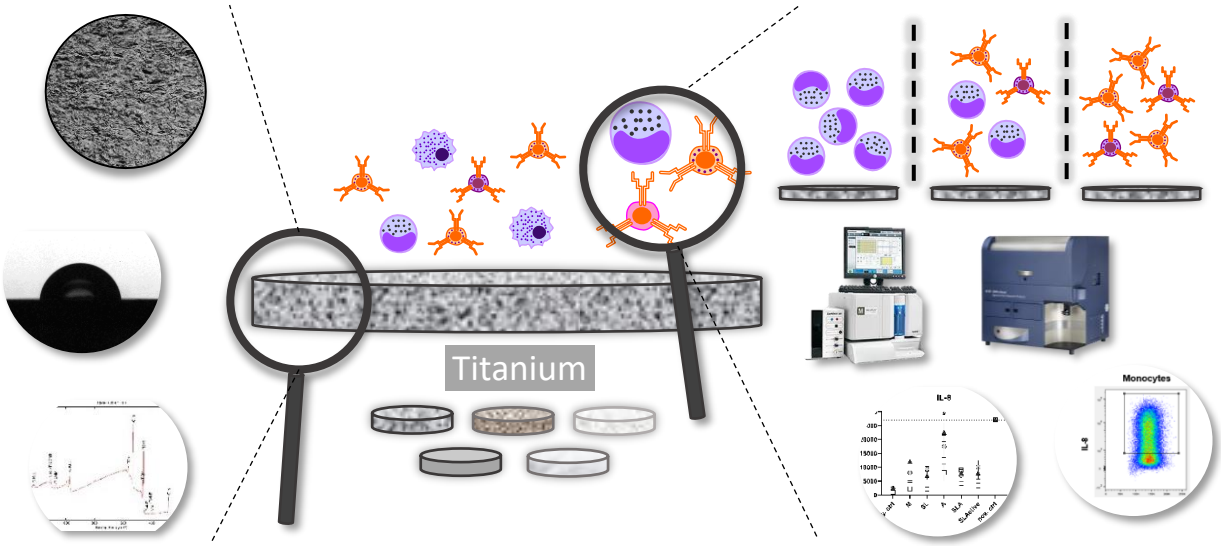

Figure 8: Investigation of the immune response to titanium biomaterials and the role of individual immune cell populations. Five differently treated titanium specimens were analysed regarding biomaterial properties (left side) and elicited immune response (right side) to link surface characteristics with immunological effects. Culturing of cellular subsets alone and at defined ratios was furthermore used to investigate the specific role of individual immune cell populations in the response to biomaterials.

3.1 Surface characteristics of clinically-used titanium dental implants

In this study, five titanium grade 2 titanium implant materials (all provided by Straumann AG, Basel, Switzerland) were investigated. During the manufacturing procedure, their surfaces have been (1) machine polished (2) acid etched (3) sandblasted (4) sandblasted and acid etched (SLA) and (5) sandblasted and acid etched including a hydrophilic treatment (SLActive). While all specimens that have been sandblasted showed a high surface roughness with an S_a value (mean arithmetic height of the surface area) of around 3.3 µm, machine polished and acid etched samples were rather smooth ($S_a \leq 0.6$ µm) (Billing F. et al., **Appendix I**, Suppl. Table 1). SLActive surface was extremely hydrophilic (contact angle below the quantification

limit of 10°), while the other surfaces showed medium (contact angle ~ 75°: machine polished; sandblasted) or high levels of hydrophobicity (contact angle ≥ 90°: acid etched; sandblasted and acid etched). XPS analysis revealed similar chemical composition between acid etched + sandblasted and acid etched surfaces.

3.2 Immune responses towards surface-treated titanium dental implants

Potential differences in the immune response to the five titanium specimens were investigated by culturing PBMCs directly on the biomaterial surfaces. For most of the analysed markers, the smooth and hydrophobic acid etched surface was found to elicit the highest release of pro-inflammatory cytokines (Billing F. et al., **Appendix I**, Suppl. Fig. 2). In contrast, the rough and medium hydrophobic sandblasted specimen resulted in the lowest level of cytokine release, thus indicating a contribution of roughness and hydrophobicity to the immunological response. Immune responses towards the remaining specimens were somewhere between. Interestingly, the specimen created by combining sandblasting and acid etching revealed very low pro-inflammatory activity as well, implying that the immunological response might depend rather on the high roughness created by the sandblasting procedure then on the pits being caused by acid etching. The very hydrophilic and rough SLActive surface was found to induce significantly lower levels of pro-inflammatory cytokines IL-6 and IL-8, as well as higher levels of the anti-inflammatory cytokine IL-10. For other cytokines studied, this trend was less obvious. Overall, the findings indicate that roughness within the investigated range may have an effect on immunological response, whereas wettability may also play a role. Because of the beneficial immunomodulating properties demonstrated here and its long and successful history as a clinical dental implant,[119–121] the SLActive surface was shifted into focus to explore the involvement of individual immune cell types in the immune response in the following.

3.3 The role of innate and adaptive immune cells

To investigate the contribution of innate and adaptive immune cells, the expression of cell surface molecules was assessed on the major types of immune cells. The population of monocytes responded with a significantly higher expression of activation markers HLA-DR (compared to the acid etched surface) and CD16 (compared to all other surfaces tested) on the SLActive surface (Billing F. et al., **Appendix I**, Suppl. Fig. 3). From the literature it is known that the presence of IL-10 promotes the expression

of the anti-inflammatory marker CD163 on monocytes.[122] In line with this, increased IL-10 levels were found to be accompanied by enhanced CD163 expression on monocytes after cultivation on the SLActive surface (Billing F. et al., **Appendix I**, Suppl. Fig. 3). Other innate immune populations, such as NK cells, did not differ significantly between the titanium samples. Adaptive immune cells such as helper T cells (T_h cells) and cytotoxic T cells (T_c cells) showed slightly increased frequencies of cells expressing HLA-DR and an enhanced signal for CD16 in response to SLActive titanium. Analysing intracellular cytokine expression in both innate and adaptive immune cells revealed that the vast majority of IL-8 and TNF-producing cells were innate monocytes, with only a small number of adaptive lymphocytes expressing these cytokines. (Billing F. et al., **Appendix I**, Suppl. Fig. 6A). As cytokine production and surface marker expression are both dynamic processes, the timing of testing can have an impact on the results. Thus, cytokine production and surface molecule expression were examined over time. While cytokine response in monocytes was immediate and peaked during the first 12 h of biomaterial contact, the expression of the antigen presentation molecule HLA-DR and the co-stimulatory molecule CD86 on the cell surface increased only after 72 h of cultivation (Billing F. et al., **Appendix I**, Suppl. Fig. 6C and D). These data suggest that in regular PBMC cultures, monocytes play a larger role and respond more quickly to titanium dental implant surfaces, while adaptive immune cells/lymphocytes appear to play a diminished role.

To further investigate the role of lymphocytes in the immune response, monocytes were isolated from the PBMC suspension using magnetic cell sorting and cultured in isolation or in set ratios with lymphocytes on SLActive titanium biomaterial. Cultures of pure monocytes were found to result in the highest concentration of pro- and anti-inflammatory cytokines, while pure lymphocyte cultures elicited the lowest secretion of these cytokines, approaching the lower limit of detection (Billing F. et al., **Appendix I**, Suppl. Fig. 4). Thus, when cultured separately, lymphocytes seem to be unaffected by the SLActive biomaterial. To investigate the potential contribution of lymphocytes to cytokine secretion in mutual interaction with monocytes, the levels of cytokine and surface marker expression in a pure monocyte culture were compared to a mixed culture containing the same absolute number of monocytes but lymphocytes in addition. Cultivation on the SLActive titanium surface revealed that cytokine concentrations (IL-8, TNF-α, IL-6 and IL-1β) and expression of monocyte surface

markers (CD16, CD86, and CD163) were unaffected by the presence of lymphocytes (Billing F. et al., **Appendix I**, Suppl. Fig. 4 and 5). In exception, expression of the antigen presentation molecule HLA-DR on monocytes was slightly elevated with high numbers of lymphocytes being present in the culture. Notably, when substantial numbers of monocytes were present, there was an increase in CD16 expression and an increase in the frequency of HLA-DR positive cells on T_h and T_c cells, indicating a general responsiveness of these populations to monocyte-derived stimuli. However, no effects of mutual activation were seen testing physiological ratios of monocytes and lymphocytes.

This work demonstrated that differential immune responses occur to differently treated titanium biomaterials in terms of pro- and anti-inflammatory cytokines and cell surface proteins. More broadly, this work indicates the importance of surface properties such as topography, chemistry, and wettability on the immune response. Cells of the innate immune system (monocytes) were found to be the predominant population driving the immune response towards the commonly-used SLActive titanium surface, while cells of the adaptive immune system were neither capable of reacting to the biomaterial nor influencing the cytokine response or surface marker expression of the innate immune system. Activation of the adaptive by the innate immune system was observed for cell surface markers, but under artificially increased numbers of monocytes only. These results imply that in the development of new surfaces the response of monocytes/macrophages should be the primary consideration.

Chapter 4

Results II:

Systematic investigation of biomaterial surface roughness

The contents of this chapter are based on:

Segan S., Jakobi M., Khokhani P., Klimosch S., **Billing F.** et al. Systematic Investigation of Polyurethane Biomaterial Surface Roughness on Human Immune Responses in vitro. *BioMed Research International, Volume 2020*

4 Results II: Systematic investigation of biomaterial surface roughness

The immune system is the first site of biological interaction between the body and the implant after protein adsorption to the implant surface and a key factor in the biological integration.[7,123] It is involved in inflammatory processes and the foreign body reaction, but is also essential for biological processes enhancing biomaterial integration, such as wound healing and osseointegration.[4,7] To selectively guide the immune response in a desired way, the topographical structure of a biomaterial might be a powerful tool. Topographic features like microstructures and surface roughness can direct migration and proliferation of osteoblasts, drive activation and differentiation of macrophages, modulate cell morphology, promote osseointegration, and alter healing.[15,16,124–128] Thus, the topography of a biomaterial can be an important parameter affecting the immune response to implant surfaces. However, existing studies often rely on different experimental concepts regarding cellular models, interspecies differences, or readout parameters. In addition, systematic studies examining the effect of this single parameter in a complex human-derived immunological setting are lacking.

The aim of this study was to evaluate if surface roughness alone could be a decisive factor in determining the immune response to biomaterials. Therefore, three in vitro models of the human immune system of varying biological complexity were applied: (1) the widely used THP-1-derived model using a macrophage cell line as a system of reduced complexity, (2) the multifaceted PBMC model using primary immune cells isolated from human blood and (3) a whole blood model culturing the biomaterial directly in isolated human blood. Medical grade polyurethane (Pellethane® 2363-75D) was chosen as biomaterial substrate. Polyurethane is a polymeric material that is widely used in medical devices like breast implants, dermal scaffolds, bone and tissue engineering, as well as other applications due to its high level of biocompatibility.[129–133] The influence of the single parameter surface topography on the immune response was specifically examined by generating polyurethane samples with graded roughness in eight distinct levels (S_a = 0.3 – 19 µm; with S_a indicating the mean arithmetic height of the surface area) (Figure 9).

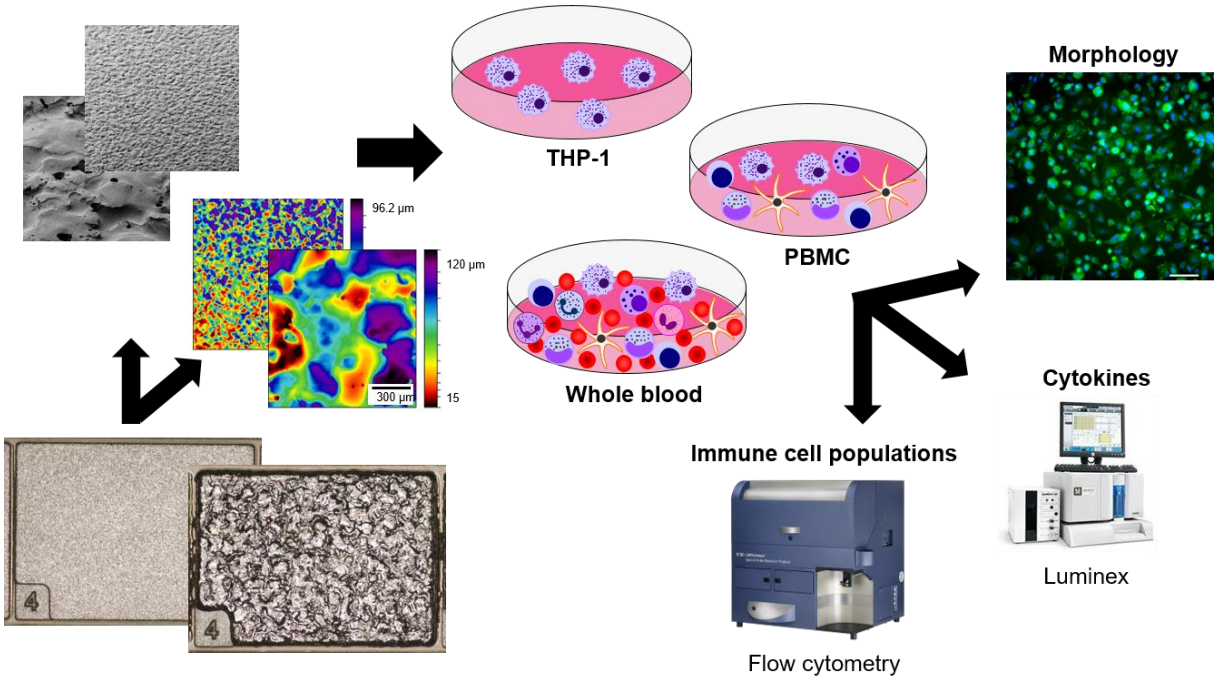

Figure 9: Systematic investigation of biomaterial surface roughness. Surface properties of eight polyurethane samples with defined roughness grades (VDI 0 – VDI 45) were analysed using SEM and confocal scanning microscopy. Three different culturing models of increasing biological complexity (THP-1 cell line, PBMC, whole blood) were used to investigate the immunological response towards the polyurethane surfaces. As readout parameters, morphological differentiation, secretion of immunomodulatory cytokines, and surface marker expression of distinct immune cell populations were assessed.

4.1 Creation and characterization of polyurethane samples

Injection moulding was used to create polyurethane samples with eight distinct roughness grades according to the VDI 3400 industrial standard, ranging from VDI 0 (“flat” with no deliberate surface roughness) to VDI 45 (roughest surface investigated). To ensure that the polyurethane samples exhibited the intended surface characteristics, confocal scanning microscopy and SEM imaging were applied. Analysis showed a clear correlation between increasing VDI number and greater surface roughness, with a uniform distribution across the samples surface (Segan S. et al., **Appendix II**, Suppl. Fig. 1 and 2). Contact angle analysis showed polyurethane to be a hydrophobic material with no effect of surface topography on material wettability (Segan S. et al., **Appendix II**, Suppl. Fig. 3).

4.2 Cellular responses to polyurethane surface topography

THP-1 macrophage model

To investigate the biological response towards the different levels of surface roughness, THP-1-derived macrophages were cultured for 72 hours on the polyurethane specimens. The morphology (cell area, cell shape factor, and cell elongation factor) of cultured cells was analysed to distinguish between macrophages with pro-inflammatory M1-like or anti-inflammatory M2-like phenotypes. Cells that had been chemically stimulated into the M1 or M2 phenotypes were used as controls. THP-1-derived macrophages were shown to be more dispersed and cover a larger area on the two roughest polyurethane samples compared to the smoother samples, whereas cell circularity and elongation appeared to be unaffected by the degree of surface roughness. (Segan S. et al., **Appendix II**, Suppl. Fig. 5). Regarding circularity and elongation, cells cultured on polyurethane samples resembled M2-like phenotypes more than M1-like phenotypes when compared to differentiated macrophages cultured on TCP controls. This is an indicator for the relatively mild immune response to polyurethane biomaterials that also has been reported in the literature.[133] Similar effects were observed when assessing the secretion of pro- and anti-inflammatory cytokines. THP-1-derived macrophages responded to polyurethane samples with just a minor increase in pro-inflammatory cytokines compared to TCP controls (Segan S. et al., **Appendix II**, Suppl. Fig. 6). Although being still at a low level, the release of pro-inflammatory cytokines MIP-1β, MCP-1, TNF-α, and IL-8 slightly increased with increasing surface roughness.

PBMC model

After observing just a minor effect of surface roughness on the behaviour of THP-1-derived macrophages, a model with greater biological complexity, the PBMC model, was employed. Besides of monocytes, PBMCs also include lymphocytes and dendritic cells, all being isolated directly from human blood. There are several potential advantages of the PBMC model: First, primary monocytes of this model might be more susceptible to changes in biomaterial properties than the genetically modified THP-1 cell line monocytes.[92] Second, the additional presence of lymphocytes in the culturing system enables mutual interaction between innate and adaptive immune cells via secretion of soluble mediators or direct cell-cell interaction, which can affect the

general immune response.[134] Third, the presence of lymphocytes in a culturing set up was shown to significantly increase the rate of monocyte adhesion and fusion,[116] thus potentially rising the “awareness” of the monocytes to the different surface topographies. To assess if this model of enhanced biological complexity might respond to changes in surface roughness of the polyurethane samples, PBMCs obtained from three healthy donors were tested and cytokine secretion was quantified using Luminex immunoassays. Similar to the results observed in the THP-1 model, PBMCs showed generally low levels of cytokine secretion in response to the polyurethane specimens, which were comparable to the TCP negative control (Segan S. et al., **Appendix II**, Suppl. Fig. 8). No effect of surface roughness on the production of either pro-inflammatory or anti-inflammatory cytokines was detected. To evaluate the behaviour of specific immune cell populations, the activation of monocytes, lymphocytes and NK cells was assessed using flow cytometry. However, surface roughness had no effect on the level of surface marker expression in any of the immune cell populations investigated (Segan S. et al., **Appendix II**, Suppl. Fig. 7).

Whole blood model

As neither THP-1-derived macrophages nor human PBMCs responded to alterations in polyurethane surface topography, the human whole blood model was employed as it provides an additional degree of biological complexity. Unlike the two previous models, whole blood cultures additionally contain all sorts of granulocytes. Out of this group, the population of neutrophils has recently been shown to be sensitive to changes in biomaterial surface properties and to exhibit differential activation based on surface topography in general.[135,136] As regulators of the initial immune response and recruiters of monocytes and macrophages, the presence of neutrophils (accounting for more than 50% of all leukocyte cells in whole blood) might result in topography-dependent immune responses towards the polyurethane specimens in the whole blood model.[137,138] In order to get a more comprehensive assessment of potential immunological effects, the number of studied cytokines was increased from eight to 25 in addition. However, after 48 h of incubation, the cytokine response was found to be independent of topographical differences in the whole blood model, with no effect of additional cells like neutrophils (Segan S. et al., **Appendix II**, Suppl. Fig. 9).

In this study, a systematic approach was applied to investigate the impact of surface roughness on the immune response to polyurethane biomaterial. While topography-dependent immune activation has been reported in several studies,[16,33,42,128,139] no link was found between the surface roughness of polyurethane specimens and the immune response in any of the models investigated in this study. There might be several reasons for this behaviour. First, other surface characteristics like the class of the biomaterial tested could play a role in the results of a topography-based immune response. As polyurethane has low immunological impact in general, the effect of biomaterial chemistry and wettability could outweigh the effect of topography here. Studies that do find topographical-based differences mentioned at the beginning of this paragraph were conducted on different classes of biomaterials. Accordingly, when investigating titanium specimens, topography-dependent differences in pro-inflammatory cytokine secretion were observed (see chapter 3.2). Second, choosing adequate topographic characteristics may be crucial for a proper evaluation. In the present study, only the parameter S_a (mean arithmetic height of the surface area) was assessed as a distinguishing factor between the surfaces, while no other roughness-characterizing criteria were examined. In conclusion, our work demonstrates that microscale surface roughness is not solely responsible for the immune reaction to medicinal polyurethane. However, these results cannot be automatically transferred to other biomaterials or other topographical structures.

Chapter 5

Results III:

Interrelation between wettability, protein adsorption & immune response

The contents of this chapter are based on:

Billing F., et al. Altered pro-inflammatory responses to polyelectrolyte multilayer coatings are associated with differences in protein adsorption and wettability. *ACS Applied Materials & Interfaces,* Volume *13, Issue 46, 2021*

5 Results III: Interrelation between wettability, protein adsorption & immune response

During the inflammatory response, the proteins adsorbed on the biomaterial surface play an important mediating role between biomaterial and immune cells. Upon implantation, proteins from blood and interstitial fluids adsorb to the biomaterial surface, with the type, volume, and conformation of adsorbed proteins being dependent on surface parameters like wettability and surface charge.[50,52,140,141] Adsorbed serum proteins can alter immune cell behaviour, which has a direct impact on the immunological outcome of a biomaterial.[50,60,61,63,142] However, there remains a paucity of data on the interrelationship between the three essential aspects influencing the fate of a biomaterial implant – surface property, protein adsorption, and immune response. While previous in vitro studies have mainly focused on either the correlation between surface properties and protein adsorption [141,143] or the modulation of the immune response by artificial protein coatings,[61,142,144] relatively few studies have examined the interrelationship of all three factors. Furthermore, previous investigations frequently relied on simplistic models based on single cell lines that lacked the complexity of the human immune system [63] or analysed the effect of single proteins only,[61,144–146] thus missing the dynamic adsorption patterns of the full spectrum of serum proteins.

In this study, the complex nature of surface-protein interaction as well as the full spectrum of the immune response were evaluated, while the effects were pinpointed to particular differences in material properties. To link particular properties to specific immunological outcomes, three polyelectrolyte multilayer (PEM) coatings of varying wettability were created and their surface characteristics determined. The immune response was investigated by culturing PBMCs in serum-containing media on the PEM surfaces and analysing the collective secretion of immunomodulating cytokines in the cell culture supernatant, the expression of cell surface markers, and cell-specific intracellular cytokine production. To examine the influence of serum proteins on the observed immune response to the PEM coatings, PBMCs cultured in conventional cell culture media containing human serum were compared to cultures of serum-free media. In addition, the composition of the protein layers on the PEMs was examined

using LC-MS/MS to investigate if the adsorbed protein layer differs on the surfaces. Finally, using DigiWest technology, the activity of intracellular signalling pathways in immune cells was assessed.

5.1 Characterisation of surface properties and inflammatory response

Three variations of PEM coatings were created based on alternating layers of the polyanion polystyrene sulfonate (PSS) and the polycation polyallylamine hydrochloride (PAH) by adjusting the pH-sensitive charge density of the assembling polymers. Due to their cationic termination, they are referred to as PEM Cationic A, B and C. Surface characterisation revealed differences in surface wettability, with PEM Cationic A being the most hydrophilic and PEM Cationic C being the least hydrophilic surface (Billing F. et al., **Appendix III**, Suppl. Fig. 1). Mean surface charge was found to be identical for all coatings. SEM imaging revealed uniform surfaces without topographical variances, allowing cell adhesion with different morphology but apparently tight interaction to the smooth PEM coatings.

Cytokine analysis in the cell culture supernatant revealed that in response to the more hydrophobic coating Cationic C considerably higher amounts of pro-inflammatory cytokines TNF-α, MIP-1β, and IL-6 were secreted by PBMCs than in response to the other surfaces (Billing F. et al., **Appendix III**, Suppl. Fig. 2). For PEM Cationic C, the observed cytokine response was accompanied by a change in CD molecules on monocytes, including significantly increased expression of the pro-inflammatory marker CD86 and reduced expression of the anti-inflammatory marker CD163. To examine the individual contribution of the different immune cell populations being present in the PBMC suspension, cytokine expression in monocytes, T cells, and NK cells was examined intracellularly after cultivation on Cationic C coating. The findings revealed a clearly enhanced frequency of cytokine-positive monocytes for TNF-α, MIP-1β, IL-8 and MCP-1, with only minor contribution of T cells and negligible contribution of NK cells (Billing F. et al., **Appendix III**, Suppl. Fig. 3). Comparison of all three PEM coatings revealed the more hydrophobic Cationic C to show a higher frequency of cytokine-positive monocytes than Cationic A. These findings further indicated that 1) the immunological response is enhanced in response to coating Cationic C and 2) that cytokine production in response to the PEM coatings studied is mostly the responsibility of monocytes. Increasing the spectrum of biological variation using a

large panel of 24 donors generally confirmed the results of the three randomly selected donors of the previous experiments (Billing F. et al., **Appendix III**, Suppl. Fig. 4). Linear regression analysis revealed a weak age-dependent increase in TNF-α expression but no age-related trend for IL-8. No differences between male and female donors were observed for any cytokine investigated. Cytokine release itself is a dynamic process that is subject to rapid regulatory mechanisms. To reveal the process of cytokine response towards the PEM coatings across time, cytokine production by monocytes was investigated after 12, 24 and 96 h of biomaterial contact. While there were no changes in cytokine expression across the PEM surfaces after 12 and 96 h, cellular activation was evident on all PEM substrates after 24 h of cultivation, with the more hydrophobic coating Cationic C showing the greatest increase. (Billing F. et al., **Appendix III**, Suppl. Fig. 3). In summary, immunological investigations revealed a significantly enhanced pro-inflammatory immune response after cultivation on the more hydrophobic PEM coating Cationic C compared to the more hydrophilic coating Cationic A, thus indicating a strong influence of surface wettability.

5.2 Adsorbed proteins as potential causes of the observed immune response

In the next step, the influence of serum proteins on the immune response towards PEM coatings was analysed. To further explore the impact of surface wettability, the two coatings with the most hydrophilic and most hydrophobic properties were investigated. When PBMC cultures were compared in the presence and absence of human serum, the alterations in immune response were attributed to the presence of serum proteins on the coated surfaces. Under serum-free conditions, no differences in the immune response could be observed between hydrophilic and hydrophobic PEMs, thus clearly demonstrating a crucial role of the adsorbed protein layer in the immune response (Billing F. et al., **Appendix III**, Suppl. Fig. 5). In the following, protein identification using LC-MS/MS revealed surface-dependent changes in type and quantity of detected proteins. For both PEM surfaces, lipoproteins were the main class of adsorbed proteins, followed by acute inflammatory response proteins (Billing F. et al., **Appendix III**, Suppl. Fig. 6). For PEM coating Cationic C, a 4-fold increase in the amount of acute inflammatory response proteins in comparison to Cationic A was observed. Statistical analysis further showed an increased amount of apolipoproteins A-I, C-II, C-III, and J (also known as clusterin) on the more hydrophobic Cationic C surface compared to the more hydrophilic Cationic A. The presence of these proteins has been associated with

pro-inflammatory responses and an increased secretion of pro-inflammatory cytokines by monocytes in the literature, thus reflecting the differences in the immune response observed for coatings A and C.[147–153] In addition, proteins associated with anti-inflammatory effects were less abundant on coating Cationic C than on Cationic A. Apolipoproteins A-I and E are known to promote macrophage conversion from the pro-inflammatory M1-like to the anti-inflammatory M2-like phenotype and inhibit the production of pro-inflammatory cytokines.[154–156] On coating Cationic A, these two inflammation-dampening proteins accounted for 53.6 % of the total protein abundance, while their abundance on Cationic C was only 23.6 %. Taken together, the protein analysis showed that the composition of the adsorbed protein layer highly differed between PEM coatings of identical chemical substrates but distinct levels of wettability. The presence of the respective proteins may have a significant impact on the cytokine expression by monocytes and the resulting immune response.

5.3 The MAPK signalling pathway as a candidate factor in driving monocyte immune response

In a last step, intracellular processes in monocytes were examined to uncover potential changes in signalling pathways in response to different protein layers. Therefore, DigiWest technology was applied to simultaneously detect protein abundance and phosphorylation status of 67 intracellular signalling proteins.[157] Out of seven signalling proteins identified to significantly differ between PEM coatings Cationic A and C, six belonged to the MAPK signalling pathway (c-Jun, MEK1, MEK2, NF-κB, Erk 1/2 and TRAF1), showing a widespread function for this pathway in response to PEM surfaces. (Billing F. et al., **Appendix III**, Suppl. Fig. 7). Except for c-Jun, all proteins were expressed at higher quantities on coating Cationic A compared to Cationic C.

The results of this study demonstrate that the layer of proteins adsorbed to the surface has a major influence on immune responses to the different PEM coatings. Protein identification revealed an increased quantity of inflammation-associated proteins on the PEM coating with the highest pro-inflammatory immune response, and a higher abundance of proteins with anti-inflammatory association on the less inflammatory coating. In addition, variations in the expression of MAPK proteins in monocytes in response to the different surfaces were observed. As the tested PEM surfaces were highly similar in surface charge and topography but mainly differed in their surface

wettability, this characteristic is particularly interesting for the targeted design of medical implants. In this context, PEM coatings could be used as a versatile tool to modulate the immune response towards a biomaterial substrate. Furthermore, the class of apolipoproteins emerged as an important indicator for assessing a biomaterial's biocompatibility. This study thus demonstrated the interrelationship between material properties, protein adsorption and the immune response as closely related components of the biological response to foreign materials (Figure 10).

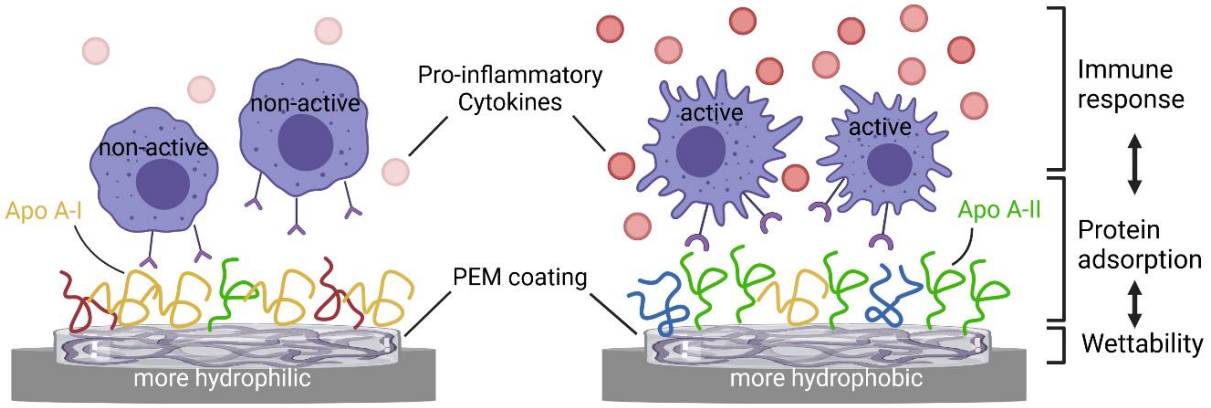

Figure 10: Schematic overview of the interrelation between surface wettability, protein adsorption and immune response. Wettability of PEM coatings was observed to be critical for the adsorption of specific human serum proteins to the biomaterial surfaces. PEM coatings of a higher hydrophilicity resulted in elevated adsorption of proteins associated with anti-inflammatory effects (e.g. apolipoprotein A-I) combined with a low number of activated monocytes and reduced levels of pro-inflammatory cytokines (left). More hydrophobic coatings, on the other hand, had higher levels of inflammation-associated proteins (e.g., apolipoprotein A-II) adsorbed to their surface, a higher number of activated monocytes, and induced significantly increased secretion of pro-inflammatory cytokines (right). Graphic was created using biorender.com.

Chapter 6

General discussion and conclusion

6 General discussion and conclusion

Biomedical implants are commonly used in medical therapies that aid in the resolution of health issues in a wide range of treatments. Existing implant devices are continuously improved, and new devices for novel applications are constantly being developed. Besides of being an essential contributor in enhancing human health, medical implant development is also a significant economic factor. In the future, strong growth rates for the number of implantations as well as the economic turnover in the medical technology industry are projected due to an aging global population and the developments in the manufacturing of medical devices.[158–160] For the patients, implant biocompatibility is a significant determinant in therapy effectiveness. A comprehensive understanding of the interplay between biomaterial features and induced immune response is crucial for implant development in order to achieve high levels of biocompatibility and associated functionality after the device is placed into the body. Various factors must be taken into account for the successful modulation of biocompatibility.

6.1 Role of innate and adaptive immune cells in response to biomaterial surfaces

Prior to focusing on gaining knowledge about possible modulation strategies of a given device's biocompatibility, a comprehensive understanding of the immune response to biomaterials in general and the involvement of participating immune cell types in particular is essential. While immunological processes in response to "natural" foreign bodies such as bacteria and viruses have been thoroughly studied, the involvement of individual immune cell types in response to "artificial" foreign bodies such as implant biomaterials remain unclear. In the context of biomaterials, it is often viewed that the adaptive immune system's participation in the first immunological response is fairly restricted. However, data to support this idea is limited. In this work, components of the innate and the adaptive immune systems were explored for their role in the initial immune response towards titanium dental implants. When cultured separately, isolated monocytes of the innate immune system were found to become activated and respond to titanium surfaces with enhanced pro-inflammatory cytokine and surface marker expression, while T cells of the adaptive immune system cultured in the absence of monocytes showed no direct biomaterial response above the level of the negative

control (Chapter 3). It is not surprising that lymphocytes do not respond when encountering a material surface without co-stimulatory cells being present. Although several studies have indicated that lymphocytes have mechanosensing properties in general, this effect was predominantly observed for changes in material stiffness and can only be induced by the artificial presence of adequate receptor binding sites.[161,162] Unlike monocytes of the innate immune system, T cells of the adaptive immune system usually require antigen presentation and priming of naïve cells for their pathogen-specific response. However, lymphocytes may also be activated non-specifically by the innate immune system through the release of soluble molecules.[163] Thus, this work was designed to test the potential of lymphocytes to indirectly respond to biomaterials through the activation by monocytes. Regarding cell surface markers, expression levels on lymphocyte populations were found to be slightly biomaterial surface-dependent. In addition, the expression of surface markers on T cells was found to be increased when high numbers of monocytes were present in PBMC cultures containing both innate and adaptive immune cells. This shows the general ability of lymphocytes to be activated depending on the monocytes being present; although the observed effects were just observable under artificially altered ratios of innate to adaptive cells.

Regarding the generation of immunoactive cytokines, the data demonstrated a monocyte-induced cytokine response following contact with titanium surfaces, while T cell mediated cytokine response in PBMC cultures containing both innate and adaptive populations was found to be quite minor. Notably, there was also no indication of lymphocytes stimulating or suppressing the cytokine response of monocytes in turn. These results are in contrast to some previous findings showing innate and adaptive cell interactions in response to biomaterials to result in lymphocyte activation, even when the populations were separated by transwell.[116,118] There could be several explanations for the absence of lymphocyte response observed in this work. The amount of cytokines generated by monocytes, for example, may be insufficient for a robust T cell activation. Following contact with the tested titanium surface, only low cytokine levels of IL-6 were found, a cytokine that plays an important role in T cell activation and differentiation.[72] This explanation is also supported by the observation that with artificially increased amounts of monocytes in the culture – and thus with higher levels of secreted cytokines – a slight increase in activation marker expression on lymphocytes could be observed. The lack of variance in the immune response of

the three biological models of various complexity explored in Chapter 4 could possibly be explained by a lack of adequate cellular activation as well. Another possibility is that T cell activation occurred, but was missed by the experimental setting. Lymphocyte proliferation and differentiation, for example, were not assessed in this work but can be strong indications of lymphocyte activation. A third explanation for the absence of observed lymphocyte response is that the three-day observation period was too short, as potential effects might not be apparent until later stages. This was also reported in other studies which found that lymphocyte effects on the release of pro-inflammatory cytokines TNF-α, IL-6 and IL-8, cytokines that were also evaluated in this work, occurred only after a 10-day interval, but not before.[164] Further investigations addressing these potential cues would be needed to clearly determine the lymphocyte response to biomaterial surfaces.

It also has to be considered that the results obtained for a single biomaterial substrate with a specific set of surface properties cannot be generalized to other materials and surface characteristics. The very low lymphocyte activation in response to the titanium surfaces employed does not imply a general inactivity of lymphocytes after contact with biomaterials. Surface properties like topography and wettability, as outlined in Chapter 1.1, have a significant impact on the immune response. This is also true for lymphocytes, which show different levels of activation depending on the biomaterial substrate. For example, both hydrophobic and anionic surfaces were shown to increase lymphocyte proliferation, while hydrophilic as well as cationic surfaces were both found to inhibit lymphocyte activity.[165] The SLActive titanium surface evaluated in the present work had a high degree of hydrophilicity as well, which could explain why the lymphocytes were not activated. The same might occur for the PEM coatings investigated in Chapter 5, which had a cationic termination layer and also showed only minor lymphocyte activity. Thus, surface properties are critical for examination and evaluation of the immune response and the role of individual immune cell populations.

The results imply that for investigations on the initial phase of biomaterial host response, in vitro models using cells of the innate immune system only might be sufficient. This was also evident in the comparison of test systems of different biological complexity, where no differences between models with and without adaptive immune cells could be found after a three-day examination period (Chapter 4). However, in the

long term, adaptive immune cells have been shown to have direct and indirect effects on material biocompatibility in vivo as mediators in tissue regeneration, fibrosis, and the foreign body reaction. In the context of biomaterials, adaptive immune cells were shown to be recruited to the implant side where they can regulate regenerative wound healing.[166,167] Cross talk between innate and adaptive cells was found to modulate the foreign body response by impairing macrophage attraction and increasing the rate of macrophage fusion into FBGCs.[116,168] Finally, T cell mediated responses were detected in implant-surrounding tissues in cases of aseptic loosening of joint replacements.[169] This demonstrates the overall importance of lymphocytes for implant biocompatibility and suggests the necessity for additional research into the processes of lymphocyte activation. The choice of test systems for the immunological evaluation of a biomaterial modification thus depends on whether the immediate inflammatory response or long-term development is to be examined.

6.2 Surface property-driven immune response

The immune response can be modulated by altering the topographical characteristics of a biomaterial,[170–172] which was also observed for the titanium samples investigated in Chapter 3. However, the results must be evaluated within the context of several limitations that also apply to many other studies in the field. First, defining a surface primarily by its manufacturing process (e.g. sandblasting, acid etching, …) rather than its particular topographical features can result in misleading comparisons because a method might create distinct topographies when applied to different materials.[173] Second, surface topography is frequently adjusted without considering the effects on other properties like surface chemistry or wettability.

In order to comprehensively investigate the effects of roughness on a given material class with equal chemical composition, seven polyurethane samples with defined roughness gradations were compared to each other in terms of immune response using the primary PBMC model. Contrary to expectations, no immunological differences were found between the tested surfaces in any of the biological models used (Chapter 4). Even though many studies in the field do propose a topography-dependent immune response, there are also some investigations observing unchanged cytokine profiles of immune cells cultured on distinct surface topographies.[174–176] One possible reason for these results is the choice of biomaterial

substrate. The polyurethane substrate employed in the present work is considered as one of the most biocompatible materials and is well-known for its low-inflammatory properties.[177] Also the other studies mentioned above that did not detect topography-dependent stimulation of the immune response used biomaterials that are normally linked with low immune responses. The observed effects might thus be attributed to the low-immunogenic surface chemistry used, which overrode possible topographical effects. To confirm this, the same topographical features would need to be transferred to a material that elicits a stronger host response. This would allow to see if specific topographical features have a mitigating effect on the immune response.

Another point to consider is that the current study did not investigate specific surface topography features like shape or spacing, which may influence immune cell behaviour. In the present study, only the parameter R_a was assessed as a distinguishing factor between the polyurethane surfaces, whereas additional criteria for characterizing roughness were not examined. R_a is a parameter that describes the mean arithmetic roughness and is commonly used in the evaluation of surface topography. However, although having comparable R_a values, the topographies of two given substrates can be highly different, with distinct nanoscopic topologies being present (see Figure 11).[17,178] At the same time, surfaces with different R_a values can be identical in terms of other topographical parameters, such as the average number of peaks (S_m). Thus, despite the differences in R_a, the polyurethane specimens investigated in this work might be similar in aspects such as nanoscale topography, which might represent the sensitive form of topography for immune cells. Further studies elucidating the role of specific surface features on the biocompatibility of a device should therefore assess a larger variety of topography-related parameters in order to determine the surface parameter(s) to which the cells respond.

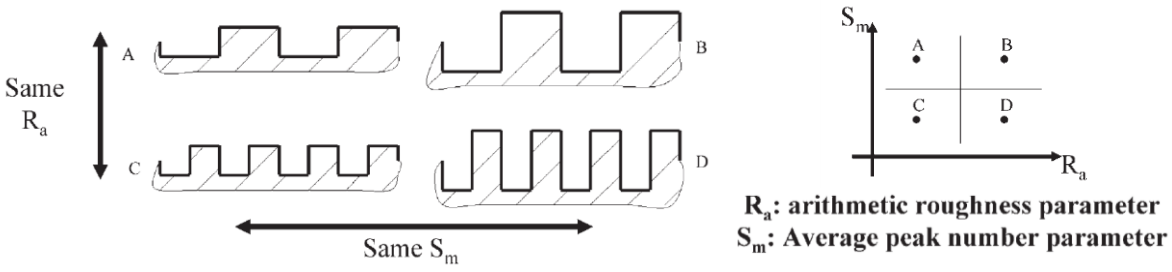

Figure 11: Example of similar topographical profiles with distinct roughness parameter R_a. Parameters R_a (A = C) ≠ (B = D) and S_m (A = B) ≠ (C = D). Adapted and modified from Ponche et al.[17]

The cellular response to different topographical features can be influenced by changes in cell-to-implant contact area dimensions, the directing effects of specific surface structures, or variances in induced cell motility.[173] However, surface topography may also have a significant impact on protein adhesion, which further mediates cellular attachment. Independent of surface chemistry, nanoscale topography was shown to influence the adsorption and conformation of integrin binding proteins, thus altering cell binding site availability and affecting integrin signalling.[179] Similar effects were also observed for other proteins like fibrinogen or vitronectin.[180] This suggests that, at least in part, the effects of surface topography are conveyed to the surrounding cells via the layer of adsorbed proteins. Thus, mass spectrometry studies could be used to determine the composition of the protein layer on the polyurethane surfaces. If identical proteins are identified on the different polyurethane specimens, this would further explain why the immune response to the polyurethane samples was found to be identical. Similar investigations on PEM coatings demonstrated a crucial influence of protein adsorption on the immune response (further discussed in Chapter 6.4).

6.3 Modulation of biocompatibility via PEM surface coating

Besides of topography, this work also focused on surface wettability and its involvement in the host immune response. Investigating materials of different chemistry revealed that hydrophilic titanium specimens and hydrophilic PEM coatings both elicited a diminished pro-inflammatory cytokine response compared to their hydrophobic counterparts (see Chapters 3 and 5). This reflects a widely observed phenomena in which an increased degree of hydrophilicity is associated with a reduced acute inflammatory response.[181] The use of PEM coatings in this work allowed for the induction of particular changes in surface wettability while maintaining topography and surface charge constant. As a result, immune responses could be directly correlated to the degree of wettability. Possible explanations for the obtained observations are discussed in Chapter 6.4.

The results of this work showed that alterations in surface wettability could be used as a strategy to modulate the host response to a medical device. In accordance with the findings on the immune-modulatory effect of PEM coatings in this work (Chapter 5.1), appropriate PEM coatings have been found to significantly influence macrophage adhesion, formation of FBGCs, and cytokine release; hence reducing the inflammatory

response of biomaterials.[182] Thus, PEM coatings could be a useful tool to passively refine immune responses based on a change in surface wettability. As shown in the physico-chemical examination (Chapter 5.1), the surface properties of PEMs can be altered during the creation process; thus enabling a wide application range with differing biocompatibility requirements. A blood-compatibility coating composed of natural polyelectrolytes heparin and chitosan, for example, has been found to improve biocompatibility of cardiovascular implants.[183] This suggests that the effects identified for the polyelectrolytes in this work may be transferable to an in vivo environment. In addition to passive modulation, PEM coatings can also be employed in drug delivery systems as a reservoir for bioactive compounds, thus combining both passive and active modulation approaches. Bioactive strategies aim for the local delivery of anti-inflammatory and/or pro wound healing molecules from a reservoir or a coating to induce desired cell responses. As especially cytokines and growth factors affect the immune cell response, these immune players are attractive components for sustained release from bioactive coatings. PEMs, when paired with immunomodulatory cytokines like IL-4, have been shown to inhibit the release of pro-inflammatory cytokines by activated monocytes.[105] This modification of the host response by bioactive surface coatings represents another strategy for the modulation of biomaterials, which has received increasing attention in recent years. Further development of the polyelectrolytes used in this work into bioactive coatings could enable targeted application of the PEMs for specific implantation requirements.

The common aim of both active and passive PEM coating approaches is to reduce the risk of chronic inflammation in the long term and to support the healing process following implantation. However, the remarkable biocompatibility of PEM coatings in these applications is mediated not directly by their physicochemical properties, but rather by the effects of an intermediary mediator: proteins adsorbed on the coating's surface.

6.4 Protein adsorption as essential marker for biocompatibility

The immediate adsorption of proteins to artificial surfaces prevents cells of any type from direct interaction with the biomaterial, both in vivo and in vitro. Instead, the adsorbed protein layer acts as a bridge, transmitting the effects of the material

properties to the immune cells.[50] In this work, it was demonstrated that a change in surface wettability can alter the immune response through a shift in the type and quantity of protein composition (Chapter 5). The effects of altered wettability were observable in the presence of proteins only, thus emphasizing the critical relevance of protein adsorption for a device's biocompatibility. Protein adsorption to a biomaterial surface appears to be the main driver of the elicited immune response and therefore provides promising strategies for the modulation of implant biocompatibility. One modulation strategy to attenuate the host inflammatory response is the general reduction of protein adsorption at the biomaterial surface, which was shown to prevent adhesion of monocytes / macrophages and expression of pro-inflammatory cytokines.[101] However, although showing beneficial effects in vitro and during the acute phase within the initial days after implantation, this strategy lacks long-term stability and failed to keep its favourable responses for chronic inflammation in vivo.[183] Thus, rather than protecting the implanted material from all interaction with the surrounding tissue, more bioactive strategies are required. A more promising strategy is the guided adsorption of desired proteins. The adsorbed protein layer usually provides binding sites for protein-specific receptors like integrins for immune cells.[184] Surface chemistry-dependent protein layer modulation may thus permit alternative receptor binding and signalling in immune cells. This idea is supported by the observation that the presence of specific integrin binding domains on a biomaterial surface was shown to promote cell-specific adhesion and to direct the responses of inflammatory cells.[185,186] By varying surface properties such as wettability, the available receptor binding sites can be altered, thereby changing the cellular immune response.

In this work, apolipoproteins emerged as a potentially interesting class of proteins in the mediation of the inflammatory response. A huge variety of apolipoproteins was found at the PEM surfaces, most of them showing very high abundance. This is of particular interest, as in the context of biomaterials apolipoproteins are known for their immunomodulating activity. Once adhered to a surface, apolipoproteins can induce pro- or anti-inflammatory effects by affecting immune cell activation and cytokine production, depending on the type of apolipoprotein.[147–156] Other studies investigating biomaterial protein adsorption have also revealed high levels of attached apolipoproteins on a variety of biomaterial surfaces.[63,187–190] Similar to the results of the present work, the amount and type of adsorbed apolipoproteins often differed

between materials with different inflammatory properties in these studies.[63,189,190] This indicates a potential critical role for apolipoproteins in the host response towards biomaterials. For apolipoprotein J (also known as clusterin), it was already shown that the adsorption of this protein directly influences macrophage activation as the presence of this protein significantly reduced the uptake of nanocarriers by macrophages.[191] Further investigation on the role of apolipoproteins is required to confirm their importance in the formation of the immune response to biomaterials. This might be accomplished through in vitro testing of biomaterials using cell cultures with apolipoprotein-depleted serum, or by using artificial coatings of single types of apolipoproteins, and subsequent immunological analysis. If a critical role of apolipoproteins were proven, this would be a significant step in predicting the biocompatibility of implants based on protein adsorption.

6.5 Conclusion

The host response to biomaterials is a very complex multifaceted process that is orchestrated by a diverse array of cellular players at different stages of progression. This process is strongly influenced by the presence or absence of certain proteins on the material surface, while their composition is defined by the combined interplay of different surface properties. In order to increase biocompatibility across a wide range of materials and application areas, the effect of individual proteins on the activation of specific (immune) cell populations must be further investigated. Although it may appear unconnected at first, a strong focus must be placed on the adherent proteins in the choice of material substrate and surface treatment. The adsorbed protein layer incorporates all physicochemical material variations since the type, level and conformation of serum proteins that adsorb to biomaterial surfaces are determined by the biomaterial's terminal chemical and physical properties. Therefore, adsorbed proteins may be the ideal marker indicating optimal surface topography and chemistry, thus being capable of predicting the immune response to a biomaterial. In this context, the class of apolipoproteins emerges as a potential key element in conveying material based effects to the host immune response. Only when solid predictions regarding the host response can be obtained, it will be possible to achieve a significant improvement in the biocompatibility of newly developed or current medical devices.

References

1. Han, H., Kim, S. & Han, D. Multifactorial evaluation of implant failure: a 19-year retrospective study. *Int. J. Oral Maxillofac. Implants* **29**, 303–310 (2014).
2. Langton, D. *et al.* Accelerating failure rate of the ASR total hip replacement. *J. Bone Joint Surg. Br.* **93**, 1011–1016 (2011).
3. Sakka, S., Baroudi, K. & Nassani, M. Z. Factors associated with early and late failure of dental implants. *J. Investig. Clin. Dent.* **3**, 258–261 (2012).
4. Anderson, J. M., Rodriguez, A. & Chang, D. T. Foreign body reaction to biomaterials. *Semin. Immunol.* **20**, 86–100 (2008).
5. Anderson, J. M. Biological responses to materials. *Annu. Rev. Mater. Sci.* **31**, 81–110 (2001).
6. Landgraeber, S., Jäger, M., Jacobs, J. J. & Hallab, N. J. The pathology of orthopedic implant failure is mediated by innate immune system cytokines. *Mediators Inflamm.* **2014**, (2014).
7. Franz, S., Rammelt, S., Scharnweber, D. & Simon, J. C. Immune responses to implants – A review of the implications for the design of immunomodulatory biomaterials. *Biomaterials* **32**, 6692–6709 (2011).
8. Tang, L., Thevenot, P. & Hu, W. Surface Chemistry Influences Implant Biocompatibility. *Curr. Top. Med. Chem.* **8**, 270–280 (2008).
9. Vishwakarma, A. *et al.* Engineering Immunomodulatory Biomaterials To Tune the Inflammatory Response. *Trends Biotechnol.* **34**, 470–482 (2016).
10. Mariani, E., Lisignoli, G., Borzì, R. M. & Pulsatelli, L. Biomaterials: Foreign Bodies or Tuners for the Immune Response? *Int. J. Mol. Sci. 2019, Vol. 20, Page 636* **20**, 636 (2019).
11. Williams, D. F. *The Williams Dictionary of Biomaterials*. vol. ISBN-10: 0853237344 (Liverpool University Press, 1999).
12. Williams, D. F. On the mechanisms of biocompatibility. *Biomaterials* **29**, 2941–2953 (2008).
13. Williams, D. F. *Essential Biomaterials Science*. (Cambridge University Press, 2014).
14. Nouri, A. & Wen, C. Introduction to surface coating and modification for metallic biomaterials. *Surf. Coat. Modif. Met. Biomater.* 3–60 (2015).
15. Bartneck, M. *et al.* Induction of specific macrophage subtypes by defined micro-patterned structures. *Acta Biomater.* **6**, 3864–3872 (2010).
16. Paul, N. E. *et al.* Topographical control of human macrophages by a regularly microstructured polyvinylidene fluoride surface. *Biomaterials* **29**, 4056–4064 (2008).
17. Ponche, A., Bigerelle, M. & Anselme, K. Relative influence of surface topography and surface chemistry on cell response to bone implant materials. Part 1: Physico-chemical effects: *Proc. Inst. Mech. Eng., Part H J. Eng. Med.* **224**, 1471–1486 (2010).
18. Flemming, R. G., Murphy, C. J., Abrams, G. A., Goodman, S. L. & Nealey, P. F. Effects of synthetic micro- and nano-structured surfaces on cell behavior. *Biomaterials* **20**, 573–588 (1999).
19. Yim, E. K. F. & Leong, K. W. Significance of synthetic nanostructures in dictating cellular response. *Nanomedicine Nanotechnology, Biol. Med.* **1**, 10–21 (2005).
20. Schwartz, Z., Kieswetter, K., Dean, D. D. & Boyan, B. D. Underlying mechanisms at the bone-surface interface during regeneration. *J. Periodontal Res.* **32**, 166–171 (1997).
21. Ogle, O. E. Implant Surface Material, Design, and Osseointegration. *Dent. Clin.* **59**, 505–520 (2015).
22. Wennerberg, A. & Albrektsson, T. Effects of titanium surface topography on bone integration: a systematic review. *Clin. Oral Implants Res.* **20**, 172–184 (2009).
23. Jemat, A., Ghazali, M. J., Razali, M. & Otsuka, Y. Surface modifications and their effects on titanium dental implants. *Biomed Res. Int.* **2015**, (2015).
24. Witherel, C. E., Abebayehu, D., Barker, T. H. & Spiller, K. L. Macrophage and Fibroblast

Interactions in Biomaterial-Mediated Fibrosis. *Adv. Healthc. Mater.* **8**, 1801451 (2019).
25. Chou, L., Firth, J. D., Uitto, V. J. & Brunette, D. M. Substratum surface topography alters cell shape and regulates fibronectin mRNA level, mRNA stability, secretion and assembly in human fibroblasts. *J. Cell Sci.* **108**, 1563–1573 (1995).
26. Schulte, V. A., Díez, M., Möller, M. & Lensen, M. C. Surface Topography Induces Fibroblast Adhesion on Intrinsically Nonadhesive Poly(ethylene glycol) Substrates. *Biomacromolecules* **10**, 2795–2801 (2009).
27. Dalby, M. J. *et al.* Increasing Fibroblast Response to Materials Using Nanotopography: Morphological and Genetic Measurements of Cell Response to 13-nm-High Polymer Demixed Islands. *Exp. Cell Res.* **276**, 1–9 (2002).
28. Steiert, A. E., Boyce, M. & Sorg, H. Capsular contracture by silicone breast implants: possible causes, biocompatibility, and prophylactic strategies. *Med. Devices (Auckl).* **6**, 211 (2013).
29. Doloff, J. C. *et al.* The surface topography of silicone breast implants mediates the foreign body response in mice, rabbits and humans. *Nat. Biomed. Eng.* **5**, 1115–1130 (2021).
30. Wong, C. H., Samuel, M., Tan, B. K. & Song, C. Capsular contracture in subglandular breast augmentation with textured versus smooth breast implants: A systematic review. *Plast. Reconstr. Surg.* **118**, 1224–1236 (2006).
31. Rich, A. & Harris, A. K. Anomalous preferences of cultured macrophages for hydrophobic and roughened substrata. *J. Cell Sci.* **50**, 1–7 (1981).
32. McWhorter, F. Y., Davis, C. T. & Liu, W. F. Physical and mechanical regulation of macrophage phenotype and function. *Cell. Mol. Life Sci. 2014 727* **72**, 1303–1316 (2014).
33. Refai, A. K., Textor, M., Brunette, D. M. & Waterfield, J. D. Effect of titanium surface topography on macrophage activation and secretion of proinflammatory cytokines and chemokines. *J. Biomed. Mater. Res. Part A* **70A**, 194–205 (2004).
34. Chen, S. *et al.* Characterization of topographical effects on macrophage behavior in a foreign body response model. *Biomaterials* **31**, 3479–3491 (2010).
35. Tan, K. S., Qian, L., Rosado, R., Flood, P. M. & Cooper, L. F. The role of titanium surface topography on J774A.1 macrophage inflammatory cytokines and nitric oxide production. *Biomaterials* **27**, 5170–5177 (2006).
36. Zhu, Y. *et al.* Regulation of macrophage polarization through surface topography design to facilitate implant-to-bone osteointegration. *Sci. Adv.* **7**, (2021).
37. Ruths, M. Surface Forces, Surface Tension, and Adhesion. *Encycl. Tribol.* 3435–3443 (2013).
38. Rupp, F. *et al.* A review on the wettability of dental implant surfaces I: Theoretical and experimental aspects. *Acta Biomater.* **10**, 2894–2906 (2014).
39. Wei, J. *et al.* Influence of surface wettability on competitive protein adsorption and initial attachment of osteoblasts. *Biomed. Mater.* **4**, 045002 (2009).
40. Arima, Y. & Iwata, H. Effect of wettability and surface functional groups on protein adsorption and cell adhesion using well-defined mixed self-assembled monolayers. *Biomaterials* **28**, 3074–3082 (2007).
41. van Kooten, T. G., Schakenraad, J. M., van der Mei, H. C. & Busscher, H. J. Influence of substratum wettability on the strength of adhesion of human fibroblasts. *Biomaterials* **13**, 897–904 (1992).
42. Hotchkiss, K. M. *et al.* Titanium surface characteristics, including topography and wettability, alter macrophage activation. *Acta Biomater.* **31**, 425–434 (2016).
43. Jones, J. A. *et al.* Proteomic analysis and quantification of cytokines and chemokines from biomaterial surface-adherent macrophages and foreign body giant cells. *J. Biomed. Mater. Res. Part A* **83A**, 585–596 (2007).
44. Dai, X. *et al.* Attenuating Immune Response of Macrophage by Enhancing Hydrophilicity of Ti Surface. *J. Nanomater.* (2015).
45. Alfarsi, M. A., Hamlet, S. M. & Ivanovski, S. Titanium surface hydrophilicity modulates the human macrophage inflammatory cytokine response. *J. Biomed. Mater. Res. Part*

A **102**, 60–67 (2014).
46. Schwarz, F. *et al.* Potential of chemically modified hydrophilic surface characteristics to support tissue integration of titanium dental implants. *J. Biomed. Mater. Res. Part B Appl. Biomater.* **88B**, 544–557 (2009).
47. Yao, K., Huang, X.-D., Huang, X.-J. & Xu, Z.-K. Improvement of the surface biocompatibility of silicone intraocular lens by the plasma-induced tethering of phospholipid moieties. *J. Biomed. Mater. Res. Part A* **78A**, 684–692 (2006).
48. Tognetto, D. *et al.* Hydrophobic acrylic versus heparin surface-modified polymethylmethacrylate intraocular lens: a biocompatibility study. *Graefe's Arch. Clin. Exp. Ophthalmol. 2003 2418* **241**, 625–630 (2003).
49. Schmidt, D. R., Waldeck, H. & Kao, W. J. Protein Adsorption to Biomaterials. *Biol. Interact. Mater. Surfaces* 1–18 (2009).
50. Wilson, C. J., Clegg, R. E., Leavesley, D. I. & Pearcy, M. J. Mediation of Biomaterial–Cell Interactions by Adsorbed Proteins: A Review. *Tissue Eng. 2005* **11**, 1–18 (2005).
51. Norde, W. Adsorption of proteins from solution at the solid-liquid interface. *Adv. Colloid Interface Sci.* **25**, 267–340 (1986).
52. Horbett, T. A. Chapter 13 Principles underlying the role of adsorbed plasma proteins in blood interactions with foreign materials. *Cardiovasc. Pathol.* **2**, 137–148 (1993).
53. Nakanishi, K., Sakiyama, T. & Imamura, K. On the adsorption of proteins on solid surfaces, a common but very complicated phenomenon. *J. Biosci. Bioeng.* **91**, 233–244 (2001).
54. Brash, J. L., Horbett, T. A., Latour, R. A. & Tengvall, P. The blood compatibility challenge Part 2: protein adsorption phenomena governing blood reactivity. *Acta Biomater.* **94**, 11 (2019).
55. Noh, H. & Vogler, E. A. Volumetric interpretation of protein adsorption: Mass and energy balance for albumin adsorption to particulate adsorbents with incrementally increasing hydrophilicity. *Biomaterials* **27**, 5801–5812 (2006).
56. Vogler, E. A. Protein Adsorption in Three Dimensions. *Biomaterials* **33**, 1201 (2012).
57. Gittens, R. A. *et al.* A review on the wettability of dental implant surfaces II: Biological and clinical aspects. *Acta Biomater.* **10**, 2907–2918 (2014).
58. Vroman, L. & Adams, A. L. Findings with the recording ellipsometer suggesting rapid exchange of specific plasma proteins at liquid/solid interfaces. *Surf. Sci.* **16**, 438–446 (1969).
59. Jung, S.-Y. *et al.* The Vroman Effect: A Molecular Level Description of Fibrinogen Displacement. *J. Am. Chem. Soc.* **125**, 12782–12786 (2003).
60. Collier, T. O. & Anderson, J. M. Protein and surface effects on monocyte and macrophage adhesion, maturation, and survival. *J. Biomed. Mater. Res.* **60**, 487–496 (2002).
61. Jenney, C. R. & Anderson, J. M. Adsorbed serum proteins responsible for surface dependent human macrophage behavior. *J Biomed Mater Res.* **Mar 15**, 435–47 (2000).
62. Jenney, C. R. & Anderson, J. M. Adsorbed IgG: A potent adhesive substrate forhuman macrophages. *World Biomater. Congr.* (2000).
63. Visalakshan, R. M. *et al.* Biomaterial Surface Hydrophobicity-Mediated Serum Protein Adsorption and Immune Responses. *ACS Appl. Mater. Interfaces* **11**, 27615–27623 (2019).
64. Brodbeck, W. G. *et al.* In vivo leukocyte cytokine mRNA responses to biomaterials are dependent on surface chemistry. *J. Biomed. Mater. Res. Part A* **64A**, 320–329 (2003).
65. Esche, C., Stellato, C. & Beck, L. A. Chemokines: Key Players in Innate and Adaptive Immunity. *J. Invest. Dermatol.* **125**, 615–628 (2005).
66. Anderson, J. M. & McNally, A. K. Biocompatibility of implants: lymphocyte/macrophage interactions. *Semin. Immunopathol. 2011 333* **33**, 221–233 (2011).
67. Xia, Z. & Triffitt, J. T. A review on macrophage responses to biomaterials. *Biomed. Mater.* **1**, R1 (2006).
68. Martin, K. E. & García, A. J. Macrophage phenotypes in tissue repair and the foreign body response: Implications for biomaterial-based regenerative medicine strategies.

Acta Biomater. **133**, 4–16 (2021).
69. Dinarello, C. A. Interleukin-1. *Cytokine Growth Factor Rev.* **8**, 253–265 (1997).
70. Dinarello, C. A. Overview of the IL-1 family in innate inflammation and acquired immunity. *Immunol. Rev.* **281**, 8 (2018).
71. Rose-John, S. Interleukin-6 Family Cytokines. *Cold Spring Harb. Perspect. Biol.* **10**, a028415 (2018).
72. Hunter, C. A. & Jones, S. A. IL-6 as a keystone cytokine in health and disease. *Nat. Immunol. 2015 165* **16**, 448–457 (2015).
73. Hurst, S. M. *et al.* IL-6 and Its Soluble Receptor Orchestrate a Temporal Switch in the Pattern of Leukocyte Recruitment Seen during Acute Inflammation. *Immunity* **14**, 705–714 (2001).
74. Harada, A. *et al.* Essential involvement of interleukin-8 (IL-8) in acute inflammation. *J. Leukoc. Biol.* **56**, 559–564 (1994).
75. Remick, D. G. Interleukin-8. *Crit. Care Med.* **33**, (2005).
76. Li, A., Dubey, S., Varney, M. L., Dave, B. J. & Singh, R. K. IL-8 Directly Enhanced Endothelial Cell Survival, Proliferation, and Matrix Metalloproteinases Production and Regulated Angiogenesis. *J. Immunol.* **170**, 3369–3376 (2003).
77. Deshmane, S. L., Kremlev, S., Amini, S. & Sawaya, B. E. Monocyte Chemoattractant Protein-1 (MCP-1): An Overview. *J. Interf. Cytokine Res.* **29**, 313 (2009).
78. Menten, P., Wuyts, A. & Van Damme, J. Macrophage inflammatory protein-1. *Cytokine Growth Factor Rev.* **13**, 455–481 (2002).
79. Zelová, H. & Hošek, J. TNF-α signalling and inflammation: interactions between old acquaintances. *Inflamm. Res. 2013 627* **62**, 641–651 (2013).
80. Bradley, J. TNF-mediated inflammatory disease. *J. Pathol.* **214**, 149–160 (2008).
81. Nelms, K., Keegan, A. D., Zamorano, J., And, J. J. R. & Paul, W. E. The IL-4 Receptor: Signaling Mechanisms and Biologic Functions. *Annu. Rev. Immunol.* **17**, 701–738 (2003).
82. Junttila, I. S. Tuning the Cytokine Responses: An Update on Interleukin (IL)-4 and IL-13 Receptor Complexes. *Front. Immunol.* **9**, (2018).
83. Martire-Greco, D. *et al.* Interleukin-10 controls human peripheral PMN activation triggered by lipopolysaccharide. *Cytokine* **62**, 426–432 (2013).
84. Moore, K. W., de Waal Malefyt, R., Coffman, R. L. & O'Garra, A. Interleukin-10 and the interleukin-10 receptor. *Annu. Rev. Immunol.* **19**, 683–765 (2001).
85. Bao, P. *et al.* The Role of Vascular Endothelial Growth Factor in Wound Healing. *J. Surg. Res.* **153**, 347–358 (2009).
86. Schwarz, F., Derks, J., Monje, A. & Wang, H.-L. Peri-implantitis. *J. Clin. Periodontol.* **45**, S246–S266 (2018).
87. Harris, W. The problem is osteolysis. *Clin. Orthop. Relat. Res.* 46–53 (1995).
88. Man, K., Jiang, L.-H., Foster, R. & Yang, X. B. Immunological Responses to Total Hip Arthroplasty. *J. Funct. Biomater. 2017, Vol. 8, Page 33* **8**, 33 (2017).
89. Abu-Amer, Y., Darwech, I. & Clohisy, J. C. Aseptic loosening of total joint replacements: mechanisms underlying osteolysis and potential therapies. *Arthritis Res. Ther. 2007 91* **9**, 1–7 (2007).
90. Prantl, L. *et al.* Clinical and morphological conditions in capsular contracture formed around silicone breast implants. *Plast. Reconstr. Surg.* **120**, 275–284 (2007).
91. Kohro, T. *et al.* A comparison of differences in the gene expression profiles of phorbol 12-myristate 13-acetate differentiated THP-1 cells and human monocyte-derived macrophage. *J. Atheroscler. Thromb.* **11**, 88–97 (2004).
92. Schildberger, A., Rossmanith, E., Eichhorn, T., Strassl, K. & Weber, V. Monocytes, peripheral blood mononuclear cells, and THP-1 cells exhibit different cytokine expression patterns following stimulation with lipopolysaccharide. *Mediators Inflamm.* **2013**, (2013).
93. Julier, Z., Park, A. J., Briquez, P. S. & Martino, M. M. Promoting tissue regeneration by modulating the immune system. *Acta Biomater.* **53**, 13–28 (2017).
94. Davenport Huyer, L. *et al.* Advanced Strategies for Modulation of the Material–

Macrophage Interface. *Adv. Funct. Mater.* **30**, (2020).
95. Anselme, K. *et al.* Qualitative and quantitative study of human osteoblast adhesion on materials with various surface roughnesses. *J. Biomed. Mater. Res.* **49**, 155–166 (2000).
96. Baharloo, B., Textor, M. & Brunette, D. M. Substratum roughness alters the growth, area, and focal adhesions of epithelial cells, and their proximity to titanium surfaces. *J. Biomed. Mater. Res. Part A* **74A**, 12–22 (2005).
97. Eisenbarth, E., Meyle, J., Nachtigall, W. & Breme, J. Influence of the surface structure of titanium materials on the adhesion of fibroblasts. *Biomaterials* **17**, 1399–1403 (1996).
98. Rostam, H. M. *et al.* The impact of surface chemistry modification on macrophage polarisation. *Immunobiology* **221**, 1237–1246 (2016).
99. Hotchkiss, K. M., Ayad, N. B., Hyzy, S. L., Boyan, B. D. & Olivares-Navarrete, R. Dental implant surface chemistry and energy alter macrophage activation in vitro. *Clin. Oral Implants Res.* **28**, 414–423 (2017).
100. Brodbeck, W. G. *et al.* Biomaterial surface chemistry dictates adherent monocyte / macrophage cytokine expression in vitro. *Cytokine* **18**, 311–319 (2002).
101. Bridges, A. W. *et al.* Reduced acute inflammatory responses to microgel conformal coatings. *Biomaterials* **29**, 4605–4615 (2008).
102. Kajahn, J. *et al.* Artificial extracellular matrices composed of collagen I and high sulfated hyaluronan modulate monocyte to macrophage differentiation under conditions of sterile inflammation. *Biomatter.* **2**, 226–273 (2012).
103. Decher, G. Fuzzy Nanoassemblies: Toward Layered Polymeric Multicomposites. *Science (80-.).* **277**, 1232–1237 (1997).
104. Richert, L. *et al.* Cell interactions with polyelectrolyte multilayer films. *Biomacromolecules* **3**, 1170–1178 (2002).
105. Knopf-Marques, H. *et al.* Immunomodulation with Self-Crosslinked Polyelectrolyte Multilayer-Based Coatings. *Biomacromolecules* **17**, 2189–2198 (2016).
106. Mendelsohn, J. D., Yang, S. Y., Hiller, J., Hochbaum, A. I. & Rubner, M. F. Rational Design of Cytophilic and Cytophobic Polyelectrolyte Multilayer Thin Films. *Biomacromolecules* **4**, 96–106 (2002).
107. Thompson, M. T., Berg, M. C., Tobias, I. S., Rubner, M. F. & Van Vliet, K. J. Tuning compliance of nanoscale polyelectrolyte multilayers to modulate cell adhesion. *Biomaterials* **26**, 6836–6845 (2005).
108. Tryoen-Tóth, P. *et al.* Viability, adhesion, and bone phenotype of osteoblast-like cells on polyelectrolyte multilayer films. *J. Biomed. Mater. Res.* **60**, 657–667 (2002).
109. Yoo, D., Shiratori, S. S. & Rubner, M. F. Controlling Bilayer Composition and Surface Wettability of Sequentially Adsorbed Multilayers of Weak Polyelectrolytes. *Macromolecules* **31**, 4309–4318 (1998).
110. Criado-Gonzalez, M., Mijangos, C. & Hernández, R. Polyelectrolyte Multilayer Films Based on Natural Polymers: From Fundamentals to Bio-Applications. *Polym. 2021, Vol. 13, Page 2254* **13**, 2254 (2021).
111. Guo, S., Zhu, X. & Loh, X. J. Controlling cell adhesion using layer-by-layer approaches for biomedical applications. *Mater. Sci. Eng. C* **70**, 1163–1175 (2017).
112. Ogle, M. E., Segar, C. E., Sridhar, S. & Botchwey, E. A. Monocytes and macrophages in tissue repair: Implications for immunoregenerative biomaterial design. *Exp Biol Med* **241**, 1084–1097 (2016).
113. Mosser, D. M. & Edwards, J. P. Exploring the full spectrum of macrophage activation. *Nat. Rev. Immunol. 2008 812* **8**, 958–969 (2008).
114. Sridharan, R., Cameron, A. R., Kelly, D. J., Kearney, C. J. & O'Brien, F. J. Biomaterial based modulation of macrophage polarization: a review and suggested design principles. *Mater. Today* **18**, 313–325 (2015).
115. Klopfleisch, R. & Jung, F. The pathology of the foreign body reaction against biomaterials. *J. Biomed. Mater. Res. Part A* **105**, 927–940 (2017).
116. Brodbeck, W. G., MacEwan, M., Colton, E., Meyerson, H. & Anderson, J. M. Lymphocytes and the foreign body response: Lymphocyte enhancement of macrophage

adhesion and fusion. *J. Biomed. Mater. Res. Part A* **74A**, 222–229 (2005).
117. Chen, H. *et al.* The promotion of type 1 T helper cell responses to cationic polymers in vivo via toll-like receptor-4 mediated IL-12 secretion. *Biomaterials* **31**, 8172–8180 (2010).
118. Chang, D. T., Colton, E., Matsuda, T. & Anderson, J. M. Lymphocyte adhesion and interactions with biomaterial adherent macrophages and foreign body giant cells. *J. Biomed. Mater. Res. Part A* **91A**, 1210–1220 (2009).
119. Bornstein, M. M., Wittneben, J.-G., Brägger, U. & Buser, D. Early Loading at 21 Days of Non-Submerged Titanium Implants With a Chemically Modified Sandblasted and Acid-Etched Surface: 3-Year Results of a Prospective Study in the Posterior Mandible. *J. Periodontol.* **81**, 809–818 (2010).
120. Lang, N. P. *et al.* Early osseointegration to hydrophilic and hydrophobic implant surfaces in humans. *Clin Oral Implant. Res* **Apr**, 349–56 (2011).
121. Nicolau, P. *et al.* 10-year outcomes with immediate and early loaded implants with a chemically modified SLA surface. *Quintessence Int* **50**, 114–124 (2019).
122. Sulahian, T. H. *et al.* Human monocytes express CD163, which is upregulated by IL-10 and identical to p155. *Cytokine* **12**, 1312–1321 (2000).
123. Major, M. R., Wong, V. W., Nelson, E. R., Longaker, M. T. & Gurtner, G. C. The Foreign Body Response: At the Interface of Surgery and Bioengineering. *Plast. Reconstr. Surg.* **135**, 1489–1498 (2015).
124. Owen, G. R., Jackson, J., Chehroudi, B., Burt, H. & Brunette, D. M. A PLGA membrane controlling cell behaviour for promoting tissue regeneration. *Biomaterials* **26**, 7447–7456 (2005).
125. Barth, K. A., Waterfield, J. D. & Brunette, D. M. The effect of surface roughness on RAW 264.7 macrophage phenotype. *J. Biomed. Mater. Res. Part A* **101A**, 2679–2688 (2013).
126. del Fabbro, M. *et al.* Osseointegration of Titanium Implants with Different Rough Surfaces: A Histologic and Histomorphometric Study in an Adult Minipig Model. *Implant Dent.* **26**, 357–366 (2017).
127. Buser, D. *et al.* Influence of surface characteristics on bone integration of titanium implants. A histomorphometric study in miniature pigs. *J. Biomed. Mater. Res.* **25**, 889–902 (1991).
128. Bota, P. C. S. *et al.* Biomaterial topography alters healing in vivo and monocyte/macrophage activation in vitro. *J. Biomed. Mater. Res. Part A* **95A**, 649–657 (2010).
129. Castel, N., Soon-Sutton, T., Deptula, P., Flaherty, A. & Parsa, F. D. Polyurethane-Coated Breast Implants Revisited: A 30-Year Follow-Up. *Arch. Plast. Surg.* **42**, 186 (2015).
130. Greenwood, J. E. & Wagstaff, M. J. D. The use of biodegradable polyurethane in the development of dermal scaffolds. *Adv. Polyurethane Biomater.* 631–662 (2016).
131. Fernando, S., McEnery, M. & Guelcher, S. A. Polyurethanes for bone tissue engineering. *Adv. Polyurethane Biomater.* 481–501 (2016).
132. Hong, Y. Electrospun fibrous polyurethane scaffolds in tissue engineering. *Adv. Polyurethane Biomater.* 543–559 (2016).
133. Schutte, R. J., Parisi-Amon, A. & Reichert, W. M. Cytokine profiling using monocytes/macrophages cultured on common biomaterials with a range of surface chemistries. *J. Biomed. Mater. Res. Part A* **88A**, 128–139 (2009).
134. Monaco, C., Andreakos, E., Kiriakidis, S., Feldmann, M. & Paleolog, E. T-cell-mediated signalling in immune, inflammatory and angiogenic processes: The cascade of events leading to inflammatory diseases. *Curr. Drug Targets Inflamm. Allergy* **3**, 35–42 (2004).
135. Abaricia, J. O., Shah, A. H., Musselman, R. M. & Olivares-Navarrete, R. Hydrophilic titanium surfaces reduce neutrophil inflammatory response and NETosis. *Biomater. Sci.* **8**, 2289–2299 (2020).
136. Abaricia, J. O. *et al.* Control of innate immune response by biomaterial surface topography, energy, and stiffness. *Acta Biomater.* **133**, 58–73 (2021).
137. Butterfield, T. A., Best, T. M. & Merrick, M. A. The Dual Roles of Neutrophils and

Macrophages in Inflammation: A Critical Balance Between Tissue Damage and Repair. *J. Athl. Train.* **41**, 457 (2006).
138. Selders, G. S., Fetz, A. E., Radic, M. Z. & Bowlin, G. L. An overview of the role of neutrophils in innate immunity, inflammation and host-biomaterial integration. *Regen. Biomater.* **4**, 55–68 (2017).
139. Shayan, M. *et al.* Nanopatterned bulk metallic glass-based biomaterials modulate macrophage polarization. *Acta Biomater.* **75**, 427–438 (2018).
140. Baier, R. E. & Dutton, R. C. Initial events in interactions of blood with a foreign surface. *J. Biomed. Mater. Res.* **3**, 191–206 (1969).
141. George B. Sigal, Milan Mrksich, and & Whitesides*, G. M. Effect of Surface Wettability on the Adsorption of Proteins and Detergents. *J. Am. Chem. Soc.* **120**, 3464–3473 (1998).
142. Kim, Y. K., Que, R., Wang, S.-W. & Liu, W. F. Modification of Biomaterials with a Self-Protein Inhibits the Macrophage Response. *Adv. Healthc. Mater.* **3**, 989–994 (2014).
143. Kang, C.-K. & Lee, Y.-S. The surface modification of stainless steel and the correlation between the surface properties and protein adsorption. *J. Mater. Sci. Mater. Med. 2007 187* **18**, 1389–1398 (2007).
144. Brodbeck, W. G., Colton, E. & Anderson, J. M. Effects of adsorbed heat labile serum proteins and fibrinogen on adhesion and apoptosis of monocytes/macrophages on biomaterials. *J. Mater. Sci. Mater. Med. 2003 148* **14**, 671–675 (2003).
145. Maciel, J., Oliveira, M. I., Gonalves, R. M. & Barbosa, M. A. The effect of adsorbed fibronectin and osteopontin on macrophage adhesion and morphology on hydrophilic and hydrophobic model surfaces. *Acta Biomater.* **8**, 3669–3677 (2012).
146. Battiston, K. G. *et al.* Interaction of a block-co-polymeric biomaterial with immunoglobulin G modulates human monocytes towards a non-inflammatory phenotype. *Acta Biomater.* **24**, 35–43 (2015).
147. Yang, M. *et al.* Apolipoprotein A-II induces acute-phase response associated AA amyloidosis in mice through conformational changes of plasma lipoprotein structure. *Sci. Reports 2018 81* **8**, 1–11 (2018).
148. Thompson, P. A., Berbée, J. F. P., Rensen, P. C. N. & Kitchens, R. L. Apolipoprotein A-II augments monocyte responses to LPS by suppressing the inhibitory activity of LPS-binding protein: *Innate Immun.* **14**, 365–374 (2008).
149. Barlage, S. *et al.* Changes in HDL-associated apolipoproteins relate to mortality in human sepsis and correlate to monocyte and platelet activation. *Intensive Care Med. 2009 3511* **35**, 1877–1885 (2009).
150. Medeiros, L. A. *et al.* Fibrillar Amyloid Protein Present in Atheroma Activates CD36 Signal Transduction. *J. Biol. Chem.* **279**, 10643–10648 (2004).
151. Zewinger, S. *et al.* Apolipoprotein C3 induces inflammation and organ damage by alternative inflammasome activation. *Nat. Immunol. 2019 211* **21**, 30–41 (2019).
152. Han, X. *et al.* Apolipoprotein CIII regulates lipoprotein-associated phospholipase A 2 expression via the MAPK and NFkB pathways. *Biol Open.* **4(5)**, 661–5 (2015).
153. Shim, Y.-J. *et al.* Clusterin induces matrix metalloproteinase-9 expression via ERK1/2 and PI3K/Akt/NF-B pathways in monocytes/macrophages. *J. Leukoc. Biol* **90**, 761–769 (2011).
154. Hyka, N. *et al.* Apolipoprotein A-I inhibits the production of interleukin-1β and tumor necrosis factor-α by blocking contact-mediated activation of monocytes by T lymphocytes. *Blood* **97**, 2381–2389 (2001).
155. Baitsch, D. *et al.* Apolipoprotein E Induces Antiinflammatory Phenotype in Macrophages. *Arterioscler. Thromb. Vasc. Biol.* **31**, 1160–1168 (2011).
156. Murphy, A. J. *et al.* High-Density Lipoprotein Reduces the Human Monocyte Inflammatory Response. *Arterioscler. Thromb. Vasc. Biol.* **28**, 2071–2077 (2008).
157. Treindl, F. *et al.* A bead-based western for high-throughput cellular signal transduction analyses. *Nat. Commun. 2016 71* **7**, 1–11 (2016).
158. Bhatia, N. & El-Chami, M. Leadless pacemakers: a contemporary review. *J. Geriatr. Cardiol.* **15**, 249 (2018).

159. Rupp, M., Lau, E., Kurtz, S. M. & Alt, V. Projections of Primary TKA and THA in Germany from 2016 through 2040. *Clin. Orthop. Relat. Res.* **478**, 1622–1633 (2020).
160. Price, A. J. *et al.* Knee replacement. *Lancet* **392**, 1672–1682 (2018).
161. Jin, W. *et al.* T cell activation and immune synapse organization respond to the microscale mechanics of structured surfaces. *Proc. Natl. Acad. Sci.* **116**, 19835–19840 (2019).
162. Judokusumo, E., Tabdanov, E., Kumari, S., Dustin, M. L. & Kam, L. C. Mechanosensing in T Lymphocyte Activation. *Biophys. J.* **102**, L5–L7 (2012).
163. Murphy, K. & Casey, W. *Janeway's Immunobiology - 9th Edition*. (Garland science, 2016).
164. Chang, D. T., Colton, E. & Anderson, J. M. Paracrine and juxtacrine lymphocyte enhancement of adherent macrophage and foreign body giant cell activation. *J. Biomed. Mater. Res. Part A* **89A**, 490–498 (2009).
165. MacEwan, M. R., Brodbeck, W. G., Matsuda, T. & Anderson, J. M. Monocyte/lymphocyte interactions and the foreign body response: In vitro effects of biomaterial surface chemistry. *J. Biomed. Mater. Res. Part A* **74A**, 285–293 (2005).
166. Sadtler, K. *et al.* The Scaffold Immune Microenvironment: Biomaterial-Mediated Immune Polarization in Traumatic and Nontraumatic Applications. *Tissue Eng. Part A* **23**, 1044 (2017).
167. Griffin, D. R. *et al.* Activating an adaptive immune response from a hydrogel scaffold imparts regenerative wound healing. *Nat. Mater. 2020 204* **20**, 560–569 (2020).
168. van Luyn, M. J., Khouw, I. M., van Wachem, P. B., Blaauw, E. H. & Werkmeister, J. A. Modulation of the tissue reaction to biomaterials. II. The function of T cells in the inflammatory reaction to crosslinked collagen implanted in T-cell-deficient rats. *J. Biomed. Mater. Res.* **39**, 398–406 (1998).
169. Revell, P. A. The combined role of wear particles, macrophages and lymphocytes in the loosening of total joint prostheses. *J. R. Soc. Interface* **5**, 1263–1278 (2008).
170. Bettinger, C. J., Langer, R. & Borenstein, J. T. Engineering Substrate Topography at the Micro- and Nanoscale to Control Cell Function. *Angew. Chemie Int. Ed.* **48**, 5406–5415 (2009).
171. Ross, A. M., Jiang, Z., Bastmeyer, M. & Lahann, J. Physical aspects of cell culture substrates: Topography, roughness, and elasticity. *Small* **8**, 336–355 (2012).
172. Harvey, A., Hill, T. & Bayat, A. Designing implant surface topography for improved biocompatibility. *Expert Rev. Med. Devices* **10**, 257–267 (2013).
173. Anselme, K., Ploux, L. & Ponche, A. Cell/material interfaces: Influence of surface chemistry and surface topography on cell adhesion. *J. Adhes. Sci. Technol.* **24**, 831–852 (2010).
174. Miao, X. *et al.* The response of human osteoblasts, epithelial cells, fibroblasts, macrophages and oral bacteria to nanostructured titanium surfaces: a systematic study. *Int. J. Nanomedicine* **12**, 1415 (2017).
175. Roch, T. *et al.* Immunological evaluation of polystyrene and poly(ether imide) cell culture inserts with different roughness. *Clin. Hemorheol. Microcirc.* **52**, 375–389 (2012).
176. Singh, S. *et al.* Unbiased Analysis of the Impact of Micropatterned Biomaterials on Macrophage Behavior Provides Insights beyond Predefined Polarization States. *ACS Biomater. Sci. Eng.* **3**, 969–978 (2017).
177. Zdrahala, R. J. & Zdrahala, I. J. Biomedical applications of polyurethanes: a review of past promises, present realities, and a vibrant future. *J. Biomater. Appl.* **14**, 67–90 (1999).
178. Anselme, K., Ponche, A. & Bigerelle, M. Relative influence of surface topography and surface chemistry on cell response to bone implant materials. Part 2: biological aspects. *Proc. Inst. Mech. Eng. H.* **224**, 1487–1507 (2010).
179. Webster, T., Schadler, L., Siegel, R. & Bizios, R. Mechanisms of enhanced osteoblast adhesion on nanophase alumina involve vitronectin. *Tissue Eng.* **7**, 291–301 (2001).
180. Lord, M. S., Foss, M. & Besenbacher, F. Influence of nanoscale surface topography on protein adsorption and cellular response. *Nano Today* **5**, 66–78 (2010).

181. Rostam, H. M., Singh, S., Vrana, N. E., Alexander, M. R. & Ghaemmaghami, A. M. Impact of surface chemistry and topography on the function of antigen presenting cells. *Biomater. Sci.* **3**, 424–441 (2015).
182. Zhou, G., Niepel, M. S., Saretia, S. & Groth, T. Reducing the inflammatory responses of biomaterials by surface modification with glycosaminoglycan multilayers. *J. Biomed. Mater. Res. Part A* **104**, 493–502 (2016).
183. Meng, S. *et al.* The effect of a layer-by-layer chitosan-heparin coating on the endothelialization and coagulation properties of a coronary stent system. *Biomaterials* **30**, 2276–2283 (2009).
184. García, A. J. Get a grip: integrins in cell–biomaterial interactions. *Biomaterials* **26**, 7525–7529 (2005).
185. Shin, H., Jo, S. & Mikos, A. G. Biomimetic materials for tissue engineering. *Biomaterials* **24**, 4353–4364 (2003).
186. Hersel, U., Dahmen, C. & Kessler, H. RGD modified polymers: biomaterials for stimulated cell adhesion and beyond. *Biomaterials* **24**, 4385–4415 (2003).
187. Cornelius, R. M., Archambault, J. & Brash, J. L. Identification of apolipoprotein A-I as a major adsorbate on biomaterial surfaces after blood or plasma contact. *Biomaterials* **23**, 3583–3587 (2002).
188. Magnani, A. *et al.* Two-step elution of human serum proteins from different glass-modified bioactive surfaces: A comparative proteomic analysis of adsorption patterns. *Electrophoresis* **25**, 2413–2424 (2004).
189. Rostam, H. M. *et al.* Immune-Instructive Polymers Control Macrophage Phenotype and Modulate the Foreign Body Response In Vivo. *Matter* **2**, 1564–1581 (2020).
190. Romero-Gavilan, F. *et al.* Bioactive potential of silica coatings and its effect on the adhesion of proteins to titanium implants. *Colloids Surfaces B Biointerfaces* **162**, 316–325 (2018).
191. Schöttler, S. *et al.* Protein adsorption is required for stealth effect of poly(ethylene glycol)- and poly(phosphoester)-coated nanocarriers. *Nat. Nanotechnol. 2016 114* **11**, 372–377 (2016).

Acknowledgements

Eine Promotionsarbeit ist nicht das Werk eines einzelnen, sondern entsteht durch die Zusammenarbeit vieler Personen. Bedanken möchte ich mich daher bei Prof. Katja Schenke-Layland für das Ermöglichen der Promotion am NMI sowie die fachliche Unterstützung und den Blick auf das große Ziel. Ebenso bedanken möchte ich mich bei meinem Zweitprüfer Prof. Alexander Weber für wissenschaftliche Diskussionen und den kritischen Blick von außen.

Ein sehr großer Dank geht an meine Betreuer Dr. Christopher Shipp und Dr. Hanna Hartmann, die mir in den verschiedenen Abschnitten der Promotion mit wissenschaftlichen Ideen, kritischen Rückfragen und Verbesserungsvorschlägen zur Seite standen, jederzeit eine sprichwörtlich offene Tür bei Fragen oder Problemen hatten und mir den Arbeitsgruppenwechsel leichtgemacht haben.

Auch bei allen Personen, die am experimentellen Inhalt an dieser Arbeit und den Publikationen mitgewirkt haben möchte ich mich herzlich bedanken. Nur durch ausgezeichnete Zusammenarbeit war es möglich, Erkenntnisse aus Immunologie und Materialwissenschaft zu vereinen. Hier habe ich auch die offene und einfache Kommunikation untereinander sehr geschätzt.

Ein weiterer Dank gilt allen Freunden und Kollegen, die als Teil meiner beiden Arbeitsgruppen stets bereit waren über wissenschaftliche Probleme und Ideen zu diskutieren und zugleich meinen Arbeitsalltag verschönert haben: Nora, Bernie, Elena, Kathi, Dmitri und Isi.

Auch bei vielen weiteren Doktoranden des NMI sowie insbesondere der Innovationsallianz möchte ich mich für das fantastische soziale Umfeld und die vielen gemeinsamen Stunden innerhalb und außerhalb des Institutes bedanken.

Bedanken möchte ich mich auch bei dir Marie für die regelmäßig benötigte Motivation sowie die große Geduld für die lange Ausbildungs- und Doktorandenzeit. Es ist jetzt geschafft.

Declaration

Ich erkläre hiermit, dass ich die zur Promotion eingereichte Arbeit mit dem Titel “Systematic investigation of the interplay between biomaterials and the immune system in vitro ” selbstständig verfasst, nur die angegebenen Quellen und Hilfsmittel benutzt und wörtlich oder inhaltlich übernommene Zitate also solche gekennzeichnet habe. Ich erkläre, dass die Richtlinien zur Sicherung guter wissenschaftlicher Praxis der Universität Tübingen beachtet wurden. Ich versichere an Eides statt, dass diese Angaben wahr sind und dass ich nichts verschwiegen habe. Mir ist bekannt, dass die falsche Angabe einer Versicherung an Eides statt mit Freiheitsstrafe bis zu drei Jahren oder mit Geldstrafe bestraft wird.

Florian Billing

Appendices

Appendix I

Billing F., et al. The immune response to the SLActive titanium dental implant surface in vitro is predominantly driven by innate immune cells. *Journal of Immunology and Regenerative Medicine. 13, 2021*

Journal of Immunology and Regenerative Medicine 13 (2021) 100047

Contents lists available at ScienceDirect

Journal of Immunology and Regenerative Medicine

journal homepage: www.elsevier.com/locate/regen

The immune response to the SLActive titanium dental implant surface in vitro is predominantly driven by innate immune cells

Florian Billing [a,*], Meike Jakobi [a], Dagmar Martin [a], Karin Gerlach [a], Elsa Arefaine [a], Martin Weiss [a,b], Nicole Schneiderhan-Marra [a], Hanna Hartmann [a], Christopher Shipp [a]

[a] NMI, Natural and Medical Sciences Institute at the University of Tübingen, Markwiesenstr. 55, 72770, Reutlingen, Germany
[b] Department of Women's Health, University of Tübingen, Calwerstraße 7, 72076, Tübingen, Germany

ARTICLE INFO

Keywords:
Titanium dental implants
Immune response
Monocytes
Adaptive immune cells
PBMC

ABSTRACT

Biomaterial characteristics such as topography and wettability have been shown to influence the immune response to implanted medical devices. Thus, appropriate surface design considering the immune system has moved more into focus. Previous in vitro studies have commonly employed simplistic immune models and as such, the role of different immune cell populations, particularly those of the adaptive immune system, is still poorly understood. Here, we employed a biologically complex human-based in vitro model consisting of peripheral blood mononuclear cells (PBMC) to examine interactions between cells of the innate and adaptive immune system in the context of clinically used implants. To achieve this, five differently treated titanium surfaces were characterised in terms of physicochemical properties using contact angle measurement, XPS and confocal scanning microscopy. Cytokine analysis revealed different material surface properties to result in different immune responses with SLActive surface showing low levels of IL-6 and IL-8 but high levels of MCP-1. Cytokine and surface marker analysis in isolated populations of monocytes and lymphocytes and defined ratios revealed lymphocytes alone to be unaffected by the SLActive biomaterial and except for a slight effect on HLA-DR expression indicated no activation of monocytes by lymphoid cells. On lymphocytes, CD16 and HLA-DR expression was unaffected by monocytes under physiological conditions but was elevated with high levels of monocytes present. Intracellular cytokine staining in whole PBMC cultures confirmed monocytes to be responsible for the observed immune response, with minimal involvement of lymphocytes. Expression of the pro-inflammatory cytokines IL-8 and TNF-α in monocytes peaked 12 h after biomaterial contact, while the expression of surface markers HLA-DR and CD86 continued to rise 72 h following contact. These results collectively suggest the immune response to titanium biomaterials in the first 72 h in vitro to be almost exclusively driven by the innate rather than the adaptive immune system.

1. Introduction

The performance of an implanted medical device largely depends on a patient's immune response to that device. While some implants are typically well tolerated by the immune system, others have been found to provoke excessive inflammatory responses or to result in patient side effects.[1–4] The immune response to a biomaterial is primarily dependent on its physical and chemical properties, particularly on the surface of the implant. Specifically, characteristics including surface roughness and wettability can influence the immune response towards a biomaterial, resulting in either a pro-healing response or in the development of chronic inflammation that may contribute to fibrotic encapsulation or other local tissue reactions such as bone loss and implant loosening.[5] Hence in addition to the choice of a suitable material type, the role of surface design has drawn more and more attention.[6,7] For example, while titanium has become the gold standard material for dental implants, there is increasing interest in understanding how this material may be modified to influence the biological response to it.[8–10] Consequently, there are now a number of titanium implants in clinical use that have been manufactured with different surface characteristics.[9,11,12]

Upon biomaterial implantation in the body, monocytes and macrophages are one of the primary cell types involved in initiating the host response to the foreign material. Already during the process of implantation, foreign material makes contact with blood and is therefore

* Corresponding author.
E-mail address: florian.billing@nmi.de (F. Billing).

https://doi.org/10.1016/j.regen.2021.100047
Received 22 December 2020; Received in revised form 12 March 2021; Accepted 6 May 2021
Available online 24 May 2021

confronted by large numbers of monocytes and neutrophils as part of the initial immune response. If the foreign material has characteristics that initiate monocytes activation, these monocytes may adhere and release cytokines and chemokines which can then induce the migration and differentiation of other immune cell types such as T cells or additional monocytes from the blood.[13] If this response is sustained long enough the monocytes may mature into macrophages. Both myeloid cell types have the ability to initiate pro-inflammatory responses by releasing chemoattractants and inflammatory cytokines. Conversely, they play an essential role in wound healing and tissue regeneration following the resolution of inflammation.[14] Whether the inflammatory immune response resolves into a pro-generative state depends largely on the polarisation of the local myeloid cells. For example, their polarisation may tend towards a more pro-inflammatory M1-like phenotype, which perpetuates the ongoing inflammation, or may instead develop more into an M2-like phenotype, which curbs inflammation and promote tissue regeneration. This polarisation can also be observed in vitro, where biomaterial contact induces myeloid cells to develop into M1-or M2-like monocyte-derived macrophages.[15] It has become increasingly clear that implant surface characteristics, among other factors, play a major role in determining the polarisation state of local myeloid cells.[13,16,17]

In addition to monocytes and macrophages, other types of immune cells are also reported to influence the immune response to biomaterials. Lymphocytes, for example, can be activated by inflammatory processes and modulate the immune response by the nature and level of cytokines they produce. In the context of biomaterials, lymphocytes were demonstrated to have mechanosensing properties[18] and to be activated by cytokines released from macrophages, thus contributing to the immune response to biomaterials.[19] In one study, the degree of monocyte adhesion was found to be dependent on the presence of lymphocytes, while lymphocytes themselves strongly associated with the adherent monocytes. Furthermore, lymphocytes were shown to adhere to material surfaces like tissue culture polystyrene directly and their proliferation rate to be increased by the presence of macrophages.[20] Interestingly, biomaterial surface characteristics have also been shown to influence the nature of the interactions between lymphocytes and monocytes.[21] Collectively, these results demonstrate bi-directional interactions between monocytes/macrophages and lymphocytes. However, despite these early reports there is still a limited understanding of the possible interactions between different immune cell populations in the context of biomaterials. To address this, the aim of our study was to examine the immune response towards distinct titanium surfaces and furthermore investigate the interplay between lymphoid and myeloid cell types in the context of a biomaterial-induced immune response.

Previous studies investigating the effect of biomaterial surface properties on the immune response have typically employed simplistic models of the immune system, for example with the use of human or animal cell lines. Therefore, studies that consider the interplay of different immune cells in more biologically complex patient-derived models are lacking. As such, for this study we employed an immune model derived from peripheral blood consisting of innate immune cells like monocytes and natural killer cells along with components of the adaptive immune system such as helper and cytotoxic T cells, as well as a number of other immune cell types (collectively termed peripheral blood mononuclear cells or PBMCs). Using this model combined with single cell analysis techniques, our goal was to gain new insights into the nature of immune responses to titanium biomaterials with different surface characteristics. Specifically, we aimed to identify the major populations of immune cells which respond to clinically used titanium, and were furthermore interested in studying potential interactions between the different populations of immune cells. For this investigation, we studied a biomaterial with a well-documented history of clinical performance for use as a dental implant, the SLActive titanium material from the Straumann group.[22–24] The highly hydrophilic SLActive surface is reported to enable reduction of primary healing time and more rapid loading of implants,[25,26] is thought to induce low levels of inflammation[9] and has a well-documented history of good clinical performance for use as a dental implant.[27] Therefore, the SLActive surface represents an interesting biomaterial for immunological studies.

2. Experimental section

2.1. Materials

Experiments were performed using gamma-radiation sterilized grade 2 titanium implant materials, each manufactured to produce different surface characteristics. The five specimens investigated in this study had been (1) machine polished (2) acid etched (3) sandblasted (4) sandblasted and acid etched (SLA) and (5) sandblasted and acid etched including a hydrophilic treatment (SLActive) (all provided by Straumann AG, Basel, Switzerland). All disks were sized with a diameter of 15 mm in order to fit securely in 24 well plates. No pre-treatment was applied to the titanium specimens prior to culture.

2.2. White light confocal scanning microscopy

The surface of the titanium samples was characterised by a white light confocal microscope (ConScan, CSM Instruments, Peseux, Switzerland) using a white light beam of 2 μm Ø. An area of 2.5 mm × 2.5 mm of the titanium samples was scanned with a lateral resolution of 500 pixels per mm to summarise their topographical characteristics as an overall image with axial accuracy in the nanometer range. The raw data was levelled by the subtraction of the mean plane computed from all image points. To separate the roughness dataset from the waviness dataset, the levelled primary dataset was filtered by a phase correct Gaussian filter using a cut-off wavelength λc of 80 μm for the machine polished sample and 250 μm for all other samples. From these filtered roughness data surface texture parameters were derived (for example Sa representing average roughness).

2.3. Photoelectron spectroscopy (XPS)

The measurements of the titanium specimens were conducted in a scanning XPS microprobe (Quantera SXM, Physical Electronics Inc., Chanhassen MN, USA), which is equipped with a monochromatic Al Kα source. Survey spectra were measured at 240 eV pass energy and individual high-resolution core level spectra at 55 eV pass energy. Both were subsequently calibrated to the C 1s signal at 284.8 eV (adventitious carbon). All measurements were performed using an x-ray beam of 50 W and 200 μm beam diameter. The spectra were analysed using MultiPak software version 9.9.0.9 (Ulvac-PHI).

2.4. Water contact angle measurement

The wettability of each sample was determined by sessile drop measurements of the water contact angle (θ) using a Krüss EasyDrop contact angle goniometer (Hamburg, Germany). To perform the measurements, a static drop was used, maintaining a constant volume during the measurement. This was performed with the addition of 2 μL distilled water to the samples. After 20 s, an image was recorded and transferred to the software for analysis of the static (equilibrium) contact angles. Ten independent measurements were performed to give mean values ± standard deviation. With this method, contact angles from 10° (hydrophilic surface) to 100° (hydrophobic surface) can be quantified.

2.5. Isolation of PBMC from whole blood

Whole blood samples of healthy volunteers were taken at the Department of Women's Health in Tübingen between February 2019 and March 2020 after written informed consent. The scientific use of the whole blood samples was approved by the Ethical Committee of the

Medical Faculty of the Eberhard-Karls-University Tübingen (495-2018BO2). In total, blood from six different donors (three males, age 27–60 and three females, age 31–54) was used for the experiments. Potential donors were screened with exclusion criteria (chronic inflammatory disease, surgical intervention within the last three months, infection or use of medications affecting the immune system in the past two weeks, vaccination in the previous six weeks, excess alcohol consumption or strenuous exercise prior to donation) to minimise the influence by environmental factors known to alter the immune system. All blood draws took place in the morning hours (9–11 a.m.) to ensure consistency. Immediately after the blood drawn, PBMCs were isolated by density gradient centrifugation using SepMate™ isolation tubes (StemCell Technologies, Cologne, Germany) according to the manufacturer's protocol. Testing for isolation quality showed purity of PBMCs population to be 99.76%. Isolated PBMCs were stored at −150 °C in medium containing 10% DMSO (Sigma-Aldrich, Hamburg, Germany) which was added progressively to the solution to minimise osmotic shock, 20% FCS (SAFC Biosciences (Sigma-Aldrich), Hamburg, Germany) and 70% RPMI (RPMI-1640, Gibco, Paisley, Scotland) until use. Prior to seeding, cells were thawed in a 37 °C water bath followed by serial dilution of the freezing medium, such that the initial volume was diluted 1:4 with RPMI (Gibco) before centrifugation and discard of the supernatant. The freezing/thawing procedure did not affect the cellular activity of the cells (Supplementary information 1). Viability of the PBMCs was assessed prior to each experiment by Trypan blue exclusion and was greater than 97% in all cases.

2.6. Cell culture

For all experiments, cells were cultured in IMDM (Gibco) medium containing GlutaMAX supplemented with 10% off-the-clot serum pooled from male AB blood group donors (H2B). Unless otherwise mentioned, cells were seeded at a density of 7.5×10^5 cells in 500 μL medium. A combination of PHA-L (15 μg/ml; Roche, Mannheim, Germany) and LPS (100 ng/ml; Hycultec, Uden, Netherlands) stimulation was used as a positive control to ensure cell functionality, while untreated cells served as negative controls. All cultures were performed in 24 well tissue culture treated pyrogen-free plates (Sarstedt, Nürnbrecht, Germany) and were incubated at 37 °C and 5% CO_2 in a humidified atmosphere. The culture period was 72 h, except for time-dependent analyses where samples were examined also after 12 h or 24 h. Throughout all culturing periods medium was not exchanged, which allowed non-adherent cells to remain in the culture and to potentially interact with adherent cells via contact independent mechanisms. All experiments were conducted using PBMCs of three unique donors, each tested with 3 replicates for each condition unless otherwise stated. For experiments employing intracellular cytokine staining, 1x Brefeldin A (Biolegend, Amsterdam, Netherlands) was applied to the culture 12 h prior to harvesting to prevent cytokine secretion. In the case of experiments assessing secreted cytokines, multiplex (Luminex) immunoassays were employed. For this, 190 μL cell culture medium was collected following the culture period and centrifuged at 5000 RPM for 3 min. The supernatant was then collected and stored at −80 °C until analysis. Following the culture period cells were harvested in the following manner: non-adherent cells were removed by pipette resuspension of the cell culture medium followed by rinsing with PBS (Gibco). Adherent cells were subsequently detached by incubation with 10 mM EDTA (Invitrogen, Carlsbad, USA) (diluted in PBS) at 37 °C. After 5 min, an equal volume of PBS was added and cells were detached thorough pipette resuspension. Both fractions of cells were pooled prior to flow cytometric analysis.

2.7. Cytokine analysis using multiplexed bead-based sandwich immunoassays

Levels of IL-1β, IL-1RA, IL-4, IL-6, IL-8, IL-10, IL-12p70, IL-13, GM-CSF, IFN-γ, MCP-1, MIP-1β, TNF-α and VEGF were determined using two multiplex panels of Luminex-based sandwich immunoassays developed in-house, each consisting of commercially available capture and detection antibodies and calibrator proteins. All assays were thoroughly validated ahead of the study with respect to accuracy, precision, parallelism, robustness, specificity and sensitivity.[28,29] Samples were diluted at least 1:4 or higher. After incubation of the pre-diluted samples or calibrator protein with the capture coated microspheres, beads were washed and incubated with biotinylated detection antibodies. Streptavidin-phycoerythrin was added after an additional washing step for visualization. For control purposes, calibrators and quality control samples were included on each microtiter plate. All measurements were performed on a Luminex FlexMap® 3D analyser system, using Luminex xPONENT® 4.2 software (Luminex, Austin, USA). For data analysis MasterPlex QT, version 5.0 was employed. Standard curve and quality control samples were evaluated according to internal criteria adapted to the Westgard Rules to ensure proper assay performance.[30]

2.8. Isolation of monocytes and culturing in defined ratios

Magnetic cell sorting was used to isolate monocytes from whole PBMC according to manufacturer's instructions for positive selection of $CD14^+$ cells (Miltenyi Biotec, Auburn, USA). The negative fraction of cells following isolation were utilised as lymphocytes. After isolation, cells were seeded on the titanium surfaces at the following ratio of monocytes to lymphocytes: monocytes alone (6×10^5), 2:1 (6×10^5 monocytes and 3×10^5 lymphocytes), 1:2 (2×10^5 monocytes and 4×10^5 lymphocytes), 1:9 (0.6×10^5 monocytes and 5.4×10^5 lymphocytes) and lymphocytes alone (6×10^5). Responsiveness to chemical stimulation was assessed in a preliminary experiment to ensure functionality of the isolated cells.

2.9. Flow cytometry

Freshly harvested cells were first rinsed in washing buffer (2% FCS, 2 mM EDTA, 0.05% sodium azide, pH 7.4 (Sigma-Aldrich, USA)) and centrifuged at 300 g for 5 min. After removal of the supernatant, cells were blocked using 10% human serum (diluted in washing buffer) for 20 min at RT. Samples were then washed, centrifuged and the supernatant discarded. For the labelling of cell surface proteins, antibodies were incubated for 30 min on ice (protected from light) using the antibodies in panel 1 (Supplementary information 2, Table 1,). For the staining of intracellular and cell surface proteins, antibodies recognising cell surface proteins were added first (see panel 2 in Supplementary information 2, Table 2). Following washing, intracellular proteins were labelled using a permeabilisation kit according to the manufacturer's instructions (Fixation/Permeabilisation solution kit, BD Bioscience, Heidelberg, Germany) before intracellular proteins were blocked for 10 min with 10% (v/v) human serum diluted in permeabilisation buffer. After washing, the intracellular antibodies were diluted in permeabilisation buffer and incubated for 30 min on ice in the dark (see Table 2 in Supplementary information 2 for a list of intracellular antibodies employed). After a last washing step, samples were analysed immediately following antibody staining using a BD LSRFortessa instrument (BD Bioscience) with FACS Diva software version 8.0.3 (BD Bioscience). All washing steps were performed with 1 ml washing buffer and centrifugation at 300*g* for 5 min. Data analysis was performed using FlowJo software v10 (BD) and analysed according to the gating strategy shown in Supplementary information 3 and 4.

2.10. Statistical analysis

Data are displayed as mean ± standard error mean (SEM) for each donor. Statistic was applied as follows: One-factor, equal-variance analysis of variance (ANOVA) was used in order to test the null hypothesis that the group means are equal, against an alternative hypothesis that at least two of the group means are different using a

significance threshold of 0.05. For Fig. 1, ordinary one-way ANOVA was applied followed by Tukey multiple comparison test to compare the mean of each column with the mean of every other column. For Figs. 2, 3 and 5 the option of matched data was chosen to account for the comparison across donors (repeated measurement (RM) one-way ANOVA) followed by Dunnett's multiple comparison test to compare the mean of each column with the mean of the SLActive column (Figs. 2 and 3) or the mean of pure monocyte/lymphocyte cultures (Fig. 5 A/B, respectively). The same type of analysis was applied to Fig. 6B to compare cytokine expression across time with expression after 12 h or surface marker expression across time with expression after 72 h time point.

A paired *t*-test was used in Fig. 4 to compare the group of pure monocytes with a culture containing the same absolute number of monocytes but combined with a lymphocyte fraction of 33%. A paired *t*-test was also applied to Fig. 6A to compare cytokine positive fractions of monocytes and lymphocytes. All statistical analysis and plotting was performed with GraphPad Prism 8.4.3 (GraphPad Software, San Diego, USA).

3. Results

3.1. Physicochemical characterisation of titanium biomaterials

We first performed an assessment of the physicochemical properties of the five different titanium specimens studied here. To achieve this, we employed confocal scanning microscopy to map surface topography, performed x-ray photoelectron spectroscopy (XPS) to analyse surface chemistry and used the water contact angle method to assess surface wettability. Confocal scanning microscopy revealed the roughness of these specimens to range from rather smooth (machine polished surface (M), Sa 0.11 μm) to relatively rough for all surfaces that had been sandblasted (sandblasted (SL), Sa 3.30 μm; sandblasted and acid etched (SLA), Sa 3.17 μm; a version of SLA which had undergone hydrophilic treatment (SLActive), Sa 3.52 μm). The acid etched surface (A) showed a low to moderate degree of surface roughness (Sa 0.618 μm) in comparison (Fig. 1A). In terms of wettability, we found the surfaces to differ between each other in most cases while showing slight to moderate hydrophobic characteristics with contact angles between 70.9° (SL), 77.5° (M), 90.1° (A) and 97.5° (SLA) (Fig. 1B). The SLActive surface on the other hand was extremely hydrophilic with a contact angle below the quantification limit of 10°. XPS showed all surfaces to be relatively clean and to consist predominantly of oxygen and titanium, while carbon was also detected on each specimen as expected (Fig. 1C). The detection of aluminium on the SL and SLActive surfaces likely originates from the corundum particles used in the sandblasting process. Sodium and chloride were detected on the SLActive surface, which is most likely associated with its storage in saline buffer. Scoring of the physicochemical analysis is summarized in Table 1. The direct comparison shows that the surfaces differ in at least one (A/SLA) or more surface parameters.

3.2. Characterising the immune response to titanium surfaces using a human-based immune model

We next investigated potential differences in the biological response to the five titanium specimens using an in vitro model of the human immune system. This was achieved by culturing PBMCs directly on the biomaterial surfaces for 72 h, after which the immune response was assessed by quantifying the release of 14 pro- and anti-inflammatory cytokines, chemokines and growth factors. We observed differential immune responses associated with the different titanium surfaces investigated. For example, the acid etched surface was found to provoke generally the highest release of pro-inflammatory cytokines, as could be observed by the levels of TNF-α, IL-6, IL-8, IFN-γ and IL-1β (Fig. 2A). By comparison, the rough sandblasted surface tended to result in the lowest level of cytokine release, with the remaining specimens falling somewhere between this surface and the previously mentioned acid etched specimen. Interestingly, the specimen manufactured combining sandblasting and acid etching (SLA) also showed very little pro-inflammatory activity, indicating that the sandblasting process might outweigh the effects of acid etching. As described in the introduction, we expected the hydrophilic and rather rough SLActive surface to result in low levels of inflammation. Indeed, we observed the SLActive surface to induce significant lower levels of cytokines IL-6 and IL-8 compared to the hydrophobic and relatively smooth A surface ($p < 0.05$). Surprisingly, we found SLActive to result in higher concentrations for the initially acting chemokine MCP-1 compared to M, SL and SLA surfaces (Fig. 2A). For the anti-inflammatory cytokine IL-10, SLActive surface also resulted in elevated concentrations compared to SL and SLA surfaces (Fig. 2B, $p < 0.05$). Concentrations of further anti-inflammatory markers as IL-1RA or the wound healing marker VEGF were found to be similar to all surfaces. Overall, the level of immune response to this collection of specimens was low to moderate in comparison to the positive and negative controls, with the remaining pro- and anti-inflammatory cytokines tested showing similar results as those presented in Fig. 2 A/B (data not shown).

To complement the assessment of cytokine release in response to these titanium surfaces, we additionally employed flow cytometry to characterise the expression of cell surface molecules. This technique is capable of examining the behaviour of specific immune cell populations, which might more precisely identify the major cell types involved in the observed immune response and thus reveal the presence of sub-populations, if present. Examining the major populations of immune cells revealed both T helper cells (T_h cells) and cytotoxic T cells (T_c cells) to show higher levels of activation in response to the SLActive surface compared to other specimens, as indicated by increased frequencies of cells expressing HLA-DR and an increased signal for CD16 (Fig. 3). However, the effects observed for lymphocytes were minor compared to the positive and negative control, suggesting that it is the monocytes which primarily elicit the immune response to these specimens. In line with this, the expression of HLA-DR, CD16 and CD163 on $CD14^+$ monocytes was found to be altered to a far greater extent than the lymphocyte activation markers examined (Fig. 3). Comparing SLActive to the other titanium surfaces, we found SLActive to induce higher expression of HLA-DR, CD16 and CD163 compared to A, all surfaces, and SL/SLA surface, respectively ($p < 0.05$). The additional markers tested on $CD14^+$ monocytes (CD86, CD206, CD284, CD354) as well as all markers on natural killer cells (CD25, HLA-DR, CD354) and the frequency of regulatory T cells did not differ between the different surfaces to a considerable extent (Supplementary information 5).

3.3. Monocytes but not lymphocytes are the major cell type responsible for the immune response to clinically used titanium biomaterial

The results obtained thus far hinted monocytes rather than lymphocytes to be the predominant cell type involved in the observed immune response to the titanium biomaterial surfaces. To investigate if lymphocytes contribute directly or indirectly to the immune response, we isolated monocytes from whole PBMC using magnetic cell sorting and cultured them in isolation or together with lymphocytes at defined ratios of varying monocyte content on the titanium biomaterial. We additionally included a condition containing only lymphocytes to consider any potential response solely by this cell type. The following experiments were performed using the SLActive surface only. Examining the cytokine levels across the cultures with varying monocyte and lymphocyte numbers showed the highest levels of the pro-inflammatory molecules IL-8, TNF-α, IL-6 and IL-1β to be found when monocytes fractions were highest (M100%, left), with levels progressively decreasing with lower fractions of monocytes (Fig. 4A). Noteworthy was that cultures containing only lymphocytes (L100%/M0%, far right) produced extremely low levels of cytokines approaching the lower limit of detection. Thus, when cultured alone, lymphocytes seem to be

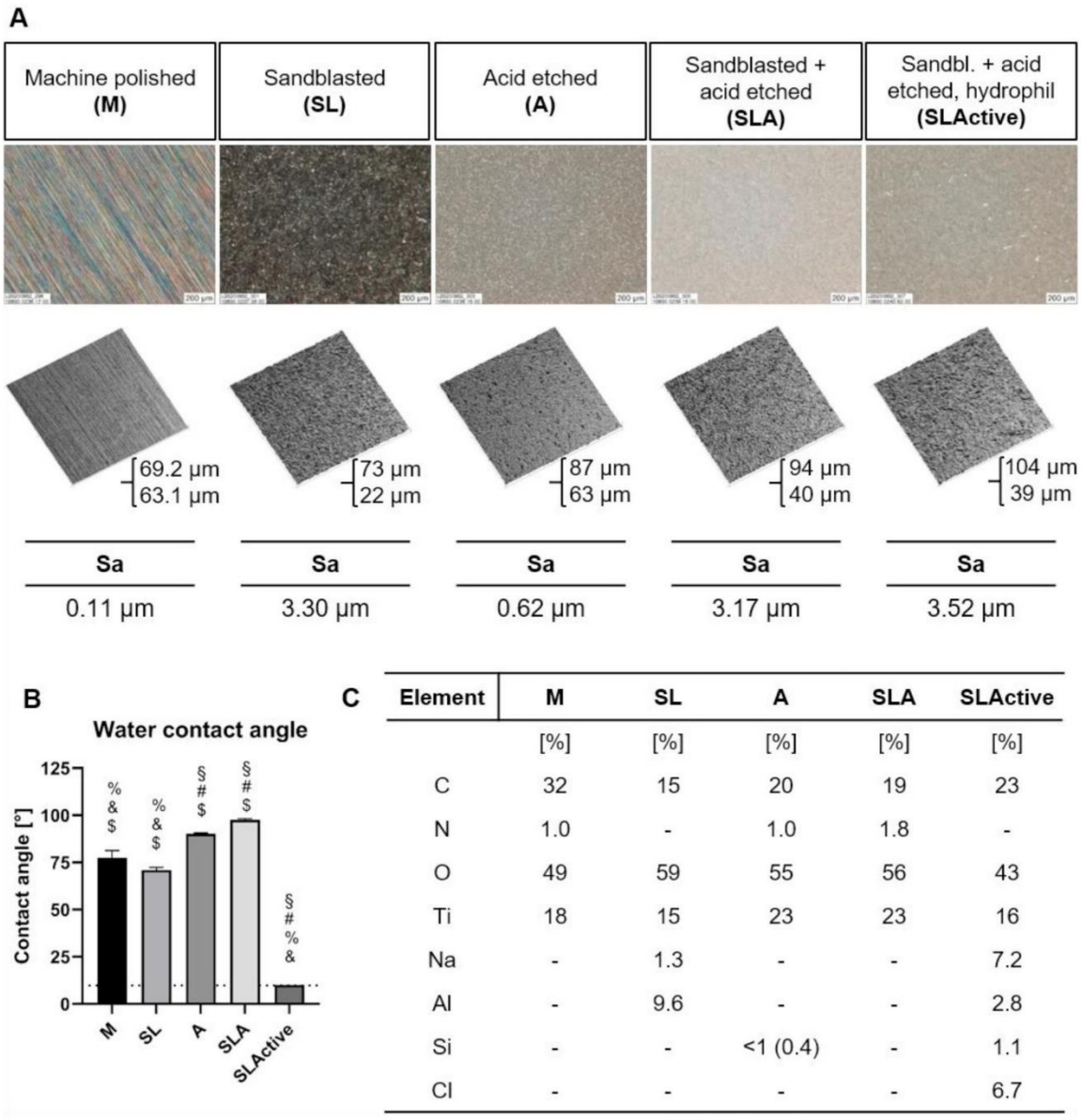

C

Element	M	SL	A	SLA	SLActive
	[%]	[%]	[%]	[%]	[%]
C	32	15	20	19	23
N	1.0	-	1.0	1.8	-
O	49	59	55	56	43
Ti	18	15	23	23	16
Na	-	1.3	-	-	7.2
Al	-	9.6	-	-	2.8
Si	-	-	<1 (0.4)	-	1.1
Cl	-	-	-	-	6.7

Fig. 1. Physicochemical characterisation of titanium implant surfaces. Machine polished (M), sandblasted (SL), acid etched (A), a combination of sandblasted and acid etched (SLA) and a hydrophilic version of SLA (SLActive) titanium specimens underwent physicochemical analysis using light microscopy, confocal scanning microscopy, water contact angle measurement and X-ray photoelectron spectroscopy (XPS). A) Light microscopy was used to visualise the surface of each specimen, while confocal scanning microscopy was used to analyse sample surface topography. Scale bar (lower right corner) equals 200 µm. 3D images depict a 2.5 × 2.5 mm area of the sample surface, numbers indicate measurement range between highest and lowest point. Sa values indicate mean height of the surface topography. B) Water contact angle measurement indicates surface wettability (n = 10 for each surface). One-way ANOVA shows significant differences ($p < 0.01$) vs. M (§), vs. SL (#), vs. A (%), vs. SLA (&) and vs. SLActive ($). C) XPS analysis shows elemental composition of the surfaces investigated. Values indicate percentage of total chemical composition.

unaffected by the SLActive biomaterial. To assess the potential influence of lymphocytes to the secretion of cytokines in mutual interaction with monocytes, we statistically compared cytokine levels of a pure monocyte culture M100% with a mixed culture L33%/M66% (first two conditions on the left). As both cultures contain the same absolute number of monocytes, a potential effect of lymphocytes would result in a different cytokine expression pattern in the L33%/M66% mixed culture. However, we were not able to detect any differences of this mixed culture compared to the pure monocyte culture (Fig. 4A). Thus, cytokine expression of monocytes seems to be unaffected by the presence of

Table 1
Scoring of surface characteristics roughness, hydrophobicity and chemistry.

Surface	Roughness	Hydrophobicity	Chemistry similar to
M	Low	Medium	–
SL	High	Medium	–
A	Low	High	SLA
SLA	High	High	A
SLActive	High	Low	–

lymphocytes. In general, the same effect was observed for the anti-inflammatory molecule IL-1RA and the wound healing marker VEGF (Fig. 4B).

As cytokine analysis only assesses the overall immune response but does not allow analysis of individual cell populations directly, in a further step we applied flow cytometry using the identical experimental setting to shed a light on the effects on the cellular level. To investigate a potential role of lymphocytes on the activation of monocytes, we compared the expression of monocyte surface markers in a pure monocyte culture with those in mixed cultures of different lymphocyte ratios. Quantifying the mean fluorescence intensity of the markers allows a comparison of the M100% culture with all mixed cultures as the parameter should be independent of the absolute monocyte cell number. Analysis showed expression of CD16, CD86 and CD163 surface markers on monocytes to be unaffected by the presence of lymphocytes (Fig. 5A). In exception, we found expression of HLA-DR on monocytes to be increased with a large number of lymphocytes being present ($p < 0.05$). In addition, to investigate the reverse effect of a possible influence of monocytes on lymphocyte activity, lymphocyte surface marker expression was measured in a pure culture and compared with those in mixed cultures with monocytes. For both lymphocyte populations – helper T cells and cytotoxic T cells – we found no difference in expression of CD25, but identified an increased expression of CD16 and an elevated frequency of HLA-DR positive cells in cultures consisting of one third lymphocytes and two third monocytes (Fig. 5B and C, $p < 0.05$). No differences were observed for a culture of 90% lymphocytes and 10% monocytes, which resembles the PBMC conditions. Taken together, the results indicate that lymphocytes themselves might not be able to respond to the SLActive titanium surface. Furthermore, the findings suggest that under physiological conditions, mutual interactions only slightly affect cellular behaviour of monocytes and lymphocytes in the context of this biomaterial, as most of the analysed markers were unaffected.

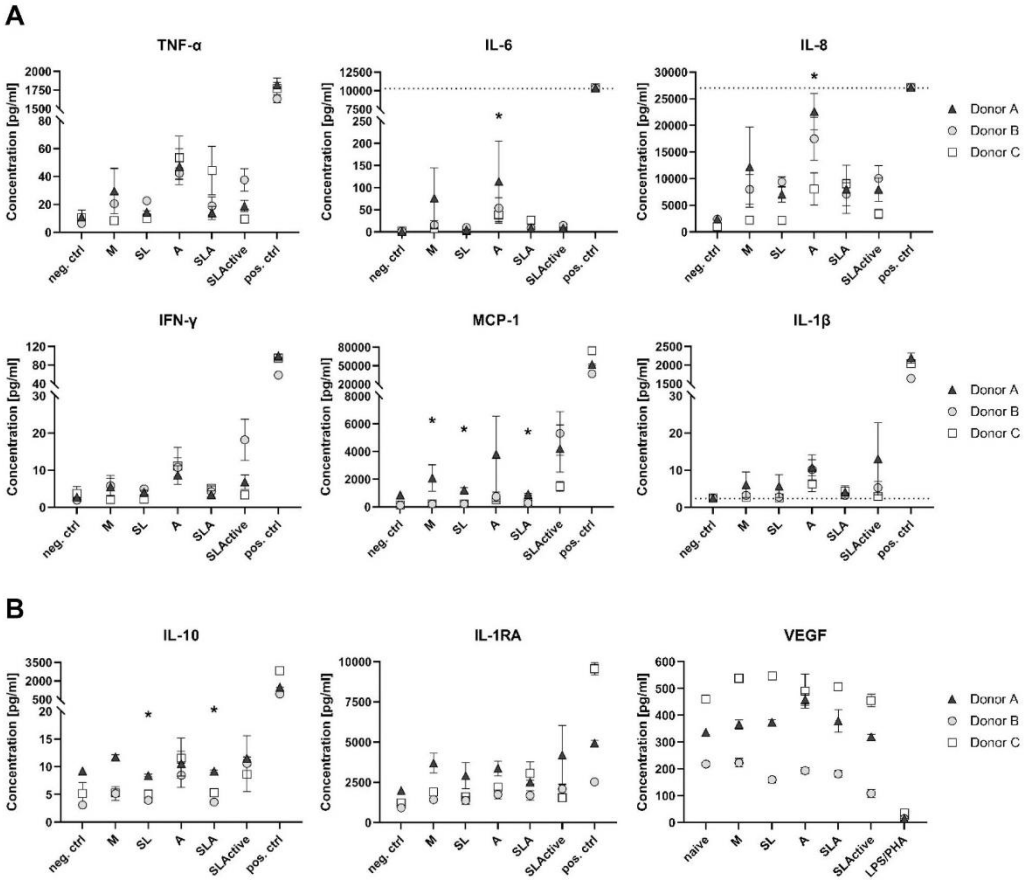

Fig. 2. Pro- and anti-inflammatory cytokine response by PBMCs cultured on titanium specimens. PBMCs from three donors were cultured on the following titanium specimens for 72 h: machine polished (M), sandblasted (SL), acid etched (A), sandblasted and acid etched (SLA) and SLA with hydrophilic treatment (SLActive). Cell culture polystyrene was used as negative control (neg. ctrl/naïve), while the positive control (pos. ctrl/LPS/PHA) was stimulated with 100 ng/ml LPS and 15 µg/ml PHA-L. A) Pro-inflammatory and B) anti-inflammatory/wound healing mediators were quantified in the cell culture medium using multiplex immunoassays. Dotted line indicates upper or lower limit of quantification. Each of the three donors was analysed in triplicate for all conditions tested (i.e. n = 3 for each donor). Graphs show mean with SEM. RM one-way ANOVA compares all means vs. the mean of SLActive, * = $p < 0.05$ vs. SLActive.

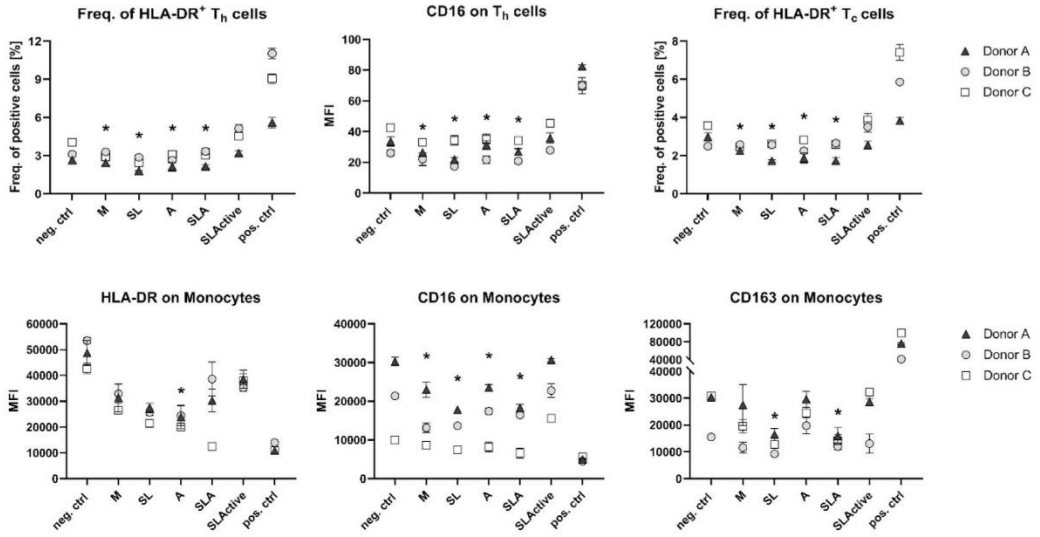

Fig. 3. Expression of cell surface molecules on PBMCs following culture on titanium specimens. PBMCs from three donors were cultured on the following titanium specimens for 72 h: machine polished (M), sandblasted (SL), acid etched (A), sandblasted and acid etched (SLA) and SLA with hydrophilic treatment (SLActive). Cell culture polystyrene was used as negative control (neg. ctrl), while the positive control (pos. ctrl) was stimulated with 100 ng/ml LPS and 15 µg/ml PHA-L. Mean fluorescence intensity (MFI) of surface marker expression or frequency of positive cells was quantified on lymphoid and myeloid cell populations including monocytes, T helper cells (T_h cells) and cytotoxic T cells (T_c cells) using flow cytometry. Each of the three donors was analysed in triplicate for all conditions tested (i.e. n = 3 for each donor). Graphs show mean with SEM. RM one-way ANOVA compares all means vs. the mean of SLActive, * = $p < 0.05$ vs. SLActive.

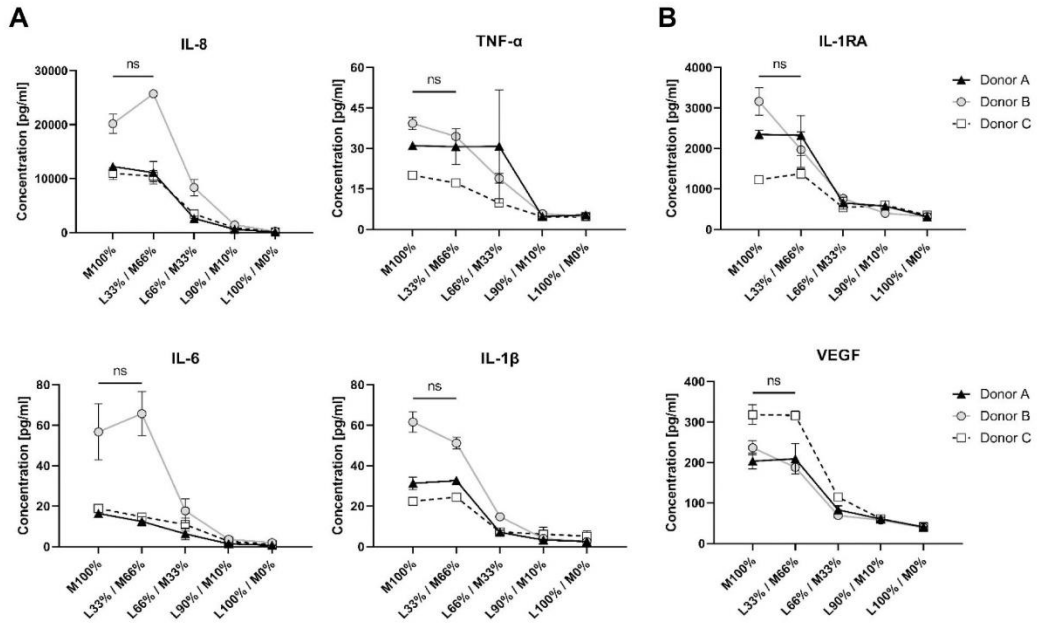

Fig. 4. Cytokine analysis of isolated monocytes and lymphocytes alone and together at defined ratios on SLActive titanium. Monocytes were isolated from whole PBMC using magnetic cell sorting and cultured at defined ratios on the SLActive titanium surface. Graphs show decreasing monocyte and increasing lymphocyte levels from left to right ranging from monocytes alone (far left, M100%) followed by monocytes and lymphocytes cultured at ratios of L33%/M66%, L66%/M33%, L90%/M10% and lymphocytes alone (far right, L100%). Levels of A) pro-inflammatory and B) anti-inflammatory/wound healing mediators of three different donors were measured after 72 h cultivation by multiplex immunoassays. Three donors were tested in triplicate (i.e. n = 3 for each donor). Graphs show mean with SEM. Absolute monocyte cell numbers were identical in groups M100% and L33%/M66%. Paired *t*-test of these two groups showed no significant differences (ns).

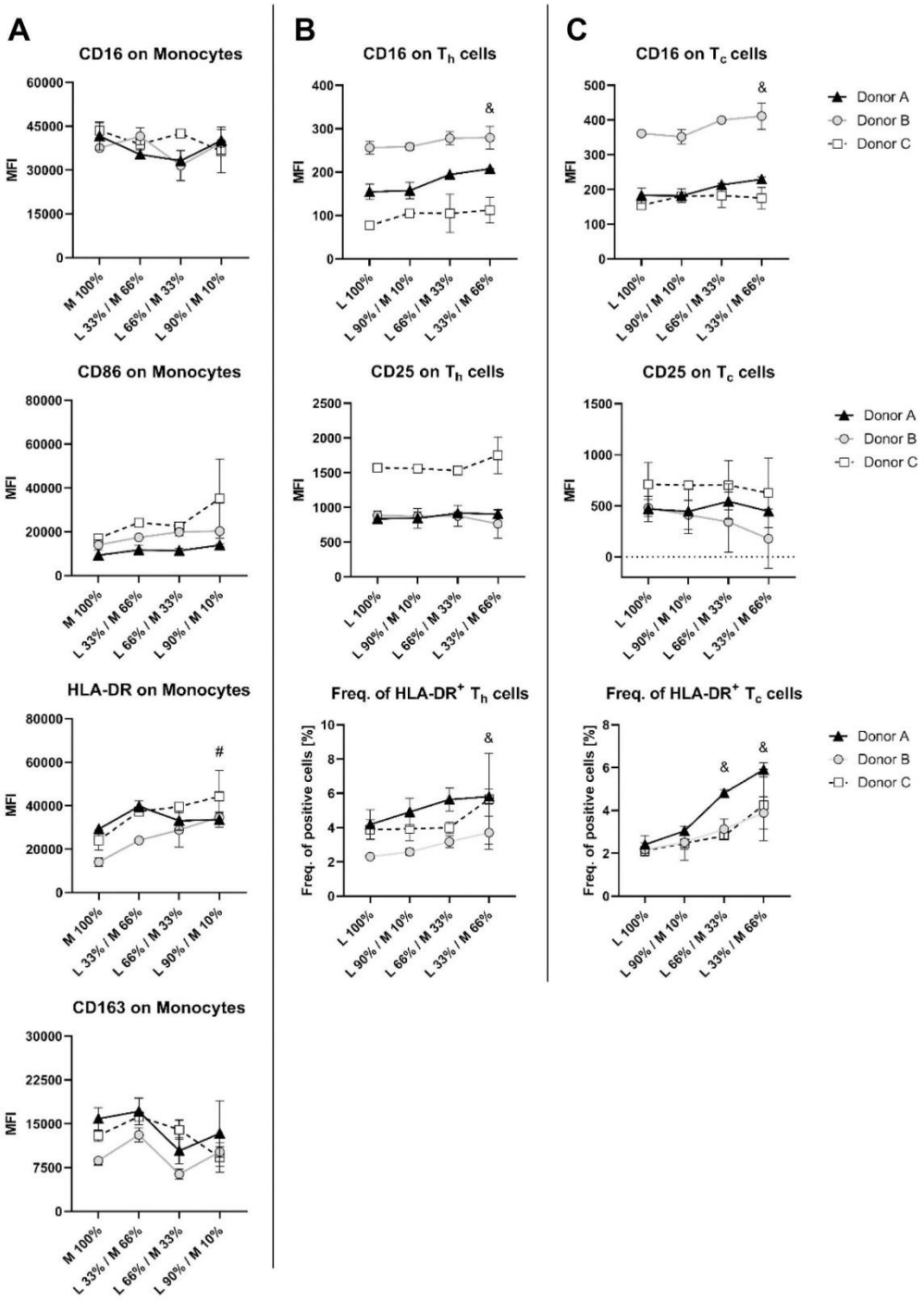

Fig. 5. Surface marker expression of isolated monocytes and lymphocytes at defined ratios on SLActive titanium. Monocytes were isolated from whole PBMC and cultured at defined ratios on the SLActive surface. Graphs show decreasing monocyte and increasing lymphocyte levels from left to right ranging from monocytes alone (far left, M100%) followed by monocytes and lymphocytes cultured at ratios of L33%/M66%, L66%/M33%, L90%/M10% and lymphocytes alone (far right, L100%). Surface marker expression was quantified on A) monocytes, B) T helper cells (T_h cells) and C) cytotoxic T-cells (T_c cells) after 72 h cultivation by flow cytometry as mean fluorescence intensity (MFI) or frequency of positive cells. Three donors were tested in triplicate (i.e. n = 3 for each donor). Graphs show mean with SEM. RM one-way ANOVA was employed to compare mixed cultures with A) pure monocyte (# = $p < 0.05$) or B) pure lymphocyte cultures (& = $p < 0.05$), respectively.

3.4. Intracellular cytokine staining in PBMC confirms monocytes as the primary cell type reactive to the SLActive titanium dental implant

Although we already showed the total cytokine concentration to be apparently unaffected by lymphocytes using isolated monocytes (Fig. 4), so far we have not investigated the cellular origin of the measured cytokines in whole PBMC cultures. While it is widely reported that myeloid cells are able to recruit and activate lymphoid cells in response to biomaterials through the action of chemo- and cytokines, lymphocytes are also capable of producing many of the cytokines we observed in

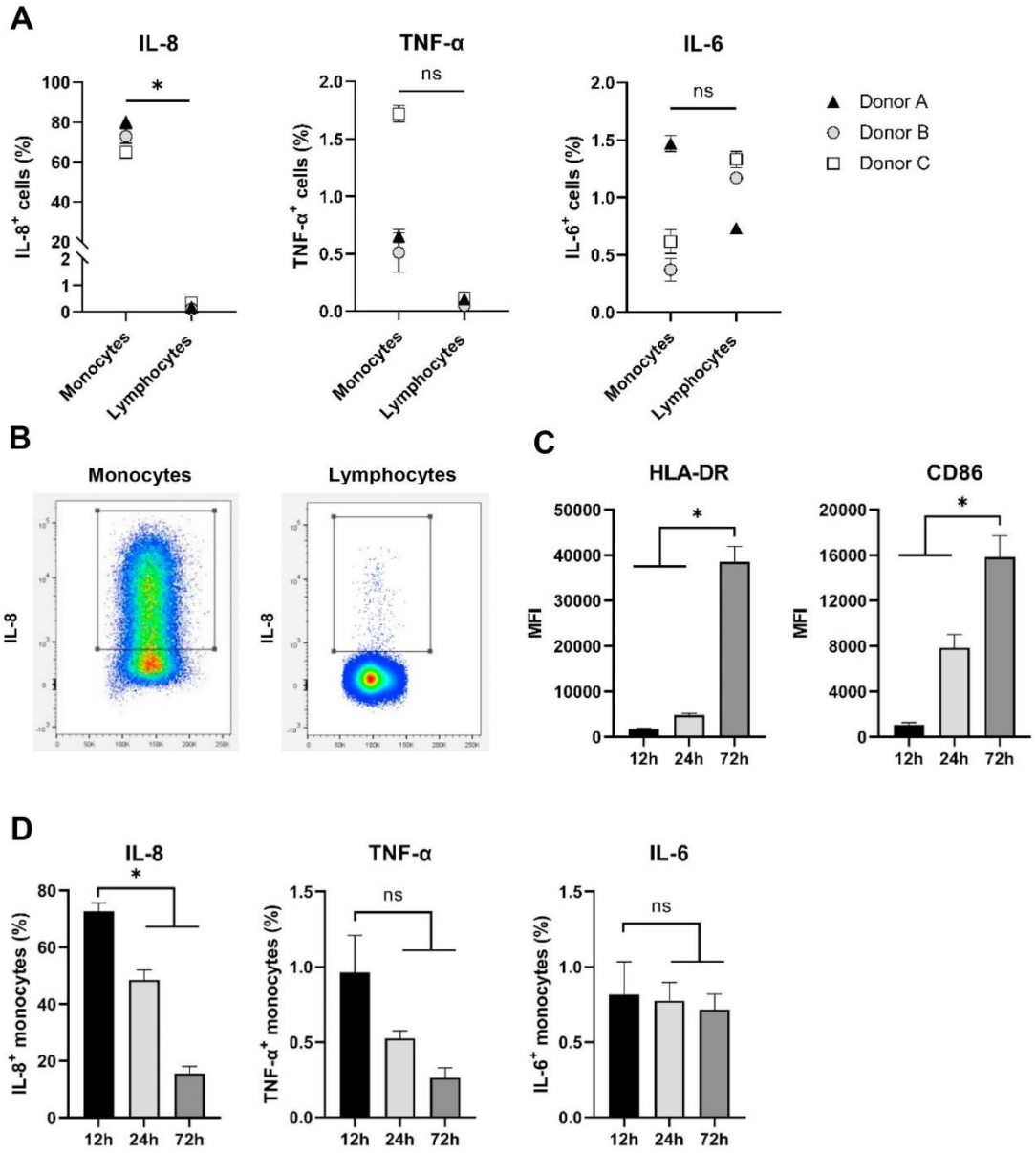

Fig. 6. Intracellular cytokine staining of monocyte and lymphocyte populations in PBMC cultured on SLActive titanium. Monocyte and lymphocyte populations in whole PBMC were assessed for intracellular expression of IL-8, TNF-α and IL-6 with flow cytometry. A) The percentage of IL-8, TNF-α and IL-6 positive monocytes and lymphocytes was compared in PBMCs after 12 h of cultivation on the SLActive titanium surface. B) Dot plot shows levels of gated IL-8 positive cells in monocytes and lymphocytes for one exemplary donor. C) The expression of HLA-DR and CD86 on monocytes and D) the percentage of IL-8, TNF-α and IL-6 positive monocytes was assessed in PBMCs after 12 h, 24 h and 72 h of cultivation on the SLActive titanium surface. All experiments were performed with three separate donors in duplicate for all conditions tested (i.e. n = 2 for each donor). Graphs show results for A) each donor presented separately or C) and D) pooled. Statistical analysis was employed to A) compare monocyte and lymphocyte populations for all donors combined or C) and D) compare frequencies of positive monocytes across time. Asterisk * indicates significant differences ($p < 0.05$). Statistical analysis was applied to all graphs shown.

response to the SLActive material themselves. To therefore investigate potential crosstalk between different cell types in our model, we cultured PBMCs on the SLActive surface and analysed cytokine production on a single cell level in monocyte and lymphocyte populations using flow cytometry. The results showed that the majority of cytokine-producing cells were monocytes, with only a small proportion of lymphocytes also showing cytokine production. For example, we found 64.9%–80.15% of the monocytes to be positive for IL-8, whereas this was 0.11%–0.34% in the lymphocyte population (Fig. 6A, $p < 0.0001$). Gating results for IL-8 on monocytes and lymphocytes of one representative donor are shown in Fig. 6B. A similar trend was observed for TNF-α, where the fraction of positive monocytes was substantially higher than for lymphocytes (0.51%–1.72% positive monocytes compared with 0.05%–0.12% positive lymphocytes, $p = 0.08$). For IL-6, however, donor-dependent differences were found with no clear trend overall. While the fraction of IL-6 positive cells was higher in monocytes than lymphocytes for Donor A (1.47% versus 0.73%), Donors B and C showed a higher fraction of lymphocytes than monocytes producing IL-6 (0.37% and 0.64% positive monocytes compared to 1.17% and 1.33% positive lymphocytes). Nevertheless, the relative magnitude of response by lymphocytes and monocytes for IL-6 was substantially lower than for TNF-α or IL-8, both showing a minimum 6 and over 100-fold higher frequency of positive cells for monocytes, respectively, compared to lymphocytes in all donors. Together, these results suggest that the initial phase of the immune response to this biomaterial surface is largely dominated by monocytes. Even in the presence of activated monocytes producing a number of cytokines and chemokines, significant levels of lymphocyte activation were not observed.

3.5. Monocyte cytokine production and surface protein expression show differential expression across time

Having identified monocytes as the major cell type that is almost exclusively responsible in the observed immune response to the SLActive biomaterial, we then focussed on characterising the monocyte response in more detail. Cytokine production and surface marker expression are dynamic processes, which is why the time point of examination can have an influence on the evaluation of the results. Thus, we were interested in examining cytokine production and the expression of surface molecules across time to reveal differences in the rate of response by these proteins. In the case of intracellular cytokines, we observed IL-8 levels to peak after 12 h of biomaterial contact, followed by a significant decrease after 24 h and a further drop after 72 h following contact with the SLActive surface (Fig. 6D, $p < 0.001$), thus indicating a relatively strong initial response after biomaterial contact. A similar trend was also observed for TNF-α. In contrast, the levels of the antigen presentation molecule HLA-DR and the co-stimulatory molecule CD86 were relatively low initially after biomaterial contact. Here, we found significant elevation in protein expression for both markers after 72 h of cultivation compared to the 12 h time point while a slightly elevated expression was observed after 24 h (Figs. 6C and 12 h vs. 72 h $p < 0.01$ for both HLA-DR and CD86; 24 h vs. 72 h $p < 0.01$ for HLA-DR). Collectively, these results point to the immediate immune response primarily involving the release of soluble signalling proteins, while molecules involved in the presentation of antigens and the priming of T cells peak much later.

4. Discussion

Surface characteristics have been widely shown to influence the immune response towards any given biomaterial.[5,31] Accordingly, the design of biomaterials to modulate the host immune response has been gaining increasing attention as an important factor influencing implant biocompatibility.[6] In the present study, we compared five titanium specimens varying in surface topography, wettability and chemical composition in terms of the immune response. Generally speaking, we observed the immune response to all five tested surfaces to range from mild to moderate. However, some differences were observed among the different samples investigated. For example, the pro-inflammatory response to the acid etched (A) sample was elevated for a number of cytokines compared to the rougher sandblasted and acid etched (SLA) surface. This is especially interesting as A and SLA surface showed a similar level of hydrophobicity and an almost identical chemical composition, but highly differed on surface roughness. Thus, this indicates an influence of surface topography on the immune response, which is in line with a previous study on titanium biomaterials that also reported low expression of pro-inflammatory cytokines like IL-6 and TNF-α to rough surfaces.[9]

In addition to surface topography, wettability has also been shown to alter biological responses to biomaterials.[32] Because the SLA and SLActive specimens undergo identical manufacturing processes, they display similar surface topography and roughness, but due to the hydrophilic treatment applied to the SLActive surface they differ significantly in their wettability. It has also been reported that an additional effect of the hydrophilic treatment and storage in saline buffer is the development of nanostructures on the surface of the SLActive specimen.[33] Accordingly, we observed the SLActive surface to show a slightly higher surface roughness compared to SLA (Fig. 1). Analysing the immune response, we found both surfaces to evoke similar expression for some cytokines but differ in MCP-1 and IL-10 levels. When comparing the in vivo performance of both surfaces, several animal investigations and clinical studies in humans reported accelerated healing for the SLActive implants.[27] Taking our findings into account, the faster healing reported for the SLActive surface in comparison with SLA may be associated with the higher levels of MCP-1 observed, a chemoattractant able to recruit cells such as macrophages, which may assist in tissue regeneration following implantation. Furthermore, the elevated levels of IL-10 after cultivation on the SLActive surface may act to dampen inflammation by contributing to the induction of regulatory T cells and driving the differentiation of macrophages to an M2-like state. Accordingly, we observed a higher expression of the M2 polarisation marker CD163 on monocytes after cultivation on the SLActive surface compared to the SLA material. In summary, we could show that distinct titanium specimen surface properties like topography and wettability are able to modulate the immune response of PBMCs.

Several studies have shown that in vitro, monocytes can get activated by biomaterial contact directly, without any other stimuli.[34,35] These in vitro observations of monocyte activation were also linked to in vivo effects.[36] While these cells are already well established to play an essential role in the initiation of the host response to foreign materials, the role of lymphocytes in such processes is still poorly understood. In order to better understand the role of lymphocytes in the immune response to a clinically used titanium implant, we therefore cultured lymphocytes alone and at defined ratios with monocytes on the SLActive material. In contrast to a previous study,[18] lymphocytes were found here to show no detectable difference in response to the biomaterial surface as the culture of a pure lymphocyte population did not result in considerable cytokine expression. Investigating the cellular origin of detected cytokines in regular PBMC cultures revealed the majority of cytokine producing cells to be monocytes, while only a very small fraction of lymphocytes was found to produce the pro-inflammatory cytokines IL-8 and TNF-α. An exception to this was IL-6, which showed more comparable cytokine levels across monocytes and lymphocytes, but with a strong donor-dependent effect. It should also be considered that supernatant levels of IL-6 secreted by PBMC after three days of contact with the SLActive biomaterial were comparable to the negative control and were very low overall, indicating the role of IL-6 produced by lymphocytes to be negligible. Considering all five specimens examined here, we did not find any that induced increased surface marker expression on lymphocytes beyond the level of negative control (Fig. 3). This suggests that the lack of involvement of the adaptive immune system is not restricted to the SLActive surface, but likely applies

to all titanium surfaces studied. In response to SLActive biomaterial, monocytes were generally unaffected by the presence of lymphocytes regarding cytokine production and surface marker expression. In turn, surface marker expression on lymphocyte populations was increased for some markers with high numbers of monocytes being present. However, it is questionable whether this strong excess of monocytes can also be expected under physiological conditions. Further studies would be required to investigate the observed effects in vivo.

The observation that lymphocytes play a minor role in response to a biomaterial may be explained by the biology of these different cell types. While the innate immune system is designed to respond non-specifically to pathogens immediately, the hallmark of the adaptive immune system is its pathogen-specific response, which requires the presentation of relevant antigen and the priming of naïve cells, which can take a number of days or weeks to be fully established. Thus, we propose that the SLActive biomaterial elicits immune mechanisms classically employed against pathogens recognized by the innate immune system. In line with this, it may be possible that adaptive immune responses by lymphocytes could occur later in response to biomaterials. Supporting this notion is our observation that molecules involved in antigen presentation and the co-stimulation of T cells (HLA-DR and CD86) were found to increase dramatically with time on monocytes. This notion is also supported by a previous study that showed enhancement of the pro-inflammatory cytokines IL-8, TNF-α and IL-6 by monocytes in direct contact with lymphocytes only after 10 days of culture, but failed to show any effect at earlier time points.[37] The SLActive titanium surface included in our study has been shown by a number of previous investigations to elicit relatively low pro-inflammatory responses.[7,9,38] This might suggest that non-specific activation of lymphocytes, for example by cytokines produced from activated monocytes, may only occur when inflammatory states are higher than those produced by the SLActive material here - for example in vitro to a biomaterial that produces strong pro-inflammatory responses or in vivo via tissue injury occurring during the process of implantation.[39] Alternatively, this may take place either in vitro or in vivo in the context of lymphocytes that have been pre-activated by additional stimuli.[7] Although the PBMC model used in this study captures the bulk of the biological complexity of the circulating human immune system, it cannot reproduce all aspects of the immune system that occur in the body. Therefore, further in vivo studies would be recommended to analyse the effect of the adaptive immune system in more detail.

5. Conclusions

In summary, this study shows altered immune responses to differently treated titanium surfaces for several pro- and anti-inflammatory cytokines and cell surface markers, revealing influence of different surface characteristics as topography, chemistry and wettability. We found the response to the clinically used SLActive material to be predominantly driven by the innate immune system, while the adaptive immune system is neither capable of reacting to the biomaterial to a measurable extent nor is it influencing the cytokine response or surface marker expression of the innate immune system. Activation of the adaptive by the innate immune system occurred under selective conditions only and might take a longer time to develop. Intracellular cytokine staining confirmed cytokine production to be mostly based on monocytes and peak already during the first 12 h, while monocyte surface markers need at least 72 h to fully set up. Collectively, our results suggest that strategies aiming to modulate the initial host response to implant materials should focus on targeting the innate immune system.

Credit author statement

Florian Billing: Conceptualisation, Investigation, Formal analysis, Visualization, Writing – original draft, Writing – Review & Editing, Meike Jakobi: Methodology, Investigation, Dagmar Martin: Funding acquisition, Resources, Karin Gerlach: Investigation. Elsa Arefaine: Investigation. Martin Weiss: Resources. Nicole Schneiderhan-Marra: Funding acquisition, Resources. Hanna Hartmann: Funding acquisition, Project administration, Supervision, Writing – Review & Editing, Christopher Shipp: Project administration, Conceptualisation, Supervision, Validation, Writing – Original draft, Writing – Review & Editing.

Declaration of competing interest

The authors declare that they have no known competing financial interests or personal relationships that could have appeared to influence the work reported in this paper.

Acknowledgements

This work received financial support by the EU-EFRE (712889), the State Ministry of Baden-Wuerttemberg for Economic Affairs, Labour and Tourism, as well as the NMI, which is also partly funded by the German State of Baden-Wuerttemberg. We are very grateful to Burkhard Schlosshauer (NMI) for his contribution to the planning and execution of this work.

Appendix A. Supplementary data

Supplementary data to this article can be found online at https://doi.org/10.1016/j.regen.2021.100047.

References

1 Bizjak M, Selmi C, Shoenfeld S, et al. Silicone implants and lymphoma: the role of inflammation. *J Autoimmun*. 2015;65. https://doi.org/10.1016/j.jaut.2015.08.009.
2 Albrektsson T, Becker W, Coli P, Jemt T, Mölne J, Sennerby L. Bone loss around oral and orthopedic implants: an immunologically based condition. *Clin Implant Dent Relat Res*. 2019;21:786–795.
3 Landgraeber S, Jäger M, Jacobs JJ, Hallab NJ. The pathology of orthopedic implant failure is mediated by innate immune system cytokines. *Mediat Inflamm*. 2014;2014. https://doi.org/10.1155/2014/185150.
4 Mahendra G, Pandit H, Kliskey K, Murray D, Gill HS, Athanasou N. Necrotic and inflammatory changes in metal-on-metal resurfacing hip arthroplasties. *Acta Orthop*. 2009;80:653–659.
5 Anderson JM, Rodriguez A, Chang DT. Foreign body reaction to biomaterials. *Semin Immunol*. 2008;20:86–100.
6 Franz S, Rammelt S, Scharnweber D, Simon JC. Immune responses to implants - a review of the implications for the design of immunomodulatory biomaterials. *Biomaterials*. 2011;32:6692–6709.
7 Vishwakarma A, Bhise NS, Evangelista MB, et al. Engineering immunomodulatory biomaterials to tune the inflammatory response. *Trends Biotechnol*. 2016;34:470–482.
8 Alfarsi MA, Hamlet SM, Ivanovski S. Titanium surface hydrophilicity modulates the human macrophage inflammatory cytokine response. *J Biomed Mater Res*. 2014;102:60–67.
9 Hotchkiss KM, Reddy GB, Hyzy SL, Schwartz Z, Boyan BD, Olivares-Navarrete R. Titanium surface characteristics, including topography and wettability, alter macrophage activation. *Acta Biomater*. 2016;31:425–434.
10 Hyzy SL, Olivares-Navarrete R, Hutton DL, Tan C, Boyan BD, Schwartz Z. Microstructured titanium regulates interleukin production by osteoblasts, an effect modulated by exogenous BMP-2. *Acta Biomater*. 2013;9:5821–5829.
11 Palmquist A, Omar OM, Esposito M, Lausmaa J, Thomsen P. Titanium oral implants: surface characteristics, interface biology and clinical outcome. *J R Soc Interface*. 2010;7(Suppl 5):S515–S527.
12 Barfeie A, Wilson J, Rees J. Implant surface characteristics and their effect on osseointegration. *Br Dent J*. 2015;218:E9.
13 Ogle ME, Segar CE, Sridhar S, Botchwey EA. Monocytes and macrophages in tissue repair: implications for immuno regenerative biomaterial design. *Exp Biol Med*. 2016;241:1084–1097.
14 Mosser DM, Edwards JP. Exploring the full spectrum of macrophage activation. *Nat Rev Immunol*. 2008;8:958–969.
15 Rostam HM, Singh S, Aemmaghami, et al. The impact of surface chemistry modification on macrophage polarisation. *Immunobiology*. 2016;221:1237–1246.
16 Klopfleisch R, Jung F. The pathology of the foreign body reaction against biomaterials. *J Biomed Mater Res*. 2017;105:927–940.
17 Sridharan R, Cameron AR, Kelly DJ, Kearney CJ, O'Brien FJ. Biomaterial based modulation of macrophage polarization: a review and suggested design principles. *Mater Today*. 2015;18:313–325.
18 Jin W, Tamzalit F, Chaudhuri PK, Black CT, Huse M, Kam LC. T cell activation and immune synapse organization respond to the microscale mechanics of structured surfaces. *Proc Natl Acad Sci U S A*. 2019;116:19835–19840.

19 Chen H, Zhang PJ, et al. The promotion of type 1 T helper cell responses to cationic polymers in vivo via toll-like receptor-4 mediated IL-12 secretion. *Biomaterials*. 2010; 31:8172–8180.

20 Brodbeck WG, Macewan M, Colton E, Meyerson H, Anderson JM. Lymphocytes and the foreign body response: lymphocyte enhancement of macrophage adhesion and fusion. *J Biomed Mater Res*. 2005;74:222–229.

21 Chang DT, Colton E, Matsuda T, Anderson JM. Lymphocyte adhesion and interactions with biomaterial adherent macrophages and foreign body giant cells. *J Biomed Mater Res*. 2009;91:1210–1220.

22 Nicolau P, Guerra F, Reis R, Krafft T, Benz K, Jackowski J. 10-year outcomes with immediate and early loaded implants with a chemically modified SLA surface. *Quintessence Int*. 2019;50:114–124. Berlin, Germany : 1985.

23 Bornstein MM, Wittneben J-G, Brägger U, Buser D. Early loading at 21 days of non-submerged titanium implants with a chemically modified sandblasted and acid-etched surface: 3-year results of a prospective study in the posterior mandible. *J Periodontol*. 2010;81:809–818.

24 Lang NP, Salvi GE, Huynh-Ba G, Ivanovski S, Donos N, Bosshardt DD. Early osseointegration to hydrophilic and hydrophobic implant surfaces in humans. *Clin Oral Implants Res*. 2011;22. https://doi.org/10.1111/j.1600-0501.2011.02172.x.

25 Buser D, Broggini N, , et alSteinemann. Enhanced bone apposition to a chemically modified SLA titanium surface. *J Dent Res*. 2004;83:529–533.

26 Schwarz F, Ferrari D, , et alBecker J. Effects of surface hydrophilicity and microtopography on early stages of soft and hard tissue integration at non-submerged titanium implants: an immunohistochemical study in dogs. *J Periodontol*. 2007;78:2171–2184.

27 Wennerberg A, Albrektsson, Galli. Current knowledge about the hydrophilic and nanostructured SLActive surface. *CCIDE*. 2011;3:59–67.

28 European Medicines Agency. Guideline on bioanalytical method validation. https://www.ema.europa.eu/en/documents/scientific-guideline/guideline-bioanalytical-method-validation_en.pdf; 2011.

29 U.S. Department of Health and Human Services, Food and Drug Administration. Bioanalytical method validation. Guidance for industry. https://www.fda.gov/downloads/drugs/guidances/ucm070107.Pdf; 2018.

30 Westgard JO, Barry PL, Hunt MR, Groth T. A multi-rule Shewhart chart for quality control in clinical chemistry. *Clin Chem*. 1981;27:493–501.

31 Thevenot P, Hu W, Tang L. Surface chemistry influences implant biocompatibility. *Curr Top Med Chem*. 2008;8:270–280.

32 Menzies KL, Jones L. The impact of contact angle on the biocompatibility of biomaterials. *Optom Vis Sci : Off Publ Am Acad Optometr*. 2010;87:387–399.

33 Kopf BS, Ruch S, Berner S, Spencer ND, Maniura-Weber K. The role of nanostructures and hydrophilicity in osseointegration: in-vitro protein-adsorption and blood-interaction studies. *J Biomed Mater Res*. 2015;103:2661–2672.

34 Schachtrupp A, Klinge U, Junge K, Rosch R, Bhardwaj RS, Schumpelick V. Individual inflammatory response of human blood monocytes to mesh biomaterials. *Br J Surg*. 2003;90:114–120.

35 Naim JO, van Oss CJ, Buehner KMLA, et al. In vitro activation of human monocytes by silicones. *Colloids Surf B Biointerfaces*. 1998;11:79–86.

36 Bota PCS, Collie AMB, Pu P, , et alStayton S. Biomaterial topography alters healing in vivo and monocyte/macrophage activation in vitro. *J Biomed Mater Res*. 2010;95: 649–657.

37 Chang DT, Colton E, Anderson JM. Paracrine and juxtacrine lymphocyte enhancement of adherent macrophage and foreign body giant cell activation. *J Biomed Mater Res*. 2009;89:490–498.

38 Hamlet SM, Lee RSB, Moon H-J, Alfarsi MA, Ivanovski S. Hydrophilic titanium surface-induced macrophage modulation promotes pro-osteogenic signalling. *Clin Oral Implants Res*. 2019;30:1085–1096.

39 Hotchkiss KM, Clark NM, Olivares-Navarrete R. Macrophage response to hydrophilic biomaterials regulates MSC recruitment and T-helper cell populations. *Biomaterials*. 2018:182. https://doi.org/10.1016/j.biomaterials.2018.08.029.

Supplemental Figures

Billing F., et al. The immune response to the SLActive titanium dental implant surface in vitro is predominantly driven by innate immune cells

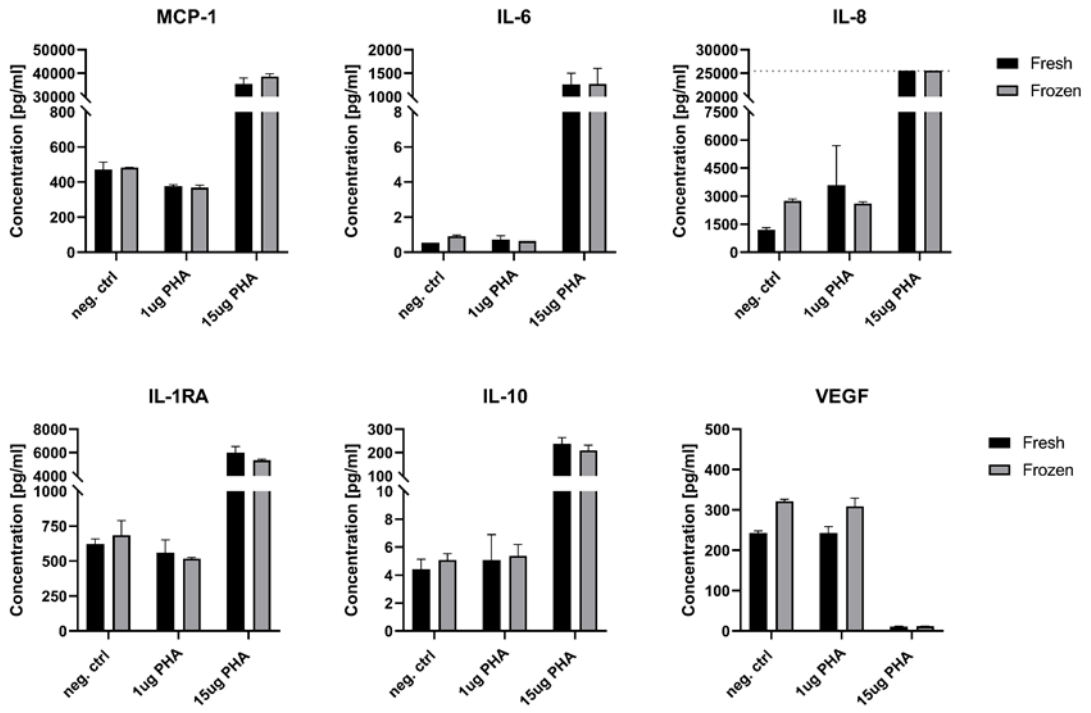

Supplementary information 1: Comparison of cytokine expression of freshly isolated PBMCs (Fresh) and PBMCs being stored at -150°C and thawed prior to the experiment (Frozen). Blood of n = 2 donors was tested.

Panel 1

Target	Fluorochrome	Clone	Company
CD3	PerCP Cy5.5	Okt.3	Biolegend
CD4	Alexa488	Okt.4	Biolegend
CD14	APC-H7	MΦP9	BD Bioscience
CD16	BV605	3G8	Biolegend
CD25	PE-Cy5	M-A251	Biolegend
CD86	BV650	IT2.2	Biolegend
CD127	BV711	A019D5	Biolegend
CD163	PE/dazzle594	GHI/61	Biolegend
CD206	PE-Cy7	15-2.	Biolegend
CD284	APC	HTA125	Biolegend
CD354	BV510	6B1	BD Bioscience
HLA-DR	BV421	L234	Biolegend

Panel 2

Target	Fluorochrome	Location	Clone	Company
CD3	PerCP Cy5.5	Cell surface	Okt.3	Biolegend
CD14	APC-H7	Cell surface	MΦP9	BD Bioscience
CD16	BV605	Cell surface	3G8	Biolegend
CD86	BV650	Cell surface	IT2.2	Biolegend
IL-6	PE-Cy7	Intracellular	MQ2-13A5	Biolegend
IL-8	APC	Intracellular	E8N1	Biolegend
TNF-α	BV711	Intracellular	MAb11	Biolegend
HLA-DR	BV421	Cell surface	L234	Biolegend

Supplementary information 2: List of antibodies used for flow cytometry

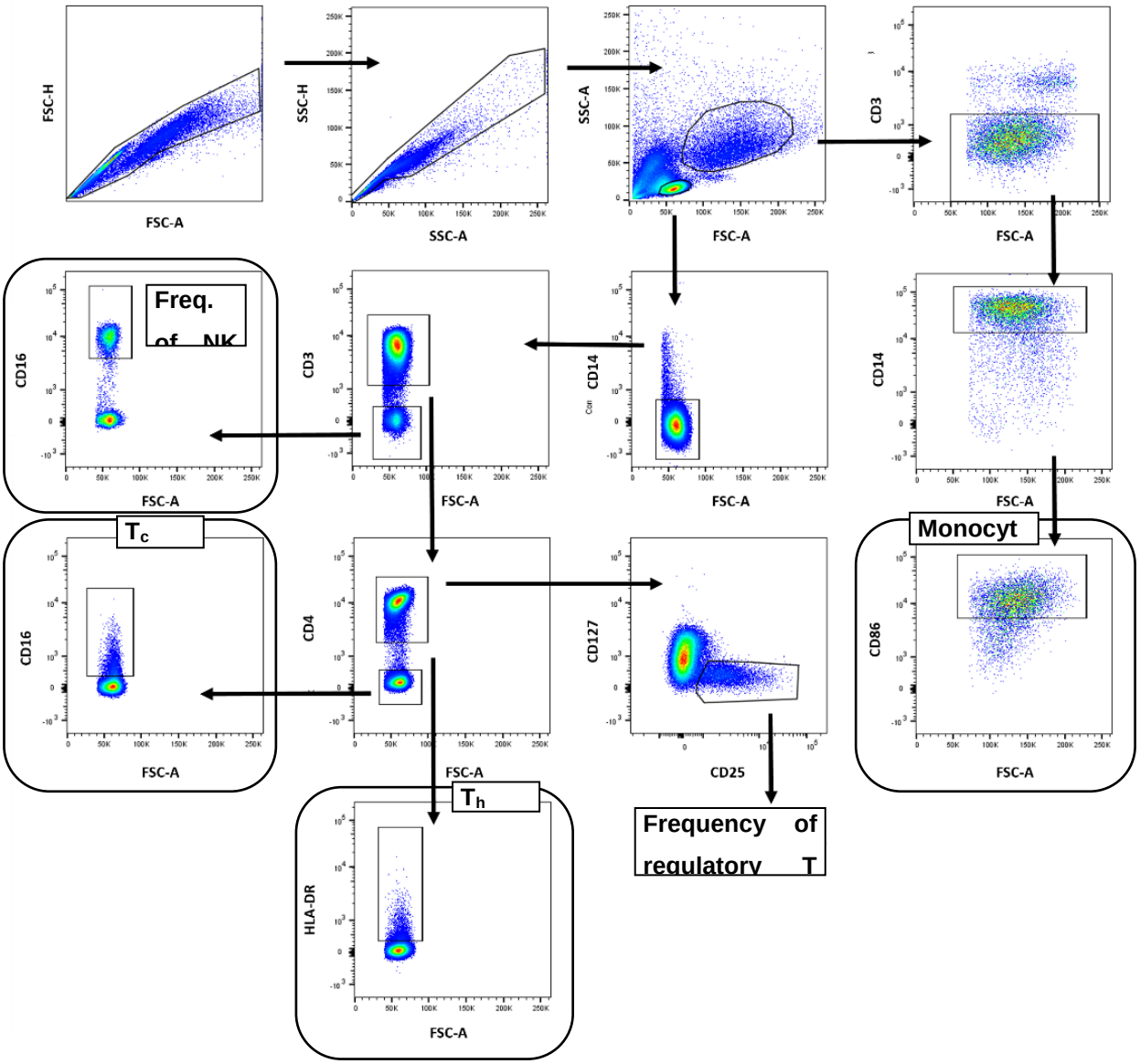

Supplementary information 3: Gating strategy for panel 1 used to identify monocytes, T helper cells (T_h cells), cytotoxic T cells (T_c cells), natural killer cells (NK cells) and regulatory T cells and analyse their activation status or frequency. Protein expression (MFI) of the markers not depicted were determined based on all cells in the relevant population.

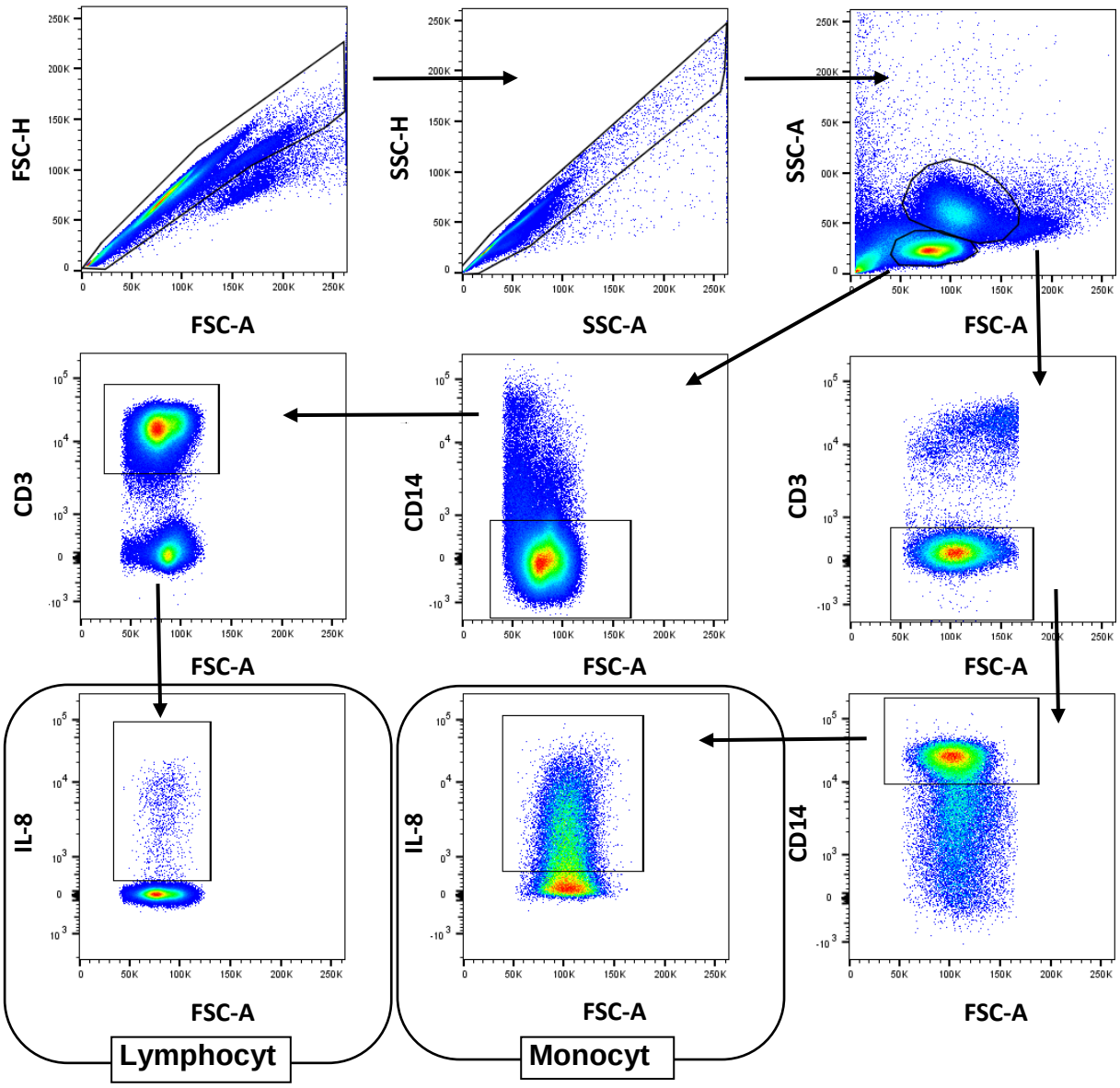

Supplementary information 4: Gating strategy for panel 2 used to analyse intracellular cytokine expression in lymphocytes and monocytes.

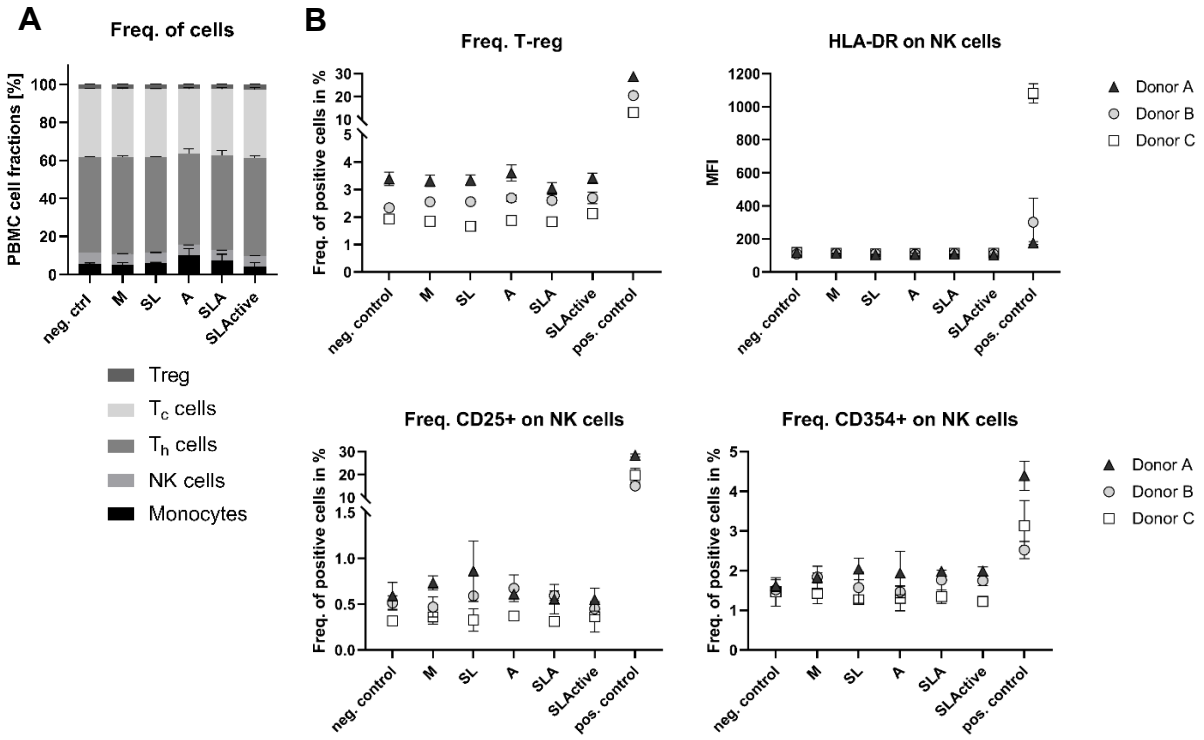

Supplementary information 5: Frequency of PBMC cell populations, regulatory T cells and expression of cell surface molecules on NK cells following culture on titanium specimens. PBMCs from three donors were cultured on the following titanium specimens for 72 hours: machine polished (M), sandblasted (SL), acid etched (A), sandblasted and acid etched (SLA) and SLA with a hydrophilic treatment (SLActive). Cell culture polystyrene was used as negative control (neg. ctrl), while the positive control (pos. ctrl) was stimulated with 100 ng/ml LPS and 15 µg/ml PHA-L. Frequencies of all analysed cell fractions cultured on titanium samples and regular tissue culture plate (neg. ctrl) of one representative donor are shown in A). B) Frequency of positive cells or mean fluorescence intensity (MFI) of surface marker expression was quantified on regulatory T cells (T-reg) and natural killer cells (NK cells) using flow cytometry. Each of the three donors was analysed in triplicate for all conditions tested (i.e. n = 3 for each donor). Graphs show mean with SEM.

Appendix II

Segan S., Jakobi M., Khokhani P., Klimosch S., **Billing F.** et al. Systematic Investigation of Polyurethane Biomaterial Surface Roughness on Human Immune Responses in vitro. *BioMed Research International, Volume 2020*.

Hindawi
BioMed Research International
Volume 2020, Article ID 3481549, 15 pages
https://doi.org/10.1155/2020/3481549

Research Article

Systematic Investigation of Polyurethane Biomaterial Surface Roughness on Human Immune Responses *in vitro*

Sören Segan,[1] Meike Jakobi,[1] Paree Khokhani,[1] Sascha Klimosch,[1,2] Florian Billing,[1] Markus Schneider,[3] Dagmar Martin,[1] Ute Metzger,[1] Antje Biesemeier,[1,4] Xin Xiong,[1] Ashutosh Mukherjee,[1] Heiko Steuer,[1] Bettina-Maria Keller,[5] Thomas Joos,[1] Manfred Schmolz,[2] Ulrich Rothbauer,[1,5] Hanna Hartmann,[1] Claus Burkhardt,[1] Günter Lorenz,[3] Nicole Schneiderhan-Marra,[1] and Christopher Shipp[1]

[1]*NMI, Natural and Medical Sciences Institute at the University of Tübingen, Markwiesenstr. 55, 72770 Reutlingen, Germany*
[2]*HOT Screen GmbH, Aspenhaustraße 25, 72770 Reutlingen, Germany*
[3]*University of Applied Sciences, Reutlingen, Alteburgstr. 150, 72762 Reutlingen, Germany*
[4]*Center for Ophthalmology, University Hospital Tübingen, Schleichstr. 12/1, 72076 Tübingen, Germany*
[5]*University of Tübingen, Geschwister-Scholl-Platz, 72074 Tübingen, Germany*

Correspondence should be addressed to Christopher Shipp; mrchristophershipp@gmail.com

Received 28 October 2019; Revised 29 January 2020; Accepted 4 March 2020; Published 12 May 2020

Academic Editor: Vasiliki Galani

It has been widely shown that biomaterial surface topography can modulate host immune response, but a fundamental understanding of how different topographies contribute to pro-inflammatory or anti-inflammatory responses is still lacking. To investigate the impact of surface topography on immune response, we undertook a systematic approach by analyzing immune response to eight grades of medical grade polyurethane of increasing surface roughness in three *in vitro* models of the human immune system. Polyurethane specimens were produced with defined roughness values by injection molding according to the VDI 3400 industrial standard. Specimens ranged from 0.1 μm to 18 μm in average roughness (Ra), which was confirmed by confocal scanning microscopy. Immunological responses were assessed with THP-1-derived macrophages, human peripheral blood mononuclear cells (PBMCs), and whole blood following culture on polyurethane specimens. As shown by the release of pro-inflammatory and anti-inflammatory cytokines in all three models, a mild immune response to polyurethane was observed, however, this was not associated with the degree of surface roughness. Likewise, the cell morphology (cell spreading, circularity, and elongation) in THP-1-derived macrophages and the expression of CD molecules in the PBMC model on T cells (HLA-DR and CD16), NK cells (HLA-DR), and monocytes (HLA-DR, CD16, CD86, and CD163) showed no influence of surface roughness. In summary, this study shows that modifying surface roughness in the micrometer range on polyurethane has no impact on the pro-inflammatory immune response. Therefore, we propose that such modifications do not affect the immunocompatibility of polyurethane, thereby supporting the notion of polyurethane as a biocompatible material.

1. Introduction

Biomaterials have become indispensable in the field of regenerative medicine, such as in the treatment of dysfunctional joints, atherosclerotic arteries, or decaying teeth. The current demand for implantable medical devices has produced a global market that exceeds the $20 billion threshold per year [1] and which is now facing further growth due to aging populations. However, the ongoing technological advances in the development of more sophisticated implants are facing considerable counter forces. This negative impact is primarily driven by an increasing level of regulation and threat of legal liability. Hybrid implants with biomimetic activity or those containing biological additives such as drug-release devices have turned into pharmacological agents according to regulatory definition and therefore have become the subject of

extensive clinical trials [2]. This is contributing to a revival of pure material-based solutions based on chemical composition and intelligent surfaces. Although less sophisticated in design, the potential in this approach is vast: A recent study showed that the addition of one methyl group to clinically relevant methacrylate produced a shift in metabolic responses of several hundred protein species by macrophages [3]. A simple yet powerful strategy to alter host response to implanted medical devices may be achieved through the modification of implant surface topography. Topographic features in the micrometer and nanometer range have been under investigation in a variety of studies to direct cell responses. For example, it was shown that microgrooves and surface roughness can be used to guide the migration and proliferation of osteoblasts and epithelial cells [4], while nanoscale topographic features can be used to modulate myofibroblast differentiation [5]. Another example is given by the use of micropatterned surfaces to control human keratocyte alignment [6], while surface topographical features can also influence endothelial cell adhesion and migration [7]. Together, these studies demonstrate the potential of using biomaterial surface topography to control the cellular host response.

Following protein adsorption to the implant surface, the immune system is the first point of cellular interaction between the body and the implant. For this reason, immune cell responses to implanted biomaterials have been claimed to pave the way for all subsequent host-material interactions [8, 9]. The immune system additionally plays roles in biological processes required for the integration of biomaterials such as wound healing, osseointegration, inflammation, and foreign body reactions [9, 10], further implicating it as a central player in the process of biological integration. Physicochemical properties such as size, shape, topography, and chemistry have been shown to provide cues to the immune system that can be used to design immune modulatory biomaterials that direct host responses towards inflammatory or wound healing phenotypes [11–13]. One such example is perfluoropolyether, where microstructures were successfully employed to drive macrophage differentiation into opposing directions. In response to regular grooves macrophages responded with a pro-inflammatory phenotype, whereas a topography containing evenly spaced pillars resulted in an anti-inflammatory M2 phenotype [14]. In another study, microstructured topographies on polyvinylidene resulted in the pro-inflammatory but also anti-inflammatory activation of macrophages, whereas relatively flat and nanotextured surfaces produced much lower levels of pro-inflammatory and anti-inflammatory responses [15]. Roughness has also been shown to be an important parameter affecting immune response to implant surfaces. For example, epoxy replicas of polished or rough titanium specimens were compared on their ability to activate macrophages. This study showed that only the rougher surface to result in increased macrophage inflammatory protein-1α (MIP-1α) and monocyte chemotactic protein-1 (MCP-1) [16]. Results from *in vivo* studies also confirm the importance of surface topography and tissue integration, as rougher surfaces have been shown to be superior for implants requiring osseointegration [17, 18].

Though a number of studies convincingly demonstrate that biomaterial surface topography has a major impact on implant-host interactions, systematic studies examining the effect of this single parameter are lacking. More comprehensive studies are required to pinpoint the surface properties most relevant for specific biological responses, as well as to eliminate bias when comparing results from different experimental concepts (cellular models, interspecies differences, and readout parameters). For this reason, we employed three *in vitro* models of the human immune system, ranging in degree of biological complexity from simple to complex: We chose a model based on THP-1-derived macrophages because this is widely regarded as a valid model to investigate biomaterials, particularly due to its demonstrated ability to relate to the host response *in vivo* [18–21]. Due to its reduced complex biology, this model also affords several advantages. This was complemented by two more complex systems: Primary peripheral blood mononuclear cells (PBMCs) and whole blood, both of which provide substantially greater biological complexity but are rarely employed in the field of biomaterials. To assess the impact of surface topography on immune response, we manufactured medical grade polyurethane (Pellethane® 2363-75D) with eight scales of surface roughness ranging from "flat" surfaces without any intentional roughness to surfaces containing a high degree of roughness. Polyurethane is a polymeric material which is generated by the reaction of polyols and toluene diisocyonate. This material is chemically inert [22] and has been used in medical devices since the second half of the 20th century [23]. Beyond its function as a coating on breast implants [24], polyurethane is also used in a multitude of settings in the health care sector, such as for dermal scaffolds [25], in bone [26] and tissue engineering [27], as artificial heart valves and arteries [28], and as insulation for pacemakers [29]. The high biocompatibility is supported by further *in vitro* studies which also show low immune responses to polyurethane [30]. By altering only a single biomaterial parameter on polyurethane specimens, we aimed to identify the impact of altered surface topography on immune response. The goal of this study was to determine if surface roughness alone could be a decisive factor in determining the immune response to a certain biomaterial.

2. Materials and Methods

2.1. Manufacture of Polyurethane Samples. The Pellethane® 2363-75D granulate used in this work is a biomedical grade thermoplastic polyurethane, commercially available from the Lubrizol corporation (Wickliffe, USA). Polyurethane specimens with defined average roughness values ranging from 0.1 μm to 18 μm were produced by injection molding utilizing steel masters. The masters, exhibiting eight grades of roughness according to the VDI (Verein Deutscher Ingenieure) 3400 industrial standard (see Table 1 for details), were manufactured by Pfletschinger & Gauch GmbH (Plochingen, Germany). Prior to use, steel masters were cleaned with propan-2-ol to remove residual anticorrosion agents. The polyurethane polymer was dried under vacuum (120 mbar) at 80°C for 24 h prior to processing. To fabricate

Table 1: Nominal average roughness values of polyurethane specimens. Polyurethane samples were manufactured according to the VDI 3400 standard ranging from the "flat" sample P0 (no intentional surface roughness) and increasing in degree of roughness to sample P7 as the roughest surface.

	VDI 0	VDI 8	VDI 14	VDI 20	VDI 27	VDI 33	VDI 39	VDI 45
Sample label	P0	P1	P2	P3	P4	P5	P6	P7
Ra in μm	0.10	0.25	0.50	1.00	2.20	4.50	9.00	18.00

the polyurethane specimens, a Boy XS injection molding machine (max clamping force = 100 kN, max injection pressure = 2298 bar, max injection speed = 35.0 g/s, max injection volume = 6.1 cm^3, screw diameter = 14 mm) was used. After the injection molding step, all samples were rinsed for 10 min with ethanol solution (70%) to remove surface residuals and subsequently dried at room temperature (RT). After drying, the samples were sterilized with 1,2-epoxyethane.

2.2. Water Contact Angle Measurement. The wettability of each sample was determined by sessile drop measurements of the water contact angle (θ) using a Krüss EasyDrop contact angle goniometer (Hamburg, Germany). To perform the measurements, a static drop was used, maintaining a constant volume during the measurement. This was performed with the deposition of 2 μL distilled water to the samples. After 20 sec, an image was recorded and transferred to the software for analysis of the static (equilibrium) contact angles. In total, nine independent measurements were performed to give mean values ± standard deviation. This method allows to quantify contact angles from 10° (hydrophilic surface) to over 90° (hydrophobic surface).

2.3. Confocal Scanning Microscopy. Surface topography was characterized by a white-light confocal microscope (STIL S.A. France, CHR 2, MG 210 Cl1). With this technique, white light is directed through a filter onto the surface of the sample. The light is separated by a filter into its component wavelengths, each corresponding to different height characteristics of the specific area. The polyurethane samples were scanned to summarize their topographical characteristics as an overall image with axial accuracy in the nanometer range. In addition, numerical characteristic of roughness was obtained (values representing average roughness, Sa). Scanning area was defined as 2.5 mm × 2.5 mm; profile filter was chosen according to DIN EN ISO 11562, and the cutoff according to DIN EN ISO 4288. A working distance of 3 mm was used for the sensor.

2.4. Scanning Electron Microscopy Assessing Material Characteristics. Scanning electron microscopy (SEM) was used to examine microtopography and nanotopography of the polyurethane samples. Samples were prepared for SEM by critical point drying and coated with a 10 nm film of gold. Surface imaging was performed with a Zeiss Auriga 40 SEM (Oberkochen, Germany) at 3 keV acceleration voltage using the chamber secondary electron detector.

2.5. Thrombin-Antithrombin (TAT) Assay. Samples were incubated with 1 mL of human blood (obtained from the local blood bank containing 1.5 U/mL heparin) in a 24 well plate (Greiner Bio-One GmbH, Frickenhausen Germany) for 2 h at 37°C with shaking at 150 RPM. Stainless steel sticks 1.401 served as positive controls (Rocholl GmbH, Aglasterhausen, Germany). Immediately after incubation, the blood was centrifuged at 2,500 g for 20 min at RT. The supernatant (plasma) was removed and stored in aliquots at -20°C. Plasma sample aliquots from negative "blank" controls (empty wells), positive controls, and experimental samples were thawed and used in ELISA for thrombin-antithrombin-complex determination (TAT) (Siemens Healthcare Diagnostics, Erlangen, Germany) according to the manufacturer's instructions.

2.6. Macrophage Cell Culture. The human monocytic leukemia cell line THP-1 (ATCC, Manassas, USA) was expanded in 75 cm^2 culture flasks (Greiner Bio-One, Kremsmünster, Austria) in RPMI 1640 (Gibco, Carlsbad, USA) supplemented with 10% heat-inactivated fetal calf serum (FCS) (Gibco) and 1% penicillin-streptomycin (Gibco) in an incubator (37°C, 5% CO_2, humidified atmosphere). Cells were subcultured routinely upon reaching a concentration between 8×10^5 and 1×10^6 cells/mL. Cells from passage 10 to 15 were used for all experiments. To induce macrophage differentiation, cells were plated in 6 well plates (Corning, Wiesbaden, Germany) at a density of 1.2×10^6 cells/well and treated with 50 ng/mL phorbol-12-myristate-13-acetate (PMA) (Sigma-Aldrich, St. Louis, USA) for 48 h. Subsequently, PMA containing media was removed and cells were cultured for a further 48 h without PMA. PMA-treated cells were detached using 0.05% trypsin/EDTA (Gibco) and reseeded onto polyurethane samples at a density of 5×10^4 cells/cm^2 in a nontransparent black 24 well plate (ibidi, Planegg, Germany) for a period of 72 h. To generate M1 or M2 macrophage phenotypes, cells were stimulated 3 h after seeding onto tissue culture plates for 72 h with either 50 ng/mL lipopolysaccharide (LPS) derived from *E. coli* (Merck Millipore, Burlington, USA) and 20 ng/mL IFN-γ (Miltenyi, Bergisch Gladbach, Germany) (M1 phenotype), or with 20 ng/mL IL-4 (Miltenyi) and 20 ng/mL IL-13 (Miltenyi) (M2 phenotype). Cells cultured on tissue culture plates without further stimuli were taken as M0 macrophages. To confirm that the M0 macrophages were in a nonactivated state, cytokine analysis was employed. Supernatants for cytokine analysis were collected, centrifuged at 5,000 RPM for 5 min to remove potential cell debris, and stored in aliquots at -80°C until analysis.

2.7. Blood Donor Selection. Peripheral blood samples were obtained from healthy donors with informed patient consent. Individuals were excluded as potential donors if they met any of the following criteria: Symptoms of systemic or local inflammatory reactions (except for single small and superficial skin lesions), last symptoms of systemic or local

inflammatory reactions of an inflammatory disease (or first symptoms of a new episode) within the last 14 days before blood donation, vaccination within the last six weeks, surgery within the last three months, chronic diseases with inflammatory components (even during symptom-free intervals), drug intake within the last 14 days (except for contraceptives) or consumption of alcohol (e.g. >0.5 L of wine or 1 L of beer on the evening prior to blood donation), or strenuous exercise performed within three hours of blood donation. Experiments with blood samples were conducted in compliance with the rules for investigation on human subjects as defined in the Declaration of Helsinki.

2.8. PBMC Cell Culture. PBMCs were isolated from whole blood of healthy volunteers by density gradient centrifugation using SepMate™ isolation tubes (StemCell Technologies, Cologne, Germany) according to the manufacturer's protocol. Isolated PBMCs were stored at -150°C in medium containing 10% DMSO, 20% FCS, and 70% RPMI until use. For seeding onto polyurethane samples, cells were thawed and resuspended in Iscove's Modified Dulbecco's Medium (IMDM) (Gibco) supplemented with 10% off-the-clot serum pooled from male AB blood group donors (H2B, Limoges, France) and seeded at a density of 0.75×10^6 cells in 750 μL medium. Phytohaemagglutinin-L (PHA-L) (15 μg/mL) (Roche, Mannheim, Germany) was used as a positive control to ensure cell functionality. Cultures were incubated at 37°C and 5% CO_2 in a humidified atmosphere for 72 h. Following culture with polyurethane samples, 200 μL cell culture medium was collected and centrifuged at 5,000 RPM for 3 min, and the supernatant was stored at -80°C until cytokine analysis.

2.9. Whole Blood Cell Culture. A testing platform based on the proprietary TruCulture® system (an established *in vitro* system for immuno-monitoring of pharmaceuticals using human whole blood) was used to assess immune response to polyurethane samples. TruCulture® tubes were loaded with polyurethane samples before the addition of TruCulture® medium. LPS (Merck, Darmstadt, Germany) and staphylococcal enterotoxin B (SEB) (BNI, Hamburg, Germany) were employed as positive controls. Blood was obtained by venepuncture, using heparinized syringes and 19 G butterfly needles. The whole blood cultures were initiated not longer than 60 min after the blood draw to prevent any loss of cell activity or nonspecific activation of the leukocytes. Heparinized human whole blood (50 IU/mL) from healthy donors was transferred to the prepared tubes and incubated at 37°C for 48 h. To prevent sedimentation of cells, the tubes were inverted for 15 min every three hours. After culture with polyurethane samples, tubes were centrifuged (500 g for 10 min), the supernatant was removed, and stored at ≤-20°C until cytokine analysis.

2.10. Cytokine Analysis Using Multiplexed Bead-Based Sandwich Immunoassays

2.10.1. Cytokine Analysis for THP-1 and PBMC Cultures. Levels of IL-1β, IL-1RA, IL-6, IL-8, IL-10, MCP-1, MIP-1β, and TNF-α were determined using the Magnetic Luminex Performance Assay, Human Cytokine Premixed Kit A (R&D Systems, Wiesbaden, Germany). The reagent volumes were adjusted for a 96 half well plate format. The following volumes were used per well: 25 μL diluted microparticle cocktail, 25 μL standard/sample volume, 30 μL diluted biotin antibody cocktail, and 30 μL streptavidin-phycoerythrin solution. All other steps were performed according to the manufacturer's instructions. Samples were thawed at 4°C and measured undiluted and at a 1 : 8 dilution. The samples were analyzed as singlets. All measurements were performed on a Luminex FlexMap® 3D analyzer system, using Luminex xPONENT® 4.2 software (Luminex, Austin, TX, USA). For data analysis, MasterPlex QT version 5.0 was employed.

2.10.2. Cytokine Analysis for Whole Blood Assays. Samples were thawed at RT, vortexed, and centrifuged for clarification (18,000 g, 1 min). The samples were successively incubated with capture microspheres, a multiplexed cocktail of biotinylated reporter antibodies and a streptavidin-phycoerythrin solution. Analysis was performed on a Luminex 100/200 instrument and data were interpreted using proprietary data analysis software developed by Myriad RBM (Austin, USA).

2.11. Scanning Electron Microscopy Assessing Cellular Morphology. After culture on polyurethane specimens, cells were washed three times with PBS (Gibco) and fixed for 2 h on ice with a PBS solution containing 4% paraformaldehyde (PFA) and 2% glutaraldehyde (both w/v). Samples were subsequently washed three times with PBS and dehydrated with a graded series of ethanol solutions (30%, 50%, 70%, 80%, 95%, and 100%). Samples were then prepared for SEM by critical point drying and coated with a 10 nm film of gold. Surface imaging was performed with a Zeiss Auriga 40 SEM (Oberkochen, Germany) at 3 keV acceleration voltage using the chamber secondary electron detector.

2.12. Microscopy and Microscopic Image Analysis

2.12.1. Fluorescent Cell Imaging. Widefield fluorescence microscopy was performed to assess cell morphology. Immunofluorescence staining was performed following a standard staining protocol. Briefly, cells were fixed in PBS containing 4% (w/v) PFA (AppliChem, Darmstadt, Germany) for 15 min at RT and then washed three times with PBS. Cells were subsequently incubated for 15 min at RT with Alexa-Fluor 555-conjugated phalloidin (Santa Cruz, Heidelberg, Germany) to stain the actin cytoskeleton and SYBR Green (Sigma-Aldrich) to stain cell nuclei. Following incubation, samples were washed three times with PBS. Images were acquired with an ImageXpress micro XL system (Molecular Devices, San José, USA).

2.12.2. Morphometric Analysis. Images were analyzed with MetaXpress software (64 bit, 6.2.3.733, Molecular Devices). For quantification, at least 200 individual cells were analyzed derived from images from three technical replicates. Using the Custom Module Editor (version 2.5.13.3) of the MetaXpress software, an image segmentation algorithm that identifies areas of interest based on the parameters of size, shape, and fluorescence intensity above local background was

established as an automated system. This led to a segmentation mask recognizing the whole cell including the nucleus. Morphological analysis and subsequent image-based quantification was performed using a set of the following predefined morphometric parameters: Cell area, cell shape factor, and cell elongation factor. Cell shape factor and cell elongation factor were used to quantify cell shape. The cell elongation factor was determined as a ratio of the long to the short axis in which a higher value indicates increased elongation. To further distinguish round macrophages from flattened or elongated macrophages, we considered the cell shape factor. This factor describes the cell circularity and takes a value between 0 and 1, whereby a value near 0 indicates a flattened object and a value of 1 indicates a perfect circle.

2.13. Flow Cytometry. For flow cytometric analysis, cells were harvested in the following manner: Nonadherent cells were first removed by pipette resuspension and rinsed with PBS, followed by the detachment of adherent cells using EDTA (Invitrogen, Carlsbad, USA) (10 mM at 37°C for 5 min) after which an equal volume of PBS was added. This was followed by pipette resuspending to lift adherent cells. Cells were then rinsed with washing buffer (2% FCS, 2 mM EDTA, 0.05% sodium azide, pH 7.4) and centrifuged at 300 g for 5 min. After supernatant removal, nonspecific binding sites were blocked using 10% human serum (diluted in washing buffer) for 20 min at RT. Cells were then washed with 1 mL washing buffer, centrifuged (300 g for 5 min), and the supernatant was removed before the labelling of immune cell populations using the following antibodies in distinct panels (incubated for 30 min on ice and protected from light): CD14-PerCP Cy5.5, CD16-PE-Cy5, CD163-PE-Dazzle594, CD3-BV421, CD86-Alexa Fluor 488, HLA-DR-PE-Cy7, and PD-1-Alexa Fluor 488 (all from Biolegend, London, UK). Cells were immediately analyzed using a BD FACSMelody instrument (BD Bioscience, Heidelberg, Germany) with FACS Chorus software (BD Biosciences). Data were analyzed using FlowJo software v10 (FlowJo LLC, Ashland, USA) according to the gating strategy in Supplementary Data 1.

2.14. Statistical Analysis. Data are expressed as the mean ± standard derivation (SD). Ordinary one-way ANOVA followed by a post hoc Tukey's test was used to compare morphometric data groups. Kruskal-Wallis ANOVA was applied to compare groups for cytokine production and CD molecule expression data, in which multiple comparisons were corrected for using a post hoc Dunn's test. Differences were considered statistically significant using a threshold of $p < 0.05$. Statistical analysis and plotting were performed with Prism software (GraphPad Software Inc., San Diego, USA). Principal component analyses (PCA) and heat maps were analyzed with ClustVis software (https://biit.cs.ut.ee/clustvis/).

3. Results

3.1. Characterization of Polyurethane Samples: Examination of Surface Topography and Material Wettability

3.1.1. Confocal Scanning Microscopy. For this study polyurethane samples were fabricated by injection molding from steel masters with eight different roughness grades according to the VDI 3400 industrial standard (for details, see Materials and Methods), ranging from VDI 0 ("flat" with no intentional surface roughness, referred to as P0) to VDI 45 (roughest surface investigated, here designated P7) (Table 1).

Selected specimens P0 (VDI 0), P4 (VDI 27), and P7 (VDI 45) were examined with confocal scanning microscopy in order to ensure that the polyurethane samples exhibited the intended surface characteristics. While visual analysis showed a clear correlation between increasing VDI number and greater surface roughness, our analysis also revealed a finer structure in addition to the microscale topography, particularly present in the valleys of samples P0 and P4 (Figure 1). Based on the images acquired, it can be seen that the topography was uniformly distributed across the samples surface. Only minor inconsistencies could be observed on samples P0 and P4, while heterogeneity is seen on sample P7 due to the high degree of an overall surface roughness.

3.1.2. Scanning Electron Microscopy. Having observed a finer surface structure present in addition to the micro roughness, we next employed SEM to examine these features in more detail at higher resolution. Similar to the results obtained with confocal scanning microscopy, the samples P0 (VDI 0), P4 (VDI 27), and P7 (VDI 45) showed the expected increased surface roughness on the microscale with higher VDI numbers (Figure 2, left panel). However, if viewed at a higher magnification, these differences were less pronounced. Notably, a finer structure of nanoscale topographies such as elevations, dips, or protrusions were observed in all samples (Figure 2, middle and right panels).

3.1.3. Water Contact Angle Measurement. Wettability of biomaterials can be a decisive factor influencing the biological response towards an implant material [31]. In this context, surface topography has also been shown to affect the wettability of a material [32]. Therefore, the drop shape analysis method was used to determine the static contact angle and to assess the wettability of polyurethane specimens with varying surface roughness. Contact angle analysis showed polyurethane to be a hydrophobic material (contact angle $(\theta) > 90°$), whereas no effect of surface topography on material wettability was observed—samples with different surface roughness were similarly hydrophobic with contact angles between 100° and 108° (Figure 3).

3.2. Cellular Responses to Polyurethane Surface Topography. Host response to foreign implant materials occurs through cellular sensing following cell adhesion to the implant surface. Thus, before directly investigating immunological responses to polyurethane, we first examined whether immune cells were capable of adhering to the material surface. We visualized the interaction of primary human PBMCs and THP-1-derived macrophages with the surface topographies of selected polyurethane samples using SEM. For both immune models, we observed cell adhesion after three days of culture (Figure 4). Cells were found to adhere in a heterogeneous fashion. For both models, we observed isolated single cells (Figure 4(c)) and small clusters of interacting cells (Figures 4(d) and

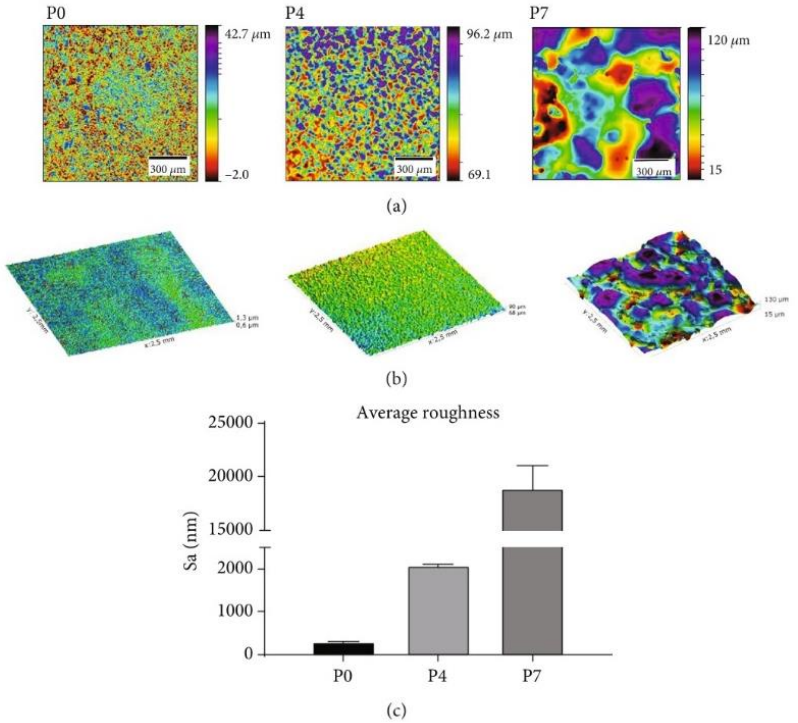

FIGURE 1: Confocal scanning microscopy of polyurethane samples with different surface roughness. (a) 2D and (b) 3D images of polyurethane samples with different roughness profiles. (c) Quantification of average surface roughness. Roughness is shown as Sa (average roughness): P0 (VDI 0) Sa 294 ± 13 nm (left), P4 (VDI 27) Sa 2,071 ± 30 nm (middle), P7 (VDI 45) Sa 18,913 ± 2,139 nm (right). The size of the analysis area for 3D images was 2.5 mm × 2.5 mm.

4(h)). Furthermore, SEM observations suggested the potential for immune cells to adapt to the underlying topographical characteristics of the polyurethane specimens.

3.2.1. Macrophage Model. Having observed that immune cells can adhere to the surface of polyurethane specimens, we next investigated the biological responses to polyurethane samples ranging in degree of surface roughness from "flat" samples without intentional roughness (P0) to polyurethane specimens with increasing levels of roughness (P1–P7). Thus, we employed THP-1 monocytes differentiated into macrophage-like cells. Similar to macrophages obtained from primary human monocytes, THP-1-derived macrophages are a commonly used model to study polarization into M1 or M2 macrophages [33]. As controls, THP-1-derived macrophages were either used in the neutral M0 state or were further polarized into the M1 (pro-inflammatory) or the M2 (anti-inflammatory) phenotype. To monitor cellular response on the single cell level, the morphology of cells cultured on different surfaces was initially characterized using widefield fluorescence microscopy. As part of this analysis, three morphometric parameters (cell area, cell shape factor, and cell elongation factor) were included. As previously reported [34] and shown in Figure 5, these parameters can be used to distinguish between macrophages showing either the M1 or the M2 phenotype: THP-1-derived M1 macrophages have a more rounded shape with a decreased cell elongation factor and an increased cell shape factor compared to M0 macrophages (Figure 5).

Compared to cells cultured on tissue culture polystyrene (TCP), cells cultured on the different polyurethane surfaces indicated a less rounded morphology (Figure 5). However, cell circularity and elongation were generally unaffected by the degree of surface roughness on the polyurethane samples. The only exception was observed for cells cultured on specimens P4 and P5, which tended to be more spread and thus to cover a greater area (the high degree of surface roughness prevented microscopically morphometric image analysis of cells cultivated on samples P6 and P7).

To complement the analysis of cell morphology, we additionally analyzed the secretion of pro-inflammatory and anti-inflammatory cytokines to examine macrophage polarization. As expected, nonactivated M0 cells cultured on TCP expressed low levels of both pro-inflammatory and anti-inflammatory cytokines. In contrast, M1 polarized cells showed an upregulation of pro-inflammatory markers, while M2 cells showed downregulated production of the pro-inflammatory cytokine IL-8. When cultured on polyurethane samples, THP-1-derived macrophages responded with marginal elevation of pro-inflammatory cytokines, clearly below the M1 level. Examining the responses of cells cultured on polyurethane with different surface topographies, despite slight tendencies for some cytokines, no clear association between the degree of surface roughness and cytokine

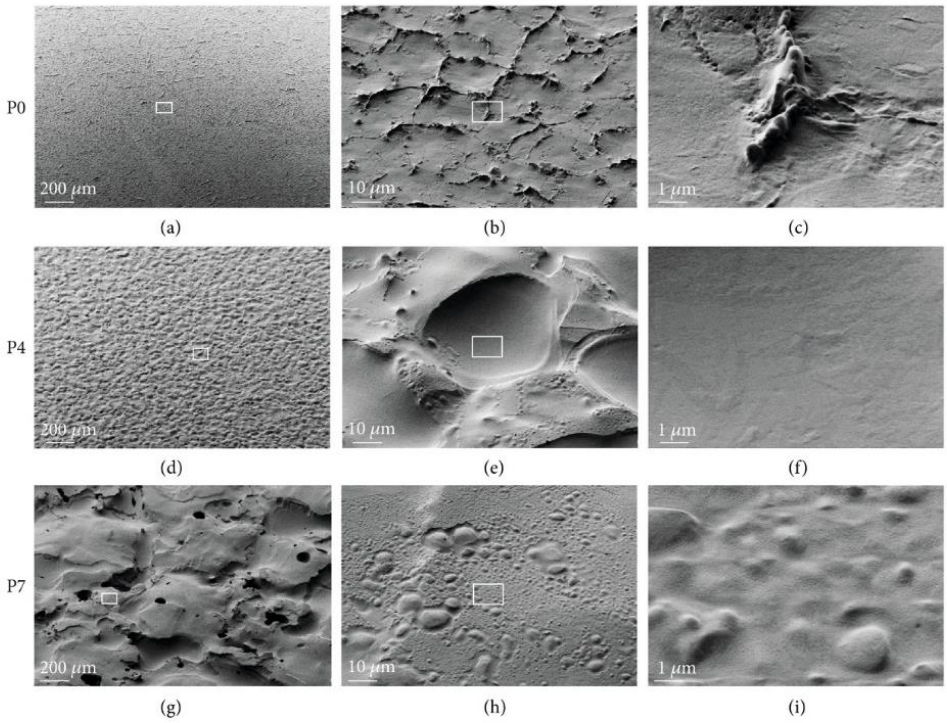

FIGURE 2: SEM micrographs of polyurethane samples with different roughness. (a-c) P0; (d-f) P4; (g-i) P7. At low magnification, the roughness corresponds well to the expected degree of roughness. However, samples additionally show features of nanoscale topographies such as elevations, dips, or protrusions that do not correlate with levels of micro roughness. Magnification increases from left to right in the figure. P0, P4, and P7 represent polyurethane surfaces with increasing roughness.

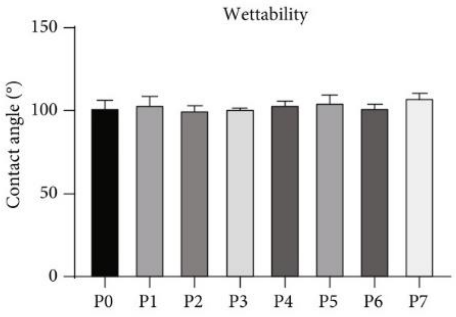

FIGURE 3: Wettability of polyurethane samples with different surface roughness. Static contact angles of polyurethane samples differing in surface roughness were analyzed from three independent measurements, each performed in triplicate and shown as mean ± standard deviation.

production could be observed (Figure 6). Results obtained for IL-6 and IL-10 are similar to those depicted in the figure and are therefore not shown.

3.2.2. Primary Human PBMC Model. Having observed only minimal effect of surface roughness on the behaviour of THP-1-derived macrophages, we next employed a model with more biological complexity. We anticipated that such a model might respond with greater sensitivity to differences in biomaterial characteristics. To this end, human primary PBMCs derived from three healthy donors encompassing the full spectrum of circulating immune cells except granulocytes were utilized to study polyurethane specimens. After three days of culture, we analyzed the behaviour of specific immune cell populations in response to different biomaterial surface roughness utilizing flow cytometry to assess the expression of cell surface markers on monocytes (HLA-DR, CD86, CD163, and CD16), T cells (HLA-DR, PD-1, and CD16), and natural killer (NK) cells (HLA-DR and PD-1). Populations of interest were identified by their specific cell surface markers: T cells ($CD3^+$), NK cells ($CD3^-/CD16^+$), and monocytes ($CD14^+$). All experiments included PHA-L as a positive control (data not shown).

Our analysis showed that T cell activation markers were slightly elevated in response to polyurethane, but the level of expression was not affected by increasing material surface roughness (Figure 7(a)). Similarly for NK cells, there was no association between degree of material roughness and expression of surface markers (Figure 7(b)). This was also the case for monocytes where neither pro-inflammatory (HLA-DR and CD86) nor anti-inflammatory markers (CD163) were found to be altered in response to surface roughness (Figure 7(c)).

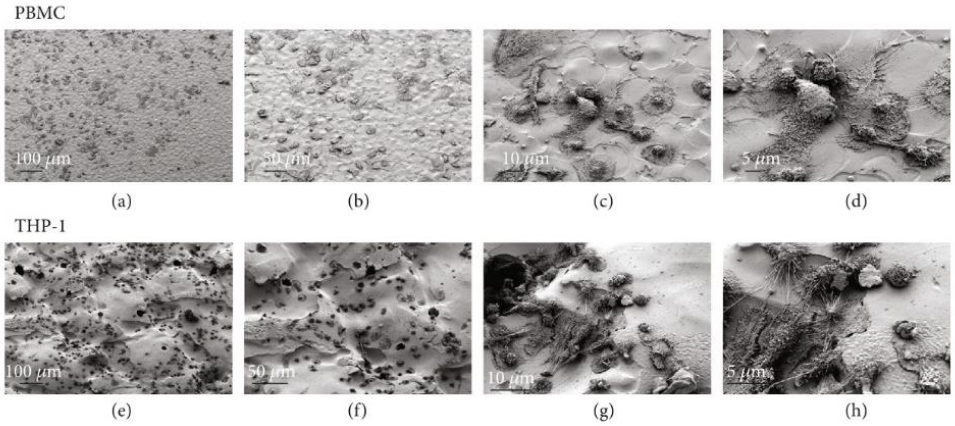

FIGURE 4: Scanning electron microscopy (SEM) images of immune cells adherent to polyurethane. Representative SEM micrographs of PBMCs (upper row, a-d) on polyurethane specimens P2 (VDI 14) or THP-1-derived macrophages (lower row, e-h) on polyurethane specimens P6 (VDI 39) following three days of culture.

Flow cytometry, which examines specific populations of immune cells, did not detect an effect of altered surface topography on the immune response. Thus, we next employed a broader assessment of immune response from all cells by characterizing cytokine production after contact with polyurethane. Quantification of the levels of pro-inflammatory cytokines Il-1β, MIP-1β, MCP-1, and TNF-α along with the anti-inflammatory cytokines IL-1RA and IL-10 following three days of culture with polyurethane specimens of varying surface roughness showed a slight pro-inflammatory response in three of the four pro-inflammatory cytokines compared to the TCP control (Figure 8(a)). However, across the polyurethane samples with different surface roughness, no difference in the levels of either pro-inflammatory or anti-inflammatory cytokines was observed (Figure 8). Results obtained for IL-6 and IL-8 are similar to those depicted in the figure and are therefore not shown. Taken together, these results show that for human PBMCs neither the expression of CD molecules nor the secretion of cytokines changed in response to differences in polyurethane surface roughness.

3.2.3. Whole Blood Models. As both THP-1-derived macrophages and human PBMCs were found not to respond to changes in polyurethane surface topography, we finally employed the human whole blood model which adds an additional degree of biological complexity. In order to obtain a broader assessment of potential immune responses, the number of investigated cytokines was further expanded from eight to 25.

According to our experimental settings, whole blood from healthy donors was cultured with all polyurethane specimens encompassing different roughness grades for two days before the spectrum of pro-inflammatory and anti-inflammatory cytokines and chemokines was quantified. Measuring this cytokine panel, we could not detect any effect of surface roughness on the production of either pro-inflammatory or anti-inflammatory cytokines in our whole blood model (Figure 9). These findings are in consistency with our previous observations of THP-1-derived macrophages and the human PBMC model.

Additionally, we also performed the whole blood experiments with LPS/SEB costimulation in order to analyze a potential immune suppressive effect of polyurethane. The results of these experiments also showed no impact of polyurethane roughness on the immune response (Supplementary Data 2). Finally, we tested the effect of surface roughness on the clotting of whole blood using the thrombin-antithrombin assay, which also showed no difference in any of the tested topographies (data not shown).

4. Discussion

In this study, we undertook a systematic approach to investigate the immune response to surface roughness, with the aim of understanding how surface topography can impact immune responses to polyurethane biomaterial. Alterations in surface topography are widely reported in the literature to be important for immune responses to biomaterials. For example, a number of studies point to differential immune activation on smooth vs. rough titanium [35–37]. This has also been shown for other classes of material such as polytetrafluoroethylene [13], glass [38], and polyvinylidene fluoride [15]. In light of these studies, it was rather unexpected that we could not observe an impact of any of the eight grades of surface roughness on immune response in our suite of immune models ranging from reductionist to highly complex *in vitro* systems. While prior studies investigating the impact of surface topography on immune response have been performed with many different classes of material, this is according to our knowledge, the first study which has been conducted utilizing polyurethane. As such, it can be speculated that biomaterial chemistry has a more pronounced effect on the immune response compared to surface topography. For example, the very low levels of immune response we observed to polyurethane may have rendered the impact of topography irrelevant. This could be partially

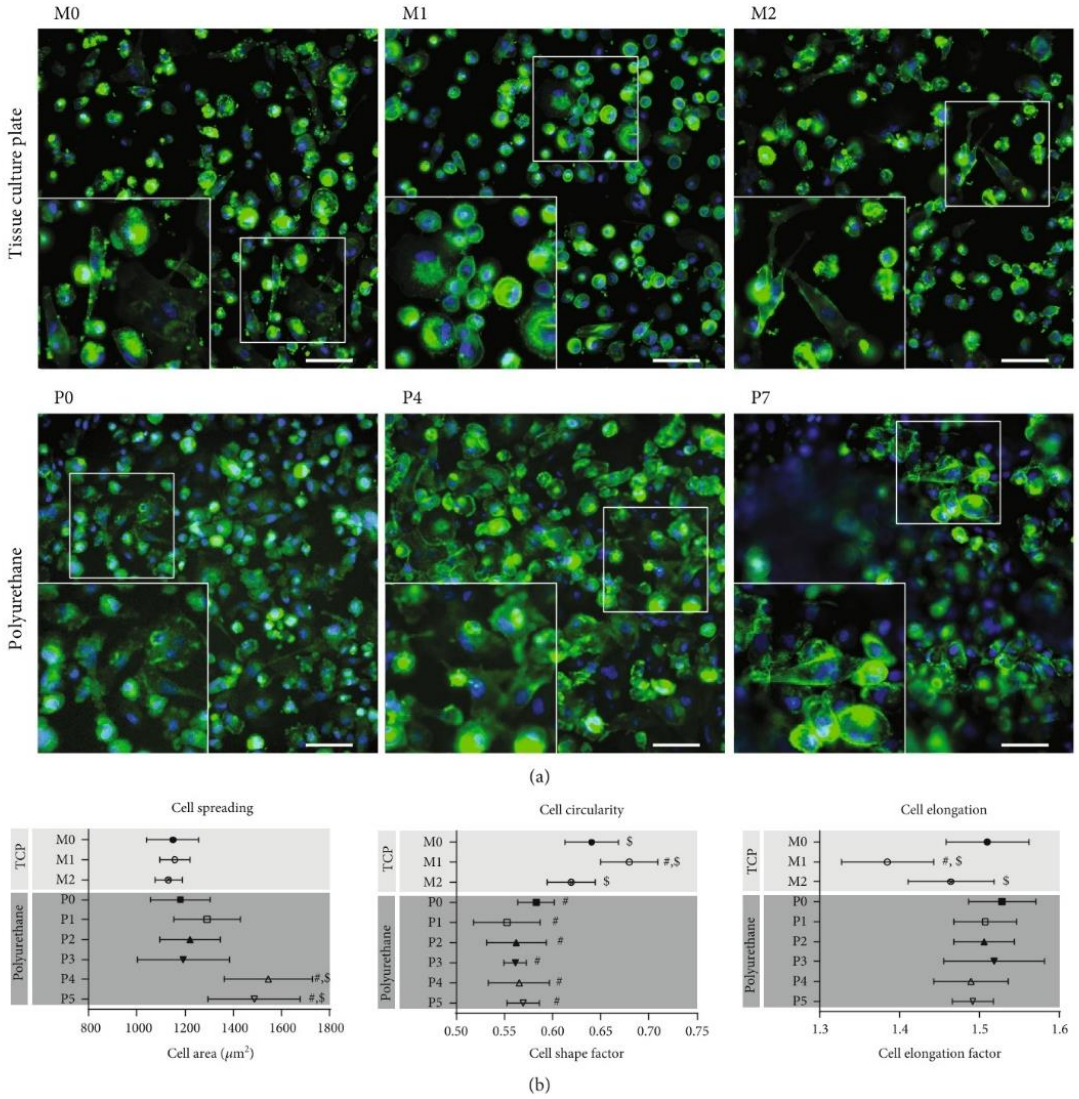

FIGURE 5: Morphology of THP-1-derived macrophages cultured on tissue culture polystyrene (TCP) or polyurethane with different surface roughness. (a) Fluorescent images of macrophages cultured on different surfaces. The upper panel shows representative images of THP-1-derived macrophages polarized as M0, M1, or M2 phenotypic cells on TCP. The lower panel shows images of THP-1-derived macrophages cultured on polyurethane surfaces with different roughness (P0, P4, and P7). For fluorescent imaging cells were stained with AlexaFluor 555-phalloidin (actin cytoskeleton, green) and SYBR Green (nucleus, blue). Scale bar: 100 μm. (b) Morphological characteristics of THP-1-derived macrophages cultured on polyurethane samples differing in surface roughness. Data are derived from automated image analysis of cells cultured either under control conditions on TCP (M0, M1, and M2 polarization) or on different polyurethane surfaces with increasing roughness from P0 (flat) to P5 (roughest). P6 and P7 samples could not be analyzed due to the high degree of surface roughness. Graphs show total cell area (spreading), cell circularity, and cell elongation. Each data point shows mean ± SD of >200 cells. $^{\#}p < 0.05$ vs. M0, $^{\$}p < 0.05$ vs. P0.

explained by the impact of material wettability, because certain hydrophobic materials such as polyurethane have shown the potential to reduce protein adsorption [39, 40] which may also dampen subsequent immune reactions. As such, we speculate that the types of surface roughness investigated in this study may nonetheless be relevant for the modulation of immune response to other classes of materials. It should, however, additionally be pointed out that our results showing no impact for microscale surface topography on biological response are not entirely at odds with the literature; a number of previous studies also report similar findings. For example, a study employing THP-1-derived macrophages found no difference in the expression of M1 or M2-associated genes on smooth vs. rough titanium surfaces [41]. Furthermore,

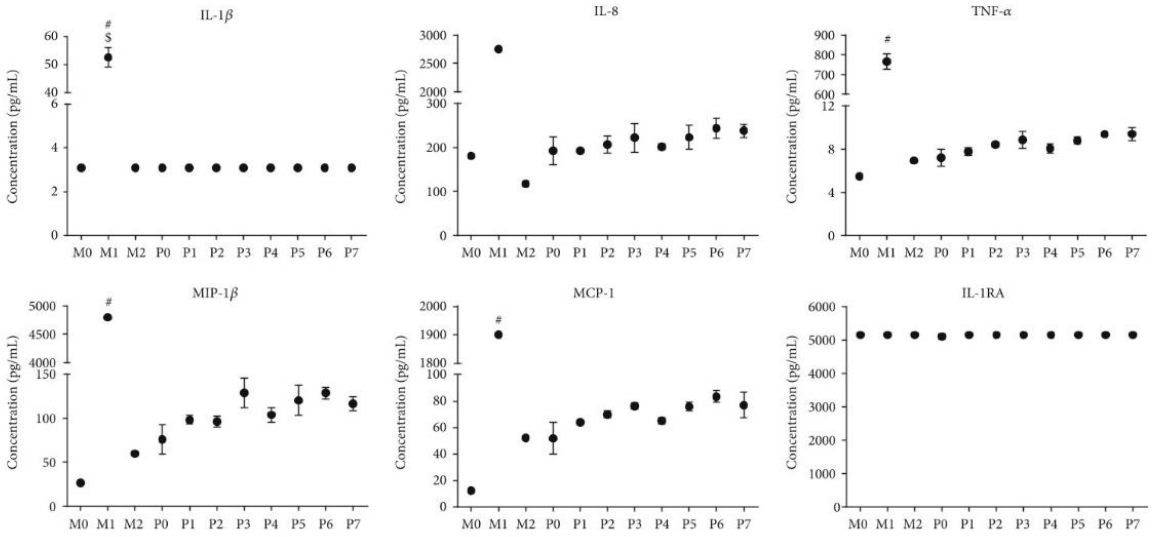

FIGURE 6: Pro-inflammatory and anti-inflammatory cytokine production from THP-1-derived macrophages cultured on polyurethane with different surface roughness. Cytokine release from control THP-1-derived macrophages (M0 (neutral), M1 (pro-inflammatory), and M2 (anti-inflammatory)) cultured for 3 days on TCP or on polyurethane with increasing surface roughness ranging from P0 (flat) to P7 (roughest). Cytokines were analyzed using multiplexed bead-based sandwich immunoassays. Shown are the expression levels (pg/mL) of the pro-inflammatory (IL-1β, MIP-1β, MCP-1, IL-8, and TNF-α) and anti-inflammatory (IL-RA) cytokines. Data are shown as mean values ± SD. If no error bars are shown in graphs, values were either above (IL-8 and IL-1RA) or below the limit of quantification (IL-1β). $^{\#}p < 0.05$ vs. M0, $^{\$}p < 0.05$ vs. P0.

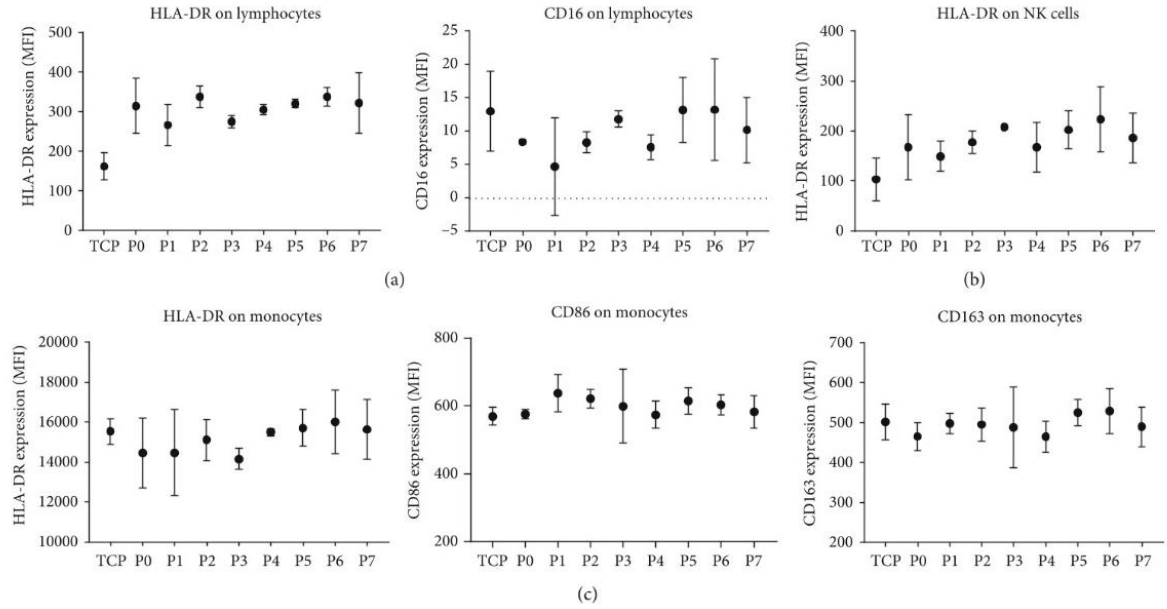

FIGURE 7: Immune response by PBMC cell surface markers to polyurethane surface roughness. PBMCs were cultured on polyurethane with different surface roughness (P0-P7) for three days, and the expression of cell surface markers on T cells (lymphocytes), NK cells, and monocytes was assessed. Expression of HLA-DR and CD16 on $CD3^+$ T cells (a) HLA-DR on $CD3^-/CD16^+$ natural killer cells (b) and HLA-DR, CD86, and CD163 on $CD14^+$ monocytes (c) from PBMCs cultured on polyurethane samples with increasing roughness from P0 (flat) to P7 (roughest). Data not shown for PD-1 on T cells/NK cells and CD16 on monocytes. Data points are derived from mean fluorescence intensity (MFI) ± SD of three technical replicates. Experiments included the testing of three donors, while graphs show one representative donor. TCP: tissue culture polystyrene.

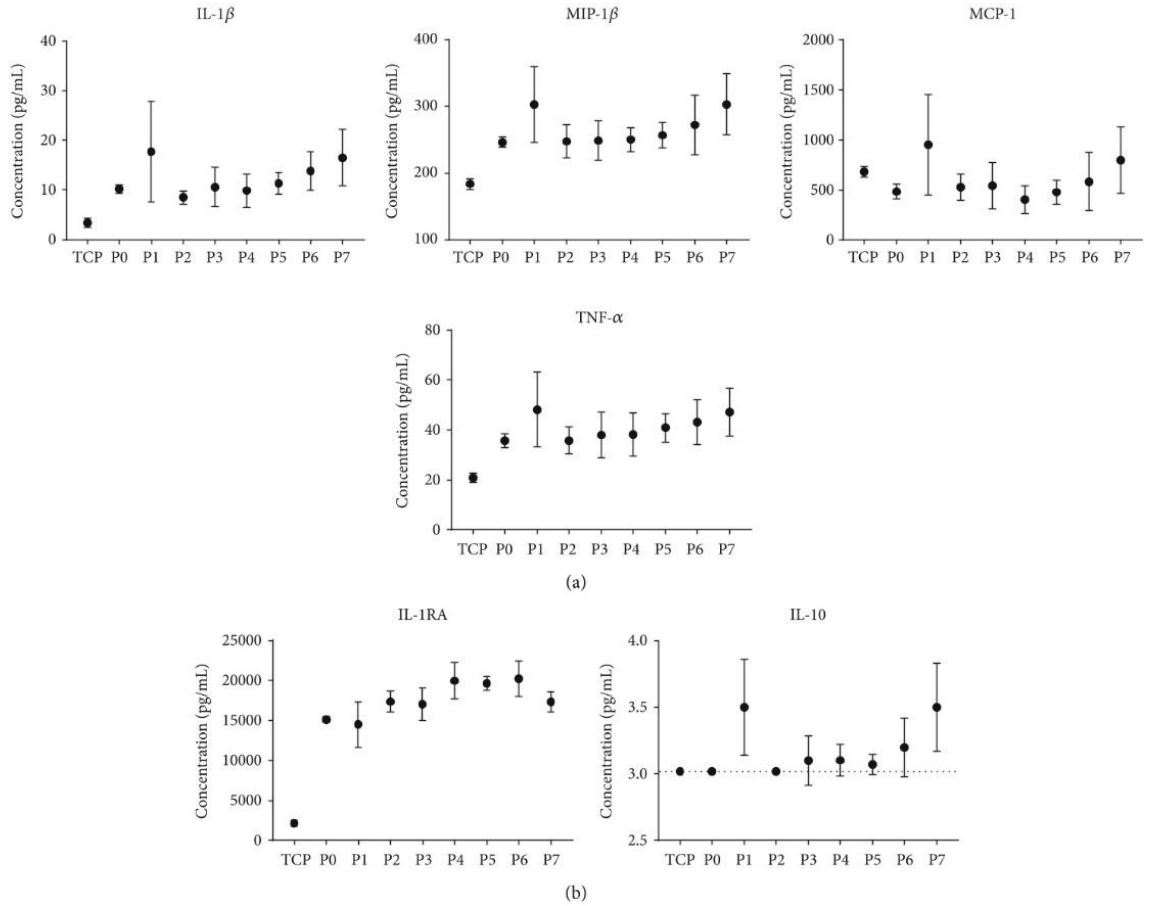

FIGURE 8: Pro-inflammatory and anti-inflammatory cytokine production from PBMCs cultured on polyurethane with different surface roughness. PBMCs were cultured for three days on polyurethane of increasing surface roughness (P0–P7), after which the concentrations of pro-inflammatory (a) and anti-inflammatory (b) cytokines were assessed using multiplexed bead-based sandwich immunoassays. For IL-10, the samples TCP, P0 and P2 were below the lower limit of quantification (3 pg/mL) and therefore do not contain error bars. Data points are derived from mean cytokine concentration (pg/mL) ± SD of three technical replicates tested for 1 representative donor (3 donors tested in total). TCP, tissue culture polystyrene.

human-derived macrophages were found to be unresponsive by cytokine production and CD molecule expression to different micropatterned hydrogel surfaces [42], and cytokine response from human whole blood was unaffected by surface roughness to polystyrene and poly(ether imide) [43]. A further consideration is that the present study did not examine specific parameters of surface topography such as shape or spacing, which may alter immune cell behaviour even when the overall degree of roughness is similar. When examining the polyurethane specimens at high resolution using SEM, we observed the samples to contain a mixture of essentially flat surfaces together with regions containing nanoscale topographical features. Therefore, it remains a possibility that immune responses to polyurethane may be more sensitive to submicron-scale types of topography designed to consider the size of adherent immune cells.

The findings presented in this study may have important clinical implications for the design of polyurethane-based biomaterials, which are considered widely for the applications including dermal scaffolds [25], bone [26] and tissue engineering [27], artificial heart valves and arteries [28], insulation for pacemakers [29], and as a coating material on silicone breast implants [24]. Silicone breast implants in particular are notorious for the relatively common presentation of patient side effects such as capsular contracture which occurs in approximately 10–20% of patients [44]. It has been shown that textured vs. smooth silicone breast implants lead to reduced rates of capsular contracture and show better biocompatibility [45]. The mechanism behind this different biological response appears to be related to the altered surface topography, which is supported by studies demonstrating that altering the surface topography of silicone results in different biological response *in vivo* and *in vitro* [46]. In contrast, our results here indicate that the biological response to polyurethane is not affected by changes in microscale surface topography, as all roughness grades produced similar

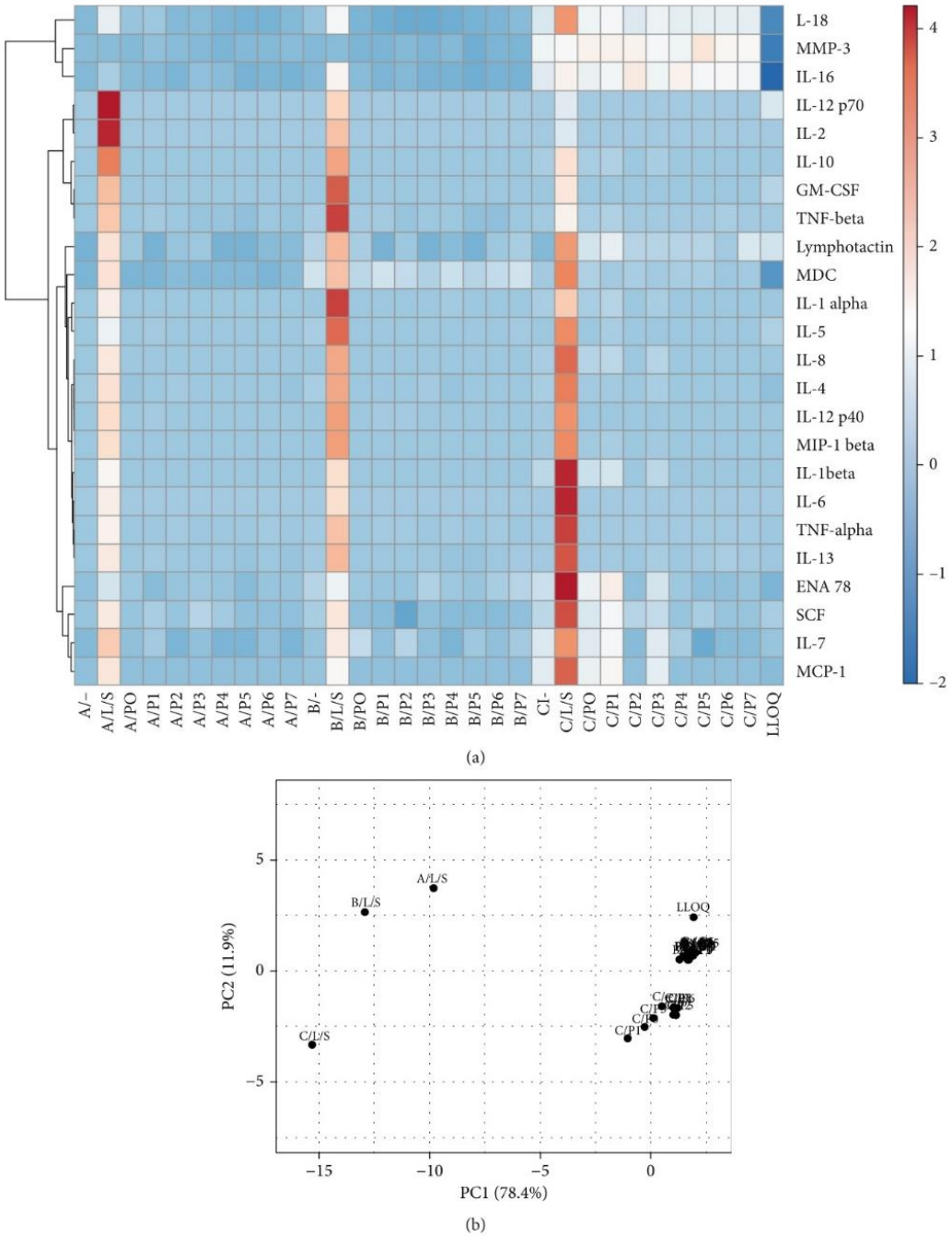

FIGURE 9: Pro-inflammatory and anti-inflammatory cytokine production from whole blood cultured on polyurethane with different surface roughness. Human whole blood was cultured for 48 hours with polyurethanes of increasing surface roughness (P0P7). The concentration of cytokines was assessed using multiplexed bead-based sandwich immunoassays. Data from three separate healthy donors analyzed in parallel are displayed as a heat map and as principal component analysis (PCA). (a) Heat map: Rows are centered; unit variance scaling is applied to rows. Rows are clustered using correlation distance and average linkage. 24 rows, 31 columns. (b) PCA: Unit variance scaling is applied to rows; SVD with imputation is used to calculate principal components. X and Y axes show principal component 1 and principal component 2 that explain 78.4% and 11.9% of the total variance, respectively. $N = 31$ data points. (https://biit.cs.ut.ee/clustvis/). Donors: $N = 3$, (a-c); L/S: LPS/SEB; LLOQ: lower limit of quantification.

immune responses. Furthermore, the degree of immune response was low compared to positive and negative controls, thereby suggesting this grade of polyurethane as an immunologically inert material that inherently produces very low immune responses independent of surface topography. This notion is supported by the clinical use of polyurethane biomaterials where polyurethane coated breast implants have been shown to be more biocompatible and result in lower rates of patient side effects like capsular contracture compared to silicone implants [24, 47, 48]. This is supported by other *in vitro* studies which also show low immune responses to polyurethane [30]. The findings here have implications for the design of biomaterials, namely, they suggest that unlike other classes of material, surface topography in the micrometer range is not a major parameter for the design of polyurethane implant biocompatibility.

5. Conclusions

In summary, this study comprehensively demonstrates that microscale surface roughness is not a decisive factor in determining immune response to medical grade polyurethane. The low levels of immune response observed to polyurethane here further support studies showing it to be a biocompatible material.

Data Availability

The data used to support the findings of this study are available from the corresponding author upon request.

Conflicts of Interest

The authors declare that there is no conflict of interest regarding the publication of this paper.

Authors' Contributions

Sören Segan and Meike Jakobi contributed equally to this work.

Acknowledgments

This work was supported by the EU-EFRE and the German State of Baden-Wuerttemberg (712889). We are very grateful to Burkhard Schlosshauer (NMI) for his contribution to the manuscript and to the planning and accompanying of this work.

Supplementary Materials

Supplementary 1. Supplementary Data 1. Gating strategy used to identify leukocyte populations from PBMCs

Supplementary 2. Supplementary Data 2. Pro-inflammatory and anti-inflammatory cytokine production from whole blood costimulated with LPS/SEB cultured on polyurethane with different surface roughness. Human whole blood was stimulated with 0.01 μg/mL LPS/SEB and cultured for 48 hours with polyurethane specimens of increasing surface roughness (P0-P7). The concentration of cytokines was assessed using multiplexed bead-based sandwich immunoassays. Data from three separate healthy donors analyzed in parallel are displayed as a heat map and as principal component analysis (PCA). (a) Heat map: Rows are centered; unit variance scaling is applied to rows. Rows are clustered using correlation distance and average linkage. 22 rows, 23 columns. (b) PCA: Unit variance scaling is applied to rows; SVD with imputation is used to calculate principal components. *X* and *Y* axes show principal component 1 and principal component 2 that explain 55.7% and 33.2% of the total variance, respectively. $N = 33$ data points (https://biit.cs.ut.ee/clustvis/). Donors: $N = 3$, A-C; L/S: LPS/SEB; LLOQ: lower limit of quantification

References

[1] B. M. Holzapfel, J. C. Reichert, J. T. Schantz et al., "How smart do biomaterials need to be? A translational science and clinical point of view," *Advanced Drug Delivery Reviews*, vol. 65, no. 4, pp. 581–603, 2013.

[2] P. S. Kowalski, C. Bhattacharya, S. Afewerki, and R. Langer, "Smart biomaterials: recent advances and future directions," *ACS Biomaterials Science and Engineering*, vol. 4, no. 11, pp. 3809–3817, 2018.

[3] M. D. Chamberlain, L. A. Wells, A. Lisovsky et al., "Unbiased phosphoproteomic method identifies the initial effects of a methacrylic acid copolymer on macrophages," *Proceedings of the National Academy of Sciences of the United States of America*, vol. 112, no. 34, pp. 10673–10678, 2015.

[4] G. R. Owen, J. Jackson, B. Chehroudi, H. Burt, and D. M. Brunette, "A PLGA membrane controlling cell behaviour for promoting tissue regeneration," *Biomaterials*, vol. 26, no. 35, pp. 7447–7456, 2005.

[5] K. E. Myrna, R. Mendonsa, P. Russell et al., "Substratum topography modulates corneal fibroblast to myofibroblast transformation," *Investigative Ophthalmology & Visual Science*, vol. 53, no. 2, pp. 811–816, 2012.

[6] C. Kilic, A. Girotti, J. C. Rodriguez-Cabello, and V. Hasirci, "A collagen-based corneal stroma substitute with micro-designed architecture," *Biomaterials Science*, vol. 2, no. 3, pp. 318–329, 2014.

[7] G. Le Saux, A. Magenau, T. Böcking, K. Gaus, and J. J. Goodin, "The relative importance of topography and RGD ligand density for endothelial cell adhesion," *PLoS One*, vol. 6, no. 7, article e21869, 2011.

[8] M. R. Major, V. W. Wong, E. R. Nelson, M. T. Longaker, and G. C. Gurtner, "The foreign body response: at the interface of surgery and bioengineering," *Plastic and Reconstructive Surgery*, vol. 135, no. 5, pp. 1489–1498, 2015.

[9] S. Franz, S. Rammelt, D. Scharnweber, and J. C. Simon, "Immune responses to implants—a review of the implications for the design of immunomodulatory biomaterials," *Biomaterials*, vol. 32, no. 28, pp. 6692–6709, 2011.

[10] L. Ginaldi and M. De Martinis, "Osteoimmunology and beyond," *Current Medicinal Chemistry*, vol. 23, no. 33, pp. 3754–3774, 2016.

[11] J. I. Andorko and C. M. Jewell, "Designing biomaterials with immunomodulatory properties for tissue engineering and regenerative medicine," *Bioengineering & Translational Medicine*, vol. 2, no. 2, pp. 139–155, 2017.

[12] S. N. Christo, K. R. Diener, A. Bachhuka, K. Vasilev, and J. D. Hayball, "Innate immunity and biomaterials at the Nexus: friends or foes," *BioMed Research International*, vol. 2015, Article ID 342304, 23 pages, 2015.

[13] P. C. Bota, A. M. Collie, P. Puolakkainen et al., "Biomaterial topography alters healing in vivo and monocyte/macrophage activation in vitro," *Journal of Biomedical Materials Research. Part A*, vol. 95, no. 2, pp. 649–657, 2010.

[14] M. Bartneck, V. A. Schulte, N. E. Paul, M. Diez, M. C. Lensen, and G. Zwadlo-Klarwasser, "Induction of specific macrophage subtypes by defined micro-patterned structures," *Acta Biomaterialia*, vol. 6, no. 10, pp. 3864–3872, 2010.

[15] N. E. Paul, C. Skazik, M. Harwardt et al., "Topographical control of human macrophages by a regularly microstructured polyvinylidene fluoride surface," *Biomaterials*, vol. 29, no. 30, pp. 4056–4064, 2008.

[16] K. A. Barth, J. D. Waterfield, and D. M. Brunette, "The effect of surface roughness on RAW 264.7 macrophage phenotype," *Journal of Biomedical Materials Research. Part A*, vol. 101, no. 9, pp. 2679–2688, 2013.

[17] M. D. Fabbro, S. Taschieri, E. Canciani et al., "Osseointegration of titanium implants with different rough surfaces: a histologic and Histomorphometric study in an adult Minipig model," *Implant Dentistry*, vol. 26, no. 3, pp. 357–366, 2017.

[18] D. Buser, R. K. Schenk, S. Steinemann, J. P. Fiorellini, C. H. Fox, and H. Stich, "Influence of surface characteristics on bone integration of titanium implants. A histomorphometric study in miniature pigs," *Journal of Biomedical Materials Research*, vol. 25, no. 7, pp. 889–902, 1991.

[19] M. A. Alfarsi, S. M. Hamlet, and S. Ivanovski, "Titanium surface hydrophilicity modulates the human macrophage inflammatory cytokine response," *Journal of Biomedical Materials Research. Part A*, vol. 102, no. 1, pp. 60–67, 2014.

[20] K. R. Fernandes, Y. Zhang, A. M. P. Magri, A. C. M. Renno, and J. van den Beucken, "Biomaterial property effects on platelets and macrophages: an in vitro study," *ACS Biomaterials Science & Engineering*, vol. 3, no. 12, pp. 3318–3327, 2017.

[21] H. S. Lee, S. J. Stachelek, N. Tomczyk, M. J. Finley, R. J. Composto, and D. M. Eckmann, "Correlating macrophage morphology and cytokine production resulting from biomaterial contact," *Journal of Biomedical Materials Research. Part A*, vol. 101, no. 1, pp. 203–212, 2013.

[22] J. O. Akindoyo, M. D. H. Beg, S. Ghazali, M. R. Islam, N. Jeyaratnam, and A. R. Yuvaraj, "Polyurethane types, synthesis and applications—a review," *RSC Advances*, vol. 6, no. 115, pp. 114453–114482, 2016.

[23] C. Scarpa, G. F. Borso, V. Vindigni, and F. Bassetto, "Polyurethane foam-covered breast implants: a justified choice?," *European Review for Medical and Pharmacological Sciences*, vol. 19, no. 9, pp. 1600–1606, 2015.

[24] N. Castel, T. Soon-Sutton, P. Deptula, A. Flaherty, and F. D. Parsa, "Polyurethane-coated breast implants revisited: a 30-year follow-up," *Archives of Plastic Surgery*, vol. 42, no. 2, pp. 186–193, 2015.

[25] J. E. Greenwood and M. J. D. Wagstaff, *The use of biodegradable polyurethane in the development of dermal scaffolds*, Advances in Polyurethane Biomaterials, Woodhead Publishing, 1st edition, 2016.

[26] S. Fernando, M. McEnery, and S. A. Guelcher, "Polyurethanes for bone tissue engineering," in *Advances in Polyurethane Biomaterials*, pp. 481–501, Woodhead Publishing, 2016.

[27] Y. Hong, "Electrospun fibrous polyurethane scaffolds in tissue engineering," in *Advances in Polyurethane Biomaterials*, pp. 543–559, Woodhead Publishing, 2016.

[28] A. Burke and N. Hasirci, "Polyurethanes in biomedical applications," *Advances in Experimental Medicine and Biology*, vol. 553, pp. 83–101, 2004.

[29] D. L. Hayes, "The next 5 years in cardiac pacemakers: a preview," *Mayo Clinic Proceedings*, vol. 67, no. 4, pp. 379–384, 1992.

[30] R. J. Schutte, A. Parisi-Amon, and W. M. Reichert, "Cytokine profiling using monocytes/macrophages cultured on common biomaterials with a range of surface chemistries," *Journal of Biomedical Materials Research. Part A*, vol. 88, no. 1, pp. 128–139, 2009.

[31] S. Spriano, V. Sarath Chandra, A. Cochis et al., "How do wettability, zeta potential and hydroxylation degree affect the biological response of biomaterials?," *Materials Science & Engineering. C, Materials for Biological Applications*, vol. 74, pp. 542–555, 2017.

[32] H. Nakae, R. Inui, Y. Hirata, and H. Saito, "Effects of surface roughness on wettability," *Acta Materialia*, vol. 46, no. 7, pp. 2313–2318, 1998.

[33] M. Genin, F. Clement, A. Fattaccioli, M. Raes, and C. Michiels, "M1 and M2 macrophages derived from THP-1 cells differentially modulate the response of cancer cells to etoposide," *BMC Cancer*, vol. 15, no. 1, 2015.

[34] F. Y. McWhorter, T. Wang, P. Nguyen, T. Chung, and W. F. Liu, "Modulation of macrophage phenotype by cell shape," *Proceedings of the National Academy of Sciences of the United States of America*, vol. 110, no. 43, pp. 17253–17258, 2013.

[35] X. Li, Q. Huang, T. A. Elkhooly et al., "Effects of titanium surface roughness on the mediation of osteogenesis via modulating the immune response of macrophages," *Biomedical Materials*, vol. 13, no. 4, article 045013, 2018.

[36] A. K. Refai, M. Textor, D. M. Brunette, and J. D. Waterfield, "Effect of titanium surface topography on macrophage activation and secretion of proinflammatory cytokines and chemokines," *Journal of Biomedical Materials Research. Part A*, vol. 70, no. 2, pp. 194–205, 2004.

[37] K. M. Hotchkiss, G. B. Reddy, S. L. Hyzy, Z. Schwartz, B. D. Boyan, and R. Olivares-Navarrete, "Titanium surface characteristics, including topography and wettability, alter macrophage activation," *Acta Biomaterialia*, vol. 31, pp. 425–434, 2016.

[38] M. Shayan, J. Padmanabhan, A. H. Morris et al., "Nanopatterned bulk metallic glass-based biomaterials modulate macrophage polarization," *Acta Biomaterialia*, vol. 75, pp. 427–438, 2018.

[39] L. C. Xu and C. A. Siedlecki, "Effects of surface wettability and contact time on protein adhesion to biomaterial surfaces," *Biomaterials*, vol. 28, no. 22, pp. 3273–3283, 2007.

[40] P. Moazzam, A. Razmjou, M. Golabi, D. Shokri, and A. Landarani-Isfahani, "Investigating the BSA protein adsorption and bacterial adhesion of Al-alloy surfaces after creating a hierarchical (micro/nano) superhydrophobic structure," *Journal of Biomedical Materials Research. Part A*, vol. 104, no. 9, pp. 2220–2233, 2016.

[41] X. Miao, D. Wang, L. Xu et al., "The response of human osteoblasts, epithelial cells, fibroblasts, macrophages and oral bacteria to nanostructured titanium surfaces: a systematic study,"

International Journal of Nanomedicine, vol. 12, pp. 1415–1430, 2017.

[42] S. Singh, D. Awuah, H. M. Rostam et al., "Unbiased analysis of the impact of micropatterned biomaterials on macrophage behavior provides insights beyond predefined polarization states," *ACS Biomaterials Science and Engineering*, vol. 3, no. 6, pp. 969–978, 2017.

[43] T. Roch, A. Krüger, K. Kratz, N. Ma, F. Jung, and A. Lendlein, "Immunological evaluation of polystyrene and poly(ether imide) cell culture inserts with different roughness," *Clinical Hemorheology and Microcirculation*, vol. 52, no. 2-4, pp. 375–389, 2012.

[44] H. Headon, A. Kasem, and K. Mokbel, "Capsular contracture after breast augmentation: an update for clinical practice," *Archives of Plastic Surgery*, vol. 42, no. 5, pp. 532–543, 2015.

[45] M. B. Calobrace, W. G. Stevens, P. J. Capizzi, R. Cohen, T. Godinez, and M. Beckstrand, "Risk factor analysis for capsular contracture: a 10-year Sientra study using round, smooth, and textured implants for breast augmentation," *Plastic and Reconstructive Surgery*, vol. 141, no. 4S, pp. 20S–28S, 2018.

[46] A. F. von Recum and T. G. van Kooten, "The influence of micro-topography on cellular response and the implications for silicone implants," *Journal of Biomaterials Science. Polymer Edition*, vol. 7, no. 2, pp. 181–198, 1995.

[47] N. Handel and J. Gutierrez, "Long-term safety and efficacy of polyurethane foam-covered breast implants," *Aesthetic Surgery Journal*, vol. 26, no. 3, pp. 265–274, 2006.

[48] G. Vazquez, "Patients' satisfaction with anatomic polyurethane implants," *Gland Surgery*, vol. 6, no. 2, pp. 185–192, 2017.

Supplemental Figures

Segan S., Jakobi M., Khokhani P., Klimosch S., **Billing F.** et al. Systematic Investigation of Polyurethane Biomaterial Surface Roughness on Human Immune Responses in vitro

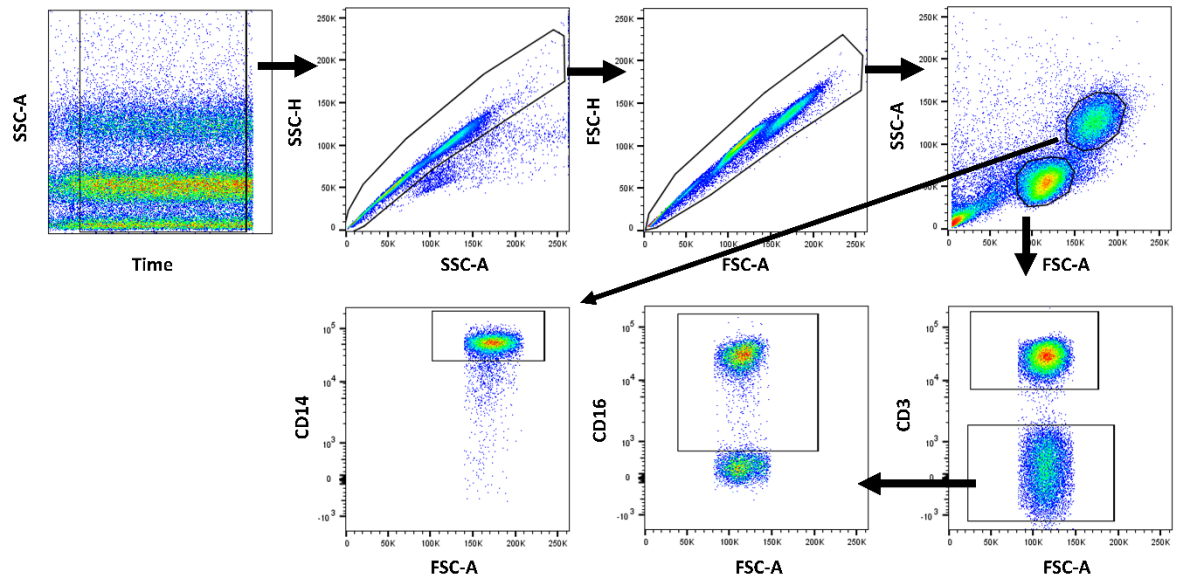

Supplementary Data 1. Gating strategy used to identify leukocyte populations from PBMC.

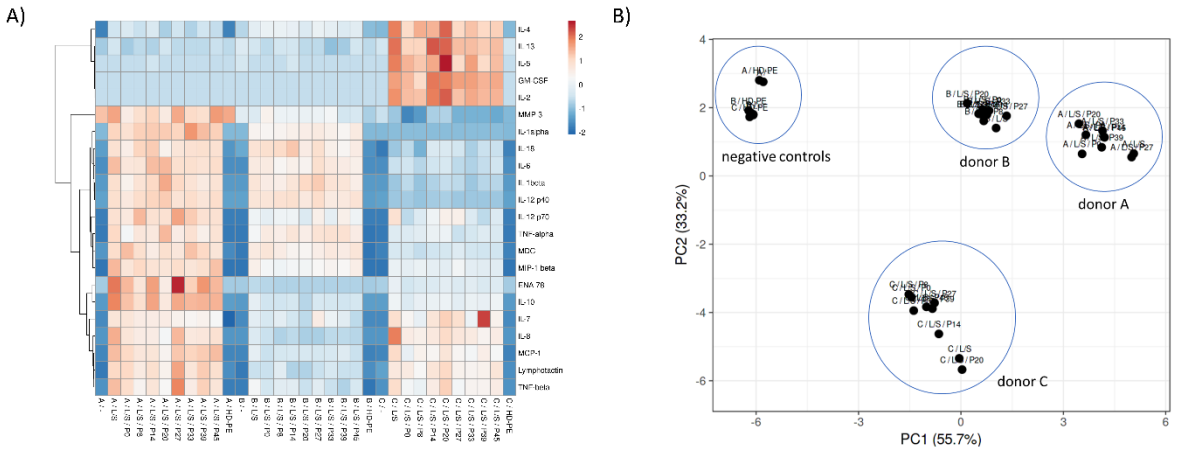

Supplementary Data 2. Pro- and anti-inflammatory cytokine production from whole blood co-stimulated with LPS/SEB cultured on polyurethane with different surface roughness. Human whole blood was stimulated with 0.01 µg/ml LPS/SEB and cultured for 48 hours with polyurethane specimens of increasing surface roughness (P0 – P7). The concentration of cytokines was assessed using multiplexed bead-based sandwich immunoassays. Data from three separate healthy donors analysed in parallel are displayed as a heat-map and as principal component analysis (PCA). A) Heat-map: Rows are centered; unit variance scaling is applied to rows. Rows are clustered using correlation distance and average linkage. 22 rows, 23 columns. B) PCA: Unit variance scaling is applied to rows; SVD with imputation is used to calculate principal components. X and Y axis show principal component 1 and principal component 2 that explain 55.7% and 33.2% of the total variance, respectively. N = 33 data points. (https://biit.cs.ut.ee/clustvis/). Donors: N = 3, A-C; L/S: LPS/SEB; LLOQ: lower limit of quantification.

Appendix III

Billing F., et al. Altered pro-inflammatory responses to polyelectrolyte multilayer coatings are associated with differences in protein adsorption and wettability. *ACS Applied Materials & Interfaces, 13 (46), 2021*

ACS APPLIED MATERIALS & INTERFACES

www.acsami.org Research Article

Altered Proinflammatory Responses to Polyelectrolyte Multilayer Coatings Are Associated with Differences in Protein Adsorption and Wettability

Florian Billing,* Bernadette Walter, Simon Fink, Elsa Arefaine, Luisa Pickarski, Sandra Maier, Robin Kretz, Meike Jakobi, Nora Feuerer, Nicole Schneiderhan-Marra, Claus Burkhardt, Markus Templin, Anne Zeck, Rumen Krastev, Hanna Hartmann, and Christopher Shipp

Cite This: https://doi.org/10.1021/acsami.1c16175 Read Online

ACCESS | Metrics & More | Article Recommendations | Supporting Information

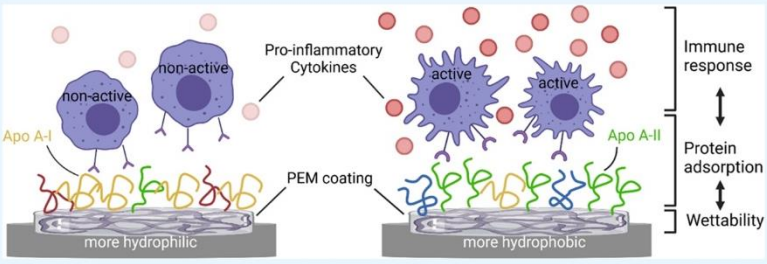

ABSTRACT: A full understanding of the relationship between surface properties, protein adsorption, and immune responses is lacking but is of great interest for the design of biomaterials with desired biological profiles. In this study, polyelectrolyte multilayer (PEM) coatings with gradient changes in surface wettability were developed to shed light on how this impacts protein adsorption and immune response in the context of material biocompatibility. The analysis of immune responses by peripheral blood mononuclear cells to PEM coatings revealed an increased expression of proinflammatory cytokines tumor necrosis factor (TNF)-α, macrophage inflammatory protein (MIP)-1β, monocyte chemoattractant protein (MCP)-1, and interleukin (IL)-6 and the surface marker CD86 in response to the most hydrophobic coating, whereas the most hydrophilic coating resulted in a comparatively mild immune response. These findings were subsequently confirmed in a cohort of 24 donors. Cytokines were produced predominantly by monocytes with a peak after 24 h. Experiments conducted in the absence of serum indicated a contributing role of the adsorbed protein layer in the observed immune response. Mass spectrometry analysis revealed distinct protein adsorption patterns, with more inflammation-related proteins (e.g., apolipoprotein A-II) present on the most hydrophobic PEM surface, while the most abundant protein on the hydrophilic PEM (apolipoprotein A-I) was related to anti-inflammatory roles. The pathway analysis revealed alterations in the mitogen-activated protein kinase (MAPK)-signaling pathway between the most hydrophilic and the most hydrophobic coating. The results show that the acute proinflammatory response to the more hydrophobic PEM surface is associated with the adsorption of inflammation-related proteins. Thus, this study provides insights into the interplay between material wettability, protein adsorption, and inflammatory response and may act as a basis for the rational design of biomaterials.

KEYWORDS: *protein adsorption, polyelectrolyte multilayers, wettability, immune response, PBMCs*

1. INTRODUCTION

The inflammatory reaction of the host is crucial for implant biocompatibility.[1] Hereby, the type of response by the recruited immune cells is a decisive factor in whether a medical implant will successfully perform its intended function or whether it results in detrimental immune responses contributing to fibrosis, chronic inflammation, or other unwanted effects.[2] To actively modulate the immune response, the implant design has moved into focus[3] as physicochemical surface properties of the applied biomaterials are found to impact the outcome of the provoked immune response.[4−8] For example, certain degrees of wettability or surface charge are associated with positive immunological effects,[8,9] although material-specific differences should not be neglected. However,

Received: August 24, 2021
Accepted: October 27, 2021

https://doi.org/10.1021/acsami.1c16175
ACS Appl. Mater. Interfaces XXXX, XXX, XXX−XXX

surface properties affect the immune response only in an indirect manner.

A decisive mediating role between the biomaterial and immune cells is performed by the proteins adsorbed on the biomaterial surface. Within seconds after the first material−tissue contact, proteins from blood and interstitial fluids begin adsorbing onto the biomaterial, thus providing the surface with a new biological identity.[10,11] Therefore, subsequently arriving immune cells mostly sense foreign surfaces through this adsorbed layer but not the surface itself. The adsorbed serum proteins can influence the behavior of immune cells, which directly affect the immunological outcome of a biomaterial.[11−16] In this context, biomaterial surface parameters such as wettability and surface charge are thought to have a significant impact on the nature, volume, and conformation of adsorbed proteins.[10,11,14,16,17] Hence, cellular responses to a biomaterial in a biological medium seem to be dependent on the adsorbed biomolecule layer, which is built up based on the material's physicochemical properties. However, there remains a paucity of data on interrelations between these three decisive factors determining the fate of a biomaterial implant. While previous in vitro studies mainly focused on either the correlation between surface properties and protein adsorption[17,18] or the modulation of the immune response by artificial protein coatings,[12,15,19] only a few included all three aspects. Moreover, previous investigations often relied on simplified models. Thus, a thorough investigation that considers the complexities of each factor is lacking. In this study, we attempt to represent the complex nature of surface−protein interactions as well as the full spectrum of the immune response, while pinpointing the effects to specific differences in material properties.

The choice of an appropriate biomaterial surface is crucial for the identification of surface parameters being specifically responsible for the observed immune response. Hereby, a precise assignment is difficult when comparing materials with different chemical compositions and a variety in several surface parameters. However, this knowledge is important for the targeted design of immunocompatible implants.[4,16] To link particular modulations to specific immunological outcomes, we employed polyelectrolyte multilayer (PEM) coatings. On a chemical level, PEMs are nanometer-scale polymer films that are generated by alternating deposition of polyelectrolytes utilizing layer-by-layer (LbL) self-assembly.[20] Due to their versatile nature, PEM coatings can be deposited on a wide range of substrates including medical devices. They have attracted attention in the field of biomedical engineering as they may be utilized to control protein adsorption, promote cell adhesion, and modulate the inflammatory response,[21] though there are still relatively few publications on the biological aspects of this technology. Modifications of certain deposition parameters, such as pH conditions, salts, temperature, etc. can be applied to impart changes in the physicochemical properties like surface charge or wettability.[22,23] For this study, we aimed for the application of a set of PEM coatings based on identical polymers that vary only in a small subset of physicochemical properties.

The complexity of the immunological model applied is another critical factor for developing a comprehensive understanding of the interrelation between surface parameters and the immune response. Here, previous investigations often rely on a simplified model of the immune system, using single populations of immune cells such as macrophage cell lines.[14] However in vivo, also other types of immune cells such as monocytes and lymphocyte populations are found in the biomaterial surrounding tissues (particularly in cases of aseptic loosening and implant failure), thus implicating a contribution of these cell types to the observed immune response.[24,25] The inclusion of all cell populations involved is therefore essential for an accurate in vitro analysis of the immune response and enables the assessment of immune-relevant cell types in addition. To investigate the influence of certain surface alterations on the immune system, we employed a human-based in vitro immune model consisting of primary peripheral blood mononuclear cells (PBMCs). These cells encompass almost the entire spectrum of circulating immune cells, including innate immune cells like monocytes and natural killer cells as well as helper and cytotoxic T cells of the adaptive immune system, among other less frequent populations. This broad immune cell spectrum resembles the in vivo situation quite closely and their patient-derived nature makes them suitable for assessing biological differences across individuals.

The use of a complex model is also critical in determining the contribution of adsorbed proteins. Many previous studies were conducted by analyzing the effect of single proteins or simple mixtures of selected proteins, e.g., albumin, fibronectin/fibrinogen, and immunoglobulin.[12,19,26,27] However, implanted devices are confronted with blood plasma containing thousands of protein compounds and the entire spectrum of extracellular matrix proteins. As a result, simplified models often fail to account for the complex and dynamic adsorption patterns in vivo.[28] Therefore, in vitro testing with human serum is likely more representative of protein adsorption in vivo.[29] Thus, in this study, human serum was included in the cell culture medium in all experiments. To identify relevant protein compounds, mass spectrometry was employed to quantify serum-derived protein adsorption. By comparing the protein composition on the different PEM coatings, we furthermore aimed to correlate the adsorbed protein layer with the observed inflammatory response. In the last step, protein expression profiling was applied using DigiWest analysis to identify alterations in cellular signal transduction in response to the distinct PEM coatings. By analyzing the adsorbed serum proteins and the potential signaling pathways, we aimed to develop a deeper understanding of the relationship between material surface properties, protein adsorption, and the resulting immune response.

2. METHODS

2.1. Material Characterization. *2.1.1. Polyelectrolyte Solutions.* For the buildup of PEMs, sodium poly(styrene sulfonate) (PSS; M_w 70 kDa) and polyethyleneimine (PEI; M_w 750 kDa) were both obtained from Sigma-Aldrich (Steinheim, Germany). Poly(allylamine hydrochloride) (PAH) was purchased from Alfa Aesar (Haverhill, Massachusetts). The polymers were used without further purification. Sodium chloride and sterile, pyrogen-free water were obtained from Carl Roth (Karlsruhe, Germany). The concentration of PSS and PAH was 2 mg/mL in 0.5 mM sodium chloride at pH values 4, 7, and 9.

2.1.2. Manufacture of Polyelectrolyte Multilayer (PEM) Coatings. The polycationic PEMs PEI(PSS/PAH)$_5$ were prepared manually at room temperature (RT) using the layer-by-layer (LbL) technique. The film buildup was prepared under sterile conditions. First, a layer of PEI (10 mg/mL, pH 7) was deposited for 10 min. After incubation, the samples were extensively rinsed with sterile, pyrogen-free water (3 × 2 min). Next, five bilayers of PSS/PAH were deposited by alternate application (i.e., 10 min PSS and PAH solutions) with an intermediate washing step, which altogether lasted over 6 min in water. Three different types of coatings using the identical PSS/PAH substrates were generated by adjusting the pH of the assembling

https://doi.org/10.1021/acsami.1c16175
ACS Appl. Mater. Interfaces XXXX, XXX, XXX−XXX

solutions during the creation process to pH values of 4, 7, and 9, which are referred to as cationic A, B, and C in this manuscript, respectively. Notably, the pH state of the assembling solution of the PEMs has no influence on the pH value in the subsequent cell culture experiments. For all experiments involving PBMCs, coatings were applied directly onto 24-well tissue culture plates (TCP, Sarstedt, Nürnbrecht, Germany), resulting in a surface area of 1.82 cm^2 per sample.

2.1.3. Ellipsometry. The film growth was monitored by means of an SENpro (SENTECH Instruments GmbH, Germany) spectroscopic ellipsometer with a wavelength range from 429 to 900 nm, at an angle of incidence of 70°. To obtain the film thickness, the raw data were fitted with a four-layer model considering the contribution from the air, PEM, SiO_2, and Si.

2.1.4. ζ Potential. The ζ potential was determined on PEM coatings (PerkinElmer Inc.) using a Zetasizer Nano ZS particle analyzer (Malvern Instruments, Herrenberg, Germany) at 25 °C and a 173° scattering angle by cumulative analysis. ζ potential analysis based on the electrophoretic mobility of the nanoplexes in aqueous buffer was performed using folded capillary cells (Malvern Instruments, Herrenberg, Germany) in automatic mode and calculated using the Smoluchowski equation. ζ potential measurements were done in triplicate and reproduced three times (n = 3 experiments and n = 9 total measurements).

2.1.5. Water Contact Angle. The wettability of each sample was determined by sessile drop measurements of the water contact angle (θ) using a Krüss Easy Drop contact angle goniometer (Hamburg, Germany). To perform the measurements, a static drop was used, maintaining a constant volume during the measurement. This was performed with the addition of 2 μL of distilled water to the samples. After 20 s, an image was recorded and transferred to the software for analysis of the static (equilibrium) contact angles. Three independent experiments were performed in triplicate to give the mean value ± standard deviation (SD).

2.1.6. Bovine Serum Albumin (BSA) Adsorption. For quantification of the protein adsorption, a solution of BSA was used. The concentration was 40 mg/mL, corresponding to the physiological concentration of human serum albumin in blood.[30] The lyophilized protein was dissolved in modified simulated body fluid (m-SBF) with ion concentrations, corresponding to those in human blood plasma.[31] The used BSA was fluorescently labeled to allow quantification of the resulting protein adsorption and was applied as a 4% additive in the used BSA−fluorescein isothiocyanate (FITC) solution. Coated well plates were washed 3× with m-SBF, incubated for 20 min with BSA−FITC in m-SBF, and washed again 3× with m-SBF before measurement. The fluorescence intensity was quantified using a PHERAstar microplate reader (BMG Labtech). Empty wells (blank), m-SBF, and BSA−FITC alone served as controls.

2.1.7. Scanning Electron Microscopy (SEM). PBMCs for SEM analysis were cultured in 24-well cell culture plates coated with PEM cationic A, B, and C for 24 h at 37 °C and 5% CO_2 in a humidified atmosphere. After culture, cells were washed three times with phosphate-buffered saline (PBS) (Thermo Fisher Scientific) and fixed for 2 h on ice with a PBS solution containing 4% paraformaldehyde (PFA) and 2% glutaraldehyde (both w/v). Subsequently, samples were washed three times with PBS. Dehydration was performed using a graded series of ethanol solutions (30, 50, 70, 80, 95, 100%). Following critical point drying (Baltec CPD 030), samples were coated with 5 nm gold−palladium (Cressington 208 HR). Surface images were taken with an Auriga 40 FIB/SEM (Zeiss, Oberkochen, Germany) at a 3 keV acceleration voltage using a chamber secondary electron detector.

2.2. Isolation of PBMCs from Whole Blood. Whole blood samples of healthy volunteers were taken between November 2018 and October 2020 after written informed consent. Potential donors were screened with exclusion criteria (chronic inflammatory disease, surgical intervention within the last 3 months, infection or use of medications affecting the immune system in the past 2 weeks, vaccination in the previous 6 weeks, excess alcohol consumption, or strenuous exercise prior to donation) to minimize the influence by environmental factors known to alter the immune system. All blood draws took place in the morning hours (9−11 am) to ensure consistency. Immediately after the blood was drawn, PBMCs were isolated by density gradient centrifugation using SepMate isolation tubes (StemCell Technologies, Cologne, Germany) according to the manufacturer's protocol. Isolated PBMCs were stored at −150 °C in a medium containing 10% dimethyl sulfoxide (DMSO) (Sigma-Aldrich, Hamburg, Germany), 20% fetal calf serum (FCS) (Sigma-Aldrich), and 70% Roswell Park Memorial Institute Medium (RPMI) 1640 (Gibco, Paisley, Scotland) until use. As shown in a previous publication,[32] the freezing/thawing procedure did not affect the cellular activity of the cells. The viability of the PBMCs was assessed prior to each experiment by the trypan blue exclusion assay and was found to be greater than 97% in all cases.

2.3. PBMC Cell Culture. Unless otherwise stated, PBMCs were cultured in Iscove's modified Dulbecco's medium (IMDM medium, Gibco, Thermo Fisher Scientific) containing GlutaMAX supplemented with 10% off-the-clot serum pooled from male AB blood group donors (human AB pooled serum (male), H2B, Limoges, France). In experiments assessing the general role of serum proteins, PBMCs were cultured in X-VIVO 15 serum-free medium (Lonza, Basel, Switzerland). In these cases, prior to culturing of the cells, the surfaces were either incubated with human serum (H2B) at 37 °C for 1 h and washed 5× with PBS, or remained untreated. For all experiments, 5.0×10^5 cells were seeded in 500 μL of medium. Cells stimulated with PHA-L (10 μg/mL, Roche, Mannheim, Germany) and lipopolysaccharides (LPSs) from *Escherichia coli* O55:B55 (100 ng/mL, Hycult Biotech, Uden, the Netherlands) served as a proinflammatory positive control to ensure cell functionality. PBMCs cultured on uncoated tissue culture plates (TCPs) without treatment were used as the negative control. Depending on the specific experiment, culture periods were 12, 24, 72, or 96 h at 37 °C and 5% CO_2 in a humidified atmosphere. Throughout all culturing periods, the medium was not exchanged, which allowed nonadherent cells to remain in the culture and to potentially interact with adherent cells via contact-independent mechanisms. For experiments employing intracellular cytokine staining, 1× Brefeldin A (BioLegend, Amsterdam, the Netherlands) was applied to the culture 12 h prior to harvesting to prevent cytokine secretion. In the case of experiments assessing secreted cytokines, multiplex (Luminex) immunoassays were employed. For this, 190 μL of cell culture medium was collected following the culture period and centrifuged at 5000 rpm for 3 min. The supernatant was then collected and stored at −80 °C until analysis.

2.4. Cytokine Analysis Using Multiplexed Bead-Based Sandwich Immunoassays. To analyze concentrations of chemo- and cytokines, collected supernatants were thawed and spun down at 10 000*g* for 5 min to remove remaining cells. Levels of interleukin (IL)-1β, IL-1RA, IL-4, IL-6, IL-8, IL-10, IL-12p70, IL-13, GM-CSF, interferon (IFN)-γ, monocyte chemoattractant protein (MCP)-1, macrophage inflammatory protein (MIP)-1β, tumor necrosis factor (TNF)-α, and vascular endothelial growth factor (VEGF) were quantified using a set of Luminex-based sandwich immunoassays, which had been developed in-house and described previously.[33] Each assay consisted of commercially available capture and detection antibodies and calibrator proteins. Assays had been thoroughly validated ahead of the study with respect to accuracy, precision, parallelism, robustness, specificity, and sensitivity.[34,35] The dilution factor of the samples was at least 1:4 or higher. After incubation of the prediluted samples or calibrator protein with the capture coated microspheres, beads were washed and incubated with biotinylated detection antibodies. Streptavidin−phycoerythrin (PE) was added after an additional washing step for visualization. As a control, calibrators and quality control samples were also tested on each microtiter plate. Plates were measured using a Luminex FlexMap 3D analyzer system with Luminex xPONENT 4.2 software (Luminex, Austin). Data was analyzed with MasterPlex QT version 5.0. Evaluation of the standard curve and quality control samples was performed in accordance with internal criteria adapted to the Westgard rules to guarantee the proper performance of assays.[36]

https://doi.org/10.1021/acsami.1c16175
ACS Appl. Mater. Interfaces XXXX, XXX, XXX−XXX

2.5. Flow Cytometry. Following the culture period, cells were harvested, as described previously.[32] Staining with extracellular antibodies was performed for 30 min on ice using the following antibodies: CD3-PerCP Cy5.5 (#317336), CD4-Alexa488 (#317420), CD16-BV605 (#302040), CD25-PE-Cy5 (#302607), CD86-BV650 (#305428), CD127-BV711 (#351328), CD163-PE/dazzle594 (#333624), CD206-PE/Cy7 (#321124), CD284-APC (#312815), and HLA-DR-BV421 (#307636), all obtained from Biolegend, and CD14-APC-H7 (#560270) and CD354-BV510 (#743739), both from BD Biosciences (Heidelberg, Germany). For the mixed surface marker/intracellular staining panel, the cells were stained with CD3-APC (#317317), CD14-PerCP/Cy5.5 (#367109), and CD16-BV605 (#302039), all obtained from Biolegend. After staining, cells were washed, spun, and the supernatant was discarded. For intracellular staining, cells were permeabilized using a Cytofix/Cytoperm Fixation/Permeabilization kit (BD) in accordance with the manufacturer's instructions before intracellular proteins were blocked for 10 min with 10% (v/v) human serum diluted in permeabilization buffer. After washing, intracellular cytokines were labeled using IL-6-PE/Dazzle594 (#501122), IL-8-Alexa Fluor488 (#511412), TNF-α-BV711 (#502940), and MCP-1-PE/Cy7 (#502614) (all Biolegend) and MIP-1β-BV421 (BD) antibodies diluted in permeabilization buffer and incubated for 30 min on ice in the dark. After the last washing step, stained cells were immediately analyzed using an LSRFortessa instrument with the FACSDiva software version 8.0.3 (BD). All washing steps were performed with 1 mL of washing buffer and centrifugation at 300g for 5 min. Data analysis was performed using FlowJo software v10.5 (BD) and analyzed according to the gating strategy shown in Figures S1 and S2.

2.6. On-Surface Trypsin Digestion and Liquid Chromatography-Mass Spectrometry (LC-MS/MS) Analysis. PEM coatings were incubated with 10% HS in IMDM medium without cells for 1 h at 37 °C. The surfaces were washed 5× with PBS and afterward incubated overnight with 5 μg of trypsin (Worthington) in 50 mM tris (Carl Roth), pH 7.5 at 37 °C. The proteolysis was stopped by adding formic acid (99% LC-MS grade from Fisher Chemicals) to a final concentration of 7% (v/v). Tryptic peptides were analyzed by liquid chromatography-mass spectrometry (LC-MS) using a QExactive mass spectrometer coupled to an UltiMate 3000 RSLCnano System (Thermo Fisher Scientific). Briefly, 5 μL of each sample was injected onto an Acclaim PepMap C18 5 mm × 0.3 mm i.d., 5 μm particle size, 100 Å pore size trapping column (Thermo Fisher) using 2% acetonitrile (LC-MS grade, Honeywell) (v/v) + 0.05% trifluoroacetic acid (VWR) as the solvent at a 120 μL/min flow rate for 0.25 min. Subsequently, the valve was switched onto the analytical column. Peptides were separated using an Acclaim PepMap RSLC C18, 15 cm × 75 μm i.d., 2 μm particle size, 100 Å pore size column (Thermo Fisher Scientific), and a linear gradient from 2.5 to 45% solvent B (80% acetonitrile v/v + 0.1% formic acid v/v) over 10.75 min. Solvent A was 0.1% formic acid in water (Honeywell) (v/v). A washing step of 3 min 99% solvent B was included and afterward, the column was re-equilibrated for 6 min at 2.5% solvent B. The complete gradient was operated at 0.6 μL/min. The total run time was 20 min. The column oven temperature was set to 50 °C. The LC system was connected to the mass spectrometer via a nanospray ion source. The mass spectrometer was operated in positive data-dependent acquisition mode and MS full scans were acquired at a resolution of 70.000 and a 200−2000 m/z range. MS full scans were followed by MS2 acquisition of the five most intense ion signals at a resolution of 17.500 and a scan range of 200−2000 m/z. Ions were fragmented using higher collision-induced dissociation (HCD) and a normalized collision energy (NCE) of 25. The automatic gain control (AGC) target and maximum injection time for MS scans were 5×10^6 and 250 ms, and for MS2 5×10^5 and 80 ms, respectively. The isolation window was set to 2.0 Da and dynamic exclusion for identified peptides was set to 2.0 s.

2.6.1. Mass Spectrometry Data Processing. Mass spectrometry raw data files were processed using MaxQuant (version 1.6.17.0).[37] Data files were searched against the human proteome (Uniprot Knowledgebase, 73.118 sequences). Variable modifications were set to oxidation (M) and acetylation (N-terminus). No fixed modifications were allowed. Label-free quantification was enabled as well as intensity-based absolute quantification (iBAQ) calculation. All other parameters were set to default. The "proteinGroups.txt" output table from MaxQuant was used for further data processing in Perseus software (version 1.6.14.0).[38] Proteins, identified "only by-site" or by matching to the reverse decoy database were removed from the analysis. Furthermore, only proteins identified at a minimum of three biological replicates of one sample were retained for downstream analysis. Since iBAQ values from MaxQuant correlate with protein abundance within a sample,[39] this metric was used for the detection of differential protein abundance between different PEM coatings. iBAQ values were log 2-transformed and the missing values were imputed by inserting the value of "10". Proteins were annotated using the Gene Ontology as well as the Kyoto Encyclopedia of Genes and Genomes (KEGG) pathway database.

2.7. Intracellular Protein Analysis (DigiWest). DigiWest was performed as recently described.[40] Briefly, gel electrophoresis and blotting onto poly(vinylidene difluoride) (PVDF) membranes were performed using the NuPAGE system as recommended by the manufacturer (Life Technologies, Carlsbad, California). Blots were washed in PBST, proteins were biotinylated on the membranes using NHS-PEG12-Biotin (50 μM) in PBST for 1 h followed by washing in PBST and drying. Individual sample lanes were cut into 96 molecular weight fractions (0.5 mm each) and proteins were eluted in 96-well plates using 10 μL of elution buffer per well (8 M urea, 1% Triton-X100 in 100 mM Tris−HCl pH 9.5). Eluted proteins from each molecular weight fraction were loaded onto color-coded, neutravidin-coated Luminex bead sets (MagPlex, Luminex, Austin, TX). Luminex bead sets (384) were employed and the protein-loaded beads from 4 different sample lanes were pooled into 1 bead-mix resulting in 3 bead-mixes for the 12 samples. The bead-mixes were sufficient for 63 antibody incubations (see Table S4). Aliquots of the DigiWest bead-mixes (1/67th per well) were added to 96-well plates containing 50 μL per well assay buffer (blocking reagent for enzyme-linked immunosorbent assay (ELISA) supplemented with 0.2% milk powder, 0.05% Tween-20, and 0.02% sodium azide, Roche). Beads were briefly incubated in assay buffer and the buffer was discarded. Antibodies were diluted in assay buffer and 30 μL were added per well. After overnight incubation at 15 °C on a shaker, bead-mixes were washed twice with PBST and phycoerythrin (PE)-labeled secondary antibodies (Dianova) were added and incubated for 1 h at 23 °C. The beads were washed twice prior to the readout on a Luminex FlexMAP 3D. Secondary antibodies were either diluted in assay buffer or a polymer buffer (blocking reagent for ELISA supplemented with 4% poly(vinylpyrrolidone) (PVP) 360.000, 1% milk powder, 0.05% Tween-20, and 0.02% sodium azide, Roche). For quantification of the antibody-specific signals, the DigiWest analysis tool (version 3.8.6.1, Excel-based) was employed. This tool uses the 96 values for each initial lane obtained from the Luminex measurements on the 96 molecular weight fractions, identifies the peaks at the appropriate molecular weight, calculates a baseline using the local background, and integrates the peaks. The values are based on relative fluorescence (accumulated fluorescence intensity, AFI). For analysis, data (measured signal intensity) was median centered, normalized to the median measured signal intensity corresponding to the sample, median centered, and log 2-transformed. The software package MEV 4.8.1 was used for data visualization, clustering, and nonparametric statistical analysis.[41]

2.8. Statistical Analysis. Apart from the intracellular protein analysis using DigiWest, all statistical analysis and plotting were performed with GraphPad Prism 9.0 (GraphPad Software, San Diego). Statistical tests were applied as indicated in the respective figure legends, with a significance threshold of $p \leq 0.05$. For all tests comparing three or more groups, the recommended correction for multiple comparisons was applied. All graphs show mean ± SD.

https://doi.org/10.1021/acsami.1c16175
ACS Appl. Mater. Interfaces XXXX, XXX, XXX−XXX

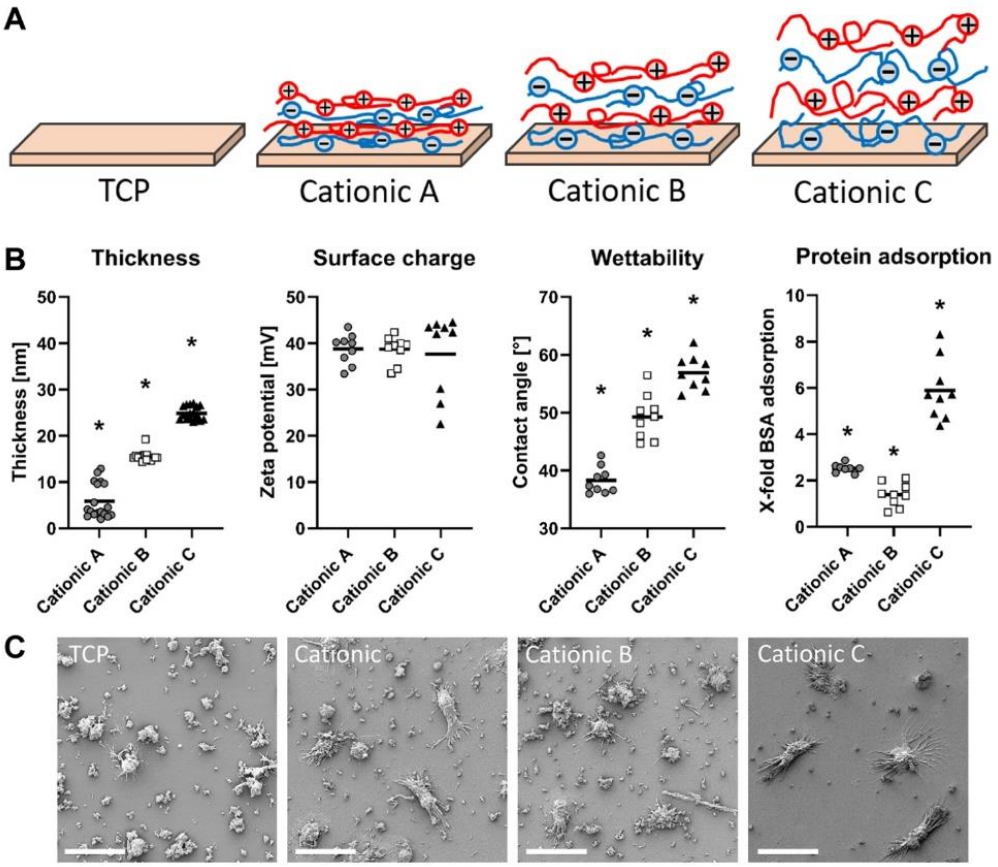

Figure 1. Physicochemical characteristics of the PEM coatings. Three different PEM coatings cationic A–C were generated by layer-by-layer deposition of polystyrene sulfonate (PSS) and polyallylamine hydrochloride (PAH) polyelectrolytes by applying different pH conditions during the assembly process. (A) Schematic overview of the deposited coatings. (B) Surface thickness (spectroscopic ellipsometry), surface charge (Zetasizer), and wettability (water contact angle) were assessed. Adsorption of BSA was quantified by measuring the fluorescence of adsorbed FITC-labeled BSA. Intensities of BSA adsorption were normalized to the FITC signal of polystyrene-adsorbed BSA, which was set to a value of 1. $n = 3$ experiments and $n = 18$ total measurements for ellipsometry and $n = 3$ experiments and $n = 9$ total measurements for all other experiments. Lines represent the mean value. The ordinary one-way analysis of variance (ANOVA) was applied to compare all PEMs and * indicates $p < 0.05$ vs all other surfaces. (C) Scanning electron microscopy images of the three PEM coatings and uncoated TCP after incubation with PBMCs for 24 h. Scale bar = 20 μm.

3. RESULTS

3.1. Physicochemical Characteristics of Material Surfaces Can Be Modulated with Polyelectrolyte Multilayers. To investigate the effect of surface properties on protein adsorption and immune response, PEM coatings that were based on identical polyelectrolyte substrates but differed in selected physicochemical properties were applied on tissue culture plate (TCP) surfaces. By adjusting the pH-sensitive charge density of the assembling polymers, three variations of PEM coatings were created, all based on alternating layers of the polyanion polystyrene sulfonate (PSS) and the polycation polyallylamine hydrochloride (PAH). A schematic view of the applied coatings and their properties can be seen in Figure 1A. In reference to the polycationic coating termination, they are referred to as PEM coating cationic A, B, and C. Although the number of applied polyelectrolyte layers was identical for all three coatings, the increasing pH of the assembly solution from coatings A to C resulted in progressively increased thickness, ranging from 5.9 ± 3.7 nm for coating cationic A to 24.9 ± 1.4 nm for cationic C as the thickest coating (Figure 1B). As parameters like surface charge and wettability can affect protein adherence, immune cell differentiation, and the immunological reactivity of a surface in general, these properties were determined employing water contact angle and Zetasizer analysis prior to assessing immunological effects. The mean surface charge was found to be identical for all coatings (Figure 1B). While all surfaces displayed hydrophilic properties, the cationic A coating was the most hydrophilic relative to the other two (contact angle 38.3 ± 2.3°) (Figure 1B). This was followed by cationic B (49.3 ± 3.9°), while the least hydrophilic coating was cationic C (56.9 ± 2.9°). Analysis of protein adsorption on these three PEM coatings showed clear differences in the amount of BSA that was adsorbed onto the surface. The most BSA was found on cationic C with a 5.9 ± 1.3-fold increase over the uncoated polystyrene (PS) control. In comparison, PEMs cationic A and B showed a 2.5 ± 0.2 and 1.4 ± 0.5-fold increase, respectively, compared to the uncoated control (Figure 1B).

https://doi.org/10.1021/acsami.1c16175
ACS Appl. Mater. Interfaces XXXX, XXX, XXX−XXX

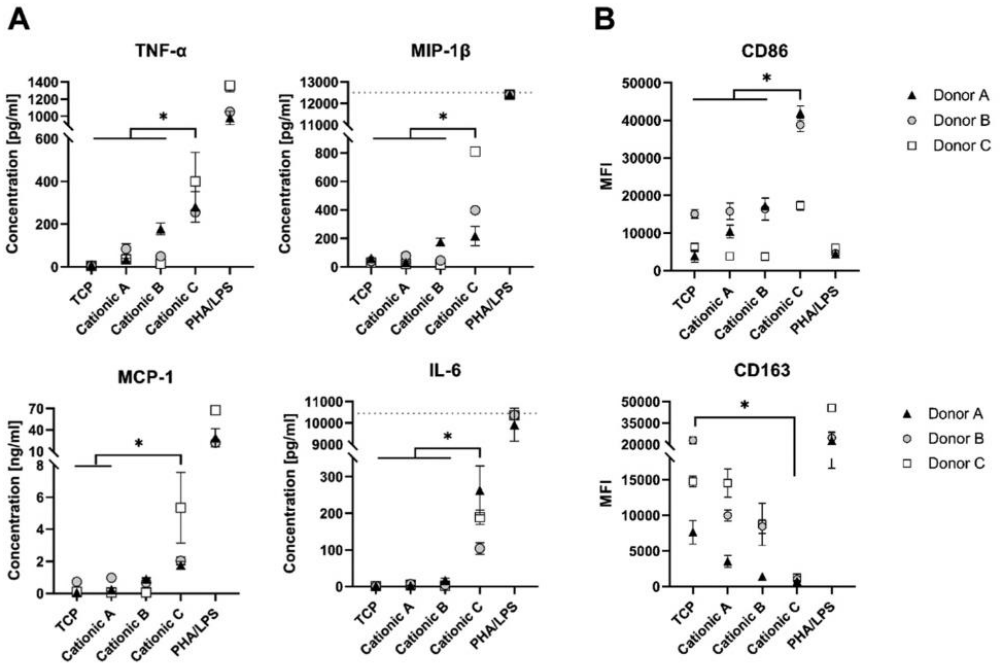

Figure 2. Proinflammatory cytokine secretion and expression of surface markers on PBMCs cultured on PEM surfaces. PBMCs from three donors were cultured for 72 h on PEM surfaces cationic A, B, and C. TCP served as a negative control and stimulation with LPS and PHA as a positive control. (A) Concentration of proinflammatory cytokines quantified in the cell culture supernatant using multiplex assays. The dotted line indicates the upper limit of quantification. (B) Expression of cell surface markers CD86 (proinflammatory) and CD163 (anti-inflammatory) on monocytes analyzed by flow cytometry. Three donors were tested with two technical replicates for all conditions. Symbols represent mean ± SD. RM one-way ANOVA compares the mean of each surface to the mean of every other surface (with the exception of the PHA/LPS condition). * indicates $p < 0.05$. MFI: mean fluorescence intensity.

To gain an initial insight into the interaction of immune cells with these coated surfaces, we cultured PBMC on the surfaces cationic A, B, and C for 24 h and visually inspected their interaction with the coatings using scanning electron microscopy. The images revealed uniform surfaces allowing cell adhesion with different morphologies but apparently a tight interaction to the smooth PEMs (Figure 1C). No consistent differences in cell morphologies between the different surfaces investigated could be observed. The structure of the deposited PEMs was quite homogeneous and no irregularities could be observed in the micrometer range. Ellipsometric measurements at 18 positions of three independent samples showed minor variations in the coating thickness for cationic B and C (coefficient of variation 7% and 6%, respectively). Only the thinnest coating cationic A showed higher variations between 2 and 13 nm (Figure 1B). Taken together, the three coatings differ in their nanometer thickness, wettability, and ability to adsorb proteins, while having a comparable microstructure and surface charge.

3.2. More Hydrophobic PEM Coating Cationic C Elicits the Highest Proinflammatory Immune Response. Having observed that immune cells made contact with and interacted with the PEM surfaces using electron microscopy, we next investigated the biological effects in response to these surfaces. To do this, PBMCs were incubated for 72 h on the three different coatings prior to the assessment of cytokine production in the cell culture supernatant and CD molecule expression on cellular immune populations. We observed the more hydrophobic cationic C surface to result in an elevated secretion of proinflammatory cytokines TNF-α, MIP-1β, and IL-6 compared to all other surfaces (Figure 2A). Similar results were also found for MCP-1, with a significantly higher level produced in response to cationic C compared to cationic A and the TCP control. Cytokine levels for cationic A and B did not differ from those found in response to the uncoated TCP control. Similar trends were observed for additionally investigated proinflammatory cytokines IL-1β, IFN-γ, and IL-8 (Figure S3). All anti-inflammatory cytokines examined either showed no change between PEM surfaces (IL-10, IL-1RA, VEGF) or were below the limit of quantification (IL-4, IL-13; data not shown). When investigating the expression of surface markers by flow cytometry, we found the observed cytokine response to be accompanied by the alteration of CD molecules on monocytes. Expression of the proinflammatory marker CD86 was substantially increased in response to PEM cationic C compared to coatings A and B and the TCP control (Figure 2B). In line with this, expression of the anti-inflammatory marker CD163 was the lowest on cationic C and was the only condition significantly lower than the negative control TCP. Levels of CD86 and CD163 in response to the positive control LPS/PHA were altered in accordance with the literature.[42] Other cell populations investigated, T and NK cells, did not show any noteworthy changes in the surface marker expression across the three PEM surfaces (data not shown). In summary, we observed the strongest immune response in contact with the more hydrophobic PEM cationic C, while the effects of coatings A and B were mild to moderate in comparison.

https://doi.org/10.1021/acsami.1c16175
ACS Appl. Mater. Interfaces XXXX, XXX, XXX−XXX

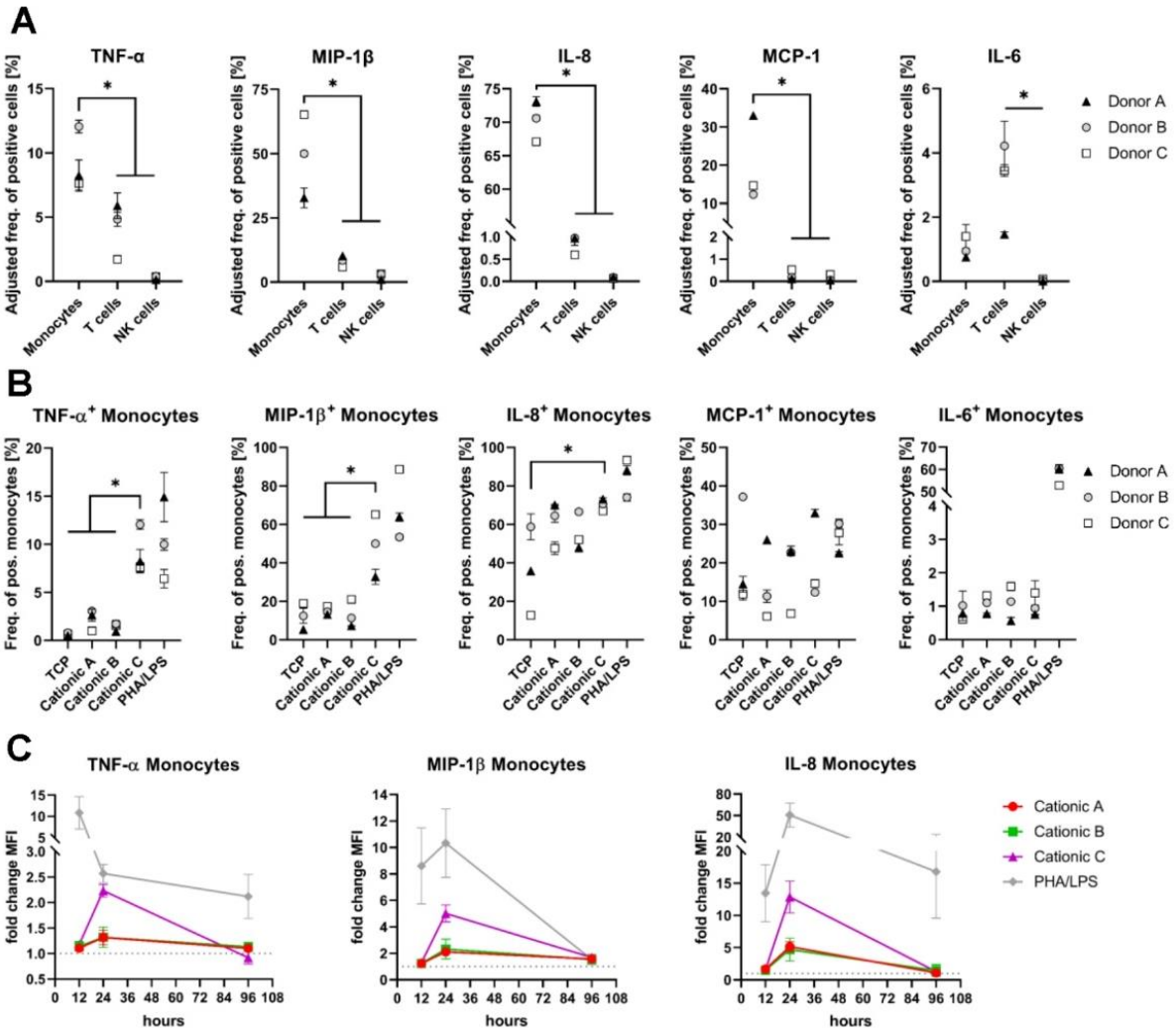

Figure 3. Intracellular cytokine analysis after cultivation of PBMCs on PEM coatings. PBMCs were cultured on PEM coatings cationic A to C and the uncoated TCP control. Intracellular staining was performed for the proinflammatory cytokines TNF-α, MIP-1β, IL-8, MCP-1, and IL-6 followed by flow cytometric analysis. (A) Frequency of positive cells for monocytes, T cells, and NK cells after cultivation of PBMC on PEM cationic C for 24 h. Frequencies of positive T cells and NK cells were adjusted to account for the differences in the relative size of these populations in relation to monocytes. $n = 3$ donors and two technical replicates. RM one-way ANOVA was applied to compare the mean of every population to the mean of every other population. * indicates $p < 0.05$. (B) Frequency of positive monocytes of three donors tested in duplicates. RM one-way ANOVA compares the mean of coating cationic C to the mean of surfaces cationic A, cationic B, and the TCP control. * indicates $p < 0.05$. (C) MFI of monocytes was quantified after culturing PBMCs for 12, 24, and 96 h. PBMCs of one donor in duplicate tested in two separate experiments. Graphs show fold change MFI of the TCP control (indicated by dotted lines) for cationic A (circles, red), cationic B (squares, green), cationic C (triangles, purple), and the positive control PHA/LPS (diamond, gray). All graphs show mean ± SD.

3.3. Proinflammatory Immune Response of PEM Cationic C Is Mediated through Monocytes and Peaks after 24 h. The results obtained by examining cytokine secretion and CD molecule expression hinted that monocytes played a major role in the immune response to the PEM surfaces. To investigate this more closely, we next examined intracellular cytokine expression in several immune cell populations in PBMC. Having observed PEM cationic C to elicit the highest proinflammatory response, this surface was chosen for analysis. Investigating the expression of proinflammatory cytokines in monocytes, T cells, and NK cells showed very low frequencies of cells expressing TNF-α, MIP-1β, IL-8 and MCP-1 in both NK cells and T cells but a significantly higher expression of these cytokines in monocytes (Figure 3A). Differences were most evident for IL-8 and MCP-1, for which on average 70.3% and 20.0% of monocytes were positive, respectively, while less than 1% of T cells and NK cells were positive for these cytokines. Similar to previous findings from our group,[32] IL-6 was an exception to this trend and showed no difference in the frequency of positive cells between monocytes and T cells. This observation might be due to the low frequency of IL-6 expressing cells for both of these populations or may more broadly reflect the ability of both monocytes and T cells to produce this molecule.[2,43] Having

https://doi.org/10.1021/acsami.1c16175
ACS Appl. Mater. Interfaces XXXX, XXX, XXX−XXX

ACS Applied Materials & Interfaces www.acsami.org Research Article

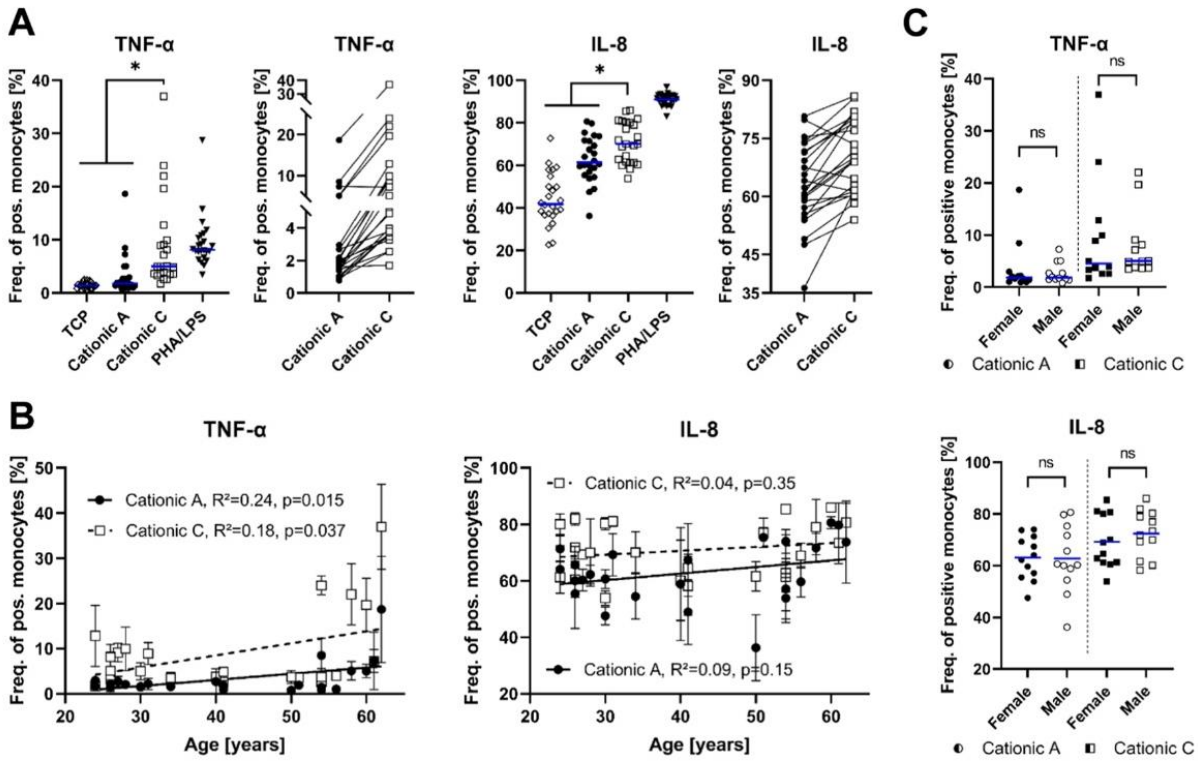

Figure 4. Intracellular expression of proinflammatory cytokines in monocytes in a cohort of 24 individuals. The frequency of TNF-α and IL-8 positive monocytes after 24 h of culture was quantified in three independent experiments using flow cytometry in 24 donors. (A) Comparison of cytokine expression on PEM cationic A and cationic C as well as TCP (negative control) and stimulated cells using PHA/LPS (positive control). RM one-way ANOVA was applied comparing cationic C vs cationic A and the TCP control, $*p \leq 0.05$. Small graphs: lines connect results of identical donors. (B) Age-dependent frequency of cytokine positive monocytes. Simple linear regression in a continuous line (cationic A) and dashed line (cationic C). (C) Analysis of PEMs cationic A and C with regard to sex. Female and male donors were compared for each surface separately using the unpaired *t*-test. Graphs in panels (A) and (C) show mean values and the blue line indicates the median. Panel (B) shows mean ± SD.

identified monocytes as the main immune cell population driving the cytokine response, differences between the immune response to cationic C and the other surfaces were assessed in monocytes. Frequencies of TNF-α and MIP-1β positive monocytes were found to be strongly enhanced on PEM cationic C compared to all other PEM surfaces and the TCP control (Figure 3B). For IL-8, a similar trend was observed with a significant increase in IL-8 positive monocytes on cationic C compared to TCP. No clear trend was observable for MCP-1 and IL-6.

Cytokine release is a dynamic process that is subject to rapid regulatory mechanisms. To reveal the process of cytokine response toward the PEM coatings across time, cytokine production by monocytes was investigated after 12, 24, and 96 h of biomaterial contact. While PHA/LPS stimulated cells showed a strong increase for MIP-1β, TNF-α, and IL-8 expression already after 12 h, no induction on the three PEM coatings was found at this time point (Figure 3C). In contrast, after 24 h of cultivation, cellular activation was observed on all PEM substrates. At this stage, coating cationic C showed the strongest cytokine expression resulting in a 2.2 (TNF-α), 5.0 (MIP-1β), and 12.9 (IL-8)-fold signal increase compared to the negative control, while this increased only 1.3/1.3 (TNF-α), 2.1/2.3 (MIP-1β), and 5.2/4.7 (IL-8)-fold for cationic A/B, respectively. After cultivation for 96 h, the cytokine response was already declined and no differences in the cytokine expression across the PEM surfaces were observed. Cytokines MCP-1 and IL-6, which have already been shown in Figure 3B to not differ in their expression levels after 24 h, were also unaffected by the different coatings after 12 and 96 h (Figure S4). Taken together, these results showed that mainly monocytes were responsible for cytokine release in response to the PEM coatings investigated and for this response to peak after 24 h of biomaterial contact. The results also confirm the cationic surface C to produce the highest proinflammatory response compared to the PEMs cationic A and B.

3.4. Testing a Large Cohort Confirms the Results Obtained with a Smaller Number of Donors. Having characterized the immune responses to these PEM coatings in a small set of donors, we then cast a wider net and investigated a broader spectrum of biological variation by employing a large panel of donors. In particular, we were interested to know if the results observed for three randomly selected donors are representative also in a larger cohort and if donor-specific characteristics such as sex or age have any impact. To achieve this, we selected 24 healthy donors (12 female and 12 male) with ages ranging from 24 to 62 years (Table S1) and examined their response to the cationic A and C surfaces, as these represent the PEMs with the lowest (cationic A) and the highest (cationic C) degree of proinflammatory response

https://doi.org/10.1021/acsami.1c16175
ACS Appl. Mater. Interfaces XXXX, XXX, XXX−XXX

ACS Applied Materials & Interfaces www.acsami.org Research Article

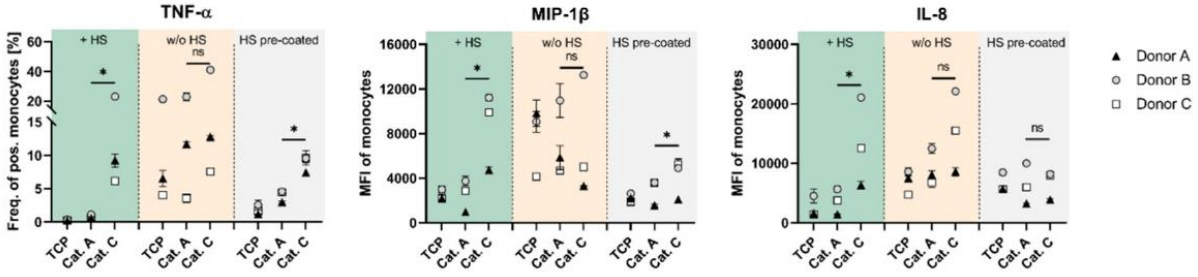

Figure 5. Influence of human serum on proinflammatory cytokine expression by PBMCs cultured on PEM coatings. PBMCs were cultured on the TCP control, PEM cationic A and PEM cationic C in human serum-containing media (+HS, green), serum-free media (w/o HS, orange), or in serum-free media after precoating of the surface with serum for 1 h (HS precoated, gray). The frequency of positive monocytes or MFI was quantified for TNF-α, MIP-1β, and IL-8 in three healthy donors with three technical replicates. Culturing period was 24 h. *t*-test was applied to compare surfaces cationic A and C within the respective culturing groups. $^*p \leq 0.05$. All graphs show mean ± SD.

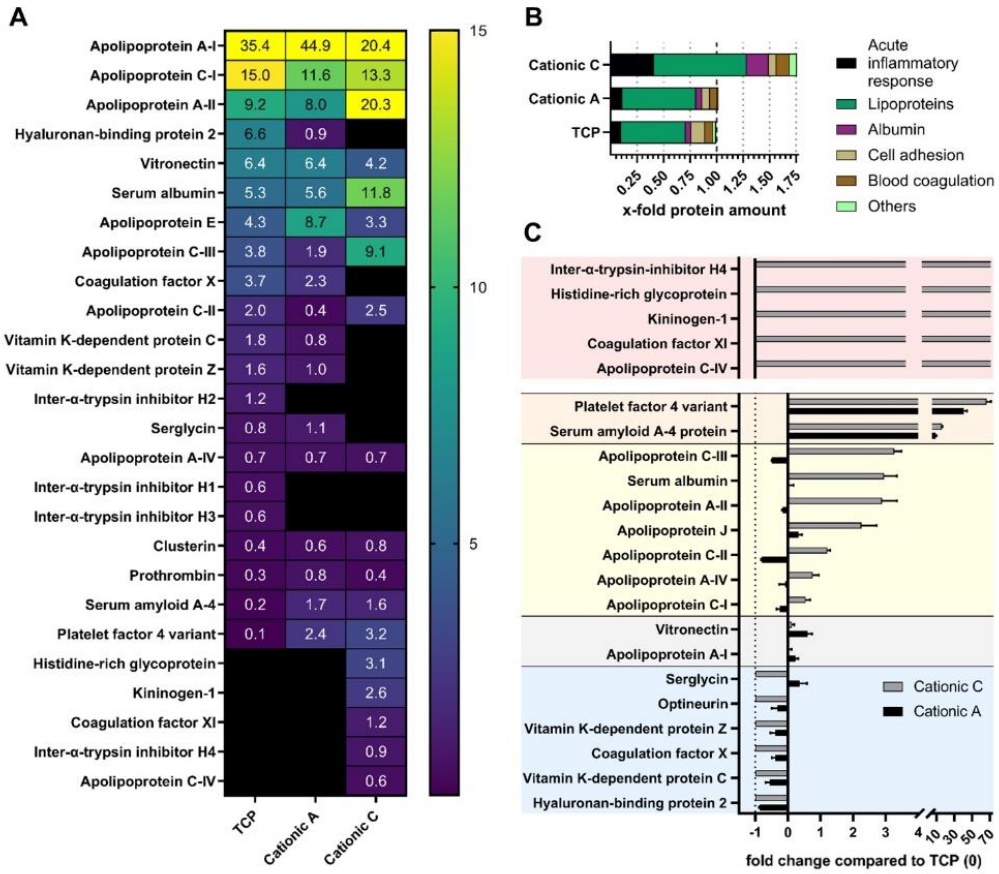

Figure 6. Quantification of protein adsorption. PEM surfaces cationic A, cationic C, and the TCP control were incubated for 1 h with media containing 10% human serum. Adsorbed proteins were determined by LC-MS with $n = 3$ for all surfaces. (A) Heatmap of all proteins identified with an abundance ≥0.5% on one of the surfaces' minimum. Values indicate the abundance percentage (total protein abundance is 100% on each surface). (B) Classification of adsorbed proteins according to their function in an *x*-fold protein amount of TCP (TCP normalized to 1). PEM cationic C 1.76-fold protein amount of TCP and PEM cationic A 1.02-fold protein amount of TCP. (C) Proteins with significantly different protein amounts on the two PEM coatings (orange, yellow, and gray backgrounds) or being present on cationic C only (red) or cationic A only (blue background) are depicted as fold change expression of TCP (TCP set to 0, level indicated by a continuous black line). Reduction by −1 (dashed line) indicates that the respective protein was not found on the corresponding surface. Multiple *t*-tests were applied ($p \leq 0.05$). Graph shows mean ± SD.

observed. We observed levels of TNF-α and IL-8 by this cohort of 24 individuals to be broadly representative of the results obtained with the initial three donors. Both cytokines were found at higher levels in response to the cationic C surface compared with cationic A and the TCP control ($p <$ 0.05 for both cytokines) (Figure 4A). However, a small

https://doi.org/10.1021/acsami.1c16175
ACS Appl. Mater. Interfaces XXXX, XXX, XXX−XXX

number of outliers did not fit the trend seen for the rest of the cohort. Three donors (representing 12.5% of the total cohort) were observed to show a slightly lower frequency of IL-8 positive monocytes for the cationic C surface compared to cationic A (see Figure 4A far right graph). For one of these donors, this was also true for TNF-α while the other two donors showed the same trend as the rest of the cohort for this marker. The outliers were not related in sex or age (two females and one male; 24, 41, and 61 years old) and were not included in other experiments. Next, we investigated whether there was an association between the features of the donors and the observed immune responses. A weak age-dependent increase in the number of TNF-α positive monocytes for both PEM surfaces (cationic A: $R^2 = 0.24$, $p = 0.015$; cationic C: $R^2 = 0.18$, $p = 0.037$) was observed (Figure 4B). No age-dependent correlation was found for IL-8 ($R^2 = 0.09$, $p = 0.15$; $R^2 = 0.03$, $p = 0.35$) or in the negative and positive control groups (Figures 4B and S5). Separating the donors by sex showed no differences between the median values of male and female donors for any cytokine or surface tested (Figure 4C). Taken together, these findings confirm our previous results also for a larger cohort while indicating occasional donor-specific differences.

3.5. Presence of Serum Influences the Immune Response to PEM Coatings. Having performed a suite of comprehensive analyses characterizing the immune response and identifying PEM cationic C as the most inflammatory coating, we next aimed to investigate potential causes of the differences in proinflammatory responses observed for the different PEM coatings tested. It is known that the immune response can be modulated by the adsorbed layer of proteins on a surface, which is in turn influenced by the surface properties of that material.[10,11,14] To analyze the influence of serum proteins on the observed immune response to our PEM coatings, we compared immune responses of PBMC cultured in standard cell culture media containing human serum with cultures of serum-free media. We observed the immune response to be dependent on the presence of proteins. In human serum-containing cultures (+HS, green), a significantly higher cytokine release on cationic C was observed for all three cytokines TNF-α, MIP-1β, and IL-8 compared to cationic A (Figure 5), as previously observed. However, when the same PEM surfaces were cultured without serum, no differences in the degree of cytokine release were found (w/o HS, orange). Interestingly, precoating the surfaces with human serum prior to culture with serum-free media (HS precoated, gray) produced similar immune responses to those observed in the presence of serum-containing media, with elevated levels of TNF-α and MIP-1β in response to cationic C compared to the cationic A surface. It is worth noting that in the absence of serum, proinflammatory responses to TCP and cationic A surfaces were found to be generally elevated compared to serum-containing cultures. Together, these results suggest a role for absorbed serum proteins in modulating the immune response to material surfaces of different wettabilities.

3.6. Adsorption of Acute Inflammatory Response Proteins Is Enhanced on More Hydrophobic PEM Cationic C. To investigate if the adsorbed protein layer differs on the two PEM surfaces and if these differences could be a cause for the distinct immune response observed between the coatings, the composition of the protein layers was analyzed following contact with human serum. PEMs cationic A and C were incubated with media containing 10% human serum, and surface proteins were quantified after on-surface trypsin digest using LC-MS/MS. In total, 26 proteins were identified on the two PEM surfaces (criteria: abundance $\geq$0.5%), with changes in the type and quantity of proteins detected when comparing cationic A with cationic C (Figure 6A). Among the most abundant proteins were several lipoproteins that were found on all three surfaces, with surface-dependent differences for the specific type of lipoprotein. While adsorption of albumin had an abundance of 5.3% and 5.6% for the TCP control and PEM cationic A, respectively, a higher abundance of albumin was observed for PEM cationic C with 11.8%. The total amount of serum proteins adsorbed was clearly enhanced on PEM cationic C (1.76-fold protein amount compared with TCP), while the total amount on PEM cationic A was similar to that in the TCP control (1.02-fold protein amount of TCP) (Figure 6B). To analyze the characteristics of the adsorbed protein layers, identified proteins were grouped based on Gene Ontology database (GOBP) functions. Lipoproteins were the main class of adsorbed proteins on all surfaces followed by proteins involved in the inflammatory response (Figure 6B). Proteins involved in other roles such as cell adhesion and blood coagulation were found in small amounts only. The comparison between surfaces cationic A and C showed a 4-fold increase in the amount of acute inflammatory response proteins on surface cationic C (0.41-fold protein amount on cationic C vs 0.11-fold protein amount on cationic A). This resembles the observed immune response.

To investigate potential differences between the two PEM coatings more closely, statistical analysis was applied to all proteins identified. The identified proteins could be subdivided into five groups (Figure 6C). The red group includes proteins that can only be found on surface cationic C but not cationic A (inter-α-trypsin inhibitor heavy chain H4, histidine-rich glycoprotein, kininogen 1, coagulation factor XI, apolipoprotein C-IV). The majority of proteins of this group are involved in regulatory roles like blood coagulation and angiogenesis. Proteins in the orange group are increased on both PEM coatings compared to the TCP surface with a statistically significant higher abundance on cationic C (platelet factor 4 variant and serum amyloid A4 (SAA4)). Notably, serum amyloids are classical acute-phase proteins that are known to induce the expression of proinflammatory cytokines TNF-α, IL-1β, and IL-8 in neutrophils and monocytes.[44,45] Proteins in the yellow protein group were found to be strongly increased on surface cationic C, while being at or below the level of the TCP control for cationic A, showing significant differences between the two PEM coatings cationic C and A (apolipoprotein C-III, serum albumin, apolipoprotein A-II, apolipoprotein J, apolipoprotein C-II, apolipoprotein A-IV, apolipoprotein C-I). Remarkably, the vast majority of proteins in this group were found to be apolipoproteins. The observation that these proteins are present in a greater amount on cationic C fits with the observation of this coating producing higher proinflammatory responses as some of these apolipoproteins have been associated with proinflammatory responses (see Section 4).[46−50] The gray group in Figure 6C includes proteins with statistically elevated protein amounts on cationic A (vitronectin and apolipoprotein A-I). Apolipoprotein A-I is known for its anti-inflammatory effects on monocytes where it inhibits the production of proinflammatory cytokines TNF-α and IL-1β[51] and is the most abundant protein on the PEM cationic A, accounting for 44.9% of the

https://doi.org/10.1021/acsami.1c16175
ACS Appl. Mater. Interfaces XXXX, XXX, XXX−XXX

ACS Applied Materials & Interfaces www.acsami.org Research Article

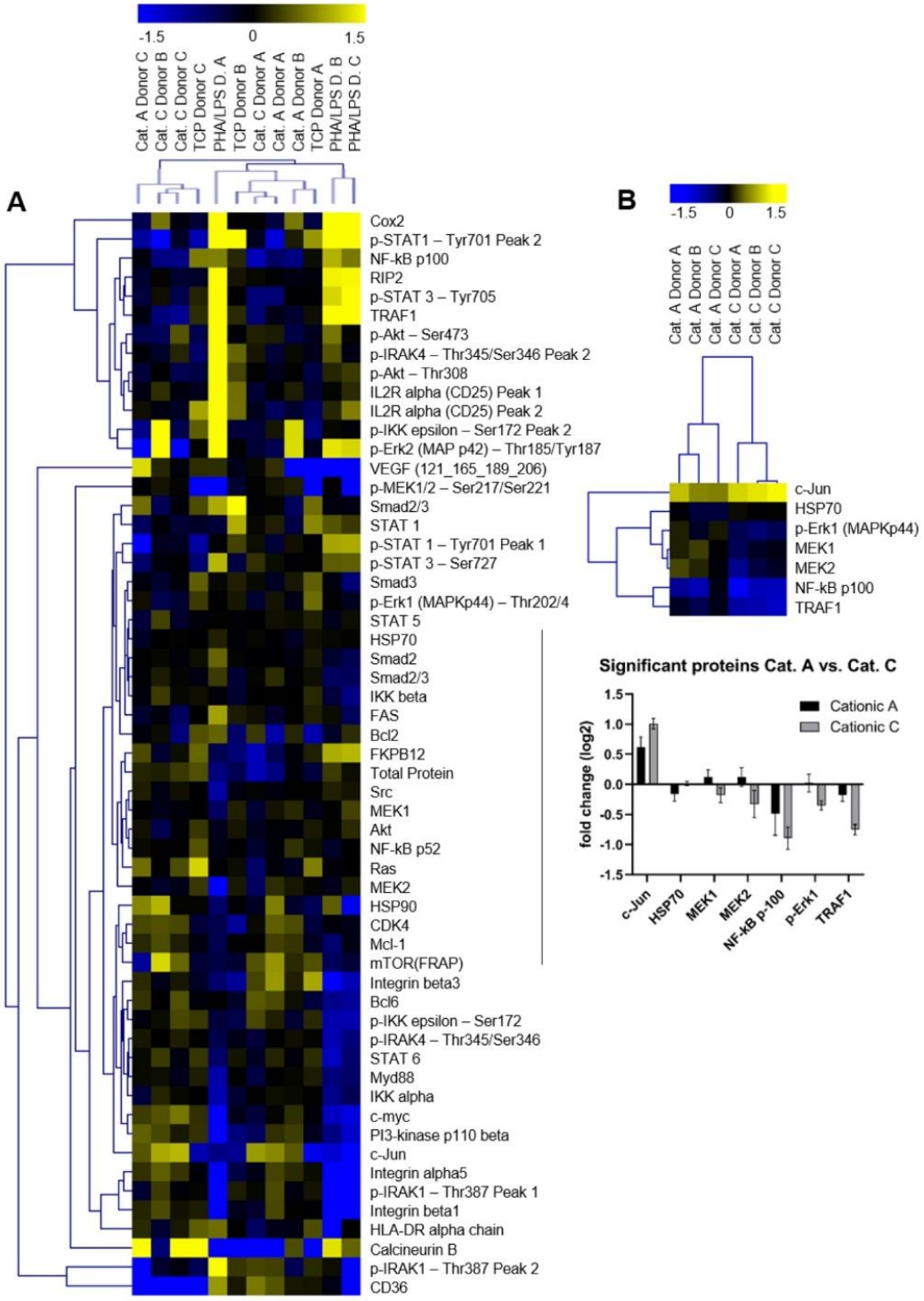

Figure 7. DigiWest-based protein expression analysis of intracellular signaling molecules in monocytes. Monocytes were isolated from the PBMC cell suspension using MACS isolation and cultured for 24 h. Protein expression of 63 cell signaling proteins and their modifications were investigated in monocytes of $n = 3$ different donors using DigiWest. (A) Hierarchically clustered protein expression of all data (Euclidean distance and complete linkage clustering). Color gradient from blue to yellow corresponds to low or high antibody-specific signals. (B) Proteins with a significant (nonparametric Wilcoxon rank-sum test, $p \leq 0.05$) difference in expression levels comparing cationic A and cationic C are shown as a hierarchically clustered heatmap (Euclidean distance and complete linkage clustering). Bar chart indicates the log fold change of significant proteins. Graph shows mean ± SD.

https://doi.org/10.1021/acsami.1c16175
ACS Appl. Mater. Interfaces XXXX, XXX, XXX−XXX

total protein amount (see Figure 6A). On the PEM cationic C, apolipoprotein A-I only accounts for 20.4% of the total protein amount. Thus, this finding is in line with the immunological results showing a lower cytokine response for cationic A compared to cationic C. The last group in Figure 6C (blue) shows proteins being present on cationic A but not cationic C. As these proteins were all identified on TCP as well, this shows a high similarity between surfaces cationic A and TCP, which was mirrored in the type of immune response that they provoked. Numerical values for data in Figure 6 can be found in Tables S2 and S3.

Taken together, proteins found to a higher extent and in large relative abundance on cationic C are acute inflammatory response proteins (e.g., SAA4) or are associated with inflammatory responses based on the literature (e.g., apolipoprotein A-II and apolipoprotein C-III), while the most abundant protein on cationic A is related to anti-inflammatory processes (apolipoprotein A-I). Thus, these observations may relate to differences in the degree of inflammatory responses found to these surfaces.

3.7. Intracellular Levels of Mitogen-Activated Protein Kinase (MAPK) Proteins in Monocytes Are Associated with the Immune Response to PEM Coatings. After having observed differences in the protein adsorption and the proinflammatory response to the PEM surfaces, we next investigated immune cells regarding intracellular signaling pathways. We were interested in identifying changes in these pathways, which could be linked to the observed immune responses. Previous experiments (Figure 3) had shown the immune response to be primarily driven by monocytes. To identify modulation of intracellular pathways in these cells, we cultured an isolated population of monocytes on the three surfaces cationic A, C, and the TCP control. After 24 h of culture, the expression of 63 intracellular signaling proteins was investigated using the DigiWest technology, which allows detection of both protein abundance as well as phosphorylation status. A heatmap of all analyzed proteins including their fold change in expression can be seen in Figure 7A (for raw data, see Table S4). Comparison between PEMs cationic A and C showed statistically significant differences in the expression of seven proteins (Figure 7B). Strikingly, six out of the seven signaling proteins identified are part of the MAPK-signaling pathways, indicating a general role of this pathway in response to PEM surfaces. Out of these, c-Jun was found to be elevated in monocytes in response to cationic C, while proteins MEK1, MEK2, NF-κB, p-Erk1, and TRAF1 were expressed at lower levels in response to cationic C compared to cationic A. It should be highlighted that qualitative differences in the response of these proteins were identified in addition to the previously mentioned differences in fold expression. As such, MEK1, MEK2, NF-κB, and Erk 1/2 increased in response to cationic A, while they were downregulated by cationic C. The only non-MAPK protein differing between cationic C and A was the molecular chaperone HSP70, which showed a higher expression on cationic C compared to cationic A. Comparison of negative (TCP) and positive controls (PHA/LPS) revealed changes in the expression and phosphorylation of 20 of the analyzed proteins (Figure S6). As reported in the literature, pharmacological stimulation of monocytes with PHA/LPS (positive control) showed a strong increase in COX2 and activation of MAPK and JAK/STAT signaling pathways.[52−54]

4. DISCUSSION

In this study, the relationship between biomaterial surface properties, adsorbed proteins, and the resultant immune response was investigated. The use of custom-modified surfaces, human serum, and a human-based primary immune cell model enabled a comprehensive analysis of the interactions between these complex aspects. We observed a material-dependent secretion of proinflammatory cytokines in response to different PEM coatings, which was largely due to monocytes. Differences in the immune response were found to be only apparent in the presence of human serum. Furthermore, we observed stronger proinflammatory responses to be associated with the adsorption of apolipoproteins A-II and C-III on the surface of the more hydrophobic PEM. Conversely, the adsorption of apolipoprotein A-I was associated with the most hydrophilic PEM coating that provoked only a mild inflammatory response.

The targeted modification of surfaces is regarded as a possible way to specifically alter the immune response to biomaterials.[4,7] Studies investigating the inflammatory effects of PEMs have reported significant alteration in macrophage adhesion, monocyte/macrophage differentiation, the secretion of inflammatory cytokines, and the formation of foreign body giant cells, depending on the respective assembling solutions used as PEM substrates.[55,56] Testing of three PEM coatings modified in a gradient fashion with respect to wettability in our study revealed distinct levels of cellular activation and cytokine release by PBMCs in response to these coatings. In accordance with previous findings on other substrates,[8,9] reduced surface wettability on the PEM coating cationic A led to a lower immune response, while the inflammatory response was enhanced in response to the more hydrophobic coating cationic C. This knowledge could be used for the modification of existing biomaterials and medical devices so that desired immune responses for any given biomaterial could be imparted to existing devices with the application of the appropriate PEM coating. Due to the low thickness of the PEMs in the nanometer range, the surface topography of the underlying materials can be preserved while physicochemical properties such as wettability can be modified in the desired way by the selected conditions in the coating process.[57] Thus, PEM coatings could be a versatile tool to maintain the functionality of a medical device while meliorating immune profiles and subsequently improving implant biocompatibility and longevity.

The distinct immune responses provoked by the PEM coatings cationic A and C were examined in detail in this study. The immune response observed by three donors was found to be broadly reflected by a larger cohort of 24 donors (Figure 4). Although the monocyte response showed a degree of variation across individuals, as expected, the overall trends for the different PEM coatings were the same for the vast majority of the 24 donors tested. Thus, the analysis of a small number of PBMC donors tested in this study seems to be representative of a larger cohort. Nevertheless, testing a large number of donors naturally increases the statistical power of the analysis, which is apparent for IL-8 in our experiments (testing three donors showed no significant difference between cationic A and C (Figure 3B), while analysis of 24 donors showed a significant increase in the IL-8 expression for cationic C (p = 0.0042, Figure 4A)). In contrast to prior studies,[58,59] no gender-specific differences were discovered and only a very

https://doi.org/10.1021/acsami.1c16175
ACS Appl. Mater. Interfaces XXXX, XXX, XXX−XXX

weak trend toward a modest rise in TNF-α expression with increasing donor age was observed. These findings suggest that demographic differences in the selection of PBMC donors are not factors of primary importance and indicate that the personalized selection of implant materials may only be necessary for the most extreme outliers in biological response. However, other factors such as environmental differences, the presence of infections, hypersensitivity, or allergies, or even activation of the immune systems in response to previously implanted biomaterials might affect the immune response but were not examined in this study.

We observed the distinct cellular response to coatings A and C to be only apparent in the presence of human serum (Figure 5). In contrast to the immune response in serum-containing cultures, cytokine release under serum-free conditions was significantly increased and no differences between the PEM coatings were discernible. By precoating the surfaces with serum, we found the difference in the inflammatory response between surfaces cationic A and C to be restored, even in cultures using serum-free media. This is in line with previous studies[60] and clearly indicates a decisive role of the adsorbed protein layer in the observed immune response toward PEM coatings. Upon implantation, biomaterials are covered by a layer of proteins within seconds.[10] Our results show that these proteins are the driving force and determine the subsequent immunological response to PEMs, while biomaterial surface properties appear to primarily influence the composition of the adsorbed proteins rather than influencing the immune response.

Examining the proteins adsorbed onto the PEMs investigated in this study identified 26 proteins on the surface of the coatings, while the total amount of proteins on the more hydrophobic cationic C surface was 1.76-fold higher than on the hydrophilic cationic A, thus indicating a wettability-associated effect. This is in line with previous findings showing that proteins bind to hydrophilic surfaces to a lower extent and less tightly than to hydrophobic surfaces.[8] All surfaces investigated here showed high abundance and number of apolipoproteins. The high affinity of apolipoproteins to biomaterial surfaces has already been reported in the literature.[14,61,62] Of note is that the adsorption of apolipoproteins onto the PEM surfaces studied here exceeded the extent of adsorption to most other materials described so far. While apolipoproteins were originally mainly associated with their function as lipid transporters in high-density lipoproteins (HDLs), very low density lipoproteins (VLDLs), or low-density lipoproteins (LDLs), there is now increasing evidence that they are also involved in the modulation of immunological processes. Apolipoprotein A-II is associated with inflammation,[46] enhances proinflammatory monocyte responses to LPS,[47] and correlates to monocyte activation in sepsis patients.[48] Apolipoprotein C-III was shown to significantly increase TNF-α, IL-6, IL-1β, and MCP-1 release from monocytes[49,50] while apolipoprotein J/Clusterin was found to induce matrix metalloproteinase-9 expression in monocytes.[63] The proinflammatory characteristic of these apolipoproteins was also shared by other identified proteins HRG and SAA4, which were shown to mediate the transition of alternatively activated (M2) to proinflammatory (M1) macrophages in a tumor model[64] and induce expression of proinflammatory cytokines TNF-α, IL-1β, and IL-8 in neutrophils and monocytes,[44,45] respectively. Together, these proteins with inflammatory function or being associated with proinflammatory effects based on the literature (HRG, SAA4, and apolipoproteins A-II, C-III, J/Clusterin) showed an abundance of 34.9% on the more proinflammatory cationic C surface, while these proteins only accounted for 12.2% of proteins on the less inflammatory cationic A coating (2.9-fold increase). When looking at the absolute amount of protein on the surfaces, this effect becomes even more pronounced. Due to the 1.76-fold increased total protein amount on surface cationic C, 5 times the amount of proinflammatory proteins is found on this surface in comparison to cationic A in absolute terms. In contrast, other apolipoproteins are associated with anti-inflammatory effects. Apolipoproteins A-I and E inhibit the production of proinflammatory cytokines and promote macrophage conversion from the proinflammatory M1 to the anti-inflammatory M2 phenotype.[51,65,66] These two inflammation-dampening proteins accounted for 53.6% of the total protein abundance on cationic A, while their abundance on cationic C was only 23.6%. Thus, the abundance of proteins with inflammation-dampening properties on the more inflammatory cationic C surface was less than half than those on the less inflammatory PEM cationic A. In addition to protein identity, wettability-dependent conformational changes and/or protein unfolding can further enhance the observed effect.[67] Hereby, nonpolar hydrophobic surfaces seem to cause the most protein unfolding, while neutrally charged hydrophilic surfaces tend to induce the least changes in the protein structure.[68] Unfolding of proteins can influence monocytes by regulating the expression of proinflammatory cytokines and modulating cell attachment.[69] Thus, these effects might be additional factors further enhancing the immune response for the more hydrophobic PEM coating cationic C. Taken together, protein analysis shows that the composition of the adsorbed protein layer can have a major impact on the cytokine expression by monocytes and the resulting immune response. In this context, the class of apolipoproteins comes into focus as a promising candidate to modulate the immune response to biomaterials.

To gain a better understanding of how the adsorbed proteins influence the observed immune responses, an analysis of intracellular signaling was performed to provide information about the type of cellular activation. We found an elevated expression of c-Jun and HSP70 in response to surface cationic C, and higher expression of MEK 1+2, NF-κB, p-Erk1, and TRAF1 to surface cationic A (Figure 7). Most of these proteins are assigned to MAPK signaling, a cascade that is well established for its role in the regulation of the inflammatory response in innate immune cells.[70] As such, the production of several proinflammatory cytokines like TNF-α, IL-6, or IL-1β as well as other inflammatory mediators are positively regulated by MAPK. While the upregulation of c-Jun, an important regulator of gene expression, on the cationic C coating is in line with the increased cytokine response to this surface, the elevated expression of other proteins of the classical MAPK pathway in response to the cationic A surface suggests that these proteins do not play a major role in mediating inflammatory responses to the coatings investigated in this study. Large pathways like MAPK also have a high level of complexity and can be modulated by various mechanisms at many steps of the pathway. As a result, differences for individual members may develop. In addition, protein conditions like phosphorylation can occur dynamically, while the measured cytokines accumulated over time. It should also be pointed out that cytokine response, in general, is a signal

https://doi.org/10.1021/acsami.1c16175
ACS Appl. Mater. Interfaces XXXX, XXX, XXX−XXX

that may undergo several steps of amplification and thus may be significantly lower at the signaling pathway level investigated here. A single-cell analysis technique would shed more light on the possible heterogeneity of responses as the results observed may have been partially masked by a fraction of cells responding in a different manner (for example, the results in Figure 3 showed a range of 25−90% of nonpositive monocytes, depending on the respective cytokines). However, the identification of multiple proteins from the MAPK pathway implicates a role for this signaling route as a mechanism that monocytes used to respond to differences in the two PEM coatings investigated.

5. CONCLUSIONS

In this study, PEM coatings were developed for the targeted modification of surface properties including wettability. We demonstrated coating-dependent adsorption of surface proteins, resulting in distinct degrees of inflammation. These effects were accompanied by differences in intracellular signaling molecules. This study thus demonstrates the interrelation of material properties, protein adsorption, and the immune response as closely connected aspects in the biological response to synthetic materials.

■ ASSOCIATED CONTENT

Supporting Information

The Supporting Information is available free of charge at https://pubs.acs.org/doi/10.1021/acsami.1c16175.

Gating strategy used to analyze surface marker proteins on PBMCs; gating strategy used for intracellular cytokine staining analysis; cytokine secretion of PBMCs cultured on PEM surfaces; intracellular cytokine analysis across time of PBMCs cultured on PEM coatings; age-associated intracellular cytokine expression in monocytes in a cohort of 24 individuals; intracellular signaling molecules in monocytes with significant differences in expression between negative and positive controls; sex, age, and frequency of major cellular populations in PBMC; abundance (percentage) of proteins identified on cationic A, cationic C, and the negative control (TCP) using LC-MS; statistical analysis comparing the amount of proteins on the cationic A and cationic C PEM surfaces; and expression levels of intracellular proteins analyzed with DigiWest technology (PDF)

■ AUTHOR INFORMATION

Corresponding Author

Florian Billing − *NMI Natural and Medical Sciences Institute at the University of Tübingen, 72770 Reutlingen, Germany;* orcid.org/0000-0002-3874-9012; Phone: +49 7121 51530843; Email: florian.billing@nmi.de

Authors

Bernadette Walter − *NMI Natural and Medical Sciences Institute at the University of Tübingen, 72770 Reutlingen, Germany*

Simon Fink − *NMI Natural and Medical Sciences Institute at the University of Tübingen, 72770 Reutlingen, Germany*

Elsa Arefaine − *NMI Natural and Medical Sciences Institute at the University of Tübingen, 72770 Reutlingen, Germany*

Luisa Pickarski − *NMI Natural and Medical Sciences Institute at the University of Tübingen, 72770 Reutlingen, Germany*

Sandra Maier − *NMI Natural and Medical Sciences Institute at the University of Tübingen, 72770 Reutlingen, Germany*

Robin Kretz − *NMI Natural and Medical Sciences Institute at the University of Tübingen, 72770 Reutlingen, Germany*

Meike Jakobi − *NMI Natural and Medical Sciences Institute at the University of Tübingen, 72770 Reutlingen, Germany*

Nora Feuerer − *NMI Natural and Medical Sciences Institute at the University of Tübingen, 72770 Reutlingen, Germany; Department of Biomedical Engineering, Eberhard Karls University Tübingen, 72076 Tübingen, Germany*

Nicole Schneiderhan-Marra − *NMI Natural and Medical Sciences Institute at the University of Tübingen, 72770 Reutlingen, Germany*

Claus Burkhardt − *NMI Natural and Medical Sciences Institute at the University of Tübingen, 72770 Reutlingen, Germany*

Markus Templin − *NMI Natural and Medical Sciences Institute at the University of Tübingen, 72770 Reutlingen, Germany*

Anne Zeck − *NMI Natural and Medical Sciences Institute at the University of Tübingen, 72770 Reutlingen, Germany*

Rumen Krastev − *NMI Natural and Medical Sciences Institute at the University of Tübingen, 72770 Reutlingen, Germany; Faculty of Applied Chemistry, Reutlingen University, 72762 Reutlingen, Germany*

Hanna Hartmann − *NMI Natural and Medical Sciences Institute at the University of Tübingen, 72770 Reutlingen, Germany*

Christopher Shipp − *NMI Natural and Medical Sciences Institute at the University of Tübingen, 72770 Reutlingen, Germany*

Complete contact information is available at: https://pubs.acs.org/10.1021/acsami.1c16175

Notes

The authors declare no competing financial interest.

■ ACKNOWLEDGMENTS

This work received financial support from the EU-EFRE and the State of Baden-Wuerttemberg (712889) as well as by the State Ministry of Baden-Wuerttemberg for Economic Affairs, Labour and Tourism. We are very grateful to Burkhard Schlosshauer (NMI) for his contribution to the initiation of the project. Further thanks go to Laura Strano (NMI) for her essential contribution to the PEMs tested here, Alexander Rudt for helpful discussions, and Hannah Graf for her assistance in the SEM analysis. The table of contents illustration was created using biorender.com.

■ REFERENCES

(1) Anderson, J. M. Biological Responses to Materials. *Annu. Rev. Mater. Res.* **2001**, *31*, 81−110.

(2) Anderson, J. M.; Rodriguez, A.; Chang, D. T. Foreign Body Reaction to Biomaterials. *Semin. Immunol.* **2008**, *20*, 86−100.

(3) Williams, D. F. On the Mechanisms of Biocompatibility. *Biomaterials* **2008**, *29*, 2941−2953.

(4) Franz, S.; Rammelt, S.; Scharnweber, D.; Simon, J. C. Immune responses to implants - a review of the implications for the design of immunomodulatory biomaterials. *Biomaterials* **2011**, *32*, 6692−6709.

(5) Rostam, H. M.; Singh, S.; Vrana, N. E.; Alexander, M. R.; Ghaemmaghami, A. M. Impact of surface chemistry and topography

on the function of antigen presenting cells. *Biomater. Sci.* **2015**, *3*, 424−441.
(6) Albanese, A.; Tang, P. S.; Chan, W. C. The effect of nanoparticle size, shape, and surface chemistry on biological systems. *Annu. Rev. Biomed. Eng.* **2012**, *14*, 1−16.
(7) Mariani, E.; Lisignoli, G.; Borzì, R. M.; Pulsatelli, L. Biomaterials: Foreign Bodies or Tuners for the Immune Response? *Int. J. Mol. Sci.* **2019**, *20*, No. 636.
(8) Thevenot, P.; Hu, W.; Tang, L. Surface chemistry influences implant biocompatibility. *Curr. Top. Med. Chem.* **2008**, *8*, 270−280.
(9) Brodbeck, W. G.; Voskerician, G.; Ziats, N. P.; Nakayama, Y.; Matsuda, T.; Anderson, J. M. In vivo leukocyte cytokine mRNA responses to biomaterials are dependent on surface chemistry. *J. Biomed. Mater. Res., Part A* **2003**, *64A*, 320−329.
(10) Horbett, T. A. Chapter 13 Principles underlying the role of adsorbed plasma proteins in blood interactions with foreign materials. *Cardiovasc. Pathol.* **1993**, *2*, 137−148.
(11) Wilson, C. J.; Clegg, R. E.; Leavesley, D. I.; Pearcy, M. J. Mediation of biomaterial-cell interactions by adsorbed proteins: a review. *Tissue Eng.* **2005**, *11*, 1−18.
(12) Jenney, C. R.; Anderson, J. M. Adsorbed serum proteins responsible for surface dependent human macrophage behavior. *J. Biomed. Mater. Res.* **2000**, *49*, 435−447.
(13) Collier, T. O.; Anderson, J. M. Protein and surface effects on monocyte and macrophage adhesion, maturation, and survival. *J. Biomed. Mater. Res.* **2002**, *60*, 487−496.
(14) Visalakshan, R. M.; MacGregor, M. N.; Sasidharan, S.; Ghazaryan, A.; Mierczynska-Vasilev, A. M.; Morsbach, S.; Mailänder, V.; Landfester, K.; Hayball, J. D.; Vasilev, K. Biomaterial Surface Hydrophobicity-Mediated Serum Protein Adsorption and Immune Responses. *ACS Appl. Mater. Interfaces* **2019**, *11* (), 27615−27623 DOI: 10.1021/acsami.9b09900.
(15) Kim, Y. K.; Que, R.; Wang, S.-W.; Liu, W. F. Modification of biomaterials with a self-protein inhibits the macrophage response. *Adv. Healthcare Mater.* **2014**, *3* (), 989−994 DOI: 10.1002/adhm.201300532.
(16) Roach, P.; Eglin, D.; Rohde, K.; Perry, C. C. Modern biomaterials: a review—bulk properties and implications of surface modifications. *J. Mater. Sci.: Mater. Med.* **2007**, *18*, 1263−1277.
(17) Sigal, G. B.; Mrksich, M.; Whitesides, G. M. Effect of Surface Wettability on the Adsorption of Proteins and Detergents. *J. Am. Chem. Soc.* **1998**, *120*, 3464−3473.
(18) Kang, C.-K.; Lee, Y.-S. The surface modification of stainless steel and the correlation between the surface properties and protein adsorption. *J. Mater. Sci.: Mater. Med.* **2007**, *18* (), 1389−1398 DOI: 10.1007/s10856-006-0079-9.
(19) Brodbeck, W. G.; Colton, E.; Anderson, J. M. Effects of adsorbed heat labile serum proteins and fibrinogen on adhesion and apoptosis of monocytes/macrophages on biomaterials. *J. Mater. Sci.: Mater. Med.* **2003**, *14*, 671−675.
(20) Decher, G.; Hong, J. D.; Schmitt, J. Buildup of ultrathin multilayer films by a self-assembly process: III. Consecutively alternating adsorption of anionic and cationic polyelectrolytes on charged surfaces. *Thin Solid Films* **1992**, *210−211*, 831−835.
(21) Detzel, C. J.; Larkin, A. L.; Rajagopalan, P. Polyelectrolyte multilayers in tissue engineering. *Tissue Eng., Part B* **2011**, *17*, 101.
(22) Yoo, D.; Shiratori, S. S.; Rubner, M. F. Controlling Bilayer Composition and Surface Wettability of Sequentially Adsorbed Multilayers of Weak Polyelectrolytes. *Macromolecules* **1998**, *31*, 4309−4318.
(23) Krastev, R.; Rudt, A.; Xiong, X.; Hartmann, H. Polyelectrolyte Coatings for Surface Modification of Medical Implants. *Curr. Dir. Biomed. Eng.* **2018**, *4*, 217−220.
(24) Trindade, M. In vitro reaction to orthopaedic biomaterials by macrophages and lymphocytes isolated from patients undergoing revision surgery. *Biomaterials* **2001**, *22*, 253−259.
(25) Brodbeck, W. G.; MacEwan, M.; Colton, E.; Meyerson, H.; Anderson, J. M. Lymphocytes and the foreign body response: Lymphocyte enhancement of macrophage adhesion and fusion. *J. Biomed. Mater. Res., Part A* **2005**, *74A*, 222−229.
(26) Jenney, C. R.; Anderson, J. M. Adsorbed IgG: A potent adhesive substrate for human macrophages. *J. Biomed. Mater. Res.* **2000**, *50*, 281−290.
(27) Maciel, J.; Oliveira, M. I.; Gonçalves, R. M.; Barbosa, M. A. The effect of adsorbed fibronectin and osteopontin on macrophage adhesion and morphology on hydrophilic and hydrophobic model surfaces. *Acta Biomater.* **2012**, *8* (), 3669−3677 DOI: 10.1016/j.actbio.2012.06.010.
(28) Park, K.; Shim, H. S.; Dewanjee, M. K.; Eigler, N. L. In vitro and in vivo studies of PEO-grafted blood-contacting cardiovascular prostheses. *J. Biomater. Sci., Polym. Ed.* **2000**, *11*, 1121−1134.
(29) Ngo, B. K. D.; Grunlan, M. A. Protein Resistant Polymeric Biomaterials. *ACS Macro Lett.* **2017**, *6*, 992−1000.
(30) Friedrichs, B. Th. Peters. Jr.: All about Albumin. Biochemistry, Genetics, and Medical Applications. XX and 432 pages, numerous figures and tables. Academic Press, Inc., San Diego, California, 1996. Price: 85.00 US $. *Food/Nahrung* **1997**, *41*, 382.
(31) Oyane, A.; Kim, H.-M.; Furuya, T.; Kokubo, T.; Miyazaki, T.; Nakamura, T. Preparation and assessment of revised simulated body fluids. *J. Biomed. Mater. Res.* **2003**, *65A*, 188−195.
(32) Billing, F.; Jakobi, M.; Martin, D.; Gerlach, K.; Arefaine, E.; Weiss, M.; Schneiderhan-Marra, N.; Hartmann, H.; Shipp, C. The immune response to the SLActive titanium dental implant surface in vitro is predominantly driven by innate immune cells. *J. Immunol. Regener. Med.* **2021**, *13*, No. 100047.
(33) Segan, S.; Jakobi, M.; Khokhani, P.; Klimosch, S.; Billing, F.; Schneider, M.; Martin, D.; Metzger, U.; Biesemeier, A.; Xiong, X.; Mukherjee, A.; Steuer, H.; Keller, B. M.; Joos, T.; Schmolz, M.; Rothbauer, U.; Hartmann, H.; Burkhardt, C.; Lorenz, G.; Schneiderhan-Marra, N.; Shipp, C. Systematic Investigation of Polyurethane Biomaterial Surface Roughness on Human Immune Responses in vitro. *BioMed Res. Int.* **2020**, *2020*, No. 3481549.
(34) European Medicines Agency. *Guideline on Bioanalytical Method Validation*; European Medicines Agency, 2011. https://www.ema.europa.eu/en/documents/scientific-guideline/guideline-bioanalytical-method-validation_en.pdf (accessed Feb 16, 2021).
(35) U.S. Department of Health and Human Services, Food and Drug Administration. *Bioanalytical Method Validation:Guidance for Industry*; U.S. Department of Health and Human Services, Food and Drug Administration, 2018. https://www.fda.gov/downloads/drugs/guidances/ucm070107.Pdf (accessed Feb 11, 2021).
(36) Westgard, J. O.; Barry, P. L.; Hunt, M. R.; Groth, T. A multi-rule Shewhart chart for quality control in clinical chemistry. *Clin. Chem.* **1981**, *27*, 493−501.
(37) Cox, J.; Mann, M. MaxQuant enables high peptide identification rates, individualized p.p.b.-range mass accuracies and proteome-wide protein quantification. *Nat. Biotechnol.* **2008**, *26*, 1367−1372.
(38) Tyanova, S.; Temu, T.; Sinitcyn, P.; Carlson, A.; Hein, M. Y.; Geiger, T.; Mann, M.; Cox, J. The Perseus computational platform for comprehensive analysis of (prote)omics data. *Nat. Methods* **2016**, *13*, 731−740.
(39) Schwanhäusser, B.; Busse, D.; Li, N.; Dittmar, G.; Schuchhardt, J.; Wolf, J.; Chen, W.; Selbach, M. Global quantification of mammalian gene expression control. *Nature* **2011**, *473*, 337−342.
(40) Treindl, F.; Ruprecht, B.; Beiter, Y.; Schultz, S.; Döttinger, A.; Staebler, A.; Joos, T. O.; Kling, S.; Poetz, O.; Fehm, T.; Neubauer, H.; Kuster, B.; Templin, M. F. A bead-based western for high-throughput cellular signal transduction analyses. *Nat. Commun.* **2016**, *7*, No. 12852.
(41) Saeed, A. I.; Bhagabati, N. K.; Braisted, J. C.; Liang, W.; Sharov, V.; Howe, E. A.; Li, J.; Thiagarajan, M.; White, J. A.; Quackenbush, J. [9] TM4 Microarray Software Suite. In *Methods in Enzymology*; Kimmel, A. R.; Oliver, B., Eds.; DNA Microarrays, Part B: Databases and Statistics; Elsevier/Academic Press, 2006; Vol. *411*, pp 134−193.
(42) Tak, T.; van Groenendael, R.; Pickkers, P.; Koenderman, L. Monocyte Subsets Are Differentially Lost from the Circulation during

https://doi.org/10.1021/acsami.1c16175
ACS Appl. Mater. Interfaces XXXX, XXX, XXX−XXX

Acute Inflammation Induced by Human Experimental Endotoxemia. *J. Innate Immun.* **2017**, *9* (), 464−474 DOI: 10.1159/000475665.
(43) Trinschek, B.; Lüssi, F.; Haas, J.; Wildemann, B.; Zipp, F.; Wiendl, H.; Becker, C.; Jonuleit, H. Kinetics of IL-6 Production Defines T Effector Cell Responsiveness to Regulatory T Cells in Multiple Sclerosis. *PLoS One* **2013**, *8*, No. e77634.
(44) Furlaneto, C. J.; Campa, A. A novel function of serum amyloid A: a potent stimulus for the release of tumor necrosis factor-alpha, interleukin-1beta, and interleukin-8 by human blood neutrophil. *Biochem. Biophys. Res. Commun.* **2000**, *268*, 405.
(45) Ribeiro, F. P.; Furlaneto, C. J.; Hatanaka, E.; Ribeiro, W. B.; Souza, G. M.; Cassatella, M. A.; Campa, A. mRNA expression and release of interleukin-8 induced by serum amyloid A in neutrophils and monocytes. *Mediators Inflammation* **2003**, *12*, 173−178.
(46) Yang, M.; Liu, Y.; Dai, J.; Li, L.; Ding, X.; Xu, Z.; Mori, M.; Miyahara, H.; Sawashita, J.; Higuchi, K. Apolipoprotein A-II induces acute-phase response associated AA amyloidosis in mice through conformational changes of plasma lipoprotein structure. *Sci. Rep.* **2018**, *8*, No. 5620.
(47) Thompson, P. A.; Berbée, J. F.; Rensen, P. C.; Kitchens, R. L. Apolipoprotein A-II augments monocyte responses to LPS by suppressing the inhibitory activity of LPS-binding protein. *Innate Immun.* **2008**, *14*, 365.
(48) Barlage, S.; Gnewuch, C.; Liebisch, G.; Wolf, Z.; Audebert, F.-X.; Glück, T.; Fröhlich, D.; Krämer, B. K.; Rothe, G.; Schmitz, G. Changes in HDL-associated apolipoproteins relate to mortality in human sepsis and correlate to monocyte and platelet activation. *Intensive Care Med.* **2009**, *35*, 1877−1885.
(49) Zewinger, S.; Reiser, J.; Jankowski, V.; Alansary, D.; Hahm, E.; Triem, S.; Klug, M.; Schunk, S. J.; Schmit, D.; Kramann, R.; Körbel, C.; Ampofo, E.; Laschke, M. W.; Selejan, S.-R.; Paschen, A.; Herter, T.; Schuster, S.; Silbernagel, G.; Sester, M.; Sester, U.; Aßmann, G.; Bals, R.; Kostner, G.; Jahnen-Dechent, W.; Menger, M. D.; Rohrer, L.; März, W.; Böhm, M.; Jankowski, J.; Kopf, M.; Latz, E.; Niemeyer, B. A.; Fliser, D.; Laufs, U.; Speer, T. Apolipoprotein C3 induces inflammation and organ damage by alternative inflammasome activation. *Nat. Immunol.* **2020**, *21*, 30−41.
(50) Han, X.; Wang, T.; Zhang, J.; Liu, X.; Li, Z.; Wang, G.; Song, Q.; Pang, D.; Ouyang, H.; Tang, X. Apolipoprotein CIII regulates lipoprotein-associated phospholipase A2 expression via the MAPK and NFκB pathways. *Biol. Open* **2015**, *4*, 661−665.
(51) Hyka, N.; Dayer, J. M.; Modoux, C.; Kohno, T.; Edwards, C. K.; Roux-Lombard, P.; Burger, D. Apolipoprotein A-I inhibits the production of interleukin-1beta and tumor necrosis factor-alpha by blocking contact-mediated activation of monocytes by T lymphocytes. *Blood* **2001**, *97*, 2381−2389.
(52) Lee, S. H.; Soyoola, E.; Chanmugam, P.; Hart, S.; Sun, W.; Zhong, H.; Liou, S.; Simmons, D.; Hwang, D. Selective expression of mitogen-inducible cyclooxygenase in macrophages stimulated with lipopolysaccharide. *J. Biol. Chem.* **1992**, *267*, 25934−25938.
(53) Bode, J. G.; Ehlting, C.; Häussinger, D. The macrophage response towards LPS and its control through the p38MAPK−STAT3 axis. *Cell. Signalling* **2012**, *24*, 1185−1194.
(54) Liu, X.; Yin, S.; Chen, Y.; Wu, Y.; Zheng, W.; Dong, H.; Bai, Y.; Qin, Y.; Li, J.; Feng, S.; Zhao, P. LPS-induced proinflammatory cytokine expression in human airway epithelial cells and macrophages via NF-κB, STAT3 or AP-1 activation. *Mol. Med. Rep.* **2018**, *17*, 5484−5491.
(55) Zhou, G.; Niepel, M. S.; Saretia, S.; Groth, T. Reducing the inflammatory responses of biomaterials by surface modification with glycosaminoglycan multilayers. *J. Biomed. Mater. Res.* **2016**, *104*, 493−502.
(56) Knopf-Marques, H.; Singh, S.; Htwe, S. S.; Wolfova, L.; Buffa, R.; Bacharouche, J.; Francius, G.; Voegel, J.-C.; Schaaf, P.; Ghaemmaghami, A. M.; Vrana, N. E.; Lavalle, P. Immunomodulation with Self-Crosslinked Polyelectrolyte Multilayer-Based Coatings. *Biomacromolecules* **2016**, *17*, 2189−2198.
(57) Hartmann, H.; Krastev, R. Biofunctionalization of surfaces using polyelectrolyte multilayers. *BioNanoMaterials* **2017**, *18*, No. 20160015.
(58) Bernin, H.; Fehling, H.; Marggraff, C.; Tannich, E.; Lotter, H. The cytokine profile of human NKT cells and PBMCs is dependent on donor sex and stimulus. *Med. Microbiol. Immunol.* **2016**, *205* (), 321−332 DOI: 10.1007/s00430-016-0449-y.
(59) Longo, D. M.; Louie, B.; Putta, S.; Evensen, E.; Ptacek, J.; Cordeiro, J.; Wang, E.; Pos, Z.; Hawtin, R. E.; Marincola, F. M.; Cesano, A. Single-cell network profiling of peripheral blood mononuclear cells from healthy donors reveals age- and race-associated differences in immune signaling pathway activation. *J. Immunol.* **2012**, *188* (), 1717−1725 DOI: 10.4049/jimmunol.1102514.
(60) Allen, L. T.; Tosetto, M.; Miller, I. S.; O'Connor, D. P.; Penney, S. C.; Lynch, I.; Keenan, A. K.; Pennington, S. R.; Dawson, K. A.; Gallagher, W. M. Surface-induced changes in protein adsorption and implications for cellular phenotypic responses to surface interaction. *Biomaterials* **2006**, *27*, 3096−3108.
(61) Magnani, A.; Barbucci, R.; Lamponi, S.; Chiumento, A.; Paffetti, A.; Trabalzini, L.; Martelli, P.; Santucci, A. Two-step elution of human serum proteins from different glass-modified bioactive surfaces: a comparative proteomic analysis of adsorption patterns. *Electrophoresis* **2004**, *25*, 2413.
(62) Cornelius, R. M.; Archambault, J.; Brash, J. L. Identification of apolipoprotein A-I as a major adsorbate on biomaterial surfaces after blood or plasma contact. *Biomaterials* **2002**, *23*, 3583−3587.
(63) Shim, Y.-J.; Kang, B.-H.; Jeon, H.-S.; Park, I.-S.; Lee, K.-U.; Lee, I.-K.; Park, G.-H.; Lee, K.-M.; Schedin, P.; Min, B.-H. Clusterin induces matrix metalloproteinase-9 expression via ERK1/2 and PI3K/Akt/NF-κB pathways in monocytes/macrophages. *J. Leukocyte Biol.* **2011**, *90*, 761−769.
(64) Rolny, C.; Mazzone, M.; Tugues, S.; Laoui, D.; Johansson, I.; Coulon, C.; Squadrito, M. L.; Segura, I.; Li, X.; Knevels, E.; Costa, S.; Vinckier, S.; Dresselaer, T.; Åkerud, P.; De, M. M.; Salomäki, H.; Phillipson, M.; Wyns, S.; Larsson, E.; Buysschaert, I.; Botling, J.; Himmelreich, U.; Van, G. J. A.; De, P. M.; Dewerchin, M.; Claesson-Welsh, L.; Carmeliet, P. HRG inhibits tumor growth and metastasis by inducing macrophage polarization and vessel normalization through downregulation of PlGF. *Cancer Cell* **2011**, *19*, 31.
(65) Baitsch, D.; Bock, H. H.; Engel, T.; Telgmann, R.; Müller-Tidow, C.; Varga, G.; Bot, M.; Herz, J.; Robenek, H.; von, E. A.; Nofer, J. R. Apolipoprotein E induces antiinflammatory phenotype in macrophages. *Arterioscler., Thromb., Vasc. Biol.* **2011**, *31*, 1160.
(66) Murphy, A. J.; Woollard, K. J.; Hoang, A.; Mukhamedova, N.; Stirzaker, R. A.; McCormick, S. P.; Remaley, A. T.; Sviridov, D.; Chin-Dusting, J. High-density lipoprotein reduces the human monocyte inflammatory response. *Arterioscler., Thromb., Vasc. Biol.* **2008**, *28*, 2071.
(67) Gittens, R. A.; Scheideler, L.; Rupp, F.; Hyzy, S. L.; Geis-Gerstorfer, J.; Schwartz, Z.; Boyan, B. D. A review on the wettability of dental implant surfaces II: Biological and clinical aspects. *Acta Biomater.* **2014**, *10*, 2907−2918.
(68) Brash, J. L.; Horbett, T. A.; Latour, R. A.; Tengvall, P. The blood compatibility challenge. Part 2: Protein adsorption phenomena governing blood reactivity. *Acta Biomater.* **2019**, *94*, 11−24.
(69) Visalakshan, R. M.; Cavallaro, A. A.; MacGregor, M. N.; Lawrence, E. P.; Koynov, K.; Hayball, J. D.; Vasilev, K. Nanotopography-Induced Unfolding of Fibrinogen Modulates Leukocyte Binding and Activation. *Adv. Funct. Mater.* **2019**, *29*, No. 1807453.
(70) Arthur, J. S. C.; Ley, S. C. Mitogen-activated protein kinases in innate immunity. *Nat. Rev. Immunol.* **2013**, *13* (), 679−692 DOI: 10.1038/nri3495.

https://doi.org/10.1021/acsami.1c16175
ACS Appl. Mater. Interfaces XXXX, XXX, XXX−XXX

Supplemental Figures

Billing F., et al. Altered pro-inflammatory responses to polyelectrolyte multilayer coatings are associated with differences in protein adsorption and wettability.

Supporting Information

Altered Pro-inflammatory Responses to Polyelectrolyte Multilayer Coatings are Associated with Differences in Protein Adsorption and Wettability

Florian Billing[1], Bernadette Walter[1], Simon Fink[1], Elsa Arefaine[1], Luisa Pickarski[1], Sandra Maier[1], Robin Kretz[1], Meike Jakobi[1], Nora Feuerer[1,2], Nicole Schneiderhan-Marra[1], Claus Burkhardt[1], Markus Templin[1], Anne Zeck[1], Rumen Krastev[1,3], Hanna Hartmann[1], Christopher Shipp[1]*

1: NMI Natural and Medical Sciences Institute at the University of Tübingen, 72770 Reutlingen, Germany

2: Department of Biomedical Engineering, Eberhard Karls University Tübingen, 72076 Tübingen, Germany

3: Reutlingen University, Faculty of Applied Chemistry, 72762 Reutlingen, Germany

* Corresponding author (Florian Billing): E-mail: florian.billing@nmi.de, Phone: +49 7121 51530843

SUPPORTING FIGURES AND TABLES

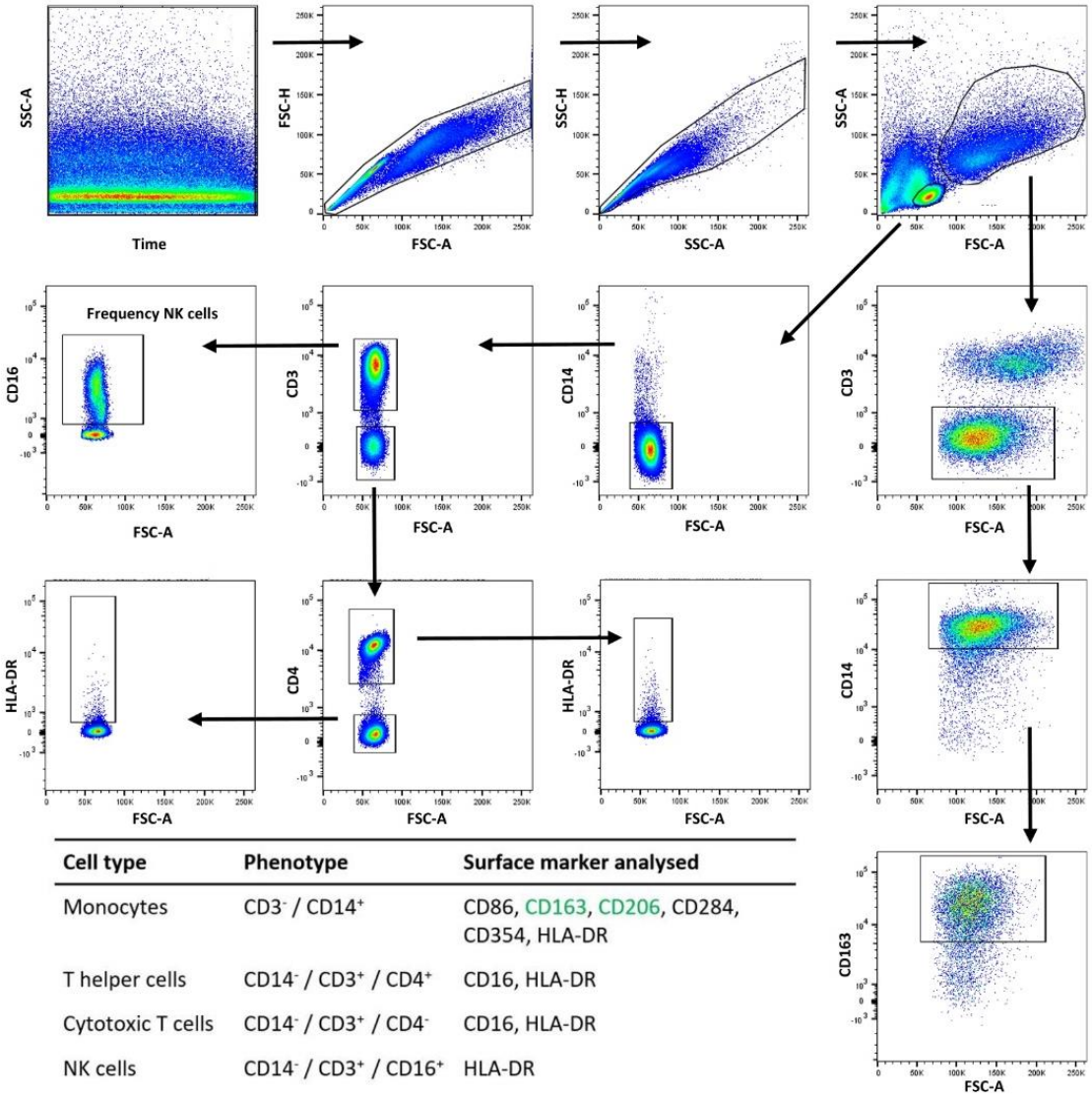

Cell type	Phenotype	Surface marker analysed
Monocytes	$CD3^-$ / $CD14^+$	CD86, CD163, CD206, CD284, CD354, HLA-DR
T helper cells	$CD14^-$ / $CD3^+$ / $CD4^+$	CD16, HLA-DR
Cytotoxic T cells	$CD14^-$ / $CD3^+$ / $CD4^-$	CD16, HLA-DR
NK cells	$CD14^-$ / $CD3^+$ / $CD16^+$	HLA-DR

Figure S1: Gating strategy used to analyse surface marker proteins on PBMCs. Gating strategy used to identify monocytes, T helper cells, cytotoxic T cells and NK cells and analyse their activation status and differentiation state. Protein expression (MFI) of the markers not depicted were determined based on all cells in the relevant population. Table shows all markers analysed for a specific cell type. Surface markers in green are related to anti-inflammatory states, surface markers in black are generally associated with pro-inflammatory effects. MFI = Mean Fluorescence Intensity.

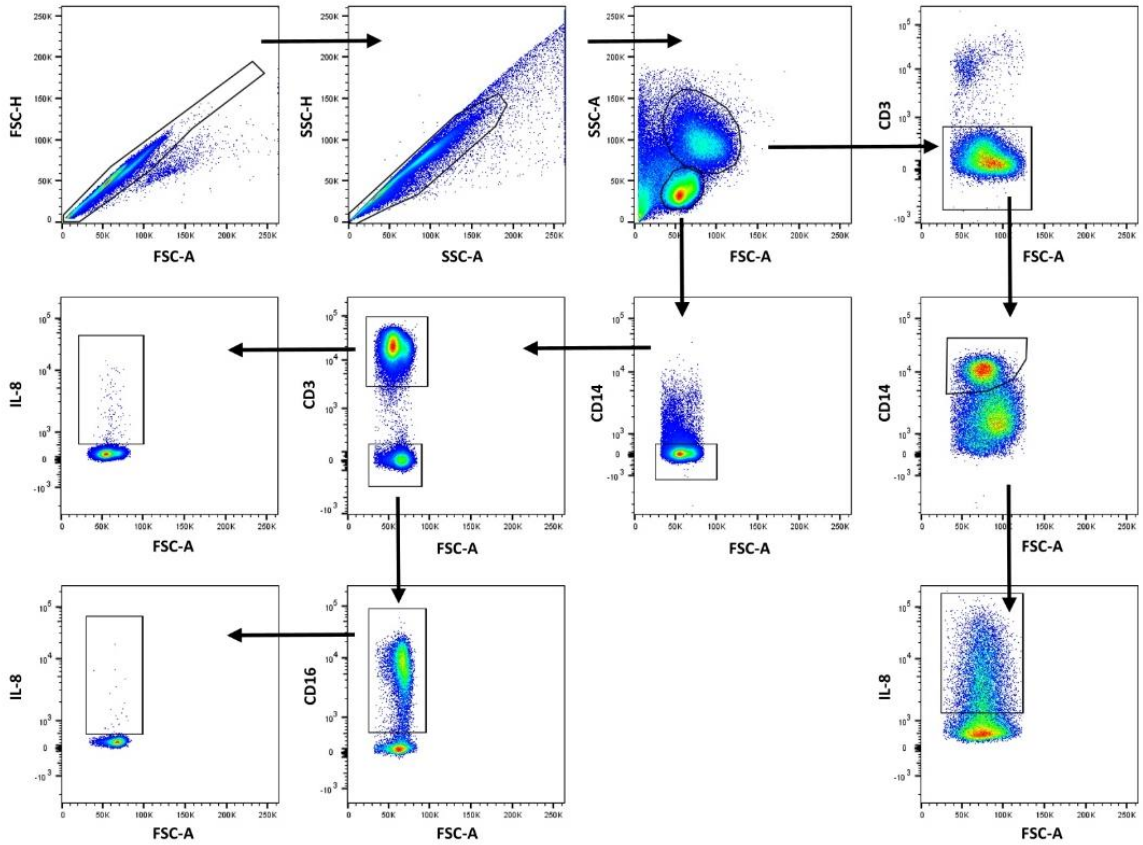

Figure S2: Gating strategy used for intracellular cytokine staining analysis. Gating strategy used to identify monocytes, T cells and NK cells and analyse the intracellular expression of cytokines. Protein expression (MFI) of the markers not depicted were determined based on all cells in the relevant population

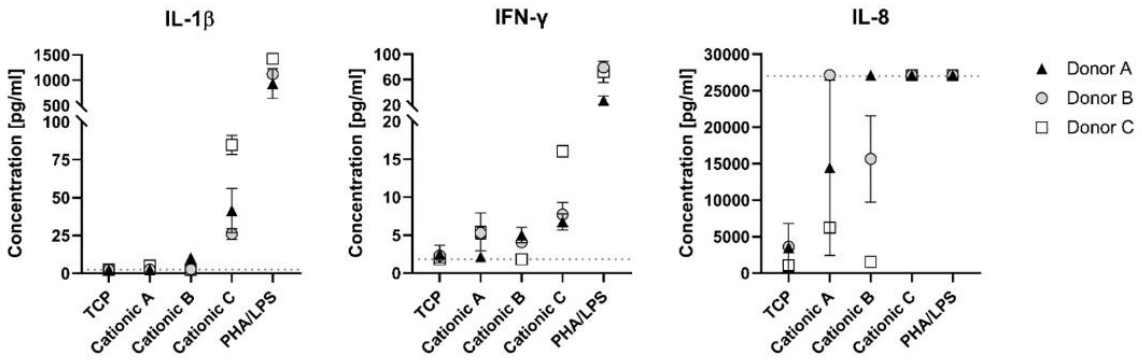

Figure S3: Cytokine secretion of PBMCs cultured on PEM surfaces. PBMCs from 3 donors were cultured for 72 h on PEM surfaces Cationic A, B and C. TCP served as a negative control, stimulation with LPS and PHA as positive control. Concentration of cytokines in pg/ml. Dotted line indicates lower limit (IL-1β, IFN-γ) or upper limit of quantification (IL-8). N = 3 donors were tested with two technical replicates. Symbols represent mean ± SD.

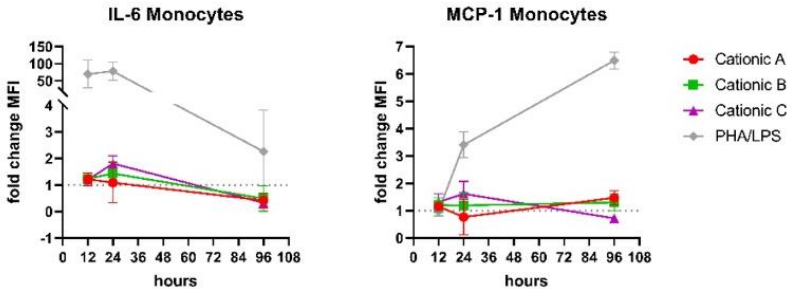

Figure S4: Intracellular cytokine analysis across time of PBMCs cultured on PEM coatings. Protein expression (MFI) of monocytes was quantified after culturing PBMCs for 12, 24 and 96 h on PEM coatings Cationic A, B and C as well as the uncoated TCP control. Graph shows results of one donor tested with two technical replicates and in two separate experiments. Graphs show fold change in protein expression (MFI) of TCP control (indicated by dotted line) for Cationic A (circles, red), Cationic B (squares, green), Cationic C (triangles, purple) and positive control PHA/LPS (diamond, grey). Symbols represent mean ± SD.

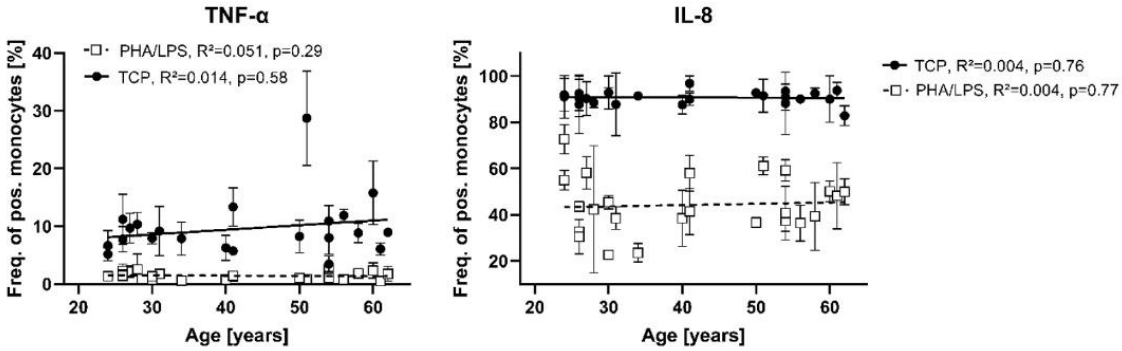

Figure S5: Age-associated intracellular cytokine expression in monocytes in a cohort of 24 individuals. Frequency of TNF-α and IL-8 positive monocytes was quantified in three independent experiments with flow cytometry in 24 donors. Graphs show age-associated frequencies of cytokine positive monocytes and simple linear regression analysis for negative control (TCP, continuous line) and positive control (PHA/LPS, dashed line). Symbols represent mean ± SD.

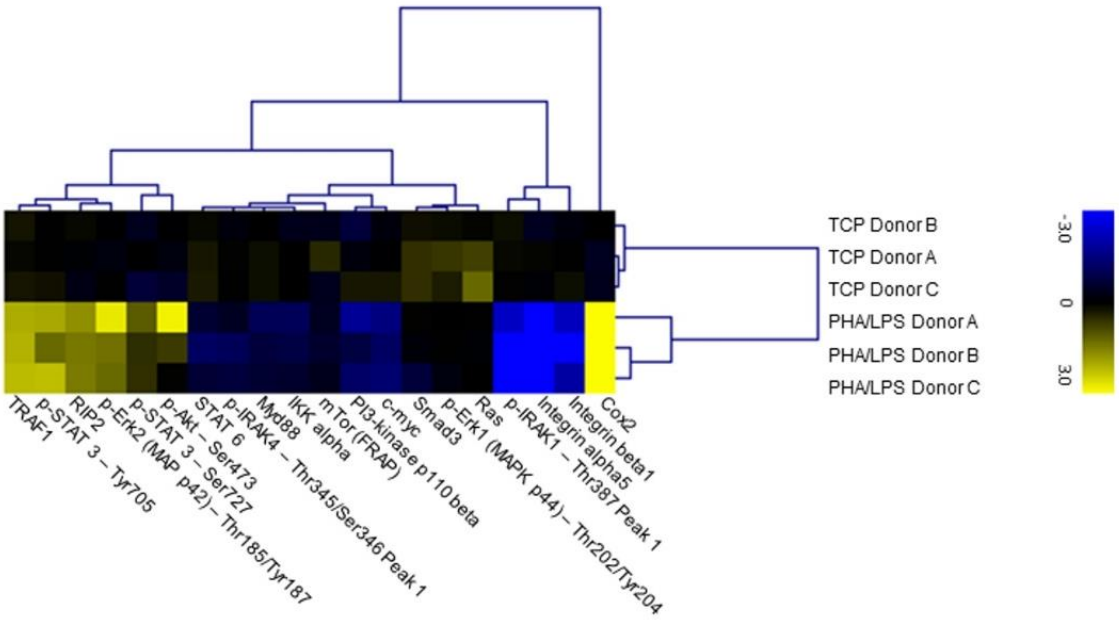

Figure S6: Intracellular signaling molecules in monocytes with significant differences in expression between negative and positive control. Monocytes were isolated from PBMC cell suspension using MACS isolation and cultured for 24 h. Protein expression of 67 cell signaling proteins and their modifications were investigated in monocytes of n = 3 different donors using DigiWest. Proteins with a significant (Nonparametric Wilcoxon Rank sum test, $p \leq 0.05$) difference in expression levels comparing TCP negative control and PHA/LPS stimulated positive control are shown as hierarchical clustered heatmap (Euclidean Distance, complete linkage clustering). Colour gradient from blue to yellow corresponds to low or high antibody-specific signals.

Donor	Sex	Age	Freq. of T helper cells	Freq. of cytotoxic T cells	Freq. of NK cells	Freq. of Monocytes
Donor 1	F	24	47.3%	13.9%	4.5%	4.9%
Donor 2	F	24	30.9%	21.0%	4.7%	7.2%
Donor 3	F	26	31.3%	25.8%	6.5%	6.1%
Donor 4	F	28	31.5%	30.0%	7.0%	4.6%
Donor 5	F	30	37.3%	20.1%	3.8%	5.9%
Donor 6	F	31	37.4%	25.3%	3.8%	4.4%
Donor 7	F	41	30.6%	19.1%	6.4%	5.1%
Donor 8	F	54	29.2%	26.1%	4.5%	2.0%
Donor 9	F	54	42.4%	12.8%	5.3%	9.9%
Donor 10	F	54	39.1%	20.0%	7.7%	5.3%
Donor 11	F	56	29.1%	19.9%	5.5%	6.7%
Donor 12	F	62	42.0%	15.3%	4.3%	3.9%
Donor 13	M	26	31.5%	17.2%	11.6%	5.1%
Donor 14	M	26	28.3%	23.8%	6.1%	5.5%
Donor 15	M	27	41.8%	23.4%	2.8%	5.8%
Donor 16	M	30	31.8%	21.2%	3.1%	13.5%
Donor 17	M	34	27.2%	23.2%	6.4%	10.5%
Donor 18	M	40	32.9%	21.7%	5.5%	8.5%
Donor 19	M	42	24.4%	19.6%	6.8%	6.7%
Donor 20	M	50	28.5%	13.3%	2.9%	12.0%
Donor 21	M	51	34.4%	20.4%	4.5%	11.9%
Donor 22	M	58	36.5%	11.5%	13.8%	7.0%
Donor 23	M	60	28.2%	16.1%	3.5%	8.7%
Donor 24	M	61	12.2%	38.5%	3.6%	7.6%

Table S1: Sex, age and frequency of major cellular populations in PBMC for donors analysed in Figure 4 (results from flow cytometric analysis of PBMC cultured on the TCP negative control for 24 h).

		Cationic A			Cationic C			TCP		
Protein names	**Gene**	Replicate 1	Replicate 2	Replicate 3	Replicate 1	Replicate 2	Replicate 3	Replicate 1	Replicate 2	Replicate 3
Apolipoprotein A-II	APOA2	8.76%	7.63%	7.54%	19.24%	19.99%	21.62%	8.75%	9.58%	9.31%
Inter-alpha-trypsin inhibitor heavy chain H4	ITIH4	0.00%	0.12%	0.00%	0.76%	0.96%	1.03%	0.00%	0.00%	0.00%
Prothrombin	F2	1.07%	0.75%	0.67%	0.44%	0.40%	0.42%	0.37%	0.31%	0.19%
Serum amyloid A-4 protein	SAA4	1.76%	1.77%	1.62%	1.65%	1.68%	1.48%	0.11%	0.42%	0.00%
Apolipoprotein A-I	APOA1	46.47%	44.28%	43.84%	22.18%	20.17%	18.70%	32.89%	38.62%	34.72%
Apolipoprotein A-IV	APOA4	0.68%	0.81%	0.55%	0.79%	0.75%	0.62%	0.74%	0.82%	0.61%
Apolipoprotein C-I	APOC1	11.55%	12.70%	10.55%	14.25%	13.26%	12.37%	14.38%	14.58%	16.02%
Apolipoprotein C-II	APOC2	0.43%	0.43%	0.34%	2.47%	2.61%	2.54%	2.61%	1.40%	2.01%
Apolipoprotein C-III	APOC3	2.19%	1.82%	1.81%	8.83%	9.39%	9.12%	4.57%	3.23%	3.46%
Apolipoprotein C-IV	APOC4	0.00%	0.00%	0.00%	0.56%	0.43%	0.71%	0.00%	0.00%	0.00%
Apolipoprotein E	APOE	8.14%	9.98%	7.88%	3.43%	3.22%	3.33%	4.13%	4.63%	4.16%
Serum albumin	ALB	6.04%	4.81%	5.98%	10.86%	12.14%	12.48%	4.78%	5.88%	5.18%
Hyaluronan-binding protein 2	HABP2	1.23%	0.69%	0.91%	0.00%	0.00%	0.00%	8.25%	4.83%	6.78%
Vitronectin	VTN	0.01%	9.68%	9.46%	3.97%	4.21%	4.28%	6.84%	6.00%	6.45%
Coagulation factor X	F10	2.87%	1.76%	2.32%	0.00%	0.00%	0.00%	4.01%	3.13%	3.89%
Coagulation factor XI	F11	0.00%	0.00%	0.00%	1.16%	1.14%	1.19%	0.00%	0.00%	0.00%
Kininogen-1	KNG1	0.00%	0.00%	0.00%	2.46%	2.59%	2.65%	0.00%	0.00%	0.00%
Platelet factor 4 variant	PF4V1;PF4	4.20%	0.00%	3.02%	3.16%	3.20%	3.27%	0.09%	0.06%	0.10%
Vitamin K-dependent protein C	PROC	1.17%	0.54%	0.78%	0.00%	0.00%	0.00%	1.97%	1.61%	1.79%
Vitamin K-dependent protein Z	PROZ	1.39%	0.72%	1.01%	0.00%	0.00%	0.00%	1.44%	1.62%	1.84%
Histidine-rich glycoprotein	HRG	0.00%	0.06%	0.00%	2.85%	3.10%	3.38%	0.00%	0.00%	0.00%
Inter-alpha-trypsin inhibitor heavy chain H1	ITIH1	0.00%	0.00%	0.02%	0.00%	0.00%	0.00%	0.73%	0.54%	0.64%
Inter-alpha-trypsin inhibitor heavy chain H2	ITIH2	0.01%	0.00%	0.02%	0.00%	0.00%	0.00%	1.26%	0.99%	1.20%
Inter-alpha-trypsin inhibitor heavy chain H3	ITIH3	0.00%	0.00%	0.00%	0.00%	0.00%	0.00%	0.94%	0.32%	0.55%
Serglycin	SRGN	1.39%	0.86%	1.08%	0.00%	0.00%	0.00%	0.68%	0.96%	0.73%

Table S2: Abundance (percentage) of proteins identified on Cationic A, Cationic C and negative control (TCP) using LC-MS. Table shows data for n = 3 samples analysed for each surface. Percentage refers to the relative abundance of a given protein in relation to the summation of all proteins found on the respective surface. Horizontal lines indicate division between groups of proteins based on their indicated GOBP (gene ontology database biological process) function (summary shown in Figure 6B). Acute inflammatory response proteins are shown at the top of the table, below are apolipoproteins (2nd from the top), then albumin (3rd position from top), cell adhesion proteins (4th position from the top) and coagulation proteins (5th from the top), while proteins not belonging to one of these categories are found at the bottom of the table.

	fold change protein amount compared to TCP (TCP normalised to 0)						Multiple unpaired t-tests, Cationic A vs. Cationic C
Protein	**Cationic A**			**Cationic C**			**p-value**
	Recplicate 1	Recplicate 2	Recplicate 3	Replicate 1	Recplicate 2	Recplicate 3	
Inter-α-trypsin-inhibitor H4	Protein not found on this surface			Protein found on Cationic C only			n.a.
Histidine-rich glycoprotein	Protein not found on this surface			Protein found on Cationic C only			n.a.
Kininogen-1	Protein not found on this surface			Protein found on Cationic C only			n.a.
Coagulation factor XI	Protein not found on this surface			Protein found on Cationic C only			n.a.
Apolipoprotein C-IV	Protein not found on this surface			Protein found on Cationic C only			n.a.
Platelet factor 4 variant	42.09	43.45	36.82	66.53	61.20	71.35	0.0019
Serum amyloid A-4 protein	8.11	9.77	9.21	16.74	15.47	15.51	0.0003
Apolipoprotein C-III	-0.50	-0.51	-0.49	3.22	3.08	3.51	0.0000
Serum albumin	-0.02	-0.08	0.19	2.69	2.75	3.39	0.0003
Apolipoprotein A-II	-0.18	-0.16	-0.14	2.74	2.53	3.35	0.0003
Apolipoprotein J / Clusterin	0.21	0.35	0.42	2.70	1.76	2.30	0.0023
Apolipoprotein C-II	-0.82	-0.78	-0.82	1.20	1.12	1.34	0.0000
Apolipoprotein A-IV	-0.19	0.14	-0.19	0.97	0.70	0.60	0.0059
Apolipoprotein C-I	-0.34	-0.14	-0.26	0.70	0.44	0.53	0.0012
Vitronectin	0.76	0.52	0.54	0.11	0.07	0.23	0.0050
Apolipoprotein A-I	0.13	0.27	0.30	0.12	-0.07	-0.02	0.0472
Serglycin	0.53	0.10	0.45	Protein not found on this surface			n.a.
Optineurin	-0.48	-0.14	-0.37	Protein not found on this surface			n.a.
Vitamin K-dependent protein Z	-0.27	-0.56	-0.36	Protein not found on this surface			n.a.
Coagulation factor X	-0.33	-0.52	-0.34	Protein not found on this surface			n.a.
Vitamin K-dependent protein C	-0.44	-0.69	-0.54	Protein not found on this surface			n.a.
Hyaluronan-binding protein 2	-0.84	-0.90	-0.86	Protein not found on this surface			n.a.

Table S3: Statistical analysis comparing the amount of proteins on the Cationic A and Cationic C PEM surfaces. Values indicate fold change protein amount compared to uncoated TCP control based on LC-MS results of n = 3 measurements. Unpaired t-tests were applied to compare statistical differences in the respective amount of each individual protein on surfaces Cationic A and C. Colour coding as described in Figure 6 and result section 3.6.

Analyte	TCP			Cationic A			Cationic C			PHA/LPS		
	Donor A [AFI]	Donor B [AFI]	Donor C [AFI]	Donor A [AFI]	Donor B [AFI]	Donor C [AFI]	Donor A [AFI]	Donor B [AFI]	Donor C [AFI]	Donor A [AFI]	Donor B [AFI]	Donor C [AFI]
Akt	5755	5619	6428	4972	4836	5559	4559	3667	5009	4616	5261	6131
Akt - phospho_Ser473	220	246	182	284	190	186	291	177	361	1856	413	260
Akt - phospho_Thr308	528	943	531	625	716	556	714	693	513	4939	827	897
Bcl2	33	33	76	33	64	52	69	57	33	33	33	66
Bcl6	62	69	76	110	86	100	118	80	113	33	33	33
Calcineurin B	666	309	9604	180	3033	6261	33	1349	8341	33	5534	3314
CD36	7439	7525	33	9728	7541	33	11270	33	33	12662	6180	33
CD69	33	33	33	33	33	33	33	33	33	33	33	33
CDK4	372	252	375	711	660	643	502	665	646	353	456	432
c-Jun	696	1019	884	3250	2671	2623	3500	3707	3945	1071	789	354
c-myc	9350	8564	11674	9847	11617	12419	7506	13539	15751	3418	4266	3836
Cox2	33	33	33	33	58	33	33	57	33	2971	5449	5532
Erk1/2 (MAPK p44/42)	49531	35104	40204	34338	28517	33741	25632	23342	25450	31693	31458	27546
Erk1/2 (MAPK p44/42) - phospho_Thr202/Tyr204	100	112	117	81	281	33	92	324	33	773	293	274
FAS	322	316	278	235	285	231	301	267	190	547	296	194
FKBP12	34618	18748	45815	21268	28090	40844	13841	24051	31759	21481	60670	63890
GATA3	66	33	33	33	33	62	33	33	33	33	33	33
HIF1 alpha	33	33	33	33	33	33	33	33	33	33	33	33
HLA-DR alpha chain	2922	2096	3108	1893	1926	2533	1416	1732	2368	3371	33	2141
HSP 90	311693	428640	456681	747342	368673	761646	380248	934781	456271	289179	656499	165851
HSP70	3639	3277	3353	3335	2904	2892	3513	3350	3439	3903	3546	3469
IKK alpha	1835	1469	1820	1935	1905	1417	1818	2115	1900	877	1041	1269
IKK beta	4675	3229	4199	3923	3960	3718	3934	5042	4080	3778	3094	2296
IKK epsilon	717	445	763	691	486	571	808	634	812	467	293	291
IKK epsilon - phospho_Ser172	33	33	78	49	110	33	33	128	33	139	33	33
IL 2R alpha (CD25)	824	1615	889	985	1150	926	807	1231	964	8116	1041	1212
IL 2R alpha (CD25)	33	63	78	33	33	43	33	37	34	313	33	67
Integrin alpha5	2560	1823	2302	3222	2906	2986	2199	3611	3026	206	174	137
Integrin beta1	385	351	441	526	396	454	321	533	422	33	33	104
Integrin beta3	788	210	334	741	451	471	525	353	437	253	142	186
IRAK1	448	469	424	562	380	334	426	527	400	33	33	33
IRAK1 - phospho_Thr387	8540	8936	5021	9328	5034	33	9561	5884	6686	29214	7601	33
IRAK4	671	588	666	652	701	723	516	653	741	484	313	391
IRAK4 -	475	816	347	424	560	511	590	452	626	3595	765	488
Mcl-1	1591	1845	1731	2434	2313	2216	1878	2578	2133	1341	1182	1696
MEK1	2001	2545	2224	2407	2613	2201	1774	2001	2093	1498	2245	2915
MEK1/2 - phospho_Ser217/Ser221	33	699	33	934	980	859	877	935	887	33	863	33
MEK2	477	518	583	557	513	451	310	390	417	33	410	522
mTOR (FRAP)	1224	710	700	1622	1052	470	1239	2128	1347	668	608	698
Myd88	2120	1906	2129	1850	1940	1965	1416	1989	1669	929	1141	1237
NF-κB p100/p52_13 - peak 1	547	610	869	340	303	488	241	303	297	879	1073	855
NF-κB p100/p52_13 - peak 2	3345	3148	4459	2975	3873	3297	2576	3117	3136	2879	2649	3153
NLRP3 (NALP3)	33	33	33	33	33	128	56	33	33	33	33	66
PI3-kinase p110 beta	1263	879	1768	1751	1855	2145	990	1933	1608	425	846	621
PI3-kinase p85 alpha	33	33	33	33	33	33	33	33	33	33	33	33
Ras	1730	1082	2442	970	876	1619	667	1021	1415	1021	982	1029
RIP2	3095	3547	2724	3168	2977	2637	3386	3318	2628	10565	8805	8917
Smad2	2335	2162	2224	2061	1962	2120	2077	2179	2029	3172	1719	1499
Smad2/3 - peak 1	574	434	500	649	527	525	558	608	557	691	366	374
Smad2/3 - peak 2	74	140	64	48	33	74	46	33	44	94	33	33
Smad3	253	194	251	145	188	158	177	139	162	176	159	104
SOCS-1	33	33	33	33	33	33	33	33	33	33	33	33
SOCS-3	53	52	33	33	33	33	33	33	33	33	33	33
Src	38188	35491	38296	35655	37952	43453	39482	34885	41265	19493	43962	41742
STAT 1	2672	3129	1297	1742	1143	1039	1573	1469	1216	1195	2161	1920
STAT 1 - phospho_Tyr701 - peak 1	97	128	49	76	105	33	103	85	84	97	192	197
STAT 1 - phospho_Tyr701 - peak 2	125	382	33	33	76	35	58	33	57	286	761	664
STAT 3 - phospho_Ser727	459	347	282	475	440	294	554	425	444	956	662	675
STAT 3 - phospho_Tyr705	155	156	182	97	157	122	97	168	114	616	376	751
STAT 5	1763	1496	1474	1651	1608	1202	1509	2021	1276	1553	1354	1626
STAT 6	5169	4712	5423	5017	4106	4533	3710	5495	3988	2792	1942	2770
TRAF1	2307	2574	2602	1956	1757	2011	1346	1303	1197	9030	9368	10026
VEGF (121_165_189_206)	33	7567	10145	10240	33	20534	8758	9846	8078	10195	33	33

Table S4: Expression levels of intracellular proteins analysed with DigiWest technology. Units of protein expression are presented in accumulated fluorescence intensity [AFI]. Values in the table are median centered and normalized to the median measured signal intensity corresponding to the sample. Table shows all values of DigiWest analysis for three donors on all surfaces tested (Cationic A and C PEM surfaces, the negative control (TCP) and the positive control (PHA/LPS)). An AFI of 33 indicates that no signal peak was detected (lower limit of detection).